Statistical Mechanics of Regularized Least Squares

Statistische Mechanik der Methode der kleinsten Quadrate mit Regularisierung

Der Technischen Fakultät der
Friedrich-Alexander-Universität Erlangen-Nürnberg
zur Erlangung des Doktorgrades

Doktor-Ingenieur

vorgelegt von

Ali Bereyhi

aus Ahvaz, Iran

Als Dissertation genehmigt von der Technischen Fakultät
der Friedrich-Alexander-Universität Erlangen-Nürnberg

Tag der mündlichen Prüfung:	26.06.2020
Vorsitzender des Promotionsorgans:	Prof. Dr.-Ing. habil. Andreas Paul Fröba
Gutachter:	Prof. Dr.-Ing. Ralf R. Müller Prof. Dr. Helmut Bölcskei

Statistical Mechanics of Regularized Least Squares

Faculty of Engineering
Friedrich-Alexander University of Erlangen-Nuremberg
for the doctoral degree

Doktor-Ingenieur

submitted by

Ali Bereyhi

from Ahvaz, Iran

Approved as doctoral dissertation by Faculty of Engineering
Friedrich-Alexander University of Erlangen-Nuremberg

Submission date:	04.11.2019
Date of doctoral defense:	26.06.2020
Dean of the doctoral committee:	Prof. Dr.-Ing. habil. Andreas Paul Fröba
Chair of the examination committee:	Prof. Dr.-Ing. Robert Schober
Reviewers:	Prof. Dr.-Ing. Ralf R. Müller Prof. Dr. Helmut Bölcskei
External authorized examiner:	Prof. Dr. Hermann Schulz-Baldes

To my Queen Saba
and
my little Princess Rima

Acknowledgment

Starting with my initial progress reports, this treatise has been developed through long iterative interactions with my supervisor Prof. Ralf R. Müller in the last five years. Doubtlessly, this dissertation would have not been accomplished without his patient superintendence. I would like to give my deepest gratitude to Prof. Müller for all his supports, patience, guidance and advices which made this milestone achievable. Furthermore, I would like to thank Prof. Hermann Schulz-Baldes from Department of Mathematics for his advices and suggestions during my study.

Throughout my PhD study, I have collaborated with several colleagues in the Institute for Digital Communications. In particular, I would like to thank my former colleague Dr. Mohammad A. Sedaghat for useful discussions regarding the applications of my results in MIMO communications, Dr. Saba Asaad whose expertise in asymptotic analysis and selection algorithms helped me understanding state-of-the-art techniques in the literature, and Bernhard Gäde for his interesting comments on hardware-related issues. Furthermore, I would like to acknowledge Jan-Nico Zäch, Viktoria Schram and Dr. Vahid Jamali for our collaborations in these five years on other research topics. I also thank head of the institute Prof. Robert Schober, as well as Prof. Wolfgang H. Gerstacker, who made these collaboration opportunities possible.

In addition to my colleagues in the Institute for Digital Communications, I would like to acknowledge Prof. Georg Fischer from the Institute for Electronics Engineering in Friedrich Alexander University, Dr. Saeid Haghighatshoar and Prof. Rafael F. Schaefer from the Information Theory and Applications Chair in Technical University of Berlin, Prof. Christoph Mecklenbräuker from the Institute for Telecommunications in Technical University of Vienna, Prof. Antonia M. Tulino from the Department of Electrical Engineering and Information Technology in University of Naples Federico II, Prof. Symeon Chatzinotas from the Interdisciplinary Centre for Security Reliability and Trust in University of Luxembourg, and Prof. Amir M. Rabiei from School of Electrical and Computer Engineering in University of Tehran.

Dedication

Despite all difficulties, these five years have passed magnificently. While being abroad, I found the opportunity to enjoy living with my family and being a father. This was made possible only with the help of Saba who was always supportive in this way. I would like to dedicate this dissertation to her and to our little princess Rima.

Abstract

Various problems in practice are mathematically described by a regression model in which the *linear* relation between possibly noisy outputs and their corresponding inputs is to be learned. An effective approach for linear regression is the *regularized* form of the *least-squares* method commonly abbreviated by RLS. This scheme specifies the linear relation, such that a penalized version of error given by the linear model is minimized. The penalty describes information known in priori about the model.

Due to the growing interest in high-dimensional applications, recent studies often desire to characterize RLS in the large-system limit. Nevertheless, for various forms of RLS, basic analytical tools fail to address this task. For these forms, numerical simulations further deal with high computational complexity. Hence, assessing the performance by numerical approaches is also intractable. The main objective of this dissertation is to address this issue by using analytical tools from statistical mechanics. To this end, RLS solution of a linear regression model is interpreted as the *ground state* of a *spin glass* whose macroscopic parameters are derived via the *replica method*. Following the relation between the spin glass and its corresponding regression problem, the asymptotic distortion achieved by RLS is analytically derived for an arbitrary distortion function. The asymptotic characterization of RLS leads to a general form of the *decoupling principle*. This result states that the regression outputs given by RLS in a high-dimensional linear model are statistically described via a *decoupled* scalar setting. When the corresponding spin glass exhibits *replica symmetry*, this decoupled setting reduces to a scalar system with independent additive Gaussian noise and recovers earlier results in the literature. For cases in which replica symmetry breaks, the Gaussianity and independency of decoupled noise are violated. Using the derivations via the replica method, the decoupled noise term is further characterized for cases with broken replica symmetry with an arbitrary number of breaking steps.

Linear regression has a diverse scope of applications from statistics and communications to information theory, signal processing and machine learning. To enlighten applications of this study, two examples of linear regression via RLS are investigated in this dissertation. The first example considers the problem of *sparse recovery*. Using the asymptotic results, the large-system performance of various recovery algorithms is studied and compared to the results in literature. For algorithms with tractable computational complexity, investigations confirm validity of the derivations. The results further characterize those recovery algorithms whose performance has remained unknown due to their intractable complexity. In the second example, *multiple-input multiple-output (MIMO) precoding* is investigated. In this respect, the problem of MIMO precoding is first interpreted as linear regression and an RLS-based scheme is proposed. The large-system performance of this scheme is then investigated by means of the asymptotic results and compared to the benchmark. Investigations depict close agreement of asymptotic characterization with finite-dimensional simulations and demonstrate significant performance enhancements in some particular cases.

Zusammenfassung

Viele Aufgabenstellungen der Signalverarbeitung können mathematisch durch ein lineares Regressionsmodell beschrieben werden. Hierbei wird eine lineare Beziehung gesucht, die das Verhältnis zwischen den Eingangs- und möglicherweise verrauschten Ausgangssignalen eines unbekannten Systems beschreibt. Die regularisierte Version der Methode der kleinsten Quadrate ist ein leistungsfähiger Ansatz für die lineare Regression, welche üblicherweise mit RLS abgekürzt wird. Diese Methode findet die lineare Beziehung welche die Summe aus den Fehlerquadraten und einem Regularisierungsterm minimiert. Letzterer beschreibt Informationen, die im Vorfeld über das Modell bekannt sind.

In letzter Zeit ist das Interesse an hochdimensionalen Problemen der Signalverarbeitung gestiegen, weshalb die asymptotischen Eigenschaften von RLS Stand aktueller Forschung sind. Allerdings können verschiedenen Formen von RLS mit üblichen analytischen Werkzeuge nicht untersucht werden. Numerische Ansätze hingegen scheiden auf Grund hoher Rechenkomplexität aus. In dieser Dissertation wird ein alternativer Ansatz mit Hilfe der analytischen Werkzeuge aus der statistischen Mechanik aufgestellt. In diesem Ansatz wird das mit RLS zulösende Problem als Spin-Glas interpretiert, dessen asymptotische Eigenschaften durch den Replika-Trick hergeleitet werden. Mit Hilfe der Analogie zwischen dem Spin-Glas und der RLS-Methode wird die asymptotische Verzerrung der RLS-Methode analytisch für eine beliebige Verzerrungsfunktion bestimmt. Diese Beschreibung der RLS-Methode führt zu einer allgemeinen Form des sogenannten *Entkopplungsprinzips*. Dieses besagt, dass die Lösungen, die durch die RLS-Methode in einem hochdimensionalen linearen Modell bestimmt werden, durch eine entkoppelte skalare Form beschrieben werden können. Wenn das entsprechende Spin-Glas die sogennante *Replika-Symmetrie* aufweist, reduziert sich diese entkoppelte Form auf ein skalares System mit unabhängigem additivem normal-

verteilen Rauschen. Diese allgemeine Erkenntnis deckt sich mit den Ergebnissen für spezielle Fälle, die bereits aus der Literatur bekannt sind. Die Normalität und die Unabhängigkeit von entkoppeltem Rauschen gilt nicht mehr für Fälle, in denen die Replika-Symmetrie gebrochen wird. Für diese Fälle wird die entkoppelte Form zum ersten Mal charakterisiert und die Verteilung des entkoppelten Rauschens ausdrücklich bestimmt.

Die Anwendungen der linearen Regression sind vielfältig, insbesondere in den Bereichen Statistik, Nachrichtentechnik, Informationstheorie, Signalverarbeitung und dem maschinellen Lernen. Um die gewonnenen Erkenntnisse zu verdeutlichen, werden zwei konkrete Anwendungsfälle der linearen Regression näher betrachtet. Als erstes Beispiel wird das Problem der komprimierten Erfassung (Compressive Sensing) herangezogen. Die Leistung verschiedener Algorithmen wird untersucht und mit aus der Literatur bekannten Ergebnissen verglichen. Numerische Simulationen bestätigen die Gültigkeit unserer Resultate für Algorithmen, deren Komplexität eine solche Untersuchungen zulässt. Die in dieser Dissertation vorgestellte Methodik erlaubt auch die Beurteilung solcher Algorithmen, deren hohe Komplexität einem numerischen Ansatz im Wege steht. Als zweites Beispiel wird die Vorcodierung in Multiple-Input Multiple-Output (MIMO) Systemen betrachtet. Dazu wird das Problem der MIMO-Vorcodierung zuerst als lineare Regression interpretiert und ein RLS-basierter Algorithmus vorgeschlagen, dessen Leistung anhand der Ergebnisse ermittelt wird. Der Vergleich des vorgeschlagenen Algorithmus mit klassischen Algorithmen zeigt signifikante Leistungssteigerungen.

Contents

List of Figures

Chapter 1

Introduction

Linear regression is doubtless one of the most studied problems in statistics, mathematics and computer science which has a large scope of applications; see [1–6] and references therein. In regression, we are provided with a vector of observed values

$$\boldsymbol{y} = \begin{bmatrix} y_1 \\ \vdots \\ y_M \end{bmatrix} \tag{1.1}$$

which are called *regressands*. The regressands depend on a set of M data vectors

$$\mathbb{D} = \{\mathbf{a}_1, \ldots, \mathbf{a}_M\} \tag{1.2}$$

where each data vector is of length N, i.e.,

$$\mathbf{a}_m = \begin{bmatrix} a_{m1} \\ \vdots \\ a_{mN} \end{bmatrix} \tag{1.3}$$

with $a_{mn} \in \mathbb{A} \subseteq \mathbb{C}$ for $m \in [M]$ and $n \in [N]$. These data vectors are referred to as the *regressors*, and N is often called *data dimension*. The main objective in this case, is to learn from $\mathbb{D}$ and $\boldsymbol{y}$, the mapping from the regressors to the regressands. In other

words, one needs to find function $f(\cdot)$ which for each data vector $\mathbf{a}_m$ determines the corresponding observation y_m as

$$y_m = f(\mathbf{a}_m). \tag{1.4}$$

Linear regression assumes that this mapping is linear, i.e.

$$y_m = \sum_{n=1}^{N} x_n a_{mn} + z_m \tag{1.5a}$$

$$= \mathbf{a}_m^{\mathsf{T}} \boldsymbol{x} + z_m \tag{1.5b}$$

for some *regression coefficients* $x_1, \ldots, x_N \in \mathbb{X}$ and *regression error* z_m which models observation noise and underdeterminacy of the problem. Here, $\boldsymbol{x} \in \mathbb{C}^N$ is defined as

$$\boldsymbol{x} = \begin{bmatrix} x_1 \\ \vdots \\ x_N \end{bmatrix}. \tag{1.6}$$

In this case, the main task is to develop a method which determines the regression coefficients from $\mathbb{D}$ and $\boldsymbol{y}$.

Several applications in communications theory, signal processing, coding and machine learning can be interpreted as linear regression. A well-known example is the problem of signal recovery from linearly mixed measurements. In this problem, samples of a signal are measured via multiple sensors in a network. Each sensor observes a linear combination of the samples. These observations are in general distorted by noise. The main task in this case is to recover the signal samples from these noisy measurements. By considering the measurements as regressands, and the linear projections from the samples to observations as regressors, signal recovery reduces to a linear regression problem whose coefficients represent the samples. There are various other applications for linear regression, such as compressive sensing, channel coding, data detection, code division multiple accsess (CDMA) systems, multiple-input multiple-

output (MIMO) precoding, hypothesis testing and dictionary learning, to name just a few. Some examples can be followed in [7–13] and references therein.

1.1 Method of Least Squares

An effective approach to learn the regression coefficients is to employ the method of least squares (LS). In this method, the coefficients in $\boldsymbol{x}$ are found such that the residual sum of squares (RSS), defined as

$$\Delta\left(\boldsymbol{x}|\mathbb{D},\boldsymbol{y}\right)=\sum_{m=1}^{M}\left|y_m-\boldsymbol{x}^{\mathsf{T}}\mathbf{a}_m\right|^2, \tag{1.7}$$

is minimized over $\mathbb{X}^N$. This approach does not necessarily lead to a unique solution, since for some choices of $\mathbb{D}$ and $\boldsymbol{y}$ the minimization might have multiple solutions.

In a Bayesian framework, LS can be considered as maximum-a-posteriori (MAP) estimation with uniform prior distribution, i.e. the maximum likelihood (ML) algorithm[1]. The assumption of uniformity on the prior distribution comes from the fact that no prior information has been provided on $\boldsymbol{x}$. In other words, the regression coefficients are not supposed to exhibit any specific behavior and can take any point in $\mathbb{X}^N$ with the same probability. This is however not the case in variety of applications. A prominent example is the problem of sparse recovery, also known as compressive sensing[2] [7]. In this problem, the regression coefficients are known to be sparse meaning that only a certain fraction of them are non-zero. In this case, the LS method needs to be modified, such that the sparsity constraint on regression coefficients is satisfied.

1.2 Regularizing via Prior Information

The prior information on the regression coefficients can be addressed in LS via penalizing the RSS. This approach is known as *regularization* in the context of regression analysis. From Bayesian inference points of view, regularized least squares (RLS) pos-

[1] We illustrate this interpretation in Chapter 2.
[2] The term *compressed sensing* is also used in the literature.

tulates a non-uniform prior distribution on the regression coefficients. This means that some points in $\mathbb{X}^N$ are believed, in priori, to be the coefficients with higher probability than other points. The penalty, referred to as the *regularization term*, should therefore be proportional to the prior information given on the regression coefficients.

Considering the example of sparse recovery, the prior information on regression coefficients is sparsity. We know that a certain fraction of the coefficients are zero. This prior information can be modeled via the ℓ_0-norm of the regularization coefficients. For vector $\boldsymbol{x}$, the ℓ_0-norm is defined as the number of non-zero entries in $\boldsymbol{x}$. As we know that the vector of regression coefficients is sparse, the points in $\mathbb{X}^N$ whose ℓ_0-norm is large are less probable to be the solution. As a result, one can regularize LS by the ℓ_0-norm and find the regression coefficients such that the regularized RSS

$$\Delta_{\mathrm{R}}\left(\boldsymbol{x}|\mathbb{D},\boldsymbol{y},\lambda_0\right)=\Delta\left(\boldsymbol{x}|\mathbb{D},\boldsymbol{y}\right)+\lambda_0\left\|\boldsymbol{x}\right\|_0 \tag{1.8}$$

is minimized over $\mathbb{X}^N$ for some real scalar λ_0.

RLS is also understood from optimization points of view: Considering the problem of sparse recovery, LS suggests to determine the regression coefficient by minimizing the RSS. It is however known in priori that some of the coefficients are zero. In this case, LS can be modified by constraining the minimization problem subject to

$$\left\|\boldsymbol{x}\right\|_0\leq\eta. \tag{1.9}$$

Consequently, RLS can be observed as a Lagrangian dual subproblem whose solution, under certain conditions, can meet the minimizer of primal constrained optimization.

Depending on the application, different prior information are provided on the regression coefficients. There are therefore various forms of regularization in the literature. The most common form is Tikhonov regularization, also known as linear regularization. In this method, the RSS is penalized by the ℓ_2-norm. In the Bayesian framework, this regularization means that the regression coefficients are postulated to have a Guassian distribution. This assumption is reasonable in many applications, in which the regression coefficients are taken from a random process in the nature. Another well-known form of regularization is least absolute shrinkage and selection

operator (LASSO) being widely used in the literature for feature selection. LASSO regularizes LS by the ℓ_1-norm which imposes the sparsity constraint on the regression coefficients via a convex function.

1.3 High-dimensional Applications of RLS

The computational complexity of RLS grows with the data dimension. The order of growth depends on the regularization term and the support from which regressors are drawn, i.e. $\mathbb{X}$. For example, for a convex choice of $\mathbb{X}$, the computational complexity of sparse recovery via with ℓ_0-norm regularization grows exponentially with dimension N. This growth is of polynomial time for Tikhonov regularization and LASSO.

In most applications of linear regression, the data dimension is large. This dimensionality is further increasing in recent applications. As a result, some forms of RLS are computationally infeasible to implement, and many others are significantly complex. Conventional approach to this complexity issue was to address high-dimensional applications of linear regression via other regression methods, such as iterative stepwise algorithms, rather than RLS. These alternative methods learn the regression coefficients with linear complexity at the expanse of poorer performance. In contrast to the initial belief, analyses based on factor graphs showed later that this trade-off between the performance and the complexity is not generic. In fact, RLS can be implemented with linear complexity for several forms of regularization via approximate message passing (AMP) algorithms.

In addition to large bodies of work on low-complexity algorithms, high dimensional applications have also brought up the necessity of asymptotic analyses. This is clarified by considering the example of sparse recovery. In this application, regression coefficients are usually determined via LASSO. This algorithm is chosen, since the alternative ℓ_0-norm regularization results in exponential complexity. Despite the reasonable performance of LASSO, the effectiveness of this algorithm in comparison with ℓ_0-norm regularization and optimal Bayesian algorithm is questionable. This question, as well as similar questions in other applications of linear regression, can be answered

via asymptotic analysis of RLS. Since basic analytic tools often fail to track such analyses, more advanced tools are required for this aim.

1.4 Contributions

The main contribution of this dissertation is to characterize the asymptotic performance of RLS with generic regularization. The analysis is based on the *replica method* developed in statistical mechanics to study the behavior of *spin glasses*. The asymptotic characterization addresses various applications of linear regression, two of whom are presented in this dissertation. In particular, the contributions of this dissertation are divided into four main groups:

1. Characterizing the RLS method in the asymptotic regime via the replica method.
2. Deriving a general form of decoupling principle for the RLS method.
3. Investigating the asymptotic performance of different sparse recovery algorithms.
4. Design and analysis of an RLS-based precoding scheme for MIMO systems.

In the following, we briefly explain each group.

1.4.1 Asymptotics of Generic RLS

The performance of RLS is described in terms of the accuracy of the linear regression model. In other words, to quantify the performance of RLS for a given regularization term and support, one needs to proceed as follows: First, the regression coefficients are explicitly derived. Then, the average distortion between a large set of observations and their corresponding estimated values, given via the linear regression model, is calculated with respect to a distortion function. This average distortion is considered as the *measure of performance*. Except for few forms of RLS, e.g. RLS with linear regularization and real support, basic analytic tools fail to characterize the performance of RLS for high-dimensional problems, as the complexity becomes analytically intractable.

We address this challenge by invoking more advanced analytic tools developed in statistical mechanics and mathematical physics. To this end, we first interpret the linear regression problem as a thermodynamic system. Following the standard stochastic model for linear regression, this problem is mathematically modeled by an imaginary spin glass. We refer to this system as the *corresponding spin glass* and show that there exists an analogy between this system and the original problem: The regression coefficients derived via an RLS method is given by the *ground state* of this spin glass, and for each distortion function, there exists a *macroscopic parameter* of this spin glass which converges to the corresponding average distortion as the spin glass freezes.

We characterize the generic RLS method in the asymptotic regime by investigating its corresponding spin glass. This task is addressed via the replica method which has been developed in statistical mechanics for analysis of spin glasses. In contrast to earlier studies, we deviate from the conventional approaches and derive the general asymptotic characterization. The result includes earlier characterizations based on *replica symmetry*, as well as derivations under *replica symmetry breaking* approach with an *arbitrary* number of breaking steps. The derivations further justifies the earlier conjecture in the literature on the *universality* of the zero-temperature entropy expression. The contributions in this respect are presented in Chapters 3 and 4.

1.4.2 Generalizing the RLS Decoupling Principle

Our analysis via the replica method demonstrates the *asymptotic decoupling property* of RLS: In the asymptotic regime, the performance of a generic RLS method is described via an equivalent scalar problem whose single regression coefficient is determined via a *decoupled* RLS method. Although this principle has been shown for some particular linear regression problems and special forms of RLS, the results of this dissertation derives a *generalized* form of the principle and clarifies several properties of the decoupled setting which have been remained unknown for more than a decade: We show that the basic form of the decoupling principle with effective Gaussian error extends only to those forms of the RLS method whose corresponding spin glass exhibits *replica symmetry*. For the forms whose corresponding spin glass violates this symmetry, the effective regression error is shown to be *non-Gaussian* and *dependent*

on the decoupled true regression coefficient. The explicit expression for effective error under replica symmetry breaking with an arbitrary number of breaking steps is derived.

The asymptotic characterization via the replica method is represented in terms of the solution of some fixed-point equations. Using the generalized form of the decoupling principle, we show that this solution can be interpreted as the *steady state* of a transition system described by the decoupled setting. This alternative representation enables us to systematically find the solution of the fixed-point equation, and give further insights on the settings characterized via replica symmetry breaking. We call this transition system the *replica simulator*. The detailed contributions in this respect are represented in Chapter 5.

1.4.3 Characterizing Sparse Recovery Algorithms

As discussed earlier, linear regression has a vast scope of applications in communications and signal processing. *Sparse recovery* is a well-known example of such applications. In this problem, samples of a signal are to be recovered from underdetermined observations, which linearly depend on the samples. Without prior information on the signal, this problem is underdetermined, and hence multiple solutions, possibly infinite, are available. The existence of prior information can however reduce the number of valid solutions to one. In sparse recovery, the prior information is given by the signal sparsity: We know in advance that a certain fraction of the samples are zero.

Most well-known methods for sparse recovery are special cases of the generic RLS method, e.g., LASSO and basis pursuit denoising. We hence employ the asymptotic characterization of RLS, derived in the first part of the dissertation, to study the performance of several sparse recovery algorithms. In particular, we consider the class of ℓ_p-norm minimization schemes, and investigate their performance for high-dimensional settings. Invoking the generality of the considered model, we study the impacts of several sensing and recovery approaches, and compare them against the benchmark techniques in the literature. Our investigations demonstrate that unlike the linear and LASSO recovery methods, ℓ_0-norm minimization scheme violates replica symme-

try and requires characterization under replica symmetry breaking. The contributions regarding the problem of sparse recovery are given in details in Chapter 6.

1.4.4 Designing a Novel Precoding Scheme

Another application of linear regression in communications is precoding over MIMO channels. In MIMO systems, specifically the recent large-scale MIMO settings, known as massive MIMO, the major processing load is desired to be shifted to the base stations. This is due to the fact that typical computational processes in these systems is still burdensome for *ordinary* low-power user equipments. The standard approach to address this issue is to alternate the order of *dominant* data processing tasks in downlink transmission: In the uplink transmission, in which users transmit information to the base station, the receive signal is *post-processed* via a *receiver* at the base station. However, while transmitting data in downlink, where the base station is the transmitter, the transmit signal is *pre-processed* by a *precoder*.

Similar to receivers, precoders aim to invert the channel impact on the information data: It is desired to construct a transmit waveform, based on users' data and the side information, such that the receive signal at each user terminal estimates the corresponding data symbol without any further data processing. Since the channel impact is modeled linearly in MIMO communications, this task reduces to linear regression. In fact, by defining channel vectors from the base station to users as the regressors and data symbols as the regressands, precoding is interpreted as the problem of finding the regression coefficients for this linear model.

The viewpoint based on linear regression provides us with a variety of new tools for precoding. In fact, regression methods available in the literature, including RLS, can be employed to perform the channel inversion task, while imposing further constraints on the transmit waveform. In this respect, we propose a generic class of precoders based on RLS. The proposed precoder finds the optimal waveform, in terms of RSS, subject to an arbitrary set of constraints at the transmit side. This novel scheme enables us to address *jointly* multiple pre-processing tasks at the precoding stage. Using this class of precoders, we are able to perform channel inversion along with several other tasks, such as antenna selection, transmit power control, peak-to-average

power ratio (PAPR) restriction and mapping to discrete constellations, simultaneously at the precoder. Invoking our asymptotic results on RLS, we study performance of the proposed class of precoders for massive MIMO settings. The precoding scheme is compared against state of the art. Our analytic investigations, confirmed by numerical simulations, demonstrate significant enhancement provided by this RLS-based scheme. The contributions in this regard are given in details in Chapter 7.

The contributions of this thesis have been partially published in the form of conference and journal papers: Some parts of the contributions discussed in Section 1.4.1 have been presented in [A1, A2]. The contributions of Section 1.4.2 are published in parts in [A1, A3]. The applications of the results to sparse recovery, i.e., contributions illustrated in Section 1.4.3, have been discussed partially in [A1, A2, A4]. The RLS-based precoding scheme and some of its applications, i.e., contributions illustrated in Section 1.4.4, have been published [A5–A9]. In addition to the contributions presented in this manuscript, some related topics have been studied whose results are published in [A4, A10–A29].

1.5 Outline of Dissertation

The remaining parts of this dissertation are given in the following order: In Chapter 2, we state the standard formulation for linear regression and illustrate the stochastic models for problem components. The generic RLS method for addressing this problem is further stated, and its well-known forms and interpretations are illustrated. To quantify discussions on performance of the regression method, various performance metrics are defined for the generic RLS method in this chapter.

We illustrate our statistical mechanical approach for asymptotic analysis in Chapter 3. To this end, the so-called *corresponding spin glass* is defined. We show that there is an analogy between this imaginary thermodynamic system and the RLS method. The analysis approach based on the replica method is then presented to characterize the asymptotic behavior of this identical object. For sake of comprehensiveness, a brief introduction to thermodynamic systems, spin glasses and their large-system characterization is given at the beginning of this chapter.

The asymptotic characterization derived by the replica method is stated in Chapter 4. The basic result is of a generic form and does not impose any pre-defined structure on the saddle-point solution. We hence refer to this result as the *replica ansatz* which contains all possible ansätze. The characterizations under *replica symmetry* and *replica symmetry breaking* are then derived from this general ansatz. For consistency check, we further determine the zero-temperature entropy for these results. For sake of simplicity, we skip the detailed derivations in this chapter and present them in the appendices. Using the replica ansatz, we demonstrates the generic form of the decoupling principle in Chapter 5. The decoupled setting is derived under replica symmetry and replica symmetry breaking. The concept of *replica simulator* is then illustrated by means of the decoupling property.

To name few applications of our investigations, we consider two applied problems, namely *sparse recovery* from signal processing literature and *MIMO precoding* in multiuser communications. The former problem is studied in Chapter 6, where we derive the asymptotic performance of various sparse recovery algorithms. The problem of MIMO precoding is then investigated in Chapter 7. In this respect, we design an RLS-based scheme for precoding and characterize its performance using our earlier derivations. We finally give some conclusions and illustrate some directions for future work in Chapter 8.

In general, the chapters of this manuscript are sorted in a consecutive order. This means that the discussions in each chapter utilize multiple results and statements from previous chapters. This sequential structure is more substantial in Chapters 2-5, where the derivations and main results are given. The last two chapters, i.e., Chapters 6 and 7, which give some applications of the results, are presented in a more self-contained form. Nevertheless, the detailed derivations in these chapters still require some knowledge from Chapters 4 and 5. Since Chapters 3-7 contain contributions, their respective literature is reviewed in a separate section titled as "Bibliographical Notes". This section enlightens the contributions in these chapters.

The roadmap of this dissertation is shown in Figure 1.1. In this figure, those parts which contain contributions are denoted by an arrow ($\leftarrow$) on the right side. The detailed contents of Chapters 6 and 7 are demonstrated in Figure 1.2.

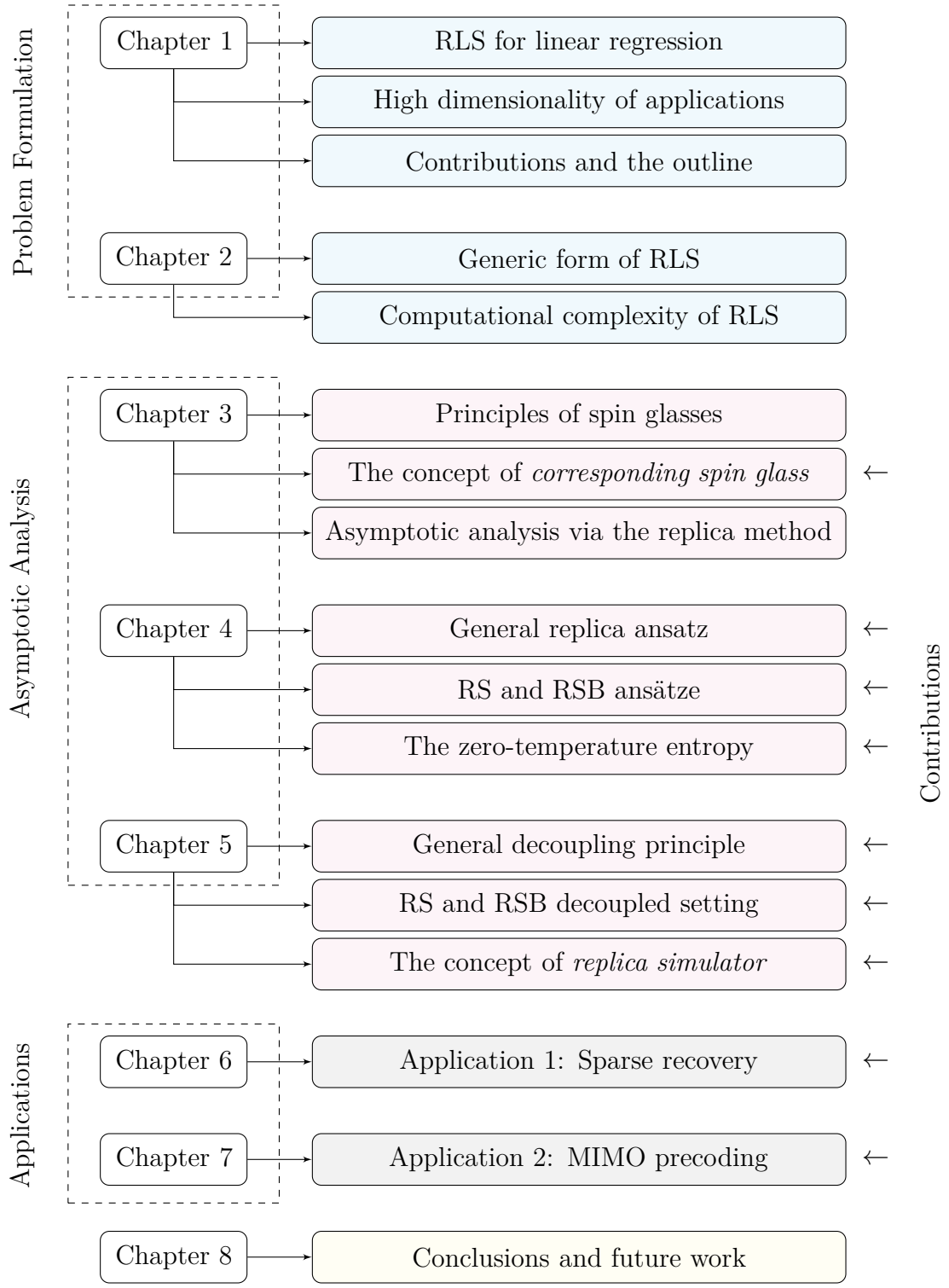

Figure 1.1: Roadmap of the dissertation.

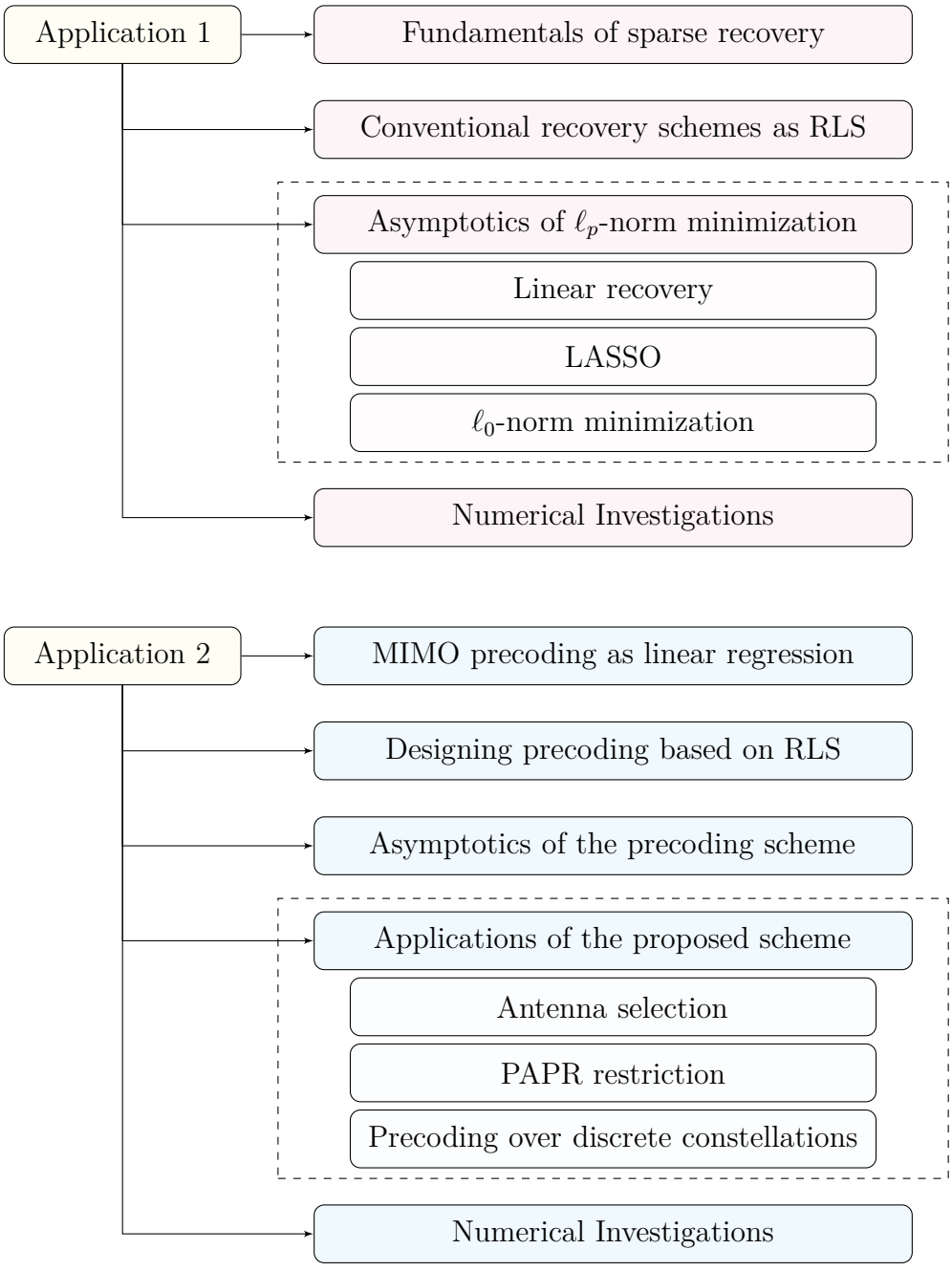

Figure 1.2: Details on the applications studied in Chapters 6 and 7.

1.6 Notations and Abbreviations

Throughout this manuscript, scalars, vectors, matrices and sets are represented with lower, bold lower, bold upper and blackboard upper case letters, respectively. $\mathbb{N}$ and $\mathbb{Z}$ are the set of natural and integer numbers, respectively. $\mathbb{R}$ denotes the real axis, and $\mathbb{C}$ represents the complex plane. For sake of compactness, the set of integers $\{i, \ldots, j\}$ for $i \leq j$ is shortened as $[i : j]$. We further simplify $[1 : j]$ by dropping the lower bound, i.e., $[1 : j]$ is denoted by $[j]$.

For a random variable x, $\mathrm{p}_x(\cdot)$ represents either the probability mass function (PMF) or probability density function (PDF), depending on the support of the variable. $\mathrm{F}_x(\cdot)$ further represents the cumulative distribution function (CDF) of x. Gaussian averaging is shown by

$$\int (\cdot)\, \mathrm{D}^{\zeta} z \coloneqq \int_{\mathbb{A}_\zeta} (\cdot)\, \phi^{\zeta}(z)\, \mathrm{d}z \tag{1.10}$$

where $\mathbb{A}_\zeta$ denotes the real axis and the complex plane for $\zeta = 1$ and $\zeta = 2$, respectively, and $\phi^{\zeta}(\cdot)$ represents the zero-mean and unit-variance Gaussian distribution over $\mathbb{A}_\zeta$. For sake of compactness, in some cases, for variables with known supports, we shorten the notations for sums, minimizations or integrals by dropping the support. For instance, knowing in advance that $x \in \mathbb{X}$, we shorten $\min_{x \in \mathbb{X}}$ by $\min_x$.

The complete list of abbreviations, operators and symbols is given at the end of this manuscript in the Glossary.

Chapter 2

RLS with Generic Regularization

The linear regression model can be compactly represented by

$$\boldsymbol{y} = \mathbf{A}\boldsymbol{x} + \boldsymbol{z}, \tag{2.1}$$

where

(a) $\boldsymbol{y}$ is an M vector enclosing the regressands.

(b) $\mathbf{A}$ is an $M \times N$ matrix containing all the M available regressors, i.e.

$$\mathbf{A} \coloneqq \begin{bmatrix} \mathbf{a}_1^{\mathsf{T}} \\ \vdots \\ \mathbf{a}_M^{\mathsf{T}} \end{bmatrix}. \tag{2.2}$$

(c) $\boldsymbol{x}$ is the N vector of regression coefficients.

(d) $\boldsymbol{z}$ is an M vector representing regression error.

Depending on the application, regressors contain either real or complex entries. Hence, we consider a general model and assume that the entries of $\mathbf{A}$ are drawn from $\mathbb{A}_\zeta$ with $\zeta \in \{1, 2\}$, where $\mathbb{A}_1 = \mathbb{R}$ and $\mathbb{A}_2 = \mathbb{C}$. As a result, $\mathbf{A} \in \mathbb{A}_\zeta^{M \times N}$ and the vectors of regressands and regression error read $\boldsymbol{y}, \boldsymbol{z} \in \mathbb{A}_\zeta^M$. The regression coefficients are moreover assumed to take values from an arbitrary set $\mathbb{X} \subseteq \mathbb{A}_\zeta$; thus, $\boldsymbol{x} \in \mathbb{X}^N$.

The regression problem is stochastic meaning that the regressors are randomly drawn from some ensemble. The regressands are hence random as well and statistically depend on the regressors. The ensemble, from which the regressors are drawn, can vary for different problems. We clarify this statement by giving the following example.

Example 2.1. *Consider the signal recovery problem, where a set of samples are to be recovered from some given linear projections of them. In this problem, regressors are the projection vectors which depend on the sensing procedure. Since sensing conditions change from an experiment to another, the projection vectors are modeled as random vectors. Nevertheless, prior knowledge on the sensing technique could restrict the ensemble from which these random projections are drawn. For instance, knowing that the linear projections are orthogonal to each other, one can conclude that* $\mathbf{A}$ *is taken from the set of row-orthogonal matrices, and hence, a matrix with two linearly dependent rows is never realized.*

In order to cover a wide scope of applications, we consider the large class of *unitarily invariant* ensembles for the regressors. In particular, we assume that $\mathbf{A}$ is randomly generated over $\mathbb{A}_{\zeta}^{M\times N}$, such that its Gramian, i.e., $\mathbf{J} = \mathbf{A}^{\mathsf{H}}\mathbf{A}$, has eigendecomposition

$$\mathbf{J} = \mathbf{U}\mathbf{D}\mathbf{U}^{\mathsf{H}} \tag{2.3}$$

with $\mathbf{D} \in \mathbb{R}^{N\times N}$ being diagonal and $\mathbf{U} \in \mathbb{A}_{\zeta}^{N\times N}$ being a so-called *Haar distributed* matrix. By a Haar distributed matrix, we refer to a random matrix which is uniformly distributed over $\mathbb{O}_N^{\zeta}$. Here, $\mathbb{O}_N^{\zeta}$ denotes the orthogonal group $\mathbb{O}_N$, and the unitary group $\mathbb{U}_N$ for $\zeta = 1$ and $\zeta = 2$, respectively. The diagonal entries of $\mathbf{D}$ are the squared singular values of $\mathbf{A}$. For a given N, we denote the empirical CDF of $\mathbf{D}$'s diagonal entries, i.e. cumulative density of states, with $\mathrm{F}_{\mathbf{J}}^{N}$ and define it as

$$\mathrm{F}_{\mathbf{J}}^{N}(\lambda) = \frac{1}{N}\sum_{n=1}^{N} \mathbf{1}\{\lambda_n^{\mathbf{J}} < \lambda\}. \tag{2.4}$$

where $\lambda_n^{\mathbf{J}}$ for $n \in [N]$ denotes the n-th diagonal entry of $\mathbf{D}$. As $N \uparrow \infty$, it is assumed that $\mathrm{F}_{\mathbf{J}}^N$ converges to a deterministic CDF $\mathrm{F}_{\mathbf{J}}$, i.e. for all $\lambda \in \mathbb{R}^+$

$$\lim_{N \uparrow \infty} \mathrm{F}_{\mathbf{J}}^N(\lambda) = \mathrm{F}_{\mathbf{J}}(\lambda). \tag{2.5}$$

The class of unitarily invariant matrices encloses various well-known models, considered for regressors in different literatures. Some few examples are as follows:

(a) *Random independent and identically distributed (i.i.d.)* model in which regressors are assumed to contain i.i.d. random variables. An example is the Rayleigh fading model for wireless channels which assumes the channel coefficients to be i.i.d. zero-mean Gaussian. Another example is the random sensing technique in signal processing, where signal samples are measured via i.i.d. linear projections.

(b) Linear regression with *row-orthogonal* regressors is another example, where the regressors are assumed to be orthogonal to each other. This model appears in several applications including the problem of signal recovery from orthogonal measurements.

2.1 Statement of the Problem

In linear regression, we are provided with a realization of $\mathbf{A}$ and $\boldsymbol{y}$. The main objective is to learn the coefficients in $\boldsymbol{x}$ from these given realizations. Another point of view is to interpret linear regression as an inference problem. By the regression model in (2.1), we assume that $\boldsymbol{y}$ is a linear combination of the regressors impaired with additive noise. In other words, there exist specific vectors $\boldsymbol{x}_0$ and $\boldsymbol{z}$, such that relate $\mathbf{A}$ to $\boldsymbol{y}$ as

$$\boldsymbol{y} = \mathbf{A}\boldsymbol{x}_0 + \boldsymbol{z}. \tag{2.6}$$

In this case, the task of learning $\boldsymbol{x}$ is mathematically equivalent to estimating $\boldsymbol{x}_0$ from $\boldsymbol{y}$, when $\mathbf{A}$ is given. We refer to $\boldsymbol{x}_0$ as the vector of *true regression coefficients*. In some applications, $\boldsymbol{x}_0$ has a physical meaning. For instance, in the problem of

signal recovery, $\boldsymbol{x}_0$ denotes true signal samples needed to be recovered from the measurements. There are however several other applications in which true coefficients do not really exist and represent only a visualization of the linear regression model. An example of such problems appears in machine learning, where a possibly nonlinear function is to be learned via a linear model.

2.1.1 Stochastic Model of Regression Error

Considering the inference viewpoint, the unknown vectors $\boldsymbol{x}_0$ and $\boldsymbol{z}$ are modeled as random vectors whose distributions are given based on the prior information. Regarding the error term $\boldsymbol{z}$, the conventional approach is to model it as a random Gaussian vector. This model follows the fact that there exists typically no prior information on the error term. For some particular examples of the linear regression model, e.g. additive white Gaussian noise (AWGN) channels, this assumed distribution can be further justified by invoking physical meaning of the error. We assume that $\boldsymbol{z} \sim \mathcal{N}^{\zeta}\left(\mathbf{0}, \sigma^2\mathbf{I}_M\right)$ for some non-negative real scalar σ, where

$$\mathcal{N}^{\zeta}\left(\mathbf{0}, \sigma^2\mathbf{I}_M\right) = \begin{cases} \mathcal{N}\left(\mathbf{0}, \sigma^2\mathbf{I}_M\right) & \zeta = 1 \\ \mathcal{CN}\left(\mathbf{0}, \sigma^2\mathbf{I}_M\right) & \zeta = 2 \end{cases}. \tag{2.7}$$

As a result, the PDF of $\boldsymbol{z}$ reads

$$\mathrm{p}_{\boldsymbol{z}}\left(\boldsymbol{z}\right) = \left(\frac{\zeta}{2\pi\sigma^2}\right)^{\frac{\zeta}{2}M} \exp\left\{-\frac{\zeta}{2\sigma^2}\|\boldsymbol{z}\|^2\right\}. \tag{2.8}$$

Due to the nature of error occurring independently, $\boldsymbol{z}$ is further assumed to be independent of regression coefficients and regressors.

2.1.2 Stochastic Model of True Coefficients

Postulations on the distribution of true coefficients depends on the application and vary from one to another. For those applications of linear regression, in which true coefficients really exist, the distribution is postulated based on the prior information

provided on $\boldsymbol{x}_0$. For instance, in signal recovery problem, the distribution is given by statistics of the true signal. In the sequel, we assume that the entries of $\boldsymbol{x}_0$ are i.i.d. according to a generic distribution. Namely, we assume that

$$\mathrm{p}_{\boldsymbol{x}_0}(\boldsymbol{x}_0) = \prod_{n=1}^{N} \mathrm{p}_0(x_{0n}). \tag{2.9}$$

Postulating a distribution for true coefficients is often required when $\boldsymbol{x}_0$ has a physical meaning. In this respect, the model in (2.9) imposes the following two assumptions:

(a) The true coefficients are independent: For a large scope of applications, this is a reasonable assumption. For instance, in signal recovery, this means that the temporal correlation among the samples is negligible. By proper sampling and preprocessing techniques, such a criteria often holds in practice.

(b) The true coefficients exhibit identical statistical behavior: For several applications, this assumption holds. However, there are some particular problems in which it is not realistic. An example of such applications is recovery of sparse signals with time-variant sparsity. In this problem, signal samples are grouped into multiple blocks, with each having a different sparsity factor.

As illustrated in Part (b), the main restriction imposed by the considered postulated distribution, is the assumption of identical statistics for all the true coefficients. This issue can be straightforwardly addressed by modifying the postulated distribution as

$$\mathrm{p}_{\boldsymbol{x}_0}(\boldsymbol{x}_0) = \prod_{b=1}^{B} \prod_{n \in \mathbb{N}_b} \mathrm{p}_b(x_{0n}) \tag{2.10}$$

with some probability distributions $\mathrm{p}_b(\cdot)$ for $b \in [B]$ and some $\{\mathbb{N}_1, \ldots, \mathbb{N}_B\}$ being a partition of $[N]$. By this modification, we assume that true coefficients are grouped into B blocks, such that in each block the coefficients have identical distribution. The distributions of coefficients from different blocks is however different.

In the sequel, we consider the i.i.d. model in (2.9). The extension of derivations to (2.10) is a straightforward task. It is further assumed that the true regression

coefficients are statistically independent of the regressors. This means that $\mathbf{A}$ and $\boldsymbol{x}_0$ are generated at random independently.

2.2 General Form of RLS

For a given matrix or regressors $\mathbf{A} \in \mathbb{A}_{\zeta}^{M\times N}$, the generic RLS method with regularization term $u_{\mathrm{v}}(\cdot) : \mathbb{X}^N \mapsto \mathbb{R}$ and tuning factor $\lambda \in \mathbb{R}$ determines the regression coefficients from the regressands in $\boldsymbol{y}$ as

$$\boldsymbol{x} = \mathbf{g}_{\mathsf{RLS}}(\boldsymbol{y}|\mathbf{A}) = \underset{\boldsymbol{v}\in\mathbb{X}^N}{\operatorname{argmin}} \ \frac{\zeta}{2\lambda}\left\|\boldsymbol{y}-\mathbf{A}\boldsymbol{v}\right\|^2 + u_{\mathrm{v}}(\boldsymbol{v}). \tag{2.11}$$

The generic RLS method in (2.11) learns the regression coefficients by minimizing the RSS term

$$\Delta(\boldsymbol{v}|\mathbf{A},\boldsymbol{y}) = \left\|\boldsymbol{y}-\mathbf{A}\boldsymbol{v}\right\|^2 \tag{2.12}$$

regularized with respect to $u_{\mathrm{v}}(\cdot)$ over $\mathbb{X}^N$. The regularization term is supposed to decouple. This means that there exists a function $u(\cdot) : \mathbb{X} \mapsto \mathbb{R}$, such that

$$u_{\mathrm{v}}(\boldsymbol{v}) = \sum_{n=1}^{N} u(v_n). \tag{2.13}$$

In a Bayesian framework, RLS can be interpreted as a MAP estimator which maximizes the posterior distribution for some postulated prior distribution on the regression coefficient. We illustrate this viewpoint further in the sequel.

2.2.1 Bayesian Interpretation of RLS

The RLS method in (2.11) can be considered as the optimal estimator in the sense that it minimizes the probability of recovery error. To clarify this viewpoint, consider a case in which true regression coefficients $\boldsymbol{x}_0$ have a physical meaning. In this case, the problem of linear regression is equivalent to recovery of true coefficients $\boldsymbol{x}_0$. Assume

that $\mathbb{X}$ is a finite set[1]. For a given regression method[2] $\mathbf{g}(\boldsymbol{y}|\mathbf{A})$, which recovers $\boldsymbol{x}$ from observations in $\boldsymbol{y}$ for known $\mathbf{A}$, we can define the probability of erroneous recovery as

$$P_{\mathrm{e}} = \Pr\{\boldsymbol{x} \neq \boldsymbol{x}_0\} \tag{2.14a}$$

$$= \Pr\{\boldsymbol{x} \neq \mathbf{g}(\boldsymbol{y}|\mathbf{A})\}. \tag{2.14b}$$

To minimize the error probability, $\mathbf{g}(\cdot|\mathbf{A})$ should be chosen such that the posterior distribution $\mathrm{p}_{\boldsymbol{x}_0}(\boldsymbol{v}|\boldsymbol{y}, \mathbf{A})$ over the support $\mathbb{X}^N$ is maximized, i.e.

$$\mathbf{g}^{\star}(\boldsymbol{y}|\mathbf{A}) = \underset{\boldsymbol{v}\in\mathbb{X}^N}{\operatorname{argmax}}\ \mathrm{p}_{\boldsymbol{x}_0}(\boldsymbol{v}|\boldsymbol{y}, \mathbf{A}) \tag{2.15a}$$

$$= \underset{\boldsymbol{v}\in\mathbb{X}^N}{\operatorname{argmax}}\ \mathrm{p}_{\boldsymbol{y}}(\boldsymbol{y}|\boldsymbol{v}, \mathbf{A})\mathrm{p}_{\boldsymbol{x}_0}(\boldsymbol{v}|\mathbf{A}) \tag{2.15b}$$

$$\overset{\star}{=} \underset{\boldsymbol{v}\in\mathbb{X}^N}{\operatorname{argmin}}\ \left[-\log \mathrm{p}_{\boldsymbol{y}}(\boldsymbol{y}|\boldsymbol{v}, \mathbf{A}) - \log \mathrm{p}_{\boldsymbol{x}_0}(\boldsymbol{v})\right]. \tag{2.15c}$$

where $\star$ comes from the independency of $\boldsymbol{x}_0$ and $\mathbf{A}$. The linearity of the regression model indicates that

$$\mathrm{p}_{\boldsymbol{y}}(\boldsymbol{y}|\boldsymbol{v}, \mathbf{A}) = \mathrm{p}_{\boldsymbol{z}}(\boldsymbol{y} - \mathbf{A}\boldsymbol{v}) \tag{2.16}$$

with $\mathrm{p}_{\boldsymbol{z}}(\cdot)$ given in (2.8). $\mathrm{p}_{\boldsymbol{x}_0}(\cdot)$ is moreover the distribution postulated for the true regression coefficient. Let us postulate that the noise variance is $\sigma^2 = \lambda$ and

$$\mathrm{p}_{\boldsymbol{x}_0}(\boldsymbol{v}) = \frac{\exp\{-u_{\mathrm{v}}(\boldsymbol{v})\}}{\sum_{\boldsymbol{v}\in\mathbb{X}^N} \exp\{-u_{\mathrm{v}}(\boldsymbol{v})\}} \tag{2.17}$$

Substituting the postulated variance and distribution into (2.15c), the optimal regression method $\mathbf{g}^{\star}(\boldsymbol{y}|\mathbf{A})$ reduces to $\mathbf{g}_{\mathsf{RLS}}(\boldsymbol{y}|\mathbf{A})$ defined in (2.11). In other words, the generic RLS method is equivalent to the optimal Bayesian recovery algorithm, in terms of the recovery error, for a linear regression method whose noise variance is equal to

[1] This means that the true coefficient are discrete random variables.
[2] A regression method in this context is equivalent to a recovery algorithm.

the tuning factor and the coefficients are postulated to be distributed proportional to $\exp\{-u_{\mathrm{v}}(\boldsymbol{x}_0)\}$.

Remark 2.1. Considering cases in which support $\mathbb{X}$ is continuous, the above argument needs some modifications. In fact, in these cases, the probability of erroneous recovery, as defined in (2.14b), is always $P_{\mathrm{e}} = 1$. Hence, it cannot be considered as a measure with respect to which the performance is optimized. Consequently, the RLS method in these cases is interpreted as a regression method which maximizes the posterior distribution postulating $\mathrm{p}_{\boldsymbol{x}_0}(\boldsymbol{v}) \propto \exp\{-u_{\mathrm{v}}(\boldsymbol{v})\}$ and noise variance $\sigma^2 = \lambda$.

2.3 Known Special Forms

The generic form of RLS recovers multiple known regression methods in the literature. Particular examples are Tikhonov regularization and LASSO. In the sequel, we shortly discuss some of these well-known forms.

2.3.1 Tikhonov Regularization

Tikhonov regularization, which is also known as linear regularization, is a well-known RLS approach to find $\boldsymbol{x}$ in

$$\boldsymbol{y} = \mathbf{A}\boldsymbol{x} \tag{2.18}$$

over $\mathbb{X}^N$ when the problem is *ill-posed*. This means that the system of linear equations is either overdetermined, i.e. $M > N$, or underdetermined, i.e. $M < N$. In this approach, the solution is found by regularizing the RSS $\Delta(\boldsymbol{v}|\mathbf{A}, \boldsymbol{y})$ with

$$f_{\boldsymbol{\Gamma}}(\boldsymbol{v}) = \|\boldsymbol{\Gamma}\boldsymbol{v}\|^2 \tag{2.19}$$

for some $\boldsymbol{\Gamma} \in \mathbb{A}_{\zeta}^{N\times N}$ referred to as Tikhonov matrix. For $\mathbb{X} = \mathbb{A}_{\zeta}$, Tikhonov regularization reduces to a linear projection, i.e.

$$\boldsymbol{x} = \underset{\boldsymbol{v}\in\mathbb{A}_{\zeta}^{N}}{\operatorname{argmin}} \ \|\boldsymbol{y} - \mathbf{A}\boldsymbol{v}\|^2 + \|\boldsymbol{\Gamma}\boldsymbol{v}\|^2 \tag{2.20a}$$

$$= \left(\mathbf{A}^{\mathsf{H}}\mathbf{A} + \mathbf{\Gamma}^{\mathsf{H}}\mathbf{\Gamma}\right)^{-1} \mathbf{A}^{\mathsf{H}}\boldsymbol{y}, \tag{2.20b}$$

if $\det\left|\mathbf{A}^{\mathsf{H}}\mathbf{A} + \mathbf{\Gamma}^{\mathsf{H}}\mathbf{\Gamma}\right| \neq 0$.

Considering a general support $\mathbb{X}$ and an invertible $\mathbf{\Gamma}$, Tikhonov regularization is addressed by the generic RLS method, when $\mathbb{X}^N$ has closure under linear projection[3] $\mathbf{\Gamma}$. To show this, let us define the vector

$$\breve{\boldsymbol{v}} \coloneqq \mathbf{\Gamma}\boldsymbol{v}. \tag{2.21}$$

Due to closure of $\mathbb{X}^N$ under $\mathbf{\Gamma}$, we have $\breve{\boldsymbol{v}} \in \mathbb{X}^N$. Moreover, as $\mathbf{\Gamma}$ is invertible, any $\boldsymbol{v} \in \mathbb{X}^N$ can be recovered from its corresponding projection $\breve{\boldsymbol{v}}$ by $\mathbf{\Gamma}^{-1}$. Hence, the solution Tikhonov regularization reads $\boldsymbol{x} = \mathbf{\Gamma}^{-1}\breve{\boldsymbol{x}}$ where

$$\breve{\boldsymbol{x}} \coloneqq \underset{\breve{\boldsymbol{v}} \in \mathbb{X}^N}{\operatorname{argmin}} \quad \left\|\boldsymbol{y} - \mathbf{A}\mathbf{\Gamma}^{-1}\breve{\boldsymbol{v}}\right\|^2 + \left\|\breve{\boldsymbol{v}}\right\|^2. \tag{2.22}$$

$\breve{\boldsymbol{x}}$ is derived by a special form of the generic RLS method represented in Section 2.2. In fact, by defining $\breve{\mathbf{A}} \coloneqq \mathbf{A}\mathbf{\Gamma}^{-1}$, we can write

$$\breve{\boldsymbol{x}} = \mathbf{g}_{\mathsf{RLS}}\left(\boldsymbol{y}|\breve{\mathbf{A}}\right) \tag{2.23}$$

for $\lambda = \zeta/2$ and $u\left(v_n\right) = \left|v_n\right|^2$.

2.3.2 ℓ_p-norm Minimization

ℓ_p-norm minimization is an approach for signal recovery and feature selection. In this algorithm, the regression coefficients are learned by minimizing the LS term penalized by the ℓ_p-norm of the coefficients, for some p. This means that $\boldsymbol{x}$ is determined by

$$\boldsymbol{x} = \underset{\boldsymbol{v} \in \mathbb{X}^N}{\operatorname{argmin}} \quad \frac{\zeta}{2\lambda}\left\|\boldsymbol{y} - \mathbf{A}\boldsymbol{v}\right\|^2 + \left\|\boldsymbol{v}\right\|_p^p \tag{2.24}$$

[3] This means that for any $\boldsymbol{v} \in \mathbb{X}^N$, $\mathbf{\Gamma}\boldsymbol{v} \in \mathbb{X}^N$.

for some $\lambda \in \mathbb{R}$, where $\|\boldsymbol{v}\|_p$ denotes the ℓ_p-norm of $\boldsymbol{v}$ and is defined as

$$\|\boldsymbol{v}\|_p \coloneqq \left(\sum_{n=1}^{N} |v_n|^p\right)^{\frac{1}{p}} . \tag{2.25}$$

Although the definition of ℓ_p-norm requires $p \geq 1$, the generalized ℓ_p-norm minimization technique considers $p > 0$. For $0 < p < 1$, the regularization term is not convex, and hence the optimization problem is not posed by convex programming even for convex choices of $\mathbb{X}$.

For some particular choices of p, ℓ_p-norm minimization is well studied. For instance, by setting $p = 2$, this technique recovers Tikhonov regularization for Tikhonov matrix

$$\boldsymbol{\Gamma} = \sqrt{\frac{\zeta}{2\lambda}}\, \mathbf{I}_N . \tag{2.26}$$

For $p = 1$, moreover, it reduces to LASSO which is an efficient approach for joint RSS minimization and variable selection. The extreme case of ℓ_p-norm minimization is given by setting $p = 0$. In this case, the ℓ_0-norm is a singular function defined as

$$\|\boldsymbol{v}\|_0 \coloneqq \sum_{n=1}^{N} \mathbf{1}\{v_n \neq 0\} \tag{2.27}$$

which determines the number of non-zero entries in $\boldsymbol{v}$. The ℓ_0-norm minimization is often referred to as the optimal RLS method for sparse recovery, since it concludes the primitive algorithm for reconstructing a sparse signal from its linear and noise-free underdetermined measurements.

From the definition, one observes that the generalized ℓ_p-norm minimization technique is a special form of the generic RLS method represented in Section 2.2. In fact, for any $p > 0$, ℓ_p-norm minimization is an RLS method with $u(v_n) = |v_n|^p$. For the case of $p = 0$, the regularization term reads $u(v_n) = \mathbf{1}\{v_n \neq 0\}$.

2.4 Performance Analysis

To quantify the performance, we need to define a metric which measures the performance of a given regression method. For the linear regression model, a classic metric is the posterior RSS, often called as the *least squares error (LSE)*.

Definition 2.1 (LSE)**.** *For method* $\mathbf{g}(\boldsymbol{y}|\mathbf{A})$ *which learns regression coefficients in* $\boldsymbol{x}$ *from the regressands in* $\boldsymbol{y}$ *and regressors in* $\mathbf{A}$*, i.e.* $\boldsymbol{x} = \mathbf{g}(\boldsymbol{y}|\mathbf{A})$*, the LSE is*

$$\mathrm{LSE}_N\{\mathbf{g}\} = \frac{1}{M}\mathbb{E}\left\{\|\boldsymbol{y} - \mathbf{A}\boldsymbol{x}\|^2\right\} = \frac{1}{M}\mathbb{E}\left\{\Delta(\boldsymbol{x}|\mathbf{A}, \boldsymbol{y})\right\} \tag{2.28}$$

where $\Delta(\cdot|\mathbf{A}, \boldsymbol{y})$*, given in* (2.12)*, determines the RSS of the linear regression model for a given choice of regression coefficients, and subscript* N *indicates the data dimension in the problem, i.e. the number of regression coefficients.*

The physical meaning of the LSE can be understood in two different ways:

- One viewpoint for interpreting the LSE is based on learning problems: Assume that an unknown function $f(\cdot)$ is desired to be learned from a set of observations $\{y, \ldots, y_M\}$ collected in $\boldsymbol{y}$ which correspond to the arguments $\{\mathbf{a}_1, \ldots, \mathbf{a}_M\}$ being the rows of matrix $\mathbf{A}$. Linear regression approximates $f(\mathbf{a})$ for a given argument $\mathbf{a} \in \mathbb{A}_\zeta^N$ with

$$\hat{f}(\mathbf{a}) = \sum_{n=1}^{N} x_n a_n = \mathbf{a}^\mathsf{T}\boldsymbol{x} \tag{2.29}$$

  where $\{x_1, \ldots, x_N\}$ are the regression coefficients determined via $\mathbf{g}(\boldsymbol{y}|\mathbf{A})$. Since the linear approximation is not necessarily exact, the outcome of learned function $\hat{f}(\cdot)$ at some arbitrary argument $\mathbf{a}^\star$ is different from the exact value of the function at this point, i.e., $y^\star = f(\mathbf{a}^\star)$. The average error of such approximation can hence be measured by determining the average Euclidean distance between approximated values $\hat{f}(\mathbf{a}_m)$ and the exact observations y_m for $m \in [M]$ for multiple realizations of $\boldsymbol{y}$ and $\mathbf{A}$. Denoting this measure by E, we have

$$\mathrm{E} = \frac{1}{M}\sum_{m=1}^{M}\mathbb{E}\left\{\left|y_m - \hat{f}(\mathbf{a}_m)\right|^2\right\} \tag{2.30a}$$

$$= \frac{1}{M}\, \mathbb{E}\left\{\|\boldsymbol{y} - \mathbf{A}\boldsymbol{x}\|^2\right\} = \mathrm{LSE}_N\left\{\mathbf{g}\right\}. \tag{2.30b}$$

Hence, the LSE represents average error caused by considering a linear model for a learning problem when the coefficients in this model are learned by $\mathbf{g}\left(\boldsymbol{y}|\mathbf{A}\right)$.

- Another way to interpret the LSE is to look at linear regression from inference points of view: Consider an estimation problem in which true regression coefficients have physical meaning, e.g. signal recovery. Let $\boldsymbol{x}_0$ contains the true coefficients. In this case, the LSE reads

$$\mathrm{LSE}_N\left\{\mathbf{g}\right\} = \frac{1}{M}\, \mathbb{E}\left\{\|\mathbf{A}\boldsymbol{x}_0 + \boldsymbol{z} - \mathbf{A}\boldsymbol{x}\|^2\right\} \tag{2.31}$$

$$= \frac{1}{M}\, \mathbb{E}\left\{\|\mathbf{A}\mathbf{e} + \boldsymbol{z}\|^2\right\} \tag{2.32}$$

where $\mathbf{e} \coloneqq \boldsymbol{x}_0 - \boldsymbol{x}$ quantifies the estimation error. From (2.32), one observes that the LSE in this case describes the estimation error when the algorithm $\mathbf{g}\left(\boldsymbol{y}|\mathbf{A}\right)$ is employed for recovery.

Considering either of the viewpoints, it is observed that the LSE is proportional to the error caused by using regression method $\mathbf{g}\left(\boldsymbol{y}|\mathbf{A}\right)$. However, in cases, in which true regression coefficients have physical meaning, the LSE is not directly quantifying the error; see (2.32). For these cases, the error can be further characterized by defining the metric *average distortion*. To this end, let us consider a general *distortion function* $\mathsf{d}\left(\cdot;\cdot\right)$ which determines the imperfection level between two variables x_0 and x in support $\mathbb{X}$, i.e.

$$\mathsf{d}\left(\cdot;\cdot\right) : \mathbb{X} \times \mathbb{X} \to \mathbb{R}. \tag{2.33}$$

A common example of such a function is the ℓ_2-norm, i.e. $\mathsf{d}(x; x_0) = |x - x_0|^2$, which determines the Euclidean distance between the two symbols. The average distortion for a given regression method $\mathbf{g}\left(\boldsymbol{y}|\mathbf{A}\right)$ with respect to $\mathsf{d}\left(\cdot;\cdot\right)$ is then defined as follows.

Definition 2.2 (Average distortion)**.** *Consider regression method* $\mathbf{g}\left(\boldsymbol{y}|\mathbf{A}\right)$ *which determines the regression coefficients in* $\boldsymbol{x}$ *from the regressands in* $\boldsymbol{y}$ *and the regressors*

in $\mathbf{A}$*. Assume that there exist true regression coefficients for the problem collected in* $\boldsymbol{x}_0$ *and let* $\mathbb{W}(N) \subseteq [N]$ *be a subset of indices. Then, the average distortion with respect to* $\mathsf{d}(\cdot;\cdot)$ *over* $\mathbb{W}(N)$ *is*

$$D_N^{\mathbb{W}}\{\mathbf{g}\} \coloneqq \frac{1}{|\mathbb{W}(N)|} \sum_{w \in \mathbb{W}(N)} \mathbb{E}\{\mathsf{d}(x_w; x_{0w})\}. \tag{2.34}$$

Depending on $\mathsf{d}(\cdot;\cdot)$, the average distortion determines several performance measures defined in various applications. For instance, assume that $\mathbb{W}(N) = [N]$, meaning that the arithmetic average in (2.34) is taken over the whole coefficients. Then,

1. By setting $\mathsf{d}(x; x_0) = |x - x_0|^2$, the average distortion reads

$$D_N^{\mathbb{W}}\{\mathbf{g}\} \coloneqq \frac{1}{N}\mathbb{E}\left\{\|\boldsymbol{x} - \boldsymbol{x}_0\|^2\right\} = \mathrm{MSE} \tag{2.35}$$

   which is the mean squared error (MSE) given by regression method $\mathbf{g}(\boldsymbol{y}|\mathbf{A})$. This metric is widely used in communications and signal processing to quantify the performance of estimation or signal shaping algorithms.

2. For cases with discrete supports, i.e. $\mathbb{X}$ is a discrete set, the distortion function $\mathsf{d}(x; x_0) = \mathbf{1}\{x \neq x_0\}$ leads to

$$D_N^{\mathbb{W}}\{\mathbf{g}\} = \frac{1}{N}\sum_{n=1}^{N} \mathbb{E}\{\mathbf{1}\{x_n \neq x_{0n}\}\} \tag{2.36a}$$

$$= \frac{1}{N}\sum_{n=1}^{N} \Pr\{x_n \neq x_{0n}\} = \mathrm{SER} \tag{2.36b}$$

   which is the average symbol error rate (SER). This metric is widely utilized in communications to measure the performance of receivers.

Although the average distortion is mainly defined for problems in which true regression coefficients are physically meaningful, it can be further employed to characterize the statistics of regression coefficients in other problems. To clarify this statement, consider the following example.

Example 2.2. *Let* $\boldsymbol{x} = \mathbf{g}(\boldsymbol{y}|\mathbf{A})$ *for some regression method* $\mathbf{g}(\boldsymbol{y}|\mathbf{A})$*. Set* $\mathsf{d}(x; x_0) = x^u$ *and* $\mathbb{W}(N) = \{n\}$*, for some integers* u *and* $1 \leq n \leq N$*, and denote the corresponding average distortion by* $D(u) = D_N^{\mathbb{W}}\{\mathbf{g}\}$*.* $D(u)$ *determines the* u*-th moment of the* n*-th regression coefficient. In this case, the distribution of coefficient* x_n *can be described from sequence* $\{D(u) : u \in \mathbb{Z}\}$*, via the moments method.*

2.4.1 Asymptotic Performance

As discussed in Chapter 1, linear regression mostly addresses high dimensional applications, and hence its performance is desired to be analyzed in the asymptotic regime. As a result, we are interested in the limit performance measures, i.e., the LSE and average distortion, for the generic RLS method when the dimension grows large. To formulate this objective, we consider a sequence of linear regression problems with data dimension N and $M(N)$ regressands. We assume that $M(N)$ is a deterministic function of N, such that

$$\lim_{N\uparrow\infty} \frac{M(N)}{N} = \alpha. \tag{2.37}$$

We refer to α as the *load*. For sake of compactness, we drop the explicit dependence of M on N. In each of these problems, the regression coefficients are determined by a generic RLS method, defined in Section 2.2, for some given function $u(\cdot)$ and tuning factor λ. We denote the corresponding sequences of LSEs by $\{\mathrm{LSE}_N\{\mathbf{g}_{\mathsf{RLS}}\}\}$, and the sequence of average distortions with respect to some distortion function $\mathsf{d}(\cdot;\cdot)$ over a sequence $\{\mathbb{W}(N)\}$ by $\left\{D_N^{\mathbb{W}}\{\mathbf{g}_{\mathsf{RLS}}\}\right\}$.

The asymptotic performance of a given generic RLS method is characterized by taking the limit of the corresponding performance metrics, when the data dimension grows unboundedly large. In this respect, we define the *asymptotic LSE* as follows.

Definition 2.3 (Asymptotic LSE)**.** *The asymptotic LSE of a generic RLS method is given by the limit of its corresponding LSE sequence, when* N *grows large, i.e.*

$$\mathrm{LSE}_{\mathsf{RLS}} \coloneqq \lim_{N\uparrow\infty} \mathrm{LSE}_N\{\mathbf{g}_{\mathsf{RLS}}\}. \tag{2.38}$$

Considering the average distortion, another asymptotic metric of performance is the *asymptotic distortion* given by the following definition.

Definition 2.4 (Asymptotic distortion)**.** *Consider distortion function* $\mathsf{d}(\cdot;\cdot)$ *and sequence of index subsets* $\{\mathbb{W}(N)\}$*, such that*

$$\lim_{N\uparrow\infty} \frac{|\mathbb{W}(N)|}{N} = \eta \tag{2.39}$$

for some $\eta \in [0,1]$*. The asymptotic distortion of a generic RLS method is given by taking the limit of sequence* $\left\{D_N^{\mathbb{W}}\left\{\mathbf{g}_{\mathsf{RLS}}\right\}\right\}$*, when* N *tends to* ∞*, i.e.,*

$$D_{\mathsf{RLS}}^{\mathbb{W}} \coloneqq \lim_{N\uparrow\infty} D_N^{\mathbb{W}}\left\{\mathbf{g}_{\mathsf{RLS}}\right\}. \tag{2.40}$$

2.4.2 Analytic and Computational Tractability

The main objective of this dissertation is to derive the asymptotic LSE and distortion for RLS in its generic form. This task is however not straightforward from both analytical and computational points of view. To illustrate this point, consider the RLS method given in Section 2.2. Depending on the regularization term and support, the method might confront one or two of the following issues.

- *Analytic intractability:* For convex choices of $u(\cdot)$ and $\mathbb{X}$, the RLS method needs to solve a convex optimization problem. This is posed as a linear programming, and hence is solved in polynomial time for a given data dimension. This computational tractability however does not guarantee that the problem is also analytically tractable. In fact, for asymptotic analysis, one needs to determine the sequence of LSEs and average distortions for any integer data dimension[4], and then take the limit when N goes to ∞. For some particular choices of the regularization term and support, this task can be done via basic analytic tools, e.g. $u(v) = |v|^2$ and $\mathbb{X} = \mathbb{C}$. There are however several forms of the problem with polynomial time complexity, for which this analytic task is not tractable.

[4]Or at least for $N > N_0$ with N_0 being some bounded integer.

- *Computational intractability:* Several forms of the generic RLS method are not only analytically, but also computationally intractable, meaning that it is commonly believed to exist no algorithm which can determine the regression coefficients in polynomial time. An example is ℓ_0-norm minimization which reduces to a nondeterministic polynomial time (NP)-hard problem [14]. For such cases, the performance cannot even be investigated for large, but finite, dimensions via numerical simulations.

To address both the analytic and computational issues, we need to deviate from basic techniques for asymptotic analysis and invoke some alternative methods. In this dissertation, we take a statistical mechanical approach for analysis. In this respect, we introduce a thermodynamic system whose macroscopic investigation is isomorphic to the asymptotic analysis of generic RLS. Using the replica method, introduced in this literature for analysis of spin glasses, we characterize RLS in the asymptotic regime.

2.5 Summary

In this chapter, the stochastic model for linear regression has been presented. This model encloses a large class of applications, some of which are discussed later. The generic form of RLS method for linear regression has been formally introduced, and several well-known special forms have been discussed. The asymptotic performance of RLS has been characterized via the large-system limit of LSE and average distortion. The final section of this chapter has illustrated the analytic and computational intractability of the asymptotic analysis, and the need for more advanced analytic tools. In the next chapter, we invoke theory of spin glasses, developed in statistical mechanics, to characterize the generic RLS method in the asymptotic regime.

Chapter 3

Modeling RLS as a Spin Glass

Statistical mechanics deals with the analysis of *thermodynamic systems* which consist of enormously large number of particles. Examples are a bottle of liquid or a certain volume of a gas, which contain significantly large numbers of molecules. These particles have *microscopic* parameters, e.g., velocity or energy, which are mutually coupled through a gigantic system of equations. The main objective of statistical mechanics is to derive the *macroscopic* features of a given system, e.g., temperature or pressure, from the microscopic parameters of its particles. The direct approach is to calculate the microscopic parameters by solving the corresponding system of equations, and determine the features as a function of them. This approach is however intractable, due to the huge dimension of the problem. Statistical mechanics has hence developed several analytic tools to address this intractability issue.

The nature of intractability issues in statistical mechanics is similar to those appear in asymptotic analysis of RLS. As a result, the advanced analytical methods developed in the context of statistical mechanics can be employed to characterize the generic RLS method in the asymptotic regime. To this end, in this chapter, we demonstrate an isomorphism between an artificial thermodynamic system and linear regression with RLS. We refer to this system as the *corresponding spin glass* and show that asymptotic performance metrics of the generic RLS method are given as macroscopic features of the corresponding spin glass. The asymptotic characterization of the regression problem is hence followed by invoking analytic techniques from theory of spin glasses, namely the replica method.

3.1 Preliminaries

Consider a thermodynamic system which consists of N particles with each having a microscopic parameter $v_n \in \mathbb{V}$ for $n \in [N]$. For this system, the *microstate* is defined as follows.

Definition 3.1 (Microstate)**.** *For a thermodynamic system, the microstate is defined as a vector in $\mathbb{V}^N$ which collects microscopic parameters of all the particles, i.e.*

$$\boldsymbol{v} = [v_1, \ldots, v_N]^{\mathsf{T}}. \tag{3.1}$$

Physical characteristics of a thermodynamic system is described in an abstract form via its Hamiltonian. The Hamiltonian is a mapping from microstate ensemble $\mathbb{V}^N$ to the right hand side of the real axis, i.e.

$$\mathcal{E}(\cdot) : \mathbb{V}^N \mapsto \mathbb{R}_0^+. \tag{3.2}$$

This function assigns to each realization of the microstate a non-negative energy level. For a physical system, the exact form of the Hamiltonian is derived via the theories which relate the microscopic parameters in the system.

In statistical mechanics, the microscopic parameters are considered to be random. This stochastic model is taken due to the fact that deterministic derivations of these parameters are intractable. Consequently, the microstate is a random vector whose distribution depends on physical characteristics of the system. Statistical mechanics tries to mathematically formulate the physical features of the given thermodynamic system via this stochastic model. To this end, some basic macroscopic parameters are defined for a given system which are introduced in the following.

3.1.1 Basic Macroscopic Parameters

Macroscopic parameters of a thermodynamic system are those features which describe the overall characterizations of the system. An example of such parameters in physics is temperature. In thermodynamic, a system is mathematically characterized by two basic macroscopic parameters, namely the *entropy* and *free energy*.

Definition 3.2 (Normalized entropy)**.** *For a given thermodynamic system with N particles, the normalized average entropy per particle at inverse temperature β is defined as*

$$\mathcal{H}_N(\beta) \coloneqq -\frac{1}{N}\mathbb{E}_{\boldsymbol{v}}\left\{\log \mathrm{p}_\beta(\boldsymbol{v})\right\}, \tag{3.3}$$

where p_β denotes the distribution of microstate $\boldsymbol{v}$ at inverse temperature β.

The normalized free energy of a thermodynamic system is further defined as follows.

Definition 3.3 (Normalized free energy)**.** *Consider a thermodynamic system with N particles and Hamiltonian $\mathcal{E}(\cdot)$. At the inverse temperature β, the normalized free energy per particle is defined as*

$$\mathcal{F}_N(\beta) \coloneqq \frac{1}{N}\mathbb{E}_{\boldsymbol{v}}\left\{\mathcal{E}(\boldsymbol{v})\right\} - \frac{1}{\beta}\mathcal{H}_N(\beta) \tag{3.4}$$

where $\mathcal{H}_N(\beta)$ denotes the normalized entropy per particle at inverse temperature β.

3.1.2 Second Law of Thermodynamics

For a given thermodynamic system, the distribution of the microstate, when it is in thermal equilibrium[1], is determined via the second law of thermodynamics. Based on this law, the microstate in thermal equilibrium is distributed such that the normalized free energy is minimized[2]. Since $\mathcal{F}_N(\beta)$ is convex with respect to the distribution of microstate $\boldsymbol{v}$, it is concluded that at inverse temperature β, the microstate is distributed with

$$\mathrm{p}_\beta(\boldsymbol{v}) = \frac{\exp\left\{-\beta\mathcal{E}(\boldsymbol{v})\right\}}{\mathcal{Z}_N(\beta)} \tag{3.5}$$

[1] In a nutshell, this means that there is no energy flow.

[2] In general, the second law of thermodynamics states that the entropy in a system with no energy flow always increases. This statement is formulated as a constrained optimization problem. The free energy is then derived as the Lagrange function which adds the constraint imposed by conservation law of energy via a Lagrange multiplier. By standard derivations temperature turns out to be the corresponding multiplier.

where subscript β indicates dependency on the inverse temperature. $\mathcal{Z}_N(\beta)$ in the denominator is a normalization factor, i.e.,

$$\mathcal{Z}_N(\beta) = \sum_{\boldsymbol{v}\in\mathbb{V}^N} \exp\{-\beta\mathcal{E}(\boldsymbol{v})\} \tag{3.6}$$

for discrete ensembles and

$$\mathcal{Z}_N(\beta) = \int_{\mathbb{V}^N} \exp\{-\beta\mathcal{E}(\boldsymbol{v})\}\,\mathrm{d}\boldsymbol{v} \tag{3.7}$$

for a continuous microstate, which is referred to as the *partition function*. The subscript N in $\mathcal{Z}_N(\beta)$ indicates the number of particles over which this partition function is calculated. $\mathrm{p}_\beta(\boldsymbol{v})$ is known as the *Boltzmann-Gibbs distribution* and reduces to some well-known distributions for several choices of the Hamiltonian.

Substituting the Boltzmann-Gibbs distribution into Definition 3.3, the normalized free energy at inverse temperature β reads

$$\mathcal{F}_N(\beta) = -\frac{1}{\beta N}\log\mathcal{Z}_N(\beta) \tag{3.8}$$

which is explicitly determined in terms of the partition function. This is in fact a fundamental property indicating that the macroscopic behavior of a thermodynamic system, when it is in thermal equilibrium, is completely described via its partition function. This property is straightforwardly investigated by substituting the Boltzmann-Gibbs distribution into Definition 3.2. In this case, we have

$$\mathcal{H}_N(\beta) = -\frac{1}{N}\mathbb{E}_{\boldsymbol{v}}\{\log\mathrm{p}_\beta(\boldsymbol{v})\} \tag{3.9a}$$

$$= \frac{\beta}{N}\mathbb{E}_{\boldsymbol{v}}\{\mathcal{E}(\boldsymbol{v})\} + \frac{1}{N}\log\mathcal{Z}_N(\beta) \tag{3.9b}$$

$$= -\frac{\beta}{N}\frac{\mathrm{d}}{\mathrm{d}\beta}\log\mathcal{Z}_N(\beta) + \frac{1}{N}\log\mathcal{Z}_N(\beta) \tag{3.9c}$$

$$= -\frac{\beta^2}{N}\frac{\mathrm{d}}{\mathrm{d}\beta}\frac{\log\mathcal{Z}_N(\beta)}{\beta} \tag{3.9d}$$

$$= \beta^2 \frac{\mathrm{d}}{\mathrm{d}\beta} \mathcal{F}_N(\beta). \tag{3.9e}$$

As it is observed, the normalized entropy is analytically derived from the normalized free energy. Hence, a thermodynamic system is completely described in thermal equilibrium with its normalized free energy. As the normalized free energy is explicitly calculated from the partition function, one can conclude that the system is mathematically characterized via its partition function.

3.1.3 Spin Glasses

Spin glasses are randomized thermodynamic systems in which the Hamiltonian assigns energy levels to realizations of the microstate conditioned to the realization of some randomizer. Given a random object $\boldsymbol{\Omega}$ taken from ensemble $\mathbb{Q}$, the energy levels are specified by a set of Hamiltonian functions which read

$$\mathcal{E}(\cdot|\boldsymbol{\Omega}) : \mathbb{V}^N \mapsto \mathbb{R}^+ \tag{3.10}$$

for all realizations of $\boldsymbol{\Omega}$. From physical points of view, spin glasses are many-body structures whose particles choose to interact randomly: Each realization of $\boldsymbol{\Omega}$ specifies a thermodynamic system being described by Hamiltonian $\mathcal{E}(\cdot|\boldsymbol{\Omega})$. The particles of spin glasses choose $\boldsymbol{\Omega}$ at random and then interact based on $\mathcal{E}(\cdot|\boldsymbol{\Omega})$. Consequently, the order of randomness in randomizer $\boldsymbol{\Omega}$ and the microstate is different. In fact, $\boldsymbol{\Omega}$ is realized once and remains unchanged for a long time. In the context of statistical mechanics, $\boldsymbol{\Omega}$ is known to have *quenched* randomness while the microstate is an *annealed* random variable.

The characterization of spin glasses is analogous to thermodynamic systems by conditioning to the given realization of the quenched randomizer. Hence, given $\boldsymbol{\Omega}$, the microstate of a spin glass is conditionally distributed in thermal equilibrium at inverse temperature β via conditional Boltzmann-Gibbs distribution

$$\mathrm{p}_\beta(\boldsymbol{v}|\boldsymbol{\Omega}) = \frac{\exp\{-\beta\mathcal{E}(\boldsymbol{v}|\boldsymbol{\Omega})\}}{\mathcal{Z}_N(\beta|\boldsymbol{\Omega})} \tag{3.11}$$

with random partition function

$$\mathcal{Z}_N(\beta|\boldsymbol{\Omega}) = \sum_{\boldsymbol{v}\in\mathbb{V}^N} \exp\{-\beta\mathcal{E}(\boldsymbol{v}|\boldsymbol{\Omega})\} \tag{3.12}$$

for discrete microstate and

$$\mathcal{Z}_N(\beta|\boldsymbol{\Omega}) = \int_{\mathbb{V}^N} \exp\{-\beta\mathcal{E}(\boldsymbol{v}|\boldsymbol{\Omega})\}\,\mathrm{d}\boldsymbol{v} \tag{3.13}$$

when $\mathbb{V}$ is continuous. The normalized free energy in this case reads

$$\mathcal{F}_N(\beta|\boldsymbol{\Omega}) = -\frac{1}{\beta N}\log\mathcal{Z}_N(\beta|\boldsymbol{\Omega}) \tag{3.14}$$

and the normalized conditional entropy is determined from the normalized free energy by

$$\mathcal{H}_N(\beta|\boldsymbol{\Omega}) = \beta^2\frac{\mathrm{d}}{\mathrm{d}\beta}\mathcal{F}_N(\beta|\boldsymbol{\Omega}). \tag{3.15}$$

3.1.4 Analysis in the Thermodynamic Limit

To study thermodynamic systems, the normalized free energy[3] should be determined in a regime referred to as the *thermodynamic limit*. In this regime, the number of particles is considered to be significantly large. Since the normalized free energy is explicitly derived from the partition function, it is expected that the partition function in this regime converges to a deterministic function. For a thermodynamic system, the main analytic task, is to determine sequence of deterministic partition functions $\{\mathcal{Z}_N(\beta) : N \in \mathbb{N}\}$, and then take the limit

$$\mathcal{F}(\beta) = \lim_{N\uparrow\infty} -\frac{1}{\beta N}\log\mathcal{Z}_N(\beta) \tag{3.16}$$

where $\mathcal{F}(\beta)$ denotes the limiting normalized free energy.

[3]Note that other macroscopic features are derived from the normalized free energy; see (3.9e) and (3.15).

For spin glasses, more tasks are required. In fact, in this case, the partition function is random. Nevertheless, physical intuitions suggest that the structure shows some deterministic macroscopic features in the thermodynamic limit. This property of spin glasses is known as *self averaging*, meaning that in the asymptotic regime each realization of the system behaves closely to what its mathematical expected characteristics describe. For some forms of spin glasses, rigorous justification of this property has been discussed [15–18]. Based on the self-averaging property, the analysis of spin glasses in the thermodynamic limit confronts the following main analytic tasks

(a) Determining sequence of partition functions $\{\mathcal{Z}_N(\beta|\mathbf{\Omega}) : N \in \mathbb{N}\}$, for each realization of randomizer $\mathbf{\Omega}$.

(b) Averaging the sequence of normalized free energy functions over all possible realizations of the randomizer, i.e., determining

$$\bar{\mathcal{F}}_N(\beta) \coloneqq \mathbb{E}_{\mathbf{\Omega}}\{\mathcal{F}_N(\beta|\mathbf{\Omega})\} \tag{3.17a}$$

$$= \mathbb{E}_{\mathbf{\Omega}}\left\{-\frac{1}{\beta N}\log \mathcal{Z}_N(\beta|\mathbf{\Omega})\right\}. \tag{3.17b}$$

for $N \in \mathbb{N}$.

(c) Taking the limit

$$\bar{\mathcal{F}}(\beta) = \lim_{N\uparrow\infty} \bar{\mathcal{F}}_N(\beta). \tag{3.18}$$

By statements similar to those given in Section 2.4.2, one concludes that this task, in a generic form, needs more advanced analytic tools. In this respect, several techniques, such as the *replica* method and the *cavity* method, have been proposed in the literature of statistical mechanics to address this task.

3.2 Corresponding Spin Glass

The problem of linear regression via RLS can be modeled via a spin glass. To show that, consider a spin glass whose microstate is taken from $\mathbb{X}^N$. For sake of simplicity, assume that $\mathbb{X}$ is a discrete set. Let the Hamiltonian be

$$\mathcal{E}\left(\boldsymbol{v}|\boldsymbol{y},\mathbf{A}\right)=\frac{\zeta}{2\lambda}\left\|\boldsymbol{y}-\mathbf{A}\boldsymbol{v}\right\|^{2}+u_{\mathrm{v}}\left(\boldsymbol{v}\right) \tag{3.19}$$

where the regressors in $\mathbf{A}$ and the regressands in $\boldsymbol{y}$ are considered to randomize the spin glass. Hence, at inverse temperature β, the microstate in thermal equilibrium is conditionally distributed with

$$\mathrm{p}_{\beta}\left(\boldsymbol{v}|\boldsymbol{y},\mathbf{A}\right)=\frac{\exp\left\{-\beta\mathcal{E}\left(\boldsymbol{v}|\boldsymbol{y},\mathbf{A}\right)\right\}}{\mathcal{Z}_{N}\left(\beta|\boldsymbol{y},\mathbf{A}\right)} \tag{3.20}$$

where partition function $\mathcal{Z}_{N}\left(\beta|\boldsymbol{y},\mathbf{A}\right)$ reads

$$\mathcal{Z}_{N}\left(\beta|\boldsymbol{y},\mathbf{A}\right)=\sum_{\boldsymbol{v}\in\mathbb{X}^{N}}\exp\left\{-\beta\mathcal{E}\left(\boldsymbol{v}|\mathbf{A},\boldsymbol{y}\right)\right\}. \tag{3.21}$$

Assume that the Hamiltonian has a unique minimizer denoted by $\boldsymbol{v}^{\star}$, and define

$$\Delta\mathcal{E}\left(\boldsymbol{v}|\boldsymbol{y},\mathbf{A}\right)=\mathcal{E}\left(\boldsymbol{v}|\boldsymbol{y},\mathbf{A}\right)-\mathcal{E}\left(\boldsymbol{v}^{\star}|\boldsymbol{y},\mathbf{A}\right). \tag{3.22}$$

The conditional Boltzmann-Gibbs distribution hence reads

$$\mathrm{p}_{\beta}\left(\boldsymbol{v}|\boldsymbol{y},\mathbf{A}\right)=\frac{\exp\left\{-\beta\mathcal{E}\left(\boldsymbol{v}|\boldsymbol{y},\mathbf{A}\right)\right\}}{\sum\limits_{\boldsymbol{v}}\exp\left\{-\beta\mathcal{E}\left(\boldsymbol{v}|\mathbf{A},\boldsymbol{y}\right)\right\}} \tag{3.23a}$$

$$=\frac{\exp\left\{-\beta\mathcal{E}\left(\boldsymbol{v}|\boldsymbol{y},\mathbf{A}\right)\right\}}{\exp\left\{-\beta\mathcal{E}\left(\boldsymbol{v}^{\star}|\boldsymbol{y},\mathbf{A}\right)\right\}\left(1+\sum\limits_{\boldsymbol{v}\neq\boldsymbol{v}^{\star}}\exp\left\{-\beta\Delta\mathcal{E}\left(\boldsymbol{v}|\mathbf{A},\boldsymbol{y}\right)\right\}\right)} \tag{3.23b}$$

$$=\frac{\exp\left\{-\beta\Delta\mathcal{E}\left(\boldsymbol{v}|\boldsymbol{y},\mathbf{A}\right)\right\}}{1+\sum\limits_{\boldsymbol{v}\neq\boldsymbol{v}^{\star}}\exp\left\{-\beta\Delta\mathcal{E}\left(\boldsymbol{v}|\mathbf{A},\boldsymbol{y}\right)\right\}}. \tag{3.23c}$$

Since $\Delta\mathcal{E}\left(\boldsymbol{v}|\boldsymbol{y},\mathbf{A}\right)>0$ for any $\boldsymbol{v}\neq\boldsymbol{v}^{\star}$, as the temperature tends to zero, i.e. $\beta\uparrow\infty$,

$$\lim_{\beta\uparrow\infty}\sum_{\boldsymbol{v}\neq\boldsymbol{v}^{\star}}\exp\left\{-\beta\Delta\mathcal{E}\left(\boldsymbol{v}|\mathbf{A},\boldsymbol{y}\right)\right\}=0. \tag{3.24}$$

Consequently, one can conclude that

$$\lim_{\beta\uparrow\infty}\mathrm{p}_{\beta}\left(\boldsymbol{v}|\boldsymbol{y},\mathbf{A}\right)=\begin{cases}1 & \boldsymbol{v}=\boldsymbol{v}^{\star}\\ 0 & \boldsymbol{v}\neq\boldsymbol{v}^{\star}\end{cases}. \tag{3.25}$$

This is a well-known property of thermodynamic systems which indicates that at zero temperature, the microstate tends to a realization whose energy level is minimized, i.e., $\boldsymbol{v}^{\star}$. This realization is called the *ground state* of the system.

Comparing the Hamiltonian in (3.19) with the generic RLS method, it is observed that $\boldsymbol{v}^{\star}=\mathbf{g}_{\mathsf{RLS}}\left(\boldsymbol{y}|\mathbf{A}\right)$. Hence, the statement in (3.25) is written as

$$\lim_{\beta\uparrow\infty}\mathrm{p}_{\beta}\left(\boldsymbol{v}|\boldsymbol{y},\mathbf{A}\right)=\mathbf{1}\left\{\boldsymbol{v}=\mathbf{g}_{\mathsf{RLS}}\left(\boldsymbol{y}|\mathbf{A}\right)\right\} \tag{3.26}$$

which indicates that the ground state of this spin glass recovers the regression coefficients of the linear regression problem, with matrix of regressors $\mathbf{A}$ and vector of regressands $\boldsymbol{y}$, when the generic RLS method is employed. This result can be interpreted in physics context as follows: Assume that this artificially defined spin glass can be realized in practice. By setting the quenched randomizer to the regressors and regressands in the linear regression problem, the microscopic parameters of the particles give the regression coefficients, when the spin glass freezes. We refer to this artificial spin glass as the *corresponding spin glass* and define it formally as follows.

Definition 3.4 (Corresponding spin glass)**.** *Consider the integer $N\in\mathbb{N}$. For a linear regression problem whose matrix of regressors is $\mathbf{A}$ and whose vector of regressands is $\boldsymbol{y}$, the corresponding spin glass is defined as a thermodynamic system with microstate $\boldsymbol{v}\in\mathbb{X}^{N}$ randomized by quenched randomizer $(\boldsymbol{y},\mathbf{A})$ with the Hamiltonian in* (3.19)*.*

3.2.1 Properties of the Corresponding Spin Glass

Invoking the connection between linear regression and its corresponding spin glass, the asymptotic performance metrics of the generic RLS method are represented as the macroscopic features of the spin glass. Hence, the asymptotic metrics can be derived by investigating the corresponding spin glass in the thermodynamic limit. To this end, we study the key properties of the corresponding spin glass. Before illustrating these properties, let us state few preliminaries.

Definition 3.5 (Asymptotic equivalence)**.** *The functions $a(\cdot)$ and $b(\cdot)$ defined over non-bounded set $\mathbb{X}$ are said to be asymptotically equivalent in exponential scale, if*

$$\lim_{x\uparrow\infty} \log \left| \frac{a(x)}{b(x)} \right| = 0 \tag{3.27}$$

for $x \in \mathbb{X}$. This equivalence is denoted by $a(x) \doteq b(x)$.

The asymptotic equivalence in exponential scale intuitively means that when $a(x) \doteq b(x)$, as x grows large

$$a(x) \approx b(x) \exp\{\epsilon(x)\} \tag{3.28}$$

for some $\epsilon(x)$ which tends to zero as x grows.

A fundamental argument from theory of large deviations which is widely utilized throughout the analyses is the *saddle-point method*. This large deviation method is illustrated in Lemma 3.1.

Lemma 3.1 (Saddle-point method)**.** *Consider function*

$$f(\cdot) : \mathbb{X}^N \mapsto \mathbb{R}^+, \tag{3.29}$$

and assume that it is bounded. Define marginalization $M_f(\beta)$ for $f(\cdot)$ as

$$M_f(\beta) \coloneqq \frac{1}{\beta} \log \sum_{\boldsymbol{v}\in\mathbb{X}^N} \exp\{-\beta f(\boldsymbol{v})\} \tag{3.30}$$

for some discrete $\mathbb{X}$*, and*

$$M_f(\beta) \coloneqq \frac{1}{\beta} \log \int_{\mathbb{X}^N} \exp\{-\beta f(\boldsymbol{v})\} \, \mathrm{d}\boldsymbol{v} \tag{3.31}$$

for some continuous $\mathbb{X}$*. Assume that* β *can grow unboundedly large. Then,*

$$\lim_{\beta \uparrow \infty} M_f(\beta) = -\min_{\boldsymbol{v} \in \mathbb{X}^N} f(\boldsymbol{v}) \,. \tag{3.32}$$

Proof. This argument in its simple form is known as Laplace method of integration. For discrete supports, the proof is straightforward. In fact, in this case, we have

$$M_f(\beta) = \frac{1}{\beta} \log \sum_{\boldsymbol{v} \in \mathbb{X}^N} \exp\{-\beta f(\boldsymbol{v})\} \tag{3.33a}$$

$$= \frac{1}{\beta} \log \left[\exp\{-\beta f(\boldsymbol{v}^\star)\} \left(1 + \sum_{\boldsymbol{v} \neq \boldsymbol{v}^\star} \exp\{-\beta [f(\boldsymbol{v}) - f(\boldsymbol{v}^\star)]\} \right) \right] \tag{3.33b}$$

$$= -f(\boldsymbol{v}^\star) + \frac{1}{\beta} \log \left(1 + \sum_{\boldsymbol{v} \neq \boldsymbol{v}^\star} \exp\{-\beta [f(\boldsymbol{v}) - f(\boldsymbol{v}^\star)]\} \right) \tag{3.33c}$$

where

$$\boldsymbol{v}^\star \coloneqq \operatorname*{argmin}_{\boldsymbol{v} \in \mathbb{X}^N} f(\boldsymbol{v}) \,. \tag{3.34}$$

Since for any $\boldsymbol{v} \neq \boldsymbol{v}^\star$

$$f(\boldsymbol{v}) - f(\boldsymbol{v}^\star) > 0, \tag{3.35}$$

it is concluded that

$$\lim_{\beta \uparrow \infty} M_f(\beta) = -f(\boldsymbol{v}^\star) = -\min_{\boldsymbol{v} \in \mathbb{X}^N} f(\boldsymbol{v}) \,. \tag{3.36}$$

For a continuous support, the lemma is directly concluded from Varadhan's lemma by setting $\epsilon = 1/\beta$, $\phi(x) = 0$ and $\{\mu_\epsilon\}$ equal to a family of non-degenerate Gaussian measures with rate function $f(\cdot)$. Details on Varadhan's lemma are given in [19]. □

As illustrated in the beginning of this section, the ground state of the corresponding spin glass recovers the regression coefficients for a discrete microstate, i.e., $\mathbb{X}$ being discrete. This is a fundamental property which relates the problem of linear regression to this spin glass, and holds in general.

Property 1. *Consider a linear regression problem with data dimension N. Let the regression coefficients be uniquely derived via an RLS method. For $N \in \mathbb{N}$, the ground state of the corresponding spin glass recovers the regression coefficients with probability one.*

Proof. For a discrete support $\mathbb{X}$, this property was shown in (3.23a)-(3.26). To justify it for a continuous support, consider the conditional Boltzmann-Gibbs distribution in (3.20). For a continuous $\mathbb{X}$, the partition function reads

$$\mathcal{Z}_N\left(\beta|\boldsymbol{y},\mathbf{A}\right) = \int\limits_{\mathbb{X}^N} \exp\left\{-\beta\mathcal{E}\left(\boldsymbol{v}|\mathbf{A},\boldsymbol{y}\right)\right\}\mathrm{d}\boldsymbol{v}. \tag{3.37}$$

By the saddle-point method, we could write

$$\lim_{\beta\uparrow\infty}\frac{1}{\beta}\log\mathcal{Z}_N\left(\beta|\boldsymbol{y},\mathbf{A}\right) = -\min_{\boldsymbol{v}\in\mathbb{X}^N}\mathcal{E}\left(\boldsymbol{v}|\boldsymbol{y},\mathbf{A}\right). \tag{3.38}$$

Hence, one could conclude that

$$\mathcal{Z}_N\left(\beta|\boldsymbol{y},\mathbf{A}\right) \doteq \exp\left\{-\beta\min_{\boldsymbol{v}\in\mathbb{X}^N}\mathcal{E}\left(\boldsymbol{v}|\boldsymbol{y},\mathbf{A}\right)\right\}, \tag{3.39}$$

or alternatively, as β grows large

$$\mathcal{Z}_N\left(\beta|\boldsymbol{y},\mathbf{A}\right) = \exp\left\{-\beta\min_{\boldsymbol{v}\in\mathbb{X}^N}\mathcal{E}\left(\boldsymbol{v}|\boldsymbol{y},\mathbf{A}\right) + \epsilon\left(\beta\right)\right\} \tag{3.40}$$

for some non-negative[4] $\epsilon(\beta) = \mathcal{O}(\beta)$. Define open ball $\mathcal{B}(\boldsymbol{v}^\star, \varepsilon)$ in $\mathbb{X}^N$ whose center is at $\boldsymbol{v}^\star$, defined as

$$\boldsymbol{v}^\star \coloneqq \underset{\boldsymbol{v}\in\mathbb{X}^N}{\operatorname{argmin}}\ \mathcal{E}(\boldsymbol{v}|\boldsymbol{y}, \mathbf{A}) = \mathsf{g}_{\mathsf{RLS}}(\boldsymbol{y}|\mathbf{A}), \tag{3.41}$$

and whose radius is ε. From the conditional Boltzmann-Gibbs distribution, the probability of $\boldsymbol{v}$ being out of $\mathcal{B}(\boldsymbol{v}^\star, \varepsilon)$ at inverse temperature β, for given $\boldsymbol{y}$ and $\mathbf{A}$, reads

$$P_\beta(\boldsymbol{v}^\star, \varepsilon) \coloneqq \Pr\{\boldsymbol{v} \notin \mathcal{B}(\boldsymbol{v}^\star, \varepsilon)\} = \int\limits_{\mathcal{B}(\boldsymbol{v}^\star,\varepsilon)^{\mathrm{c}}} \mathrm{p}_\beta(\boldsymbol{v}|\boldsymbol{y}, \mathbf{A})\,\mathrm{d}\boldsymbol{v} \tag{3.42}$$

where $\mathcal{B}(\boldsymbol{v}^\star, \varepsilon)^{\mathrm{c}}$ denotes the complement of $\mathcal{B}(\boldsymbol{v}^\star, \varepsilon)$. As β grows large, we have

$$\lim_{\beta\uparrow\infty} P_\beta(\boldsymbol{v}^\star, \varepsilon) = \lim_{\beta\uparrow\infty} \int\limits_{\mathcal{B}(\boldsymbol{v}^\star,\varepsilon)^{\mathrm{c}}} \frac{\exp\{-\beta\mathcal{E}(\boldsymbol{v}|\boldsymbol{y}, \mathbf{A})\}}{\mathcal{Z}_N(\beta|\boldsymbol{y}, \mathbf{A})}\,\mathrm{d}\boldsymbol{v} \tag{3.43a}$$

$$\overset{\dagger}{=} \lim_{\beta\uparrow\infty} \int\limits_{\mathcal{B}(\boldsymbol{v}^\star,\varepsilon)^{\mathrm{c}}} \exp\{-\beta[\mathcal{E}(\boldsymbol{v}|\boldsymbol{y}, \mathbf{A}) - \mathcal{E}(\boldsymbol{v}^\star|\boldsymbol{y}, \mathbf{A})] - \epsilon(\beta)\}\,\mathrm{d}\boldsymbol{v} \tag{3.43b}$$

$$\overset{\star}{=} 0, \tag{3.43c}$$

where $\dagger$ comes from (3.40) and $\star$ follows the fact that for any $\boldsymbol{v} \in \mathcal{B}(\boldsymbol{v}^\star, \varepsilon)^{\mathrm{c}}$,

$$\mathcal{E}(\boldsymbol{v}|\boldsymbol{y}, \mathbf{A}) - \mathcal{E}(\boldsymbol{v}^\star|\boldsymbol{y}, \mathbf{A}) > 0. \tag{3.44}$$

This limit is valid for any $\varepsilon > 0$. Hence, as at zero temperature, the probability of $\boldsymbol{v} \neq \boldsymbol{v}^\star$ tends to zero. This statement concludes the proof. □

The essential property of the corresponding spin glass is that it describes the asymptotic performance of RLS via its macroscopic features. To illustrate this property, we need to formally define a macroscopic feature. For sequence of functions

$$\psi_N(\cdot) : \mathbb{X}^N \mapsto \mathbb{R}, \tag{3.45}$$

[4]Note that $\mathcal{Z}_N(\beta|\boldsymbol{y}, \mathbf{A}) \geq \exp\left\{-\beta \min\limits_{\boldsymbol{v}\in\mathbb{X}^N} \mathcal{E}(\boldsymbol{v}|\boldsymbol{y}, \mathbf{A})\right\}$ for a bounded β. Hence, in general $\epsilon(\beta) > 0$.

the macroscopic feature is defined as the expected value in the thermodynamic limit. This means that macroscopic feature $\bar{\psi}$ corresponding to this sequence of functions is

$$\bar{\psi} = \mathbb{E}_{\boldsymbol{\Omega}} \left\{ \lim_{N\uparrow\infty} \frac{1}{N} \mathbb{E}_{\boldsymbol{v}} \left\{ \psi_N \left(\boldsymbol{v} \right) | \boldsymbol{\Omega} \right\} \right\} \tag{3.46}$$

where $\boldsymbol{v} \sim \mathrm{p}_\beta \left(\boldsymbol{v} | \boldsymbol{\Omega} \right)$ for a given randomizer $\boldsymbol{\Omega}$ with some marginal distribution $\mathrm{p}_{\boldsymbol{\Omega}}$. The direct approach for determining a macroscopic feature is to calculate the expectation over $\boldsymbol{v}$ using the conditional Boltzmann-Gibbs distribution, and then average over the randomizer. There is however a well-known trick in statistical mechanics to determine $\bar{\psi}$ implicitly from the normalized free energy. To illustrate this trick, let us assume[5] a discrete $\mathbb{X}$. The partition function is modified by dummy factor h as

$$\mathcal{Z}_N \left(\beta, h | \boldsymbol{\Omega} \right) = \sum_{\boldsymbol{v} \in \mathbb{X}^N} \exp \left\{ -\beta \mathcal{E} \left(\boldsymbol{v} | \boldsymbol{\Omega} \right) + h \psi_N \left(\boldsymbol{v} \right) \right\}. \tag{3.47}$$

For this modified partition function, the normalized free energy, conditioned to a realization of the randomizer, in thermal equilibrium reads

$$\mathcal{F}_N \left(\beta, h | \boldsymbol{\Omega} \right) = -\frac{1}{\beta N} \log \mathcal{Z}_N \left(\beta, h | \boldsymbol{\Omega} \right). \tag{3.48}$$

By standard derivation, we have

$$\frac{\partial}{\partial h} \mathcal{F}_N \left(\beta, h | \boldsymbol{\Omega} \right) = -\frac{1}{\beta N} \sum_{\boldsymbol{v} \in \mathbb{X}^N} \frac{\psi_N \left(\boldsymbol{v} \right) \exp \left\{ -\beta \mathcal{E} \left(\boldsymbol{v} | \boldsymbol{\Omega} \right) + h \psi_N \left(\boldsymbol{v} \right) \right\}}{\mathcal{Z}_N \left(\beta, h | \boldsymbol{\Omega} \right)}. \tag{3.49}$$

Hence at $h = 0$, one can write

$$\frac{\partial}{\partial h} \mathcal{F}_N \left(\beta, h | \boldsymbol{\Omega} \right) |_{h=0} = -\frac{1}{\beta N} \sum_{\boldsymbol{v} \in \mathbb{X}^N} \frac{\psi_N \left(\boldsymbol{v} \right) \exp \left\{ -\beta \mathcal{E} \left(\boldsymbol{v} | \boldsymbol{\Omega} \right) \right\}}{\mathcal{Z}_N \left(\beta, 0 | \boldsymbol{\Omega} \right)} \tag{3.50a}$$

$$= -\frac{1}{\beta N} \sum_{\boldsymbol{v} \in \mathbb{X}^N} \psi_N \left(\boldsymbol{v} \right) \mathrm{p}_\beta \left(\boldsymbol{v} | \boldsymbol{\Omega} \right) \tag{3.50b}$$

$$= -\frac{1}{\beta N} \mathbb{E}_{\boldsymbol{v}} \left\{ \psi_N \left(\boldsymbol{v} \right) | \boldsymbol{\Omega} \right\}. \tag{3.50c}$$

[5] This assumption is taken just for simplicity.

Consequently, macroscopic feature $\bar{\psi}$ is given in terms of the normalized free energy function as

$$\bar{\psi} = -\beta \mathbb{E}_{\boldsymbol{\Omega}} \left\{ \lim_{N\uparrow\infty} \frac{\partial}{\partial h} \mathcal{F}_N \left(\beta, h|\boldsymbol{\Omega}\right)|_{h=0} \right\}. \tag{3.51}$$

Assume that the limit with respect to N and derivative with respect to h exchange. Then, $\bar{\psi}$ is derived as

$$\bar{\psi} = -\beta \frac{\partial}{\partial h} \lim_{N\uparrow\infty} \mathbb{E}_{\boldsymbol{\Omega}} \left\{ \mathcal{F}_N \left(\beta, h|\boldsymbol{\Omega}\right) \right\}|_{h=0} \tag{3.52a}$$

$$= -\beta \frac{\partial}{\partial h} \bar{\mathcal{F}} \left(\beta, h\right)|_{h=0} \tag{3.52b}$$

where $\bar{\mathcal{F}}\left(\beta, h\right)$ denotes the asymptotic modified free energy. This result illustrates the fact that characteristics of a thermodynamic system is completely described by its normalized free energy function.

For the corresponding spin glass, the above result indicates that the asymptotic performance metrics of the generic RLS method is derived explicitly from its modified free energy. This property is presented and justified as follows.

Property 2. *The asymptotic performance of an arbitrary RLS regression method is completely described by the normalized free energy function of its corresponding spin glass.*

Proof. To justify this property, we need to show that the asymptotic LSE, as well as the asymptotic distortion, are derived explicitly from the normalized free energy. We start with the asymptotic distortion. Without loss of generality assume that $\mathbb{X}$ is a discrete set. Consider sequence of linear regression problems with regressands $\{\boldsymbol{y}_N\}$ and $\{\mathbf{A}_N\}$. Assume that $\boldsymbol{x}_{0N} \in \mathbb{X}^N$ contains true regression coefficients. Hence, for noise $\boldsymbol{z}_N$

$$\boldsymbol{y}_N = \mathbf{A}_N \boldsymbol{x}_{0N} + \boldsymbol{z}_N. \tag{3.53}$$

For sequence of index subsets $\{\mathbb{W}(N)\}$, define sequence $\{\psi_N(\cdot)\}$ with

$$\psi_N(\boldsymbol{v}|\boldsymbol{x}_{0N}) \coloneqq \frac{N}{|\mathbb{W}(N)|}\sum_{w\in\mathbb{W}(N)}\mathsf{d}(v_w; x_{0Nw}). \tag{3.54}$$

The partition functions, modified with sequence $\{\psi_N(\cdot)\}$, in this case read

$$\mathcal{Z}_N(\beta, h|\boldsymbol{y}_N, \mathbf{A}_N) = \sum_{\boldsymbol{v}\in\mathbb{X}^N}\exp\{-\beta\mathcal{E}(\boldsymbol{v}|\boldsymbol{y}_N, \mathbf{A}_N) + h\psi_N(\boldsymbol{v}|\boldsymbol{x}_{0N})\} \tag{3.55}$$

for the Hamiltonian given in (3.19). Here, one should note that $\boldsymbol{x}_{0N}$ is not considered as a part of randomization, since it implicitly is included in $\boldsymbol{y}_N$. The normalized free energy function in the thermodynamic limit is further determined by

$$\bar{\mathcal{F}}(\beta, h) = \lim_{N\uparrow\infty} -\frac{1}{\beta N}\mathbb{E}_{\boldsymbol{y}_N,\mathbf{A}_N}\{\log\mathcal{Z}_N(\beta, h|\boldsymbol{y}_N, \mathbf{A}_N)\}. \tag{3.56}$$

Therefore, the averaging trick concludes that

$$-\beta\frac{\partial}{\partial h}\bar{\mathcal{F}}(\beta, h)|_{h=0} = \lim_{N\uparrow\infty}\frac{1}{N}\mathbb{E}\{\psi_N(\boldsymbol{v}|\boldsymbol{x}_{0N})\} \tag{3.57a}$$

$$= \lim_{N\uparrow\infty}\frac{1}{|\mathbb{W}(N)|}\sum_{w\in\mathbb{W}(N)}\mathbb{E}\{\mathsf{d}(v_w; x_{0Nw})\} \tag{3.57b}$$

with $\boldsymbol{v}$ being distributed due to the Boltzmann-Gibbs distribution. From Property 1, we know that the ground state of the corresponding spin glass recovers the regression coefficients given by the RLS method. Thus, as the temperature tends to zero

$$\lim_{\beta\uparrow\infty} -\beta\frac{\partial}{\partial h}\bar{\mathcal{F}}(\beta, h)|_{h=0} = \lim_{\beta\uparrow\infty}\lim_{N\uparrow\infty}\frac{1}{N}\mathbb{E}\{\psi_N(\boldsymbol{v}|\boldsymbol{x}_{0N})\} \tag{3.58}$$

$$= \lim_{N\uparrow\infty}\frac{1}{N}\mathbb{E}\{\psi_N(\boldsymbol{x}_N|\boldsymbol{x}_{0N})\} \tag{3.59}$$

$$= \lim_{N\uparrow\infty}\frac{1}{|\mathbb{W}(N)|}\sum_{w\in\mathbb{W}(N)}\mathbb{E}\{\mathsf{d}(x_{Nw}; x_{0Nw})\} \tag{3.60}$$

where $\boldsymbol{x}_N = \mathbf{g}_{\mathsf{RLS}}\left(\boldsymbol{y}_N|\mathbf{A}_N\right)$. This concludes that

$$D_{\mathsf{RLS}}^{\mathbb{W}} = \lim_{\beta\uparrow\infty} -\beta\frac{\partial}{\partial h}\bar{\mathcal{F}}\left(\beta,h\right)|_{h=0}. \tag{3.61}$$

Considering the asymptotic LSE, we start with the fact that

$$\frac{\partial}{\partial\beta}\beta\bar{\mathcal{F}}\left(\beta,h\right)|_{h=0} = \lim_{N\uparrow\infty}\mathbb{E}\left\{\sum_{\boldsymbol{v}\in\mathbb{X}^N}\frac{\mathcal{E}\left(\boldsymbol{v}|\boldsymbol{y}_N,\mathbf{A}_N\right)\exp\left\{-\beta\mathcal{E}\left(\boldsymbol{v}|\boldsymbol{y}_N,\mathbf{A}_N\right)\right\}}{N\mathcal{Z}_N\left(\beta,0|\boldsymbol{y}_N,\mathbf{A}_N\right)}\right\} \tag{3.62a}$$

$$= \lim_{N\uparrow\infty}\mathbb{E}_{\boldsymbol{y}_N,\mathbf{A}_N}\left\{\mathbb{E}_{\boldsymbol{v}}\left\{\frac{1}{N}\mathcal{E}\left(\boldsymbol{v}|\boldsymbol{y}_N,\mathbf{A}_N\right)\right\}\right\}. \tag{3.62b}$$

Hence, at zero temperature, we have

$$\lim_{\beta\uparrow\infty}\frac{\partial}{\partial\beta}\beta\bar{\mathcal{F}}\left(\beta,h\right)|_{h=0} = \lim_{N\uparrow\infty}\frac{1}{N}\mathbb{E}_{\boldsymbol{y}_N,\mathbf{A}_N}\left\{\mathcal{E}\left(\boldsymbol{x}_N|\boldsymbol{y}_N,\mathbf{A}_N\right)\right\} \tag{3.63a}$$

$$= \lim_{N\uparrow\infty}\frac{1}{N}\mathbb{E}_{\boldsymbol{y}_N,\mathbf{A}_N}\left\{\frac{\zeta}{2\lambda}\left\|\boldsymbol{y}_N-\mathbf{A}_N\boldsymbol{x}_N\right\|^2+u_{\mathrm{v}}\left(\boldsymbol{x}_N\right)\right\} \tag{3.63b}$$

$$= \frac{\zeta\alpha}{2\lambda}\,\mathrm{LSE}_{\mathsf{RLS}} + \lim_{N\uparrow\infty}\frac{1}{N}\mathbb{E}_{\boldsymbol{y}_N,\mathbf{A}_N}\left\{u_{\mathrm{v}}\left(\boldsymbol{x}_N\right)\right\}. \tag{3.63c}$$

By defining sequence $\{\psi_N\left(\cdot\right)\}$ as

$$\psi_N\left(\boldsymbol{v}\right) \coloneqq \sum_{n=1}^{N} u\left(v_n\right), \tag{3.64}$$

one can use the averaging trick and write

$$\lim_{N\uparrow\infty}\frac{1}{N}\mathbb{E}_{\boldsymbol{y}_N,\mathbf{A}_N}\left\{u_{\mathrm{v}}\left(\boldsymbol{x}_N\right)\right\} = \bar{\psi} \tag{3.65}$$

which is explicitly derived from the modified free energy at zero temperature. Consequently, the asymptotic LSE is determined as

$$\mathrm{LSE}_{\mathsf{RLS}} = \frac{2\lambda}{\zeta\alpha}\left[\lim_{\beta\uparrow\infty}\frac{\partial}{\partial\beta}\beta\bar{\mathcal{F}}\left(\beta,h\right)|_{h=0}-\bar{\psi}\right]. \tag{3.66}$$

This concludes the proof. □

Remark 3.1. *Throughout the proof, we assumed that the limits with respect to the dimension and temperature are exchangeable. This assumption is just considered to keep the derivations straightforward and is not necessary to hold.*

3.3 The Replica Method

Considering the key properties of the corresponding spin glass, the asymptotic analysis of RLS reduces to deriving the modified free energy in the thermodynamic limit. This means that for a given linear regression problem with regressands $\boldsymbol{y}$, regressors $\mathbf{A}$ and true regression coefficients $\boldsymbol{x}_0$, we need to calculate the function

$$\bar{\mathcal{F}}_N(\beta, h) = -\frac{1}{\beta N}\mathbb{E}\left\{\log \mathcal{Z}_N(\beta, h|\boldsymbol{y}, \mathbf{A})\right\} \tag{3.67}$$

where partition function $\mathcal{Z}_N(\beta, h|\boldsymbol{y}, \mathbf{A})$ is given by

$$\mathcal{Z}_N(\beta, h|\boldsymbol{y}, \mathbf{A}) = \sum_{\boldsymbol{v}\in\mathbb{X}^N} \exp\left\{-\beta\mathcal{E}(\boldsymbol{v}|\boldsymbol{y}, \mathbf{A}) + h\psi_{\mathrm{v}}(\boldsymbol{v}|\boldsymbol{x}_0)\right\} \tag{3.68}$$

for discrete supports, and

$$\mathcal{Z}_N(\beta, h|\boldsymbol{y}, \mathbf{A}) = \int_{\mathbb{X}^N} \exp\left\{-\beta\mathcal{E}(\boldsymbol{v}|\boldsymbol{y}, \mathbf{A}) + h\psi_{\mathrm{v}}(\boldsymbol{v}|\boldsymbol{x}_0)\right\} \mathrm{d}\boldsymbol{v} \tag{3.69}$$

when $\mathbb{X}$ is continuous. We suppose that the modification function is of the form

$$\psi_{\mathrm{v}}(\boldsymbol{v}|\boldsymbol{x}_0) = \sum_{w\in\mathbb{W}} \psi(v_w|x_{0w}) \tag{3.70}$$

for some scalar function $\psi(\cdot|\cdot)$ and $\mathbb{W} \subseteq [N]$. This task confronts the problem of determining a logarithmic expectation which is intractable. The task can be bypassed by invoking an analytic trick which utilizes the fact that for any non-negative random variable, the expected logarithm is represented in terms of its analytic moments function. This representation is known as the *Riesz equality* [20].

Lemma 3.2 (Riesz equality)**.** *Consider random variable $z > 0$, and define continuous function $f_z(\theta)$ as*

$$f_z(\theta) \coloneqq \mathbb{E}\left\{z^{\frac{1}{\theta}}\right\}. \tag{3.71}$$

$f_z(\theta)^\theta$ is asymptotically equivalent to $\exp\{\mathbb{E}\{\log z\}\}$ in exponential scale, i.e.

$$\lim_{\theta\uparrow\infty} \theta \log f_z(\theta) = \mathbb{E}\{\log z\}. \tag{3.72}$$

Proof. The validity of this equality is straightforwardly shown by representing $f_z(\theta)$ in terms of $t = 1/\theta$ and taking the limit $t \downarrow 0$. The proof was initially given in [20]. □

Employing the Riesz equality, the modified free energy reads

$$\bar{\mathcal{F}}_N(\beta, h) = -\frac{1}{\beta N}\mathbb{E}\{\log \mathcal{Z}_N(\beta, h|\boldsymbol{y}, \mathbf{A})\} \tag{3.73a}$$

$$= -\frac{1}{\beta N}\lim_{t\downarrow 0}\frac{1}{t}\log \mathbb{E}\left\{\mathcal{Z}_N(\beta, h|\boldsymbol{y}, \mathbf{A})^t\right\}. \tag{3.73b}$$

which is represented in terms of moments function

$$f_{\mathcal{Z}}(t) = \mathbb{E}\left\{\mathcal{Z}_N(\beta, h|\boldsymbol{y}, \mathbf{A})^t\right\}. \tag{3.74}$$

Although the representation in (3.73b) bypasses the task of evaluating a logarithmic expectation, it is still intractable to be calculated, since $f_{\mathcal{Z}}(t)$ needs to be evaluated over the real axis[6].

The problem of calculating real moments appears in various studies in statistical mechanics. Several techniques have been hence developed in the literature to address this problem, at least for a class of partition functions. The proposed techniques often consider some heuristic conjectures which are concluded from physical intuitions behind the problem. The *replica method* is one of these techniques which is widely utilized in other literatures, such as information theory, communications and signal processing, and has been accepted as an efficient mathematical tools for asymptotic

[6] Or, at least, within a right neighborhood of 0.

analysis. The method is known to be non-rigorous, as it conjectures that the moments function exhibit the so-called *replica continuity*. This conjecture has been shown to hold for a certain class of partition functions. However, the proof of its validity in a general form is left open in the literature.

In order to determine $f_{\mathcal{Z}}(t)$, the replica method suggests to derive the function for an arbitrary positive integer t in an analytic form, and then consider the replica continuity conjecture given below.

Assumption 3.1 (Replica continuity)**.** *Moments function $f_{\mathcal{Z}}(t)$ analytically continues from $\mathbb{N}$ onto the real axis. This means that the analytic expression, found for an arbitrary positive integer t, directly extends to $t \in \mathbb{R}^+$.*

Replica continuity conjectures that the expression determined for $f_{\mathcal{Z}}(t)$ with integer arguments exactly recovers the real moments in the right neighborhood of $t = 0$. The validity of this conjecture is not straightforward to be investigated, since $\mathbb{N}$ is not a dense subset of the real axis. Replica continuity is the main part where the replica method lacks rigor.

By conjecturing replica continuity, calculation of the modified free energy reduces to the problem of deriving the integer moments as an analytic function in terms of the exponent. This latter task is tractable. Assuming $\mathbb{X}$ is a discrete support, we have

$$f_{\mathcal{Z}}(t) = \mathbb{E}\left\{\mathcal{Z}_N(\beta, h|\boldsymbol{y}, \mathbf{A})^t\right\} \tag{3.75a}$$

$$= \mathbb{E}\left\{\prod_{a=1}^{t} \sum_{\boldsymbol{v}_a \in \mathbb{X}^N} \exp\left\{-\beta \mathcal{E}(\boldsymbol{v}_a|\boldsymbol{y}, \mathbf{A}) + h\psi_{\mathrm{v}}(\boldsymbol{v}_a|\boldsymbol{x}_0)\right\}\right\} \tag{3.75b}$$

$$= \mathbb{E}\left\{\sum_{\{\boldsymbol{v}_a\}} \exp\left\{-\beta \sum_{a=1}^{t} \mathcal{E}(\boldsymbol{v}_a|\boldsymbol{y}, \mathbf{A}) + h \sum_{a=1}^{t} \psi_{\mathrm{v}}(\boldsymbol{v}_a|\boldsymbol{x}_0)\right\}\right\} \tag{3.75c}$$

$$= \mathbb{E}\left\{\breve{\mathcal{Z}}_{Nt}(\beta, h|\boldsymbol{y}, \mathbf{A})\right\} \tag{3.75d}$$

where we define

$$\breve{\mathcal{Z}}_{Nt}(\beta, h|\boldsymbol{y}, \mathbf{A}) \coloneqq \sum_{\{\boldsymbol{v}_a\}} \exp\left\{-\beta \sum_{a=1}^{t} \mathcal{E}(\boldsymbol{v}_a|\boldsymbol{y}, \mathbf{A}) + h \sum_{a=1}^{t} \psi_{\mathrm{v}}(\boldsymbol{v}_a|\boldsymbol{x}_0)\right\} \tag{3.76}$$

and use notation $\{\boldsymbol{v}_a\}$ to denote

$$\{\boldsymbol{v}_1, \ldots, \boldsymbol{v}_t\} \in \prod_{a=1}^{t} \mathbb{X}^N. \tag{3.77}$$

$\check{\mathcal{Z}}_{Nt}(\beta, h|\boldsymbol{y}, \mathbf{A})$ can be considered as the partition function of a spin glass with Nt particles, being randomized by $(\boldsymbol{y}, \mathbf{A})$, whose Hamiltonian is

$$\check{\mathcal{E}}(\check{\boldsymbol{v}}|\boldsymbol{y}, \mathbf{A}) \coloneqq \sum_{a=1}^{t} \mathcal{E}(\boldsymbol{v}_a|\boldsymbol{y}, \mathbf{A}) \tag{3.78}$$

and the microstate $\check{\boldsymbol{v}}$ is taken from $\mathbb{X}^{Nt}$. This new spin glass is constructed by replicating the corresponding spin glass, t times. This is in fact where the appellation comes from. The replicated versions of the original microstate, i.e., $\boldsymbol{v}_a$ for $a \in [t]$, are often referred to as the *replicas*, and $\{\boldsymbol{v}_a\}$ is called the *set of replicas*.

Starting from (3.75d), the remaining task is to derive the expectation as an analytic function in terms of t and then take the corresponding limit. This task is analytically tractable; however, it requires a variety of analytic tools from theory of random matrices to be employed. In the next chapter, we give the solution in its general form. This solution is referred to as the *general replica ansatz* and is of a complicated form. For a class of problems which exhibit the so-called *replica symmetry*, this general solution becomes of an intuitive and simple expression. When the problem does not depict replica symmetry, the general solution is analytically represented by *breaking* this symmetry via an iterative scheme. Invoking the general replica ansatz, we derive the analytic forms of the solution under both *replica symmetry* and *replica symmetry breaking* conditions.

3.4 Bibliographic Notes

Connections between information theory and statistical mechanics have been widely investigated in the literature through several concepts such as maximum entropy principle [21] and large deviation theory [19]. Discussions in [22, 23] by Jaynes, in late fifties, illustrated these connections further and introduced various directions for re-

search; see for example [24–26]. Some fundamental results have been presented by Merhav in [25], where the physical meaning of fundamental information measures, and the relation between random coding and random energy model (REM) for spin glasses [27, 28], have been illustrated.

The mean-field theory for spin glasses was developed by Sherrington and Kirkpatrick in [29, 30], where initial investigations via the replica method was given. Even though the method was developed to study spin glasses, its applications to other mathematically similar problems introduced it as an analytic tool in applied mathematics, coding theory, signal processing, multiuser communications, information theory and machine learning [26, 31–40]. Tanaka in his remarkable study [40] employed the replica method to calculate the bit error rate in a linear system followed by a class of Bayesian estimators, referred to as marginal posterior mode (MPM) detectors. The study demonstrated interesting large-system properties of multiuser estimation. Consequently, the statistical mechanical approach received more attention in the context of Bayesian estimation, and the replica method was employed for studying a large scope of problems in multiuser communications and information theory; see [41–47] and references therein for some examples from multiuser detection, MIMO systems, signal processing and channel coding. Although the replica method lacks mathematical rigor, a body of work, such as [18, 48–54], has shown the validity of several replica-based results in the literature, including Tanaka's formula in [40], using some alternative rigorous approaches.

Several problems, being studied in the literature, are special cases of RLS for the linear regression model; see for example the problems investigated in [40, 43, 45–47, 55]. The primary studies on the linear model considered a restricted class of ensembles. For instance, analyses in [40, 44] were limited to models whose regressors are i.i.d. Gaussian, and whose true coefficients are postulated to have either Bernoulli or Gaussian distributions. The scope of analyses was expanded later to wider ensembles; see for example [43, 45–47]. Nevertheless, the RLS method for linear regression with the model described in Chapter 2 has not been yet analyzed in its full generality.

3.5 Summary

This chapter has illustrated a quantitative connection between the generic RLS method for linear regression and theory of spin glasses. In this respect, some preliminaries on statistical mechanics have been presented. It has been shown that the asymptotic performance of the generic RLS regression method can be represented as macroscopic parameters of an imaginary corresponding spin glass. In the shadow of this analogy, an analytic approach based on the replica method has been proposed for asymptotic analysis of RLS. This approach is followed in the next chapter, where the generic RLS method for linear regression is tractably characterized in the asymptotic regime.

Chapter 4

Asymptotics via the Replica Method

The replica method determines the free energy of a spin glass in an analytic form in terms of the solution of a set of mutually coupled fixed-point equations. Explicit expressions for the coupled equations in the ansatz depend on the Hamiltonian. For several spin glasses, in which the Hamiltonian depicts so-called *replica symmetry*, these coupled equations reduce to a simple system of equations with two variables. In contrast to initial beliefs in the literature, several energy models, e.g. the random energy model, have been later shown to not exhibit replica symmetry. The common approach for deriving the free energy in these models is to recursively perturb the replica symmetric ansatz. This method is known as *replica symmetry breaking* in the literature and can be iterated for an arbitrary number of recursions.

In this chapter, the *generic* replica ansatz for the corresponding spin glass of RLS is derived. This ansatz represents the fixed-point equations in full generality and encloses all possible structures of the energy model, e.g. replica symmetry and broken replica symmetry. The replica symmetric ansatz, as well as its broken version with an arbitrary number of recursions, is then calculated from this generic ansatz. The *zero-temperature entropy* of the corresponding spin glass is further calculated in an analytic form for the given ansätze. This is a useful quantity whose value give some insights on the consistency of replica ansätze.

4.1 The Replica Ansatz

Starting from the formulation in Section 3.3, the generic RLS method is characterized by the statistics of true regression coefficients, regression error and regressors. The characterization is presented in this section. Before stating the replica ansatz, let us define the Stieltjes and R-transform of a probability distribution.

4.1.1 Stieltjes and R-Transform

For many random matrices the asymptotic empirical distribution of eigenvalues and singular values is not derived in a closed form. It is hence more convenient to express them by their Stieltjes or R-transforms.

Definition 4.1 (Stieltjes transform)**.** *Let random variable $x \in \mathbb{X}$, with $\mathbb{X} \subseteq \mathbb{R}$, be distributed with $\mathrm{p}_x(x)$. Then, the Stieltjes transform of $\mathrm{p}_x(x)$ over the upper complex half plane, i.e. $\mathbb{Im}\{s\} > 0$, is defined as*

$$\mathrm{G}_x(s) \coloneqq \mathbb{E}\left\{\frac{1}{x-s}\right\} = \int_{\mathbb{X}} \mathrm{p}_x(x)\,\frac{\mathrm{d}x}{x-s}. \tag{4.1}$$

The initial application of the Stieltjes transform was given in the moments problem, were the solution was simply given by the Stieltjes inversion formula. The transform is widely used in random matrix theory, as it often represents the asymptotic distribution of eigenvalues or singular values in a compact form [56–58]. A table of commonly used Stieltjes transforms in random matrix theory is given in [57].

Definition 4.2 (R-transform)**.** *Consider x with distribution with $\mathrm{p}_x(x)$ and let $\mathrm{G}_x(\cdot)$ be the Stieltjes transform. Denote the inverse with respect to composition by $\mathrm{G}_x^{-1}(\cdot)$. The R-transform of $\mathrm{p}_x(x)$ over the real axis is defined as*

$$\mathrm{R}_x(\omega) \coloneqq \mathrm{G}_x^{-1}(-\omega) - \frac{1}{\omega} \tag{4.2}$$

where $\mathrm{G}_t^{-1}(\cdot)$ is calculated such that

$$\lim_{\omega \downarrow 0} \mathrm{R}_x(\omega) = \mathbb{E}\{x\}. \tag{4.3}$$

The R-transform gives an alternative representation for asymptotic distributions in random matrix theory. The transform has some additional analytic properties, namely when multiple so-called *asymptotically free* random matrices[1] are added, the R-transform of the superposed matrix is simply derived in terms of individual summands. Details on properties of the R-transform, as well as some well-known transforms, are given in [57, 58].

The given definitions are extended to matrix arguments by a standard approach: Assume matrix $\mathbf{M} \in \mathbb{A}_{\zeta}^{N \times N}$ has real eigenvalues and is decomposed as

$$\mathbf{M} = \mathbf{U}\mathbf{\Lambda}\mathbf{U}^{-1} \tag{4.4}$$

where $\mathbf{\Lambda} \in \mathbb{R}^{N \times N}$ is a diagonal matrix of eigenvalues, i.e.,

$$\mathbf{\Lambda} = \operatorname{diag}\left\{[\lambda_1, \ldots, \lambda_N]\right\}, \tag{4.5}$$

and $\mathbf{U} \in \mathbb{A}_{\zeta}^{N \times N}$ is the matrix of eigenvectors. $\mathrm{R}_x(\mathbf{M})$ is then given by

$$\mathrm{R}_x(\mathbf{M}) = \mathbf{U} \operatorname{diag}\left\{[\mathrm{R}_x(\lambda_1), \ldots, \mathrm{R}_x(\lambda_N)]\right\} \mathbf{U}^{-1}. \tag{4.6}$$

4.1.2 Generic Form of the Replica Ansatz

The general form of the replica ansatz describes the macroscopic parameters of the corresponding spin glass in terms of a new spin glass with a finite dimension. This new spin glass, referred to as the *spin glass of replicas*, encloses only t particles where t is a finite integer denoting the number of replicas.

Definition 4.3 (Spin glass of replicas)**.** *Consider a linear regression problem with support $\mathbb{X} \subset \mathbb{A}_{\zeta}$ whose true regression coefficients are distributed with $\mathrm{p}_0(x_0)$. For a finite integer t, the spin glass of replicas is defined as a randomized thermodynamic system with t particles and quenched randomizer*

$$\mathbf{x}_t = x_0 \mathbf{1}_{t \times 1} \tag{4.7}$$

[1] The definition of asymptotic freeness is given in [57, 58].

where $x_0 \sim \mathrm{p}_0(x_0)$. *The energy model for this spin glass is described by Hamiltonian*

$$\mathcal{E}^{\mathsf{R}}(\mathbf{v}|\mathbf{x}) = (\mathbf{x}-\mathbf{v})^{\mathsf{H}}\mathbf{T}\mathrm{R}_{\mathbf{J}}(-\frac{2}{\zeta}\beta\mathbf{T}\mathbf{Q})(\mathbf{x}-\mathbf{v}) + u_{\mathrm{v}}(\mathbf{v}) \tag{4.8}$$

where $\mathbf{v} \in \mathbb{X}^t$ *represents the microstate,* $\mathrm{R}_{\mathbf{J}}(\cdot)$ *is the* R*-transform corresponding to asymptotic distribution* $\mathrm{F}_{\mathbf{J}}$ *and*

- $\mathbf{T} \in \mathbb{R}^{t\times t}$ *is defined as*

$$\mathbf{T} \coloneqq \frac{\zeta}{2\lambda}\left[\mathbf{I}_t - \frac{\beta\sigma^2}{\lambda + t\beta\sigma^2}\mathbf{1}_t\right] \tag{4.9}$$

- $\mathbf{Q}_{t\times t}$ *is the so-called replica correlation matrix given by*

$$\mathbf{Q} = \mathbb{E}\left\{(\mathbf{x}-\mathbf{v})(\mathbf{x}-\mathbf{v})^{\mathsf{H}}\right\} \tag{4.10}$$

  where the expectation is taken with respect to the Boltzmann-Gibbs distribution at thermal equilibrium, i.e.,

$$\mathrm{p}_{\beta}^{\mathsf{R}}(\mathbf{v}|\mathbf{x}) = \frac{\exp\left\{-\beta\mathcal{E}^{\mathsf{R}}(\mathbf{v}|\mathbf{x})\right\}}{\mathcal{Z}^{\mathsf{R}}(\beta|\mathbf{x})} \tag{4.11}$$

  with partition function

$$\mathcal{Z}^{\mathsf{R}}(\beta|\mathbf{x}) \coloneqq \sum_{\mathbf{v}\in\mathbb{X}^t} \exp\left\{-\beta\mathcal{E}^{\mathsf{R}}(\mathbf{v}|\mathbf{x})\right\}. \tag{4.12}$$

The spin glass of replicas can be considered as the projection of the corresponding spin glass onto the space of replicas. In fact, the Hamiltonian of this spin glass, i.e., $\mathcal{E}^{\mathsf{R}}(\cdot|\mathbf{x})$, describes a t-dimensional generic RLS regression method whose RSS term is modified with statistics of the linear regression model.

For the spin glass of replicas, the exact derivation of the macroscopic parameters requires a system of fixed-point equations to be solved. To clarify this point, note that the Boltzmann-Gibbs distribution $\mathrm{p}_{\beta}^{\mathsf{R}}(\mathbf{v}|\mathbf{x})$ depends on the replica correlation matrix

$\mathbf{Q}$. Consequently, the right hand side of (4.10) is a function of $\mathbf{Q}$, and thus (4.10) describes a fixed-point equation with respect to $\mathbf{Q}$.

To characterize the spin glass of replicas, we define some basic macroscopic parameters:

Definition 4.4 (Basic macroscopic parameters)**.** *Consider the spin glass of replicas, defined in Definition 4.3. For this spin glass,*

- *The normalized free energy at inverse temperature β is given by*

$$\mathcal{F}^{\mathsf{R}}(\beta, t) = -\frac{1}{\beta t}\mathbb{E}\left\{\log \mathcal{Z}^{\mathsf{R}}(\beta|\mathbf{x})\right\}. \tag{4.13}$$

- *The normalized conditional entropy of the system reads*

$$\mathcal{H}^{\mathsf{R}}(\beta, t) = -\frac{1}{t}\mathbb{E}\left\{\log \mathrm{p}_{\beta}^{\mathsf{R}}(\mathbf{v}|\mathbf{x})\right\} \tag{4.14a}$$

$$= \beta^2 \frac{\mathrm{d}}{\mathrm{d}\beta}\mathcal{F}^{\mathsf{R}}(\beta, t). \tag{4.14b}$$

- *The normalized average energy level of the spin glass is*

$$\bar{\mathcal{E}}^{\mathsf{R}}(\beta, t) = \frac{1}{t}\mathbb{E}\left\{\mathcal{E}^{\mathsf{R}}(\mathbf{v}|\mathbf{x})\right\} \tag{4.15a}$$

$$= \frac{\mathrm{d}}{\mathrm{d}\beta}\beta\mathcal{F}^{\mathsf{R}}(\beta, t). \tag{4.15b}$$

- *The average distortion of replicas with respect to $\mathsf{d}(\cdot,\cdot)$ at given β is*

$$D^{\mathsf{R}}(\beta, t) = \frac{1}{t}\mathbb{E}\left\{\sum_{a=1}^{t}\mathsf{d}(\mathrm{v}_a, x_0)\right\}. \tag{4.16}$$

The macroscopic parameters in Definition 4.4 are tractably calculated as a function of dimension t, since t is finite. The general replica ansatz describes the asymptotic performance of RLS in terms of these macroscopic parameters.

Proposition 4.1 (General replica ansatz)**.** *For a linear regression problem with a generic RLS method, let the spin glass of replicas be defined as in Definition 4.3 and denote the set of all possible replica correlation matrices satisfying the fixed-pint equation by* $\mathbb{F}$*. Then, the free energy of the corresponding spin glass is given by*

$$\bar{\mathcal{F}}(\beta) = \frac{\zeta\alpha\sigma^2}{2\lambda} + \Delta E(\beta) + \mathcal{F}^{\mathsf{R}}(\beta) \tag{4.17}$$

where $\mathcal{F}^{\mathsf{R}}(\beta)$ *represents the limiting free energy of the spin glass of replicas, i.e.,*

$$\mathcal{F}^{\mathsf{R}}(\beta) = \lim_{t\downarrow 0} \mathcal{F}^{\mathsf{R}}(\beta, t), \tag{4.18}$$

function $\Delta E(\beta)$ *reads*

$$\Delta E(\beta) \coloneqq \lim_{t\downarrow 0} \frac{1}{t}\left[\int_0^1 \operatorname{tr}\left\{\mathbf{TQ}\mathrm{R}_{\mathbf{J}}(-\frac{2}{\zeta}\beta\omega\mathbf{TQ})\right\}\,\mathrm{d}\omega - \operatorname{tr}\left\{\mathbf{Q}^{\mathsf{T}}\mathbf{T}\mathrm{R}_{\mathbf{J}}(-\frac{2}{\zeta}\beta\mathbf{TQ})\right\}\right] \tag{4.19}$$

and is referred to as the energy difference at β*, and* $\mathbf{Q} \in \mathbb{F}$*, such that the free energy is minimized. The asymptotic distortion of the generic RLS method is given by*

$$D^{\mathbb{W}}_{\mathsf{RLS}} = \lim_{\beta\uparrow\infty}\lim_{t\downarrow 0} D^{\mathsf{R}}(\beta, t). \tag{4.20}$$

and the asymptotic LSE is determined by

$$\mathrm{LSE}_{\mathsf{RLS}} = \sigma^2 + \frac{2\lambda}{\zeta\alpha}\lim_{\beta\uparrow\infty}\left[L(\beta) + \frac{\partial}{\partial\beta}\beta\Delta E(\beta)\right] \tag{4.21}$$

where $L(\beta)$ *is defined as*

$$L(\beta) \coloneqq \frac{\partial}{\partial\beta}\beta\mathcal{F}^{\mathsf{R}}(\beta) - \lim_{t\downarrow 0}\frac{1}{t}\mathbb{E}\left\{u_{\mathrm{v}}(\mathbf{v})\right\} \tag{4.22}$$

Proof. The proof is given in Appendix A. However, we explain briefly the strategy: We intend to determine the moments function. To this end, we start from (3.76) where

the moments function is given in terms of expected value of the replicated partition function, i.e.,

$$f_{\mathcal{Z}}(t) = \mathbb{E}\left\{\breve{\mathcal{Z}}_{Nt}(\beta, h|\boldsymbol{y}, \mathbf{A})\right\}. \tag{4.23}$$

The expectation with respect to regression error is straightforwardly taken by Gaussian integration. The expectation with respect to the regressors, i.e., $\mathbf{A}$, is represented as a spherical integral where the results from [59] can be employed to determine it in the large-system limit. The expected value is represented in terms of replicas $\{\boldsymbol{v}_a\}$ and true regression coefficients in $\boldsymbol{x}_0$. Considering the following variable exchange,

$$[\mathbf{Q}]_{ab} = \frac{1}{N}(\boldsymbol{x}_0 - \boldsymbol{v}_a)^{\mathsf{H}}(\boldsymbol{x}_0 - \boldsymbol{v}_b). \tag{4.24}$$

for $a, b \in [t]$, moments function $f_{\mathcal{Z}}(t)$ is expressed in terms of the replica correlation matrix $\mathbf{Q}$. By employing the law of large numbers, it finally reads

$$f_{\mathcal{Z}}(t) = \mathbb{E}_{\boldsymbol{x}_0}\left\{\int \exp\left\{-N\left[\mathcal{G}(\mathbf{TQ}) - \mathcal{I}(\mathbf{Q})\right] + \epsilon_N\right\} \mathrm{d}\mathbf{Q}\right\} \tag{4.25}$$

where $\mathrm{d}\mathbf{Q}$ is defined as

$$\mathrm{d}\mathbf{Q} \coloneqq \prod_{a=1}^{t}\prod_{b=a+1}^{t} \mathrm{d}[\mathbf{Q}]_{ab} \tag{4.26}$$

following the fact that $\mathbf{Q}$ is Hermitian symmetric, and ϵ_N tends to zero as $N \uparrow \infty$. The term $\exp\{N\mathcal{I}(\mathbf{Q})\}$ denotes a density measure over the set of correlation matrices and is explicitly determined in Appendix A. Moreover, $\mathcal{G}(\cdot)$ reads

$$\mathcal{G}(\mathbf{M}) = \int_0^{\beta} \mathrm{tr}\left\{\mathbf{M}\mathrm{R}_{\mathbf{J}}(-\frac{2}{\zeta}\omega\mathbf{M})\right\} \mathrm{d}\omega \tag{4.27}$$

for some square matrix $\mathbf{M}$.

It is shown that $\exp\{N\mathcal{I}(\mathbf{Q})\}\,\mathrm{d}\mathbf{Q}$ satisfies the large deviations property [60]. Hence, using results from large deviations, the integral in (4.25) for large values of N is asymptotically equivalent, in exponential scale, to the integrand at saddle point $\tilde{\mathbf{Q}}$,

$$f_{\mathcal{Z}}(t) \doteq K_N \exp\left\{-N\left[\mathcal{G}(\mathbf{T}\tilde{\mathbf{Q}}) - \mathcal{I}(\tilde{\mathbf{Q}})\right]\right\} \tag{4.28}$$

for some bounded sequence K_N. By substituting $f_{\mathcal{Z}}(t)$ and taking the limits with respect to N, t and β, as suggested by replica continuity, the macroscopic parameters of the corresponding spin glass are determined, noting the fact that free energy is minimized in thermal equilibrium. □

4.1.3 Replica Symmetry and Its Breaking

The generic replica ansatz introduces a tractable way to characterize the asymptotic performance of the generic RLS method. Here, the term *generic* indicates the fact that this ansatz only depends on replica continuity and imposes no further major assumptions. To utilize this general result, one needs to solve the fixed-point equation for correlation matrix $\mathbf{Q}$ with finite dimension t, and calculate the macroscopic parameters as analytic functions of the dimension. This direct approach is however not recommended in the literature, due to the following reasons:

1. *Complexity:* The direct approach to find the correlation matrix needs a complete search which is computationally complex with multiple solutions.

2. *Analyticity:* Replica continuity assumption requires the moments function, and as a result the free energy, to be derived as analytic functions in terms of dimension t. In this respect, the solutions derived by this direct approach for the correlation matrix are not guaranteed to result in an analytic expression for the free energy, and hence might be of no use.

These issues together are addressed in the literature of spin glasses by invoking a well-known indirect approach. The trick is to restrict the search space to a set of parameterized matrices. The structure of these parameterized matrices is set based on physical intuitions behind the study and mathematical investigations of the energy

model. In this case, the fixed-point problem with a matrix argument reduces to a system of equations whose unknown variables are the parameters of the restricted structure. To clarify the idea further, assume that we force the correlation matrix to be of the form

$$\tilde{\mathbf{Q}}\left(q_1, \ldots, q_L\right) \tag{4.29}$$

where $\tilde{\mathbf{Q}}\left(q_1, \ldots, q_L\right)$ is a $t \times t$ matrix parameterized with scalars $q_1, \ldots, q_L$, and L is a constant number which does not depend on t. In this case, by inserting $\tilde{\mathbf{Q}}\left(q_1, \ldots, q_L\right)$ into fixed-point equation (4.10), it reduces to a system of L coupled equations in terms of $q_1, \ldots, q_L$. Denoting the solution of this system of equations with $(q_1^\star, \ldots, q_L^\star)$, the correlation matrix is finally calculated as

$$\mathbf{Q} = \tilde{\mathbf{Q}}\left(q_1^\star, \ldots, q_L^\star\right). \tag{4.30}$$

By this indirect approach, the fixed-point equation is tractably followed in an analytic way. There are however two main questions which raise in this respect:

1. What is the proper choice for the parameterized structure $\tilde{\mathbf{Q}}\left(q_1, \ldots, q_L\right)$?

2. How can we assure that the correlation matrix with the enforced structure is the exact solution to the fixed-point equation?

These questions have been answered in the literature of spin glasses based on the physical meaning of the correlation matrix. In fact, due to some specific properties of the moment function at its saddle-point, the initial conjecture on the structure is given by assuming so-called replica symmetry (RS) which postulates that the replicas of the spin glass behave symmetrically such that any permutation of them results in a similar correlation matrix.

Although physical intuitions initially suggest RS, there is no necessity for RS in general to hold. There are hence several analyses in the literature which discuss stability of the RS ansatz; see for example discussions in [26, 61, 62]. Invoking these stability tests, various energy models are shown to not exhibit RS. This observation means that for these energy models, the free energy derived via the replica method,

under RS, does not describe the exact free energy of the spin glass, at least for some temperatures. The inconsistency of the replica ansatz in these cases comes from the fact that the replicated spin glass for these energy models do not show RS. To find the proper replica ansatz, it is suggested by Parisi in [63] to *break* RS structure gradually in a systematic manner. The proposed scheme by Parisi is hence named as replica symmetry breaking (RSB). For the energy models, whose RS ansatz fails to derive the free energy, the replica solution under RSB is shown to be stable.

Considering the generic RLS regression method, the Hamiltonian of the corresponding spin glass describes various energy models depending on support $\mathbb{X}$ and regularization term $u_{\mathrm{v}}(\cdot)$. As a result, there might be some choices for the support and regularization, for which the corresponding spin glass does not show RS and the exact derivation of the free energy requires RSB. We hence derive the replica ansatz under both RS and RSB in the sequel.

4.2 The RS Ansatz

The most basic parameterized structure for the correlation matrix is suggested by RS which is proposed based on observations in analyses of basic energy models. The physical meaning of RS is that the replicas of the spin glass are independent of any permutation on their order. This means that any change on the indices of replicas $\{\boldsymbol{v}_a\}$ results in the same correlation matrix. Following the mathematical formulation, RS suggests to consider the parameterized structure

$$\tilde{\mathbf{Q}}(\chi, q) = \frac{\chi}{\beta}\mathbf{I}_t + q\mathbf{1}_t \tag{4.31}$$

at inverse temperature β for some scalars χ and q. Considering the definition of $\mathbf{Q}$ in (4.24), this structure assumes that for each two replicas $\boldsymbol{v}_a$ and $\boldsymbol{v}_b$

$$\frac{1}{N}\left\|\boldsymbol{x}_0 - \boldsymbol{v}_a\right\|^2 = \frac{\chi}{\beta} \tag{4.32a}$$

$$\frac{1}{N}\left(\boldsymbol{x}_0 - \boldsymbol{v}_a\right)^{\mathsf{H}}\left(\boldsymbol{x}_0 - \boldsymbol{v}_b\right) = q + \frac{\chi}{\beta}. \tag{4.32b}$$

In other words, RS postulates that correlations between each two distinct replicas are the same, which might be different from each replica's self-correlation.

By substituting the RS parameterized structure into the general replica ansatz, the fixed-point equation reduces to a system of two equations which determines χ and q. The substitution moreover lets us to compute limits in the general ansatz analytically. The result is referred to as the *RS ansatz* and is represented in Proposition 4.2.

Proposition 4.2 (RS Ansatz)**.** *Consider a regression problem with linear model whose regression coefficients are determined by the generic RLS method, given in Chapter 2, from support* $\mathbb{X} \subseteq \mathbb{A}_\zeta$*. Assume that the corresponding spin glass exhibits RS. For some non-negative real variables* χ *and* q*, define*

$$\theta_0^2 \coloneqq \left[\mathrm{R}_{\mathbf{J}}(-\frac{\chi}{\lambda})\right]^{-2} \frac{\partial}{\partial \chi}\left[\left(\sigma^2\chi - \lambda q\right)\mathrm{R}_{\mathbf{J}}(-\frac{\chi}{\lambda})\right] \tag{4.33a}$$

$$\tau \coloneqq \left[\mathrm{R}_{\mathbf{J}}(-\frac{\chi}{\lambda})\right]^{-1} \lambda. \tag{4.33b}$$

Let x_0 *be distributed with* $\mathrm{p}_0(\mathrm{x}_0)$ *and*

$$\mathrm{y} = \mathrm{x}_0 + \theta_0 \mathrm{z} \tag{4.34}$$

for some $\mathrm{z} \in \mathbb{A}_\zeta$*. Define* x *as*

$$\mathrm{x} = \underset{v \in \mathbb{X}}{\operatorname{argmin}} \ \frac{\zeta}{2\tau}\left|\mathrm{y} - v\right|^2 + u(v). \tag{4.35}$$

Set χ *and* q *such that they satisfy*

$$\chi = \frac{\tau}{\theta_0}\ \mathbb{E}_{\mathrm{x}_0}\left\{\int \mathbb{Re}\left\{(\mathrm{x} - \mathrm{x}_0)\,\mathrm{z}^*\right\}\mathrm{D}^\zeta \mathrm{z}\right\} \tag{4.36a}$$

$$q = \mathbb{E}_{\mathrm{x}_0}\left\{\int \left|\mathrm{x} - \mathrm{x}_0\right|^2 \mathrm{D}^\zeta \mathrm{z}\right\}. \tag{4.36b}$$

Then, the free energy of the corresponding spin glass at zero temperature is

$$\bar{\mathcal{F}}_{\mathrm{RS}}^0 = \Delta\mathcal{F}_{\mathrm{RS}} + \frac{\zeta}{2\tau}\left[\mathbb{E}_{\mathrm{x}_0}\left\{\int \left|\mathrm{y} - \mathrm{x}\right|^2 + u(\mathrm{x})\,\mathrm{D}^\zeta \mathrm{z}\right\} - \theta_0^2\right] \tag{4.37}$$

where $\Delta\mathcal{F}_{\mathrm{RS}}$ *is*

$$\Delta\mathcal{F}_{\mathrm{RS}} \coloneqq \frac{\zeta}{2\lambda}\left[\alpha\sigma^2 + G\left(\chi\right) - \chi G'\left(\chi\right) - q\mathrm{R}_{\mathbf{J}}(-\frac{\chi}{\lambda})\right]. \tag{4.38}$$

with function $G\left(\cdot\right)$ *being defined as*

$$G\left(\omega\right) \coloneqq \left[q - \frac{\sigma^2}{\lambda}\omega\right]\mathrm{R}_{\mathbf{J}}(-\frac{\omega}{\lambda}). \tag{4.39}$$

Moreover, the asymptotic LSE reads

$$\mathrm{LSE}_{\mathsf{RLS}} = \sigma^2 + \alpha^{-1}R'_{\mathrm{LSE}}\left(\chi\right), \tag{4.40}$$

with $R_{\mathrm{LSE}}\left(\omega\right) = \omega G\left(\omega\right)$*, and the asymptotic distortion is determined as*

$$D^{\mathbb{W}}_{\mathsf{RLS}} = \mathbb{E}\left\{\int \mathsf{d}\left(\mathrm{x};\mathrm{x}_0\right)\mathrm{D}^{\zeta}\mathrm{z}\right\}. \tag{4.41}$$

In case of multiple solutions for χ *and* q*, the one is chosen whose zero-temperature free energy is minimized.*

Proof. By inserting the RS correlation matrix into the fixed-point equation (4.10), the coupled equations in (4.36a) and (4.36b) are derived using the eigendecomposition of the correlation matrix. The free energy, as well as the asymptotic LSE and distortion, is moreover calculated by replacing the RS correlation matrix into Proposition 4.1 and taking the limits. Detailed derivations are given in Appendix B. □

The RS ansatz describes the asymptotic performance of the generic RLS via a scalar RLS problem. In fact, considering y to be the regressand for a scalar regression problem, (4.35) can be interpreted as an RLS method which recovers scalar regression coefficient x. This observation describes the *decoupling property* of RLS which will be discussed in details in the next chapter.

4.3 Consistency Test via Zero-temperature Entropy

As discussed earlier, not all the energy models necessarily exhibit RS. In other words, for some specific choices of the Hamiltonian, the solution to the fixed-point equation is not of the RS form. This means that, in such scenarios, the asymptotic performance measures given by the RS ansatz are not exact, and hence RS needs to be broken by some number of breaking steps. In the literature of spin glasses, the validity of RS postulation is often addressed by consistency and stability tests.

A primary test for consistency of the RS ansatz is based on calculating the *zero-temperature entropy* of the corresponding spin glass. This consistency test follows the following property of spin glasses.

Property 3 (Zero-temperature entropy)**.** *As a spin glass freezes, i.e.,* $1/\beta$ *tends to zero, its normalized entropy converges to zero.*

Proof. In Chapter 3, it was shown that at zero temperature the Boltzmann-Gibbs distribution converges to an indicator function. In other words, at zero temperature, the microstate converges to its deterministic *ground state*. Noting that the entropy of the corresponding spin glass is the conditional entropy of the microstate[2], it is concluded that at zero temperature, the normalized entropy is zero. □

The zero-temperature entropy is in fact a well-known property of any thermodynamic system. From the physical point of view, it simply says that the system at zero temperature has no probabilistic ambiguity. This is intuitive, since at zero temperature, the particles are all frozen to the ground state. Invoking this property, a basic consistency test is designed as follows: Assuming that the initial conjecture of replica continuity is valid, the exact replica ansatz should give the true free energy. Consequently, the corresponding entropy should be exact. This means that, when a postulated structure for the replica correlation matrix, e.g., RS, is correct, the derived entropy at zero temperature should be *zero*. It is clear that this test gives only necessary conditions, and not sufficient criteria, for consistency. In other words, when at zero temperature the entropy is not converging to zero, it is concluded that the

[2]This holds in fact for discrete supports. For a continuous $\mathbb{X}$, it represents the conditional differential entropy of the microstate.

postulated structure is not giving the true replica ansatz. Nevertheless, for cases with converging entropy, it does not guarantee validity of the postulation.

Regarding the linear regression problem, several particular cases are available in the literature whose RS ansätze fail to achieve zero entropy at zero temperature. More interestingly, in these inconsistent cases, the entropy takes negative values which is *theoretically impossible*[3]. For these cases other stability tests further demonstrate inconsistency of the RS ansatz; see for example [64]. The replica ansatz, in these particular examples, after breaking RS with some steps of RSB depicts consistency with simulations, and the entropy derived by the corresponding RSB ansatz converges to zero. Inspired by these results, we evaluate the zero-temperature entropy of the corresponding spin glass considering the generic replica ansatz, and utilize it as a measure of consistency in the sequel.

Proposition 4.3 (Zero-temperature entropy)**.** *Consider the spin glass corresponding to a linear regression problem with a generic RLS method. The zero-temperature entropy, given by the general replica ansatz in Proposition 4.1, reads*

$$\bar{\mathcal{H}}^0 \coloneqq \lim_{\beta\uparrow\infty} \bar{\mathcal{H}}\left(\beta\right) = \lim_{\beta\uparrow\infty} \beta^2 \frac{\partial}{\partial\beta} \Delta E\left(\beta\right), \tag{4.42}$$

where $\Delta E\left(\beta\right)$ is the energy difference function.

Proof. Starting from Proposition 4.1, the entropy at inverse temperature β reads

$$\bar{\mathcal{H}}\left(\beta\right) = \beta^2 \frac{\mathrm{d}}{\mathrm{d}\beta} \bar{\mathcal{F}}\left(\beta\right) \tag{4.43a}$$

$$\overset{\star}{=} \beta^2 \frac{\partial}{\partial\beta} \left[\Delta E\left(\beta\right) + \mathcal{F}^{\mathsf{R}}\left(\beta\right)\right] \tag{4.43b}$$

$$= \beta^2 \frac{\partial}{\partial\beta} \Delta E\left(\beta\right) + \lim_{t\downarrow 0} \beta^2 \frac{\partial}{\partial\beta} \mathcal{F}^{\mathsf{R}}\left(\beta, t\right) \tag{4.43c}$$

$$= \beta^2 \frac{\partial}{\partial\beta} \Delta E\left(\beta\right) + \lim_{t\downarrow 0} \mathcal{H}^{\mathsf{R}}\left(\beta, t\right) \tag{4.43d}$$

[3]Note that the entropy is always non-negative.

where $\star$ comes from Proposition 4.1, and $\mathcal{H}^{\mathsf{R}}(\beta, t)$ denotes the entropy of the spin glass of replicas defined in Definition 4.4. Since this spin glass is a thermodynamic system, for any $t \in \mathbb{N}$, we have

$$\lim_{\beta \uparrow \infty} \mathcal{H}^{\mathsf{R}}(\beta, t) = 0. \tag{4.44}$$

Consequently, the real continuation of the entropy function fulfills the same property, and hence, the zero-temperature entropy reduces to

$$\bar{\mathcal{H}}^{0} = \lim_{\beta \uparrow \infty} \beta^2 \frac{\partial}{\partial \beta} \Delta E(\beta) \tag{4.45}$$

which concludes the proof. □

4.3.1 RS Zero-temperature Entropy

Proposition 4.3 indicates that the zero-temperature entropy directly depends on the structure of replica correlation matrix. This demonstrates the fact that it is an effective consistency measure. In Appendix B, it is shown that for the RS correlation matrix, the energy difference function reads

$$\Delta E(\beta) = \frac{\zeta \chi}{2\lambda\beta} \left[\int_0^1 \mathrm{R}_{\mathbf{J}}(-\frac{\chi}{\lambda}\omega)\mathrm{d}\omega - \mathrm{R}_{\mathbf{J}}(-\frac{\chi}{\lambda}) \right] + \Delta\mathcal{F}_{\mathrm{RS}} - \frac{\zeta\alpha\sigma^2}{2\lambda}\,. \tag{4.46a}$$

Hence, the zero-temperature entropy under RS is given by

$$\bar{\mathcal{H}}^{0}_{\mathrm{RS}} = \frac{\zeta\chi}{2\lambda} \left[\mathrm{R}_{\mathbf{J}}(-\frac{\chi}{\lambda}) - \int_0^1 \mathrm{R}_{\mathbf{J}}(-\frac{\chi}{\lambda}\omega)\mathrm{d}\omega \right]. \tag{4.47}$$

It is later shown that (4.47) gives a generic expression for the zero-temperature entropy which holds for RS and RSB structures.

4.4 Replica Symmetry Breaking Ansätze

There are several energy models for which, despite the initial intuition, the correlation matrix at the saddle-point does not exhibit RS. From mathematical points of view, this states that the solution to fixed-point equation (4.10), which minimizes the free energy, is not of the symmetric form in (4.31). Based on discussions in Section 4.1.3, we need to extend the search for $\mathbf{Q}$ to a wider set of parameterized matrices which encloses asymmetric structures as well. This task is done by the RSB scheme introduced by Parisi in [63]. Parisi's scheme starts from RS and widens the structure recursively. In the context of the replica method, this recursive widening is called *breaking* and is performed as follows.

Definition 4.5 (Parisi's breaking scheme)**.** *Let t be a multiple of integer ξ, and $\mathbf{Q}^{[\ell]}$ represent a $\xi \times \xi$ correlation matrix. Parisi's breaking scheme constructs a new $t \times t$ correlation matrix $\mathbf{Q}^{[\ell+1]}$ as*

$$\mathbf{Q}^{[\ell+1]} = \mathbf{I}_{\frac{t}{\xi}} \otimes \mathbf{Q}^{[\ell]} + q\mathbf{1}_t \tag{4.48}$$

for some real scalar q.

The RSB scheme suggests that we start with an RS matrix, i.e.,

$$\mathbf{Q}^{[0]} = \frac{\chi}{\beta}\mathbf{I}_\xi + p\mathbf{1}_\xi \tag{4.49}$$

for some scalars χ and p. In this case, $\mathbf{Q}^{[1]}$ reads

$$\mathbf{Q}^{[1]} = \frac{\chi}{\beta}\mathbf{I}_t + p\mathbf{I}_{\frac{t}{\xi}} \otimes \mathbf{1}_\xi + q\mathbf{1}_t. \tag{4.50}$$

$\mathbf{Q}^{[1]}$ describes an RSB structure with one step of breaking which we refer to as *one-RSB*. More breaking steps can be achieved by repeating Parisi's breaking scheme for more number of recursions. For instance, two steps of RSB is obtained by inserting $\mathbf{Q}^{[1]}$ in the breaking scheme and determining $\mathbf{Q}^{[2]}$.

In the sequel, the replica ansätze for RSB structured correlation matrices are determined. We start with one step of breaking, and then extend the approach to an RSB structure with an arbitrary number of breaking steps.

4.4.1 One-step RSB

Due to some analyticity issues, ξ in the RSB structures is often set to

$$\xi = \frac{\mu}{\beta} \tag{4.51}$$

for some scalar μ. Consequently, one-RSB considers parameterized structure

$$\tilde{\mathbf{Q}}\left(\chi, p, \mu, q\right) = \frac{\chi}{\beta}\mathbf{I}_t + p\mathbf{I}_{\frac{t\beta}{\mu}} \otimes \mathbf{1}_{\frac{\mu}{\beta}} + q\mathbf{1}_t \tag{4.52}$$

for scalars χ, p, μ and q. By setting $p = 0$, the one-RSB matrix is reduced to an RS matrix. This indicates that the set of RS-structured matrices is a subset of one-RSB matrices, and hence RSB structure encloses the RS correlation matrices, as well.

Substituting into the general replica ansatz, the one-RSB ansatz is derived as given in the following proposition.

Proposition 4.4 (One-RSB Ansatz)**.** *Consider a regression problem with linear model whose coefficients are determined by the generic RLS method, given in Chapter 2, from support $\mathbb{X} \subseteq \mathbb{A}_\zeta$. Assume that the corresponding spin glass exhibits one step of RSB. For some non-negative real variables χ, p, μ and q, define*

$$\theta_0^2 = \left[\mathrm{R}_{\mathbf{J}}(-\frac{\chi}{\lambda})\right]^{-2} \frac{\partial}{\partial\chi}\left[\left(\sigma^2\tilde{\chi} - \lambda q\right)\mathrm{R}_{\mathbf{J}}(-\frac{\tilde{\chi}}{\lambda})\right] \tag{4.53a}$$

$$\theta_1^2 = \left[\mathrm{R}_{\mathbf{J}}(-\frac{\chi}{\lambda})\right]^{-2} \frac{\lambda}{\mu}\left[\mathrm{R}_{\mathbf{J}}(-\frac{\chi}{\lambda}) - \mathrm{R}_{\mathbf{J}}(-\frac{\tilde{\chi}}{\lambda})\right], \tag{4.53b}$$

$$\tau = \left[\mathrm{R}_{\mathbf{J}}(-\frac{\chi}{\lambda})\right]^{-1}\lambda \tag{4.53c}$$

where $\tilde{\chi} = \chi + \mu p$. *Let* x_0 *be distributed with* $\mathrm{p}_0(\mathrm{x}_0)$ *and*

$$\mathrm{y} = \mathrm{x}_0 + \theta_0 \mathrm{z}_0 + \theta_1 \mathrm{z}_1 \tag{4.54}$$

for some $\mathrm{z}_0, \mathrm{z}_1 \in \mathbb{A}_\zeta$. *Define* x *as*

$$\mathrm{x} = \underset{v \in \mathbb{X}}{\operatorname{argmin}} \ \frac{\zeta}{2\tau} |\mathrm{y} - v|^2 + u(v) \tag{4.55}$$

and let

$$\bar{\Lambda}(\mathrm{z}_0, \mathrm{z}_1 | \mathrm{x}_0) \coloneqq \frac{\Lambda(\mathrm{z}_0, \mathrm{z}_1 | \mathrm{x}_0)}{\int \Lambda(\mathrm{z}_0, \mathrm{z}_1 | \mathrm{x}_0) \, \mathrm{D}^\zeta \mathrm{z}_1} \tag{4.56}$$

with $\Lambda(\mathrm{z}_0, \mathrm{z}_1 | \mathrm{x}_0)$ *being*

$$\Lambda(\mathrm{z}_0, \mathrm{z}_1 | \mathrm{x}_0) = \exp\left\{ -\mu \left[\frac{\zeta}{2\tau} |\mathrm{y} - \mathrm{x}|^2 - \frac{\zeta}{2\tau} |\mathrm{y} - \mathrm{x}_0|^2 + u(\mathrm{x}) \right] \right\}. \tag{4.57}$$

Moreover, define function $G(\omega)$ *as*

$$G(\omega) \coloneqq \left[q - \frac{\sigma^2}{\lambda} \omega \right] \mathrm{R}_{\mathbf{J}}(-\frac{\omega}{\lambda}). \tag{4.58}$$

Then, the zero-temperature free energy reads

$$\bar{\mathcal{F}}^{0(1)}_{\mathrm{RSB}} = \Delta \mathcal{F}^{(1)}_{\mathrm{RSB}} + \frac{1}{\mu} \left[\Delta L^{(1)}_{\mathrm{R}} - \mathbb{E}_{\mathrm{x}_0} \left\{ \int \log \int \Lambda(\mathrm{z}_0, \mathrm{z}_1 | \mathrm{x}_0) \, \mathrm{D}^\zeta \mathrm{z}_1 \mathrm{D}^\zeta \mathrm{z}_0 \right\} \right], \tag{4.59}$$

with $\Delta \mathcal{F}^{(1)}_{\mathrm{RSB}}$ *and* $\Delta L^{(1)}_{\mathrm{R}}$ *being*

$$\Delta \mathcal{F}^{(1)}_{\mathrm{RSB}} \coloneqq \frac{\zeta}{2\lambda} \left[\alpha \sigma^2 + G(\tilde{\chi}) - \tilde{\chi} G'(\tilde{\chi}) - q \mathrm{R}_{\mathbf{J}}(-\frac{\tilde{\chi}}{\lambda}) \right], \tag{4.60a}$$

$$\Delta L^{(1)}_{\mathrm{R}} \coloneqq \int_\chi^{\tilde{\chi}} \mathrm{R}_{\mathbf{J}}(-\frac{\omega}{\lambda}) \mathrm{d}\omega - L_{\mathrm{R}} \tag{4.60b}$$

and

$$L_{\mathrm{R}} \coloneqq \tilde{\chi}\mathrm{R}_{\mathbf{J}}(-\frac{\tilde{\chi}}{\lambda}) - \chi\mathrm{R}_{\mathbf{J}}(-\frac{\chi}{\lambda}). \tag{4.61}$$

Moreover, the asymptotic LSE reads

$$\mathrm{LSE}_{\mathsf{RLS}} = \sigma^2 + \alpha^{-1}\left[R'_{\mathrm{LSE}}(\chi) + \frac{1}{\mu}L_{\mathrm{R}}\right], \tag{4.62}$$

with $R_{\mathrm{LSE}}(\omega) \coloneqq \omega G(\omega)$*, and the asymptotic distortion is given by*

$$D^{\mathbb{W}}_{\mathsf{RLS}} = \mathbb{E}_{\mathrm{x}_0}\left\{\int \mathsf{d}(\mathrm{x},\mathrm{x}_0)\,\bar{\Lambda}(\mathrm{z}_0,\mathrm{z}_1|\mathrm{x}_0)\,\mathrm{D}^{\zeta}\mathrm{z}_1\mathrm{D}^{\zeta}\mathrm{z}_0\right\}. \tag{4.63}$$

The parameters χ*,* p*,* q *and* μ *are found, such that they satisfy*

$$\tilde{\chi} = \frac{\tau}{\theta_0}\mathbb{E}_{\mathrm{x}_0}\left\{\int \mathbb{R}\mathrm{e}\left\{(\mathrm{x}-\mathrm{x}_0)\,\mathrm{z}_0^*\right\}\,\bar{\Lambda}(\mathrm{z}_0,\mathrm{z}_1|\mathrm{x}_0)\;\mathrm{D}^{\zeta}\mathrm{z}_1\;\mathrm{D}^{\zeta}\mathrm{z}_0\right\} \tag{4.64a}$$

$$\tilde{\chi} + \mu q = \frac{\tau}{\theta_1}\mathbb{E}_{\mathrm{x}_0}\left\{\int \mathbb{R}\mathrm{e}\left\{(\mathrm{x}-\mathrm{x}_0)\,\mathrm{z}_1^*\right\}\,\bar{\Lambda}(\mathrm{z}_0,\mathrm{z}_1|\mathrm{x}_0)\;\mathrm{D}^{\zeta}\mathrm{z}_1\;\mathrm{D}^{\zeta}\mathrm{z}_0\right\} \tag{4.64b}$$

$$q + p = \mathbb{E}_{\mathrm{x}_0}\left\{\int |\mathrm{x}-\mathrm{x}_0|^2\,\bar{\Lambda}(\mathrm{z}_0,\mathrm{z}_1|\mathrm{x}_0)\;\mathrm{D}^{\zeta}\mathrm{z}_1\;\mathrm{D}^{\zeta}\mathrm{z}_0\right\} \tag{4.64c}$$

and

$$\frac{\zeta}{2\lambda}\left[(p+q)\,\mathrm{R}_{\mathbf{J}}(-\frac{\chi}{\lambda}) - q\mathrm{R}_{\mathbf{J}}(-\frac{\tilde{\chi}}{\lambda}) - \frac{1}{\mu}\int_{\chi}^{\tilde{\chi}}\mathrm{R}_{\mathbf{J}}(-\frac{\omega}{\lambda})\mathrm{d}\omega\right] = \frac{1}{\mu}\,\mathrm{Div}\,(\mu) \tag{4.65}$$

where

$$\mathrm{Div}\,(\mu) \coloneqq \mathbb{E}_{\mathrm{x}_0}\left\{\int \bar{\Lambda}(\mathrm{z}_0,\mathrm{z}_1|\mathrm{x}_0)\log\bar{\Lambda}(\mathrm{z}_0,\mathrm{z}_1|\mathrm{x}_0)\;\mathrm{D}^{\zeta}\mathrm{z}_1\;\mathrm{D}^{\zeta}\mathrm{z}_0\right\}. \tag{4.66}$$

Proof. Similar to RS, the one-RSB ansatz is derived by substituting the corresponding structure in the general replica ansatz and taking the limits. The detailed derivations are given in Appendix C. □

4.4.2 B-steps RSB

Although there are particular instances for which the replica correlation matrix is of one-RSB form, most non-RS energy models require multiple number of breaking steps. The general belief in this respect is that an energy model either exhibits RS or requires infinite number of RSB, unless it shows specific properties; see for example discussions on the REM in [61].

To perturb the RS structure further, Parisi's breaking scheme is recursed for extra steps: Starting from an RS-structured matrix $\mathbf{Q}^{[0]}$, the breaking scheme is repeated for B steps, such that in each step $\mathbf{Q}^{[\ell]}$ is set to be the structure determined in previous step. $\mathbf{Q}^{[B]}$ is hence parameterized with $2B+2$ parameters. We refer to this perturbed structure as B-RSB which is of the following form:

$$\tilde{\mathbf{Q}}\left(\chi, \{p_b\}, \{\mu_b\}, q\right) = \frac{\chi}{\beta}\mathbf{I}_t + \sum_{b=1}^{B} p_b \mathbf{I}_{\frac{t\beta}{\mu_b}} \otimes \mathbf{1}_{\frac{\mu_b}{\beta}} + q\mathbf{1}_t \tag{4.67}$$

for some real χ and q, and sequences $\{p_b\}$ and $\{\mu_b\}$ with $b \in [B]$. For recursive breaking, we further restrict μ_b, for $b \in [B-1]$, to satisfy

$$\frac{\mu_{b+1}}{\mu_b} \in \mathbb{N}. \tag{4.68}$$

The B-RSB structure recover the RS, as well as ℓRSB for $\ell < B$, as a special case. For instance, by setting $p_b = 0$ for $b > \ell$, the structure reduces to ℓ-RSB.

Proposition 4.5 (B-RSB Ansatz)**.** *Consider a regression problem with linear model whose coefficients are determined by the generic RLS method, given in Chapter 2, from the support $\mathbb{X} \subseteq \mathbb{A}_\zeta$. Assume that the corresponding spin glass exhibits B steps of RSB. For some scalars χ and q, and some sequences $\{p_b\}$ and $\{\mu_b\}$, define $\tilde{\chi}_0 \coloneqq \chi$ and*

$$\tilde{\chi}_b \coloneqq \chi + \sum_{\kappa=1}^{b} \mu_\kappa p_\kappa \tag{4.69}$$

for $b \in [B]$. Let τ, θ_0 and θ_b for $b \in [B]$ be defined as

$$\theta_0^2 = \left[\mathrm{R}_{\mathbf{J}}(-\frac{\tilde{\chi}_0}{\lambda})\right]^{-2} \frac{\partial}{\partial \tilde{\chi}_b} \left\{ \left[\sigma^2 \tilde{\chi}_b - \lambda q\right] \mathrm{R}_{\mathbf{J}}(-\frac{\tilde{\chi}_b}{\lambda}) \right\}, \tag{4.70a}$$

$$\theta_b^2 = \left[\mathrm{R}_{\mathbf{J}}(-\frac{\tilde{\chi}_0}{\lambda})\right]^{-2} \left[\mathrm{R}_{\mathbf{J}}(-\frac{\tilde{\chi}_{b-1}}{\lambda}) - \mathrm{R}_{\mathbf{J}}(-\frac{\tilde{\chi}_b}{\lambda})\right] \lambda \mu_b^{-1}, \tag{4.70b}$$

$$\tau = \left[\mathrm{R}_{\mathbf{J}}(-\frac{\tilde{\chi}_0}{\lambda})\right]^{-1} \lambda. \tag{4.70c}$$

For $\mathrm{x}_0 \sim \mathrm{p}_0(\mathrm{x}_0)$, define the random variable y as

$$\mathrm{y} = \mathrm{x}_0 + \sum_{b=0}^{B} \theta_b \mathrm{z}_b \tag{4.71}$$

where $\mathrm{z}_b \in \mathbb{A}_\zeta$, and let

$$\mathrm{x} = \underset{v \in \mathbb{X}}{\operatorname{argmin}} \ \frac{\zeta}{2\tau} |\mathrm{y} - v|^2 + u(v). \tag{4.72}$$

Denoting $\{\mathrm{z}_\kappa\}_b^B \coloneqq \{\mathrm{z}_b, \ldots, \mathrm{z}_B\}$ for $b \in [B]$, define $\bar{\Lambda}^{(b)}\left(\{\mathrm{z}_\kappa\}_{\kappa=b}^B, \mathrm{z}_0|\mathrm{x}_0\right)$ as

$$\bar{\Lambda}^{(b)}\left(\{\mathrm{z}_\kappa\}_{\kappa=b}^B, \mathrm{z}_0|\mathrm{x}_0\right) \coloneqq \frac{\Lambda^{(b)}\left(\{\mathrm{z}_\kappa\}_{\kappa=b}^B, \mathrm{z}_0|\mathrm{x}_0\right)}{\int \Lambda^{(b)}\left(\{\mathrm{z}_\kappa\}_{\kappa=b}^B, \mathrm{z}_0|\mathrm{x}_0\right) \mathrm{D}^\zeta \mathrm{z}_b} \tag{4.73}$$

where $\Lambda^{(1)}\left(\{\mathrm{z}_\kappa\}_{\kappa=1}^B, \mathrm{z}_0|\mathrm{x}_0\right)$ is defined as

$$\Lambda^{(1)}\left(\{\mathrm{z}_\kappa\}_{\kappa=1}^B, \mathrm{z}_0|\mathrm{x}_0\right) = \exp\left\{-\mu_1 \left[\frac{\zeta}{2\tau}|\mathrm{y} - \mathrm{x}|^2 - \frac{\zeta}{2\tau}|\mathrm{y} - \mathrm{x}_0|^2 + u(\mathrm{x})\right]\right\}. \tag{4.74}$$

and $\Lambda^{(b)}\left(\{\mathrm{z}_\kappa\}_{\kappa=b}^B, \mathrm{z}_0|\mathrm{x}_0\right)$ for $b \geq 2$ are recursively determined by

$$\Lambda^{(b)}\left(\{\mathrm{z}_\kappa\}_{\kappa=b}^B, \mathrm{z}_0|\mathrm{x}_0\right) \coloneqq \left[\int \Lambda^{(b-1)}\left(\{\mathrm{z}_\kappa\}_{\kappa=b-1}^B, \mathrm{z}_0|\mathrm{x}_0\right) \mathrm{D}^\zeta \mathrm{z}_{b-1}\right]^{\frac{\mu_b}{\mu_{b-1}}}. \tag{4.75}$$

Furthermore, define functions $G(\omega)$ *and* $\Delta \mathrm{R}_b(\cdot)$ *as*

$$G(\omega) \coloneqq \left[q - \frac{\sigma^2}{\lambda}\omega\right] \mathrm{R}_{\mathbf{J}}(-\frac{\omega}{\lambda}) \tag{4.76a}$$

$$\Delta \mathrm{R}_b(\omega) \coloneqq \tilde{\chi}_b \mathrm{R}_{\mathbf{J}}(-\frac{\tilde{\chi}_b}{\lambda}\omega) - \tilde{\chi}_{b-1}\mathrm{R}_{\mathbf{J}}(-\frac{\tilde{\chi}_{b-1}}{\lambda}\omega), \tag{4.76b}$$

and the probability measure $\mathrm{D}^{\zeta}\mathrm{F}_{\mathrm{RSB}}\left(\{\mathrm{z}_\kappa\}_{\kappa=0}^{B}|x_0\right)$ *as*

$$\mathrm{D}^{\zeta}\mathrm{F}_{\mathrm{RSB}}\left(\{\mathrm{z}_\kappa\}_{\kappa=0}^{B}|\mathrm{x}_0\right) \coloneqq \prod_{b=1}^{B} \bar{\Lambda}^{(b)}\left(\{\mathrm{z}_\kappa\}_{\kappa=b}^{B}, \mathrm{z}_0|\mathrm{x}_0\right) \mathrm{D}^{\zeta}\mathrm{z}_b\, \mathrm{D}^{\zeta}\mathrm{z}_0\,. \tag{4.77}$$

Find χ, $\{p_b\}$ *and* q *such that the following system of equations is satisfied*

$$\sum_{b=1}^{B} p_b + q = \mathbb{E}_{\mathrm{x}_0}\left\{\int |\mathrm{x}-\mathrm{x}_0|^2\, \mathrm{D}^{\zeta}\mathrm{F}_{\mathrm{RSB}}\left(\{\mathrm{z}_\kappa\}_{\kappa=0}^{B}|\mathrm{x}_0\right)\right\}, \tag{4.78a}$$

$$\tilde{\chi}_B = \frac{\tau}{\theta_0}\mathbb{E}_{\mathrm{x}_0}\left\{\int \mathbb{R}\mathrm{e}\left\{(\mathrm{x}-\mathrm{x}_0)\,\mathrm{z}_0^*\right\} \mathrm{D}^{\zeta}\mathrm{F}_{\mathrm{RSB}}\left(\{\mathrm{z}_\kappa\}_{\kappa=0}^{B}|\mathrm{x}_0\right)\right\} \tag{4.78b}$$

$$\tilde{\chi}_{b-1} + \mu_b\left(\sum_{\kappa=b}^{B} p_\kappa + q\right) = \frac{\tau}{\theta_b}\mathbb{E}_{\mathrm{x}_0}\left\{\int \mathbb{R}\mathrm{e}\left\{(\mathrm{x}-\mathrm{x}_0)\,\mathrm{z}_b^*\right\} \mathrm{D}^{\zeta}\mathrm{F}_{\mathrm{RSB}}\left(\{\mathrm{z}_\kappa\}_{\kappa=0}^{B}|\mathrm{x}_0\right)\right\} \tag{4.78c}$$

for $b \in [B]$. *Then, the zero-temperature free energy is given by minimizing*

$$\bar{\mathcal{F}}_{\mathrm{RSB}}^{0(B)} = \Delta\mathcal{F}_{\mathrm{RSB}}^{(B)} + \sum_{b=1}^{B}\frac{1}{\mu_b}\Delta L_{\mathrm{R}}^{(b)} - \frac{1}{\mu_B}\mathbb{E}_{\mathrm{x}_0}\left\{\int \log \int \Lambda^{(B)}\left(\mathrm{z}_B, \mathrm{z}_0|\mathrm{x}_0\right) \mathrm{D}^{\zeta}\mathrm{z}_B \mathrm{D}^{\zeta}\mathrm{z}_0\right\}. \tag{4.79}$$

over $\{\mu_b\} \in \mathbb{R}^{+B}$, *where* $\Delta\mathcal{F}_{\mathrm{RSB}}^{(B)}$ *and* $\Delta L_{\mathrm{R}}^{(b)}$ *are given by*

$$\Delta\mathcal{F}_{\mathrm{RSB}}^{(B)} \coloneqq \frac{\zeta}{2\lambda}\left[\alpha\sigma^2 + G(\tilde{\chi}_B) - \tilde{\chi}_B G'(\tilde{\chi}_B) - q\mathrm{R}_{\mathbf{J}}(-\frac{\tilde{\chi}_B}{\lambda})\right], \tag{4.80a}$$

$$\Delta L_{\mathrm{R}}^{(b)} \coloneqq \frac{\zeta}{2\lambda}\int_0^1 \left(\Delta \mathrm{R}_b(\omega) - \Delta \mathrm{R}_b(1)\right) \mathrm{d}\omega \tag{4.80b}$$

Setting $\{\mu_b\}$ *to the solution of this minimization problem, the asymptotic LSE is calculated by*

$$\mathrm{LSE}_{\mathsf{RLS}} = \sigma^2 + \frac{1}{\alpha}\left[R'_{\mathrm{LSE}}\left(\tilde{\chi}_B\right) + \sum_{b=1}^{B}\frac{1}{\mu_b}L_{\mathrm{R},b} + L_{\mathrm{R},0}\right]. \tag{4.81}$$

Here, $L_{\mathrm{R},b}$ *for* $b \in [B]$ *is defined as*

$$L_{\mathrm{R},b} \coloneqq \frac{2\lambda}{\zeta}\mathrm{Div}_b + \Delta\mathrm{R}_b\left(1\right) + \int \Delta\mathrm{R}_b\left(\omega\right)\mathrm{d}\omega, \tag{4.82}$$

where

$$\mathrm{Div}_b \coloneqq \mathbb{E}_{\mathrm{x}_0}\left\{\int \log\bar{\Lambda}^{(b)}\left(\{\mathrm{z}_\kappa\}_b^B, \mathrm{z}_0|\mathrm{x}_0\right)\mathrm{D}^{\zeta}\mathrm{F}_{\mathrm{RSB}}\left(\{\mathrm{z}_\kappa\}_{\kappa=0}^B|\mathrm{x}_0\right)\right\}, \tag{4.83}$$

$L_{\mathrm{R},0}$ *is given by*

$$L_{\mathrm{R},0} \coloneqq -q\mathrm{R}_{\mathbf{J}}(-\frac{\tilde{\chi}_B}{\lambda}) - \left(\sum_{b=1}^{B}p_b + q\right)\mathrm{R}_{\mathbf{J}}(-\frac{\chi}{\lambda}), \tag{4.84}$$

and $R_{\mathrm{LSE}}\left(\omega\right) \coloneqq \omega G\left(\omega\right)$*. The asymptotic distortion is further determined as*

$$D^{\mathbb{W}}_{\mathsf{RLS}} = \mathbb{E}_{\mathrm{x}_0}\left\{\int \mathsf{d}\left(\mathrm{x};\mathrm{x}_0\right)\mathrm{D}^{\zeta}\mathrm{F}_{\mathrm{RSB}}\left(\{\mathrm{z}_\kappa\}_{\kappa=0}^B|\mathrm{x}_0\right)\right\}. \tag{4.85}$$

When the system of fixed-point equations has multiple solutions, the solution is chosen whose resulting zero-temperature free energy is minimal.

Proof. The proof follows same approach as in Propositions 4.2 and 4.4. The detailed derivations are presented in Appendix D. □

4.4.3 RSB Zero-temperature Entropy

The zero-temperature entropy of the corresponding spin glass for a bRSB correlation matrix is derived by substituting the structure into Proposition 4.3. This substitution results in

$$\bar{\mathcal{H}}^0_{\mathrm{RSB}}[B] = \frac{\zeta\chi}{2\lambda}\left[\mathrm{R}_{\mathbf{J}}(-\frac{\chi}{\lambda}) - \int_0^1 \mathrm{R}_{\mathbf{J}}(-\frac{\chi}{\lambda}\omega)\mathrm{d}\omega\right] \tag{4.86}$$

which is straightforwardly derived from the results in Section D.3.2 in Appendix D.

Comparing $\bar{\mathcal{H}}^0_{\mathrm{RSB}}[B]$ with $\bar{\mathcal{H}}^0_{\mathrm{RS}}$, it is observed that the zero-temperature entropy has a generic form which does not depend on the number of breaking steps in RSB. This generic form only depends on χ. This result was conjectured in [64]. Nevertheless, the derivations therein showed the validity of the conjecture only for one step of RSB. The result in (4.86) justifies the validity of this belief.

By setting $\chi = 0$ in this generic form, the zero temperature entropy reduces to

$$\bar{\mathcal{H}}^0_{\mathrm{RSB}}[B] = 0 \tag{4.87}$$

for any integer B including $B = 0$ which denotes $\bar{\mathcal{H}}^0_{\mathrm{RS}}$. This means that $\chi = 0$ is a *sufficient* condition for having the zero-temperature entropy equal to zero. It is moreover known that for any probability distribution different from a single mass point[4], the R-transform is a *strictly increasing function* wherever its derivative with respect to a real argument exists; for the proof of this statement see [64, Appendix E]. Consequently, we can conclude that for any regression problem whose matrix of regressors is not a scaled version of the identity matrix, we have

$$\mathrm{R}_{\mathbf{J}}(-\frac{\chi}{\lambda}) \leq \int_0^1 \mathrm{R}_{\mathbf{J}}(-\frac{\chi}{\lambda}\omega)\mathrm{d}\omega \tag{4.88}$$

where the equality occurs if and only if $\chi = 0$. As a result, $\chi = 0$ is further a *necessary* condition to have a vanishing zero-temperature entropy. This imply that parameter χ in the RS and RSB ansätze determines the consistency of the ansatz. We hence can intuitively say that *the ansatz with smaller χ is more reliable.*

[4]It means for any $\mathrm{p}_x(x) \neq \delta(x - C)$ for a constant $C \neq 0$.

Remark 4.1. *Note that although the zero-temperature entropy is of a similar form in RS and RSB, it does not necessarily take the same value in these cases. In fact, χ in RS and RSB ansätze is calculated from different systems of fixed-point equations, and hence can take different values depending on the number of breaking steps.*

4.5 Bibliographic Notes

In the initial development of the mean-field theory by Sherrington and Kirkpatrick, the investigations were based on the RS assumption [29, 30]. The instability of this ansatz was later shown for some cases by Almeida and Thouless in [65]. Parisi hence introduced the RSB methodology to perturb RS iteratively [63,66,67]. Analyses under Parisi's scheme showed that the instability in the ansatz of Sherrington-Kirkpatrick model was due to the RS assumption [68, 69]. Following this result, Parisi provided some physical interpretation on RSB in [70]. This direction of study was further developed in a body of work by Mézard et al.; see for example [71, 72].

In the context of information theory, the primary work by Tanaka in [40] considered the RS ansatz to derive the asymptotics of MPM detectors. The similar approach was taken for later replica-based investigations in the literature; for example the studies in [43, 44, 46, 73]. The results given via the RS ansatz in these studies were intuitively correct, matched numerical simulations in computationally tractable cases, and were consistent with available rigorous bounds in the literature. As a result, further investigations under RSB were not addressed in these studies. The validity of the RS ansatz for some of these problems, including Tanaka's formula, was later shown via alternative rigorous approaches in [18, 48, 49, 51–54, 74].

Investigation of an information theoretic problem under the assumption of RSB was first considered by Yoshida et al. in [75] where the authors derived both the RS and one-RSB ansätze for the problem of multiuser detection in CDMA systems and discussed the impact of RSB on the asymptotic characterization in low noise scenarios. The initial information theoretic problem which showed clear inconsistency under RS was the problem of *vector precoding* primarily investigated in [45]. For the case with quadrature phase-shift-keying symbols, the asymptotic expression derived for the

energy penalty via the RS ansatz was observed to violate the rigorous lower bound derived in [76] when the load, i.e., α, exceeds 0.2. As a result, the authors further determined the one-RSB ansatz for this problem in [64]. Numerical investigations showed that the energy penalty given via the one-RSB ansatz was consistent with the lower bound for all loads in $[0, 1]$.

Several other problems in information theory are available which require investigations under RSB. An example is the ℓ_0-norm minimization problem. In [77], Kabashima et al. characterized the asymptotic performance of typical ℓ_p-norm minimization techniques for sparse recovery via the replica method. The study considered the RS ansatz for characterization. The stability analysis showed that for the case of $p = 0$, the solution given via the RS ansatz is instable and further investigations under RSB are required. In Chapter 6, we use the replica ansätze derived in this chapter and show that the asymptotic performance characterization of ℓ_0-norm minimization under RS is invalid for small loads. The one-RSB ansatz is however consistent with available bounds for a larger interval of loads. In Chapter 7, we demonstrate the similar behavior for some particular cases of MIMO precoding based on the RLS method.

4.6 Summary

In this chapter, the generic replica ansatz has been derived. The particular ansätze under the RS or RSB assumptions have been then derived as special cases of this generic solutions. Under RS, the ansatz is of the conventional form with a single auxiliary variable. This variable is shown by z in the ansatz and disappears in the final expressions by integrating with respect to Gaussian measure. The RSB ansätze are modified versions of this standard RS ansatz in which the auxiliary variable is summed with some *correction* terms. For B steps of RSB, there are B correction terms which are shown with $\mathrm{z}_1, \ldots, \mathrm{z}_B$ in the B-RSB ansatz. The zero-temperature entropy has been was further calculated for the generic replica ansatz. It has been shown that for RS and RSB ansätze, the zero-temperature entropy is of the similar form which only depends on the scalar parameter χ. Following the properties of the

R-transform, it has been concluded that the zero-temperature entropy converges to zero, if and only if parameter χ of the given ansatz tends to zero.

The derived RSB ansätze can be alternatively represented in terms of a scalar linear regression problem with RLS method. This point is illustrated in the subsequent chapter where we demonstrate the concept of decoupling principle.

Chapter 5

Decoupling Property of RLS

The asymptotic characterization of the generic RLS method under the B-RSB ansatz can be represented in terms of a scalar regression problem. This property is often referred to as the *decoupling principle*. In its generic form, the decoupling principle indicates that the regression coefficients determined via the generic RLS method converge in distribution to the outputs of a bank of the scalar linear regression problems. This result can significantly simplify the derivations and the representation of asymptotic characterization.

The RS decoupling principle has been known for some special case of linear regression problem with RLS method. In this chapter, we derive this principle for a wider class of settings. In the RS form of the principle, the scalar setting has Guassian error. Such an observation agrees with the initial intuition on the decoupling principle: It is intuitively expected that the impact of regression error and the coupling introduced by the linear system and RLS method be Guassian in the large-system limit. We further extend the scope of decoupling principle into cases whose corresponding spin glasses do not exhibit RS. These derivations demonstrate an interesting result: Under RSB with B steps of breaking, decoupled regression error is *not* Gaussian and *statistically depends* on the true regression coefficients. We try to provide some illustrations for this new finding.

The alternative representation of the replica ansatz enables us to formulate the fixed-point equations of the B-RSB ansatz as the *steady state* of a transition system. We call this system the *replica simulator* and illustrate its properties via some examples.

5.1 An Illustrative Example

A simple way to understand the concept of asymptotic decoupling is to look at linear regression from the inference point of view. To this end, let us consider the particular example of signal recovery problem: In this problem, the vector of regressands, i.e., $\boldsymbol{y} \in \mathbb{A}_{\zeta}^{M}$, denotes the vector of observations which are obtained by linearly measuring the true signal samples in $\boldsymbol{x}_0 \in \mathbb{X}^N$ via the projectors collected in $\mathbf{A} \in \mathbb{A}_{\zeta}^{M \times N}$. Following the statistical model represented in Chapter 2, we assume that the signal samples are i.i.d. distributed with $\mathrm{p}_0(\cdot)$. Using the generic RLS method, the signal samples are estimated as

$$\boldsymbol{x} = \mathbf{g}_{\mathsf{RLS}}(\boldsymbol{y}|\mathbf{A}) \tag{5.1}$$

with $\mathbf{g}_{\mathsf{RLS}}(\cdot|\cdot)$ being defined in (2.11). In this case, the distortion achieved by the RLS method averaged over all the samples, i.e., $\mathbb{W}(N) = [N]$, with respect to distortion function $\mathsf{d}(\cdot;\cdot)$ is

$$D_N^{[N]}\{\mathbf{g}_{\mathsf{RLS}}\} = \frac{1}{N}\sum_{n=1}^{N}\mathbb{E}\left\{\mathsf{d}(x_n; x_{0n})\right\}. \tag{5.2}$$

To characterize the asymptotic performance of signal recovery, let us assume that the problem exhibits RS[1]. In this case, the asymptotic limit of the average distortion is calculated via Proposition 4.2 in Chapter 4 as

$$\lim_{N\uparrow\infty} D_N^{[N]}\{\mathbf{g}_{\mathsf{RLS}}\} = \lim_{N\uparrow\infty}\frac{1}{N}\sum_{n=1}^{N}\mathbb{E}\left\{\mathsf{d}(x_n; x_{0n})\right\} \tag{5.3a}$$

$$= \mathbb{E}\left\{\int \mathsf{d}(\mathrm{x};\mathrm{x}_0)\,\mathrm{D}^{\zeta}\mathrm{z}_0\right\}, \tag{5.3b}$$

where the random variables x_0 and x are specified as follows:

- x_0 is distributed with $\mathrm{p}_0(\cdot)$.

[1] Note that this assumption is not necessarily valid and depends on $\mathbb{X}$ and the regularization term in general.

- x is determined as

$$\mathrm{x} = \underset{v \in \mathbb{X}}{\operatorname{argmin}} \ \frac{\zeta}{2\tau} \left| \mathrm{y} - v \right|^2 + u\left(v\right). \tag{5.4}$$

  for $\mathrm{y} = \mathrm{x}_0 + \theta_0 \mathrm{z}_0$, where θ_0 and τ are explicitly calculated in Proposition 4.2.

In (5.4), x can be interpreted as the estimation of x_0 from the noisy observation y via the RLS method with regularization term $u\left(\cdot\right)$ and tuning factor τ.

Considering the above interpretation and noting that $\int \mathrm{D}^{\zeta}\mathrm{z}_0$ determines expectation with respect to $\mathcal{N}^{\zeta}\left(0,1\right)$, z_0 can be observed as Gaussian noise, and hence (5.3b) can be rewritten as

$$\mathbb{E}\left\{ \int \mathsf{d}\left(\mathrm{x};\mathrm{x}_0\right) \mathrm{D}^{\zeta}\mathrm{z}_0 \right\} = \mathbb{E}_{\mathrm{x}_0,\mathrm{z}_0}\left\{ \mathsf{d}\left(\mathbf{g}_{\mathsf{RLS}}\left(\mathrm{x}_0 + \theta_0 \mathrm{z}_0 | 1\right) ; \mathrm{x}_0 \right) \right\} \tag{5.5a}$$

$$\overset{\dagger}{=} \mathbb{E}_{x_{0n},\mathrm{z}_n}\left\{ \mathsf{d}\left(\mathbf{g}_{\mathsf{RLS}}\left(x_{0n} + \mathrm{z}_n | 1\right) ; x_{0n} \right) \right\} \tag{5.5b}$$

$$\overset{\star}{=} \frac{1}{N} \sum_{n=1}^{N} \mathbb{E}_{x_{0n},\mathrm{z}_n}\left\{ \mathsf{d}\left(\mathbf{g}_{\mathsf{RLS}}\left(x_{0n} + \mathrm{z}_n | 1\right) ; x_{0n} \right) \right\} \tag{5.5c}$$

where $\mathrm{z}_1, \ldots, \mathrm{z}_N$ is an i.i.d. sequence whose entries are distributed with $\mathrm{z}_n \sim \mathcal{N}^{\zeta}\left(0, \theta_0^2\right)$. In (5.5c), $\dagger$ follows the fact that the entries of $\boldsymbol{x}_0$ are i.i.d. and distributed identical to x_0. Moreover, $\star$ follows the fact that

$$\mathbb{E}_{x_{0n},\mathrm{z}_n}\left\{ \mathsf{d}\left(\mathbf{g}_{\mathsf{RLS}}\left(x_{0n} + \mathrm{z}_n | 1\right) ; x_{0n} \right) \right\} \tag{5.6}$$

is constant in n. By substituting (5.5c) to (5.3b), it is concluded that as N grows large

$$\frac{1}{N} \sum_{n=1}^{N} \mathbb{E}\left\{ \mathsf{d}\left(x_n; x_{0n}\right) \right\} = \frac{1}{N} \sum_{n=1}^{N} \mathbb{E}_{x_{0n},\mathrm{z}_n}\left\{ \mathsf{d}\left(\mathbf{g}_{\mathsf{RLS}}\left(x_{0n} + \mathrm{z}_n | 1\right) ; x_{0n} \right) \right\}. \tag{5.7}$$

The right hand side of (5.7) describes the average distortion of a bank of N decoupled measuring systems: In system $n \in [N]$, the sample x_{0n} is measured as

$$\mathrm{y}_n = x_{0n} + \mathrm{z}_n \tag{5.8}$$

with a unit projecting coefficient where z_n is effective additive Gaussian noise. The samples are then recovered by the scalar RLS method in (5.4) with effective tuning factor, in parallel. The equality in (5.7) indicates that the average distortion calculated in this decoupled setting is asymptotically equivalent to the one calculated in the original system which is coupled linearly in measuring and nonlinearly in recovery. This result can be interpreted as follows: Due to the linear mixture in $\mathbf{A}$, and nonlinear coupling imposed by the RLS method, signal recovery in the original problem performs degraded compared to the case of identical and orthogonal sampling, i.e., when $M = N$ and $\mathbf{A} = \mathbf{I}_N$. This degradation, can be modeled via a higher noise power in the sensing process, and an effective tuning factor in the recovery algorithm.

The equivalence in (5.7) follows the asymptotic *decoupling* property of the generic RLS method. This property in its basic form indicates that the n-th recovered sample, conditioned to the n-th signal sample, converges in distribution to the output of an *effective scalar* RLS algorithm reconstructing the n-th signal sample from an *effective scalar* noisy observation. When the corresponding spin glass of the original problem exhibits RS, the effective noisy observation follows the simple additive Gaussian form. However, for problems with no RS, this term is of more complicated forms.

5.2 Basic Definitions

To present the decoupling property of the generic RLS method, let us first state some basic definitions.

Definition 5.1 (Conditional distribution of regression coefficients)**.** *Consider a linear regression problem with the vector of regressands $\boldsymbol{y}$, matrix of regressors $\mathbf{A}$, and true regression coefficients which are collected in $\boldsymbol{x}_0$. Assume that the entries of $\boldsymbol{x}_0$ are distributed i.i.d. with $\mathrm{p}_0(\cdot)$. Let the regression coefficients in $\boldsymbol{x}$ be calculated via the RLS method, i.e., $\boldsymbol{x} = \mathbf{g}_{\mathsf{RLS}}(\boldsymbol{y}|\mathbf{A})$. For a given $n \in [N]$, the distribution of regression coefficient x_n conditioned to the true coefficient x_{0n} at the mass point $(x, x_0) \in \mathbb{X} \times \mathbb{X}$ is defined as*

$$\mathrm{p}_n^N(x|x_0) \coloneqq \frac{\mathrm{p}_{x_n,x_{0n}}^N(x, x_0)}{\mathrm{p}_0(x_0)} \tag{5.9}$$

where $\mathrm{p}^N_{x_n,x_{0n}}(x,x_0)$ *is the joint distribution of* x_n *and* x_{0n} *at the math point* (x,x_0).

In Definition 5.1, the superscript N indicates the dependency of the conditional distribution to the problem dimension. For the sequence of linear regression problems specified in Chapter 2, $\mathrm{p}^N_n(x|x_0)$ describes a sequence of distribution functions whose asymptotic limit is defined as follows:

Definition 5.2 (Asymptotic conditional distribution)**.** *Consider a sequence of linear regression problems with data dimension* N *and* $M(N)$ *regressands. Assume that* $M(N)$ *is a deterministic function of* N*, such that the load*

$$\alpha(N) = \frac{M(N)}{N} \tag{5.10}$$

is bounded for any integer N *and has an asymptotic limit. Then, the asymptotic distribution of regression coefficient* x_n *conditioned to the true coefficient* x_{0n} *at the mass point* $(x,x_0) \in \mathbb{X} \times \mathbb{X}$ *is defined as*

$$\mathrm{p}_n(x|x_0) \coloneqq \lim_{N\uparrow\infty} \mathrm{p}^N_n(x|x_0)\,. \tag{5.11}$$

The existence of the asymptotic conditional distribution for a given regression coefficient, i.e., when the limit in (5.11) exists, can be alternatively stated with the notion of *convergence in law*[2].

Definition 5.3 (Convergence in law)**.** *Let*

$$\{t_N\} = t_1, t_2, \ldots, \tag{5.12}$$

with $t_N \in \mathbb{T}$ *for all* N*, be a sequence of random variables whose* N*-th entry is distributed with* $\mathrm{p}^N_t(\cdot)$*. Then,* $\{t_N\}$ *is said to converge in law to* $t \sim \mathrm{p}_t(\cdot)$*, if*

$$\lim_{N\uparrow\infty} \mathrm{p}^N_t(v) = \mathrm{p}_t(v)\,, \tag{5.13}$$

for any $v \in \mathbb{T}$.

[2]Also referred to as *convergence in distribution.*

From Definition 5.3, it is concluded that when the asymptotic limit $\mathrm{p}_n(\cdot|\cdot)$ exists, the pair (x_n, x_{0n}) converges in law to $(\mathrm{x}_n, \mathrm{x}_{0n})$ which is distributed with $\mathrm{p}_0(\mathrm{x}_0)\,\mathrm{p}_n(\mathrm{x}|\mathrm{x}_0)$ at the math point $(\mathrm{x}, \mathrm{x}_0)$.

5.3 Generic Form of the Decoupling Principle

The decoupling principle is concluded from the asymptotic characterization of the RLS method given in Chapter 4. This principle in its generic form does not rely on any symmetry assumption at the saddle point, e.g. RS or RSB, and is directly deduced from the generic replica ansatz given in Proposition 4.1.

In a nutshell, the decoupling principle indicates that the asymptotic conditional distribution of regression coefficients exists and is of the same form for all coefficients. This means that the regression coefficients determined via the RLS method are identically[3] distributed in the large-system limit. Hence, each coefficient is statistically similar to the coefficient of an equivalent scalar linear regression problem derived via an equivalent scalar RLS algorithm. Unlike the principle, the exact form of this equivalent problem depends on the symmetry property of the corresponding spin glass. We derive the equivalent problem for both the RS and RSB scenarios. The generic form of the decoupling principle is formally presented in the following proposition.

Proposition 5.1 (Generic Decoupling Principle)**.** *Consider a linear regression problem with a generic RLS method whose true regression coefficients are i.i.d. distributed as*

$$\mathrm{p}_{\boldsymbol{x}_0}(\boldsymbol{x}_0) = \prod_{n=1}^{N} \mathrm{p}_0(x_{0n})\,. \tag{5.14}$$

Let the spin glass of replicas be defined as in Definition 4.3, and $\mathbf{Q}$ *denote the replica correlation matrix which satisfies the fixed-pint equation and minimizes the free energy. For* $n \in [N]$*, the asymptotic conditional distribution of the regression coefficients de-*

[3] But of course not independently.

fined in Definition 5.2 exists and is independent of n *almost sure in* $\mathbf{A}$*. Namely, there exists a pair of correlated random variables* $(\mathrm{x}, \mathrm{x}_0)$*, in which* $\mathrm{x}_0 \sim \mathrm{p}_0(\cdot)$ *and*

$$\mathrm{p}_{\mathrm{x}|\mathrm{x}_0}(x|x_0) = \mathrm{q}(x|x_0), \tag{5.15}$$

for some conditional distribution $\mathrm{q}(\cdot|\cdot)$*, such that for all* $n \in [N]$*,* (x_n, x_{0n}) *converges in law to* $(\mathrm{x}, \mathrm{x}_0)$*. The explicit form of* $\mathrm{q}(x|x_0)$ *depends on the symmetry property of* $\mathbf{Q}$*.*

Proof. The proof follows the generic replica ansatz stated in Proposition 4.1 using the following standard argument from the Hamburger moment problem:

Statement 5.1 (Classical moment problem)**.** *Consider the tuple of real-valued random variables* (t_1, t_2) *which are jointly distributed with* $\mathrm{p}_{t_1,t_2}(\cdot,\cdot)$*. For integers* K *and* L*, let*

$$\mathsf{M}_{K,L} \coloneqq \mathbb{E}\left\{t_1^K t_2^L\right\} \tag{5.16}$$

be the (K, L) *moment of this tuple. If the sequence* $\{\mathsf{M}_{K,L}\}$ *for all integers* K *and* L *is uniformly bounded; then, there exists a unique map from* $\{\mathsf{M}_{K,L}\}$ *to* $\mathrm{p}_{t_1,t_2}(\cdot,\cdot)$*. This means that there exists only one probability measure whose moments are* $\mathsf{M}_{K,L}$*. Hence, one can uniquely specify* $\mathrm{p}_{t_1,t_2}(\cdot,\cdot)$ *by the sequence* $\{\mathsf{M}_{K,L}\}$*.*

The above statement includes the Carleman's condition which can be followed in the literature of the classical moment problems in [78–81]. Although the statement is given for real-valued random variables, it is extended to complex-valued variables as well, since it holds for tuples of an arbitrary number of random variables. As a result, without loss of generality, we focus in the reminder of the proof on real-valued cases, i.e., when we have $\mathbb{X} \subseteq \mathbb{R}$.

Let us now consider the n-th regression coefficient x_n and its corresponding true one x_{0n}. For a generic replica correlation matrix, we set the distortion function

$$\mathsf{d}(x, x_0) = x^K x_0^L \tag{5.17}$$

and the index set to

$$\mathbb{W}(N) = \mathbb{W}_{\eta}(N) = [n : n + \lfloor \eta N \rfloor] \tag{5.18}$$

in Proposition 4.1 for $\eta \in (0, 1]$. In this case, the asymptotic average distortion $D_{\mathsf{RLS}}^{\mathbb{W}_{\eta}}$ determines the arithmetic average of the (K, L) moments of

$$(x_n, x_{0n}), \ldots, (x_{(n+\lfloor \eta N \rfloor)}, x_{0(n+\lfloor \eta N \rfloor)}). \tag{5.19}$$

Let $\mathsf{M}_{K,L}(n)$ denote the (K, L) moment of (x_n, x_{0n}). Hence, from the definition it is clear that in this case

$$\mathsf{M}_{K,L}(n) = \lim_{\eta \downarrow 0} D_{\mathsf{RLS}}^{\mathbb{W}_{\eta}}. \tag{5.20}$$

Substituting the distortion function and the index set in Proposition 4.1, the asymptotic average distortion reads

$$D_{\mathsf{RLS}}^{\mathbb{W}_{\eta}} = \lim_{\beta \uparrow \infty} \lim_{t \downarrow 0} D^{\mathsf{R}}(\beta, t), \tag{5.21}$$

where $D^{\mathsf{R}}(\beta, t)$ is given by Definition 4.4 as

$$D^{\mathsf{R}}(\beta, t) = \frac{1}{t} \mathbb{E} \left\{ \sum_{a=1}^{t} \mathrm{v}_a^K \mathrm{x}_0^L \right\}. \tag{5.22}$$

with $\mathbf{v} \in \mathbb{X}^t$ being a random vector whose distribution is given in Definition 4.3 and $\mathrm{x}_0 \sim \mathrm{p}_0(\cdot)$. In (5.22), $\mathbf{v}$ and x_0 disappear after taking expectation; hence, the limit in the right hand side of (5.21) only depends on K and L, i.e.,

$$\lim_{\beta \uparrow \infty} \lim_{t \downarrow 0} D^{\mathsf{R}}(\beta, t) = f_{K,L} \tag{5.23}$$

From (5.23), it is observed that $D_{\mathsf{RLS}}^{\mathbb{W}_{\eta}}$ depends neither on index n nor on η. Hence, its limit with respect to η exists, and we have

$$\mathsf{M}_{K,L}(n) = f_{K,L}. \tag{5.24}$$

Noting that the $f_{K,L}$ is uniformly bounded by definition, it is inferred that the asymptotic joint distribution of this tuple does not depend on the index n. This means that there exist a deterministic joint distribution $\mathrm{q}(\cdot,\cdot)$, such that

$$\lim_{N\uparrow\infty} \mathrm{p}^{N}_{x_n,x_{0n}}(x|x_0) = \mathrm{q}(x,x_0) \tag{5.25}$$

for $n \in [N]$. This concludes that

$$\mathrm{p}_n(x|x_0) = \frac{\mathrm{q}(x,x_0)}{\mathrm{p}_0(x_0)} \coloneqq \mathrm{q}(x|x_0). \tag{5.26}$$

The exact expression for $\mathrm{q}(\cdot|\cdot)$ is given by calculating the sequence $\{f_{K,L}\}$ which depends on the replica correlation matrix $\mathbf{Q}$. □

Proposition 5.1 guarantees the existence of an equivalent scalar system. The exact form of this decoupled system however depends on the symmetry properties of the replica correlation matrix. For regression problems in which the replica correlation matrix exhibits RS, this system becomes of the standard linear form with additive Gaussian regression error. Nevertheless, as the RS breaks, the effective regression error deviates from the Gaussian distribution. In the sequel, we derive the explicit form of the decoupled system for both the RS and RSB cases.

5.4 Decoupled Setting of the Generic RLS Method

From the RS and RSB ansätze, it is observed that the decoupled regression coefficient x is derived in terms of the decoupled regressand y via the same scalar RLS algorithm[4]. Moreover, the decoupled regressand y is always on the same additive form

$$\mathrm{y} = \mathrm{x}_0 + \mathrm{z} \tag{5.27}$$

for some z and $\mathrm{x}_0 \sim \mathrm{p}_0(\cdot)$. We hence define the decoupled RLS algorithm and the decoupled regression problems as follows:

[4]Check the definition of x in Propositions 4.2, 4.3 and 4.4.

Definition 5.4 (Decoupled RLS algorithm)**.** *Given the scalar regressand* y*, the decoupled RLS algorithm* $\mathrm{g}_{\mathsf{RLS}}(\cdot|\tau)$ *with tuning factor* τ *and the utility function* $u(\cdot)$ *determines the regression coefficient* x *as*

$$\mathrm{g}_{\mathsf{RLS}}(\mathrm{y}|\tau) \coloneqq \underset{v\in\mathbb{X}}{\operatorname{argmin}} \ \frac{\zeta}{2\tau}|\mathrm{y}-v|^2 + u(v). \tag{5.28}$$

The decoupled RLS algorithm is an special case of the generic RLS scheme defined in Section 2.2 whose dimension is one and whose single regressor is $\mathbf{A} = 1$.

Definition 5.5 (Decoupled setting)**.** *Consider a linear regression model whose true regression coefficients are distributed with*

$$\mathrm{p}_{\boldsymbol{x}_0}(\boldsymbol{x}_0) = \prod_{n=1}^{N} \mathrm{p}_0(x_{0n}). \tag{5.29}$$

Assume that the regression coefficients for this model are determined via a generic RLS method with regularization term $u_{\mathrm{v}}(\cdot) : \mathbb{X}^N \mapsto \mathbb{R}$*. Let* $u_{\mathrm{v}}(\cdot)$ *decouple as*

$$u_{\mathrm{v}}(\boldsymbol{v}) = \sum_{n=1}^{N} u(v_n) \tag{5.30}$$

for some function $u(\cdot) : \mathbb{X} \mapsto \mathbb{R}$*. The decoupled setting corresponding to this problem consists of*

- *A single true regression coefficient* $\mathrm{x}_0 \in \mathbb{X}$ *which is distributed with* $\mathrm{p}_0(\cdot)$*.*
- *A single regressand* y *which is correlated with* x_0 *as*

$$\mathrm{y} = \mathrm{x}_0 + \mathrm{z}. \tag{5.31}$$

  for some scalar effective regression error z*.*

- *The effective regression error is distributed conditioned to* x_0 *with* $\mathrm{p}_{\mathsf{dec}}(\mathrm{z}|\mathrm{x}_0)$*.*
- *The regression coefficient is found via the decoupled RLS algorithm, i.e.,*

$$\mathrm{x} = \mathrm{g}_{\mathsf{RLS}}(\mathrm{y}|\tau) \tag{5.32}$$

for some τ, where the regularization term is set to $u(\cdot)$.

The decoupled regression setting describes a special linear model of dimension one, in which the single regressor is $\mathbf{A} = 1$. In general, the decoupled setting is always of the above form, and the symmetry property of the problem only changes the conditional distribution of the effective regression error, i.e., $\mathrm{p}_{\mathsf{dec}}(\mathrm{z}|\mathrm{x}_0)$. In the following, we derive this distribution for the RS, as well as the RSB, ansatz.

5.4.1 Effective Regression Error under RS

Following the discussions in Section 5.1, it is observed that when the regression problem exhibits RS, the effective regression error is *independent* of x_0 and distributed *Gaussian*. Such an observation intuitively indicates that the linear mixture in the regression model, as well as the nonlinear mixture imposed by the RLS method, asymptotically behave similar to an independent Gaussian process. This result is formally stated in the following proposition.

Proposition 5.2 (RS Decoupling Principle)**.** *Consider a linear regression problem whose true regression coefficients are collected in $\boldsymbol{x}_0$ and distributed as*

$$\mathrm{p}_{\boldsymbol{x}_0}(\boldsymbol{x}_0) = \prod_{n=1}^{N} \mathrm{p}_0(x_{0n}). \tag{5.33}$$

Assume that the vector of the regression coefficients $\boldsymbol{x}$ is determined by the generic RLS method whose regularization term is

$$u_{\mathrm{v}}(\boldsymbol{v}) = \sum_{n=1}^{N} u(v_n) \tag{5.34}$$

and whose tuning factor is λ. Assume that the spin glass corresponding to this problem exhibits RS. Let (χ, q) be the solution to the fixed-point equations in Proposition 4.2 which minimize the zero-temperature free energy and τ and θ_0 be defined as in Proposition 4.2. Then, for $n \in [N]$, the tuple (x_n, x_{0n}) converges in law to tuple $(\mathrm{x}, \mathrm{x}_0)$ given

in Definition 5.5 when the decoupled RLS algorithm is tuned with τ and the effective regression error is set to

$$\mathrm{z} = \theta_0 \mathrm{z}_0, \tag{5.35}$$

for an independent zero-mean and unit-variance Gaussian random variable z_0*, i.e.,* $\mathrm{z} \sim \mathcal{N}^{\zeta}(0, \theta_0^2)$.

Proof. The generic decoupling principle indicates that for any two different indices $n \neq \hat{n} \in [N]$, we have

$$\mathrm{p}_n(x|x_0) = \mathrm{p}_{\hat{n}}(x|x_0) \tag{5.36}$$

at any mass point (x, x_0) which conclude that as N grows large

$$\mathbb{E}\left\{x_n^K x_{0n}^L\right\} = \mathbb{E}\left\{x_{\hat{n}}^K x_{0\hat{n}}^L\right\}. \tag{5.37}$$

Therefore, for $n \in [N]$, we have

$$\mathsf{M}_{K,L}(n) = \mathbb{E}\left\{x_n^K x_{0n}^L\right\} = \lim_{N \uparrow \infty} \frac{1}{N} \sum_{j=1}^{N} \mathbb{E}\left\{x_j^K x_{0j}^L\right\}. \tag{5.38}$$

As a result, given the RS assumption, the asymptotic (K, L) moment of (x_n, x_{0n}) is determined by calculating the asymptotic distortion in Proposition 4.2 for $\mathbb{W}(N) = [N]$ and distortion function

$$\mathsf{d}(x; x_0) = x^K x_0^L. \tag{5.39}$$

Substituting in Proposition 4.2, the asymptotic (K, L) moment reads

$$\mathsf{M}_{K,L}(n) = \mathbb{E}_{\mathrm{x}_0}\left\{\int \mathrm{x}^K \mathrm{x}_0^L \mathrm{D}^{\zeta} \mathrm{z}_0\right\} \tag{5.40}$$

where $\mathrm{x} = \mathsf{g}_{\mathsf{RLS}}\left(\mathrm{x}_0 + \theta_0 \mathrm{z}_0 | \tau\right)$ with τ and θ_0 being defined in (4.33b) and (4.33a), respectively, and $\mathrm{x}_0 \sim \mathrm{p}_0\left(\cdot\right)$. Note that for a given function $f\left(\cdot\right)$

$$\int f\left(y\right) \mathrm{D}^{\zeta} y = \mathbb{E}_z \left\{ f\left(z\right) \right\} \tag{5.41}$$

where $z \sim \mathcal{N}^{\zeta}\left(0, 1\right)$. Hence, one can define random variable $\mathrm{z} \sim \mathcal{N}^{\zeta}\left(0, \theta_0^2\right)$ and write

$$\int \mathrm{x}^K \mathrm{x}_0^L \mathrm{D}^{\zeta} \mathrm{z}_0 = \mathbb{E}_{\mathrm{z}} \left\{ \mathrm{x}^K \mathrm{x}_0^L \right\}. \tag{5.42}$$

Substituting into (5.40), we have

$$\mathsf{M}_{K,L}\left(n\right) = \mathbb{E}_{\mathrm{x}_0,\mathrm{z}} \left\{ \mathrm{x}^K \mathrm{x}_0^L \right\}. \tag{5.43}$$

The right hand side of (5.43) describes the (K, L) moment of $(\mathrm{x}, \mathrm{x}_0)$ in the decoupled RLS setting defined in Definition 5.5, when $\mathrm{z} \sim \mathcal{N}^{\zeta}\left(0, \theta_0^2\right)$, and τ and θ_0 are set as in Proposition 4.2. Following the standard argument in classical moment problems, given in Statement 5.1, the proof is concluded. □

5.4.2 Impact of RSB

Reminding the example of signal recovery in Section 5.1, the decoupled setting under the RS assumption indicates that for a large number of samples, the effective impairment caused by both sampling noise and mixture among the samples can be modeled by an independent Gaussian process. Although this result intuitively looks true, it is not always correct. To illustrate this, let us now consider a linear regression problem whose corresponding spin glass exhibits one step of RSB. From Proposition 4.3, it is observed that the decoupled regressand is of the following form

$$\mathrm{y} = \mathrm{x}_0 + \theta_0 \mathrm{z}_0 + \theta_1 \mathrm{z}_1. \tag{5.44}$$

From the definition, it is shown that z_0 can be modeled by a Gaussian process; however, z_1 is of a more complicated form.

The new term in (5.44) can be interpreted as a correction term to the basic setting described by RS. In other words, one can conclude that the decoupled setting derived under RS is a special case of a more precise setting given by RSB ansätze which reduces to a simple additive Gaussian setup, when the problem shows RS. This intuitive result is formally formulated in the following proposition.

Proposition 5.3 (RSB Decoupling Principle)**.** *Consider a linear regression problem whose true regression coefficients are collected in* $\boldsymbol{x}_0$ *and distributed as*

$$\mathrm{p}_{\boldsymbol{x}_0}\left(\boldsymbol{x}_0\right) = \prod_{n=1}^{N} \mathrm{p}_0\left(x_{0n}\right). \tag{5.45}$$

Assume that the vector of the regression coefficients $\boldsymbol{x}$ *is determined by the generic RLS method whose regularization term is*

$$u_{\mathrm{v}}\left(\boldsymbol{v}\right) = \sum_{n=1}^{N} u\left(v_n\right) \tag{5.46}$$

and whose tuning factor is λ*. Assume that the spin glass corresponding to this problem exhibits* B *steps of RSB. Let* $\left(\chi, \left\{p_b\right\}, \left\{\mu_b\right\}, q\right)$ *be the solution to the fixed-point equations in Proposition 4.5, minimizing the zero-temperature free energy, and define the parameters* τ*,* θ_0*,* $\left\{\theta_b\right\}$ *and* $\left\{\tilde{\chi}_b\right\}$ *as in Proposition 4.5. For* $n \in [N]$*, the tuple* $\left(x_n, x_{0n}\right)$ *converges in law to tuple* $\left(\mathrm{x}, \mathrm{x}_0\right)$ *given in Definition 5.5 when the decoupled RLS algorithm is tuned with* τ *and the effective regression error is given by*

$$\mathrm{z} = \theta_0 \mathrm{z}_0 + \sum_{b=1}^{B} \theta_b \mathrm{z}_b. \tag{5.47}$$

Here, the random variable z_0 *is zero-mean Gaussian with unit variance and is distributed independent of* x_0*. Moreover, for* $b \in [B]$*,* z_b *is a random variable which is distributed conditioned to* x_0*,* z_0 *and* $\left(\mathrm{z}_{b+1}, \ldots, \mathrm{z}_B\right)$ *according to*

$$\mathrm{p}\left(\mathrm{z}_b | \mathrm{z}_{b+1}, \ldots, \mathrm{z}_B, \mathrm{z}_0, \mathrm{x}_0\right) \coloneqq \tilde{\Lambda}_b\left(\mathrm{z}_b | \mathrm{z}_{b+1}, \ldots, \mathrm{z}_B, \mathrm{z}_0, \mathrm{x}_0\right) \phi\left(\mathrm{z}_b\right) \tag{5.48}$$

with $\tilde{\Lambda}_b\left(\mathrm{z}_b | \mathrm{z}_{b+1}, \ldots, \mathrm{z}_B, \mathrm{z}_0, \mathrm{x}_0\right)$ *being defined in Proposition 4.5.*

Proof. The proof follows exactly the same steps as in the proof of Proposition 5.2 while replacing the RS ansatz with the B-RSB ansatz. We therefore skip the detailed proof to avoid repetition. □

The RSB decoupling principle can be observed as an extension of the simple RS form which gradually corrects the asymptotic distribution of the effective noise. In fact this result indicates that in settings whose corresponding spin glass does not possess a symmetric replica correlation matrix, the asymptotic effective noise is of an asymmetric form, as well. The level of asymmetry in these settings is directly related to the number of breaking steps exhibited by the corresponding spin glass.

5.5 Replica Simulator

The decoupling principle simplifies various analytic and computational tasks. The fact that a coupled vector system is represented via a bank of decoupled scalar setups let us investigate the RLS method in a tractable way. In addition to these benefits, this principle can also provide a straightforward approach to solve the fixed-point equations via Monte-Carlo methods. In this section, we illustrate this approach and give some examples.

Invoking the decoupling principle, a replica ansatz is completely represented in terms of its decoupled setting. More precisely, for a given problem, the macroscopic parameters determined by a replica ansatz, as well as the fixed-point equations, are explicitly described in terms of the decoupled setting. This property enables us to solve the fixed-point equations of the ansatz and determine the asymptotic parameters directly via Monte-Carlo methods without any analytic derivations. To show this result, let us first define some basic definitions:

Definition 5.6 (Basic statistics of the decoupled setting)**.** *Consider the decoupled setting defined in Definition 5.5 and let effective noise follows the one given by the B-RSB ansatz in Proposition 5.3. For this setting, we define the following parameters:*

- *The b-th, $b \in [B]$ impairment-error correlation is defined as*

$$C_b = \frac{1}{\theta_b}\mathbb{E}\left\{\mathbb{R}\mathrm{e}\left\{(\hat{\mathrm{x}} - \mathrm{x})\,\mathrm{z}_b^*\right\}\right\}. \tag{5.49}$$

- *The MSE is given by*

$$\mathrm{MSE} = \mathbb{E}\left\{|\hat{\mathrm{x}} - \mathrm{x}|^2\right\}. \tag{5.50}$$

The above definition lets us compactly represent the fixed-point equations of the B-RSB ansatz in terms of the statistics of the decoupled setting. To illustrate this point, consider the following examples:

Example 5.1 (RS ansatz)**.** *Let $B = 0$. The RS fixed-point equations read*

$$q = \mathrm{MSE}, \tag{5.51a}$$

$$\chi = \tau\, C_0\ . \tag{5.51b}$$

Example 5.2 (One step of RSB)**.** *The first three fixed-point equations of the one-RSB ansatz are given by*

$$q + p = \mathrm{MSE}, \tag{5.52a}$$

$$\chi + \mu p = \tau\, C_0\ , \tag{5.52b}$$

$$\tilde{\chi} + \mu q = \tau\, C_1\ . \tag{5.52c}$$

The last equation is further represented in terms of the decoupled system as

$$f_{\text{fix}}\left(\chi, p, q, \mu\right) = \mathrm{I}\left(\mathrm{z}_1; \mathrm{z}_0, \mathrm{x}_0\right) + D_{\mathsf{KL}}\left(\mathrm{p}_{\mathrm{z}_1} \| \phi\right) \tag{5.53}$$

with

$$f_{\text{fix}}\left(\chi, p, q, \mu\right) \coloneqq \frac{\zeta}{2\lambda}\left[(p+q)\,\mathrm{R}_{\mathbf{J}}(-\frac{\chi}{\lambda}) - q\mathrm{R}_{\mathbf{J}}(-\frac{\tilde{\chi}}{\lambda}) - \frac{1}{\mu}\int_{\chi}^{\tilde{\chi}} \mathrm{R}_{\mathbf{J}}(-\frac{\omega}{\lambda})\mathrm{d}\omega\right] \tag{5.54}$$

where $\mathrm{I}(\mathrm{z}_1;\mathrm{z}_0,\mathrm{x}_0)$ *is the mutual information between* z_1 *and* $(\mathrm{z}_0,\mathrm{x}_0)$*, and* $D_{\mathsf{KL}}(\mathrm{p}_{\mathrm{z}_1}\|\phi)$ *denotes the Kullback-Leibler divergence between the marginal distribution of* z_1*, i.e.,* $\mathrm{p}_{\mathrm{z}_1}$*, and the Gaussian distribution. The Kullback-Leibler divergence*[5] *between distributions* p_x *and* q_x *is defined as*

$$D_{\mathsf{KL}}(\mathrm{p}_x\|\mathrm{q}_x) \coloneqq \mathbb{E}_x\left\{\log\frac{\mathrm{p}_x}{\mathrm{q}_x}\right\} \tag{5.55}$$

where $x \sim \mathrm{p}_x$*.*

This alternative representation of the fixed-point equations leads us to a new interpretation of the replica ansätze. In fact, for a given replica ansatz, one can define a *transition system* whose state is specified by parameters of the ansatz. In this case, the decoupled setting defines the transition rule of this system, and the solution to the fixed-point equations represent the *steady state* [82, 83]. This interpretation is clarified via the following example.

Example 5.3 (Transition system described by the RS ansatz)**.** *Consider a transition system whose state is* $\mathbf{s} = [\chi, q]^{\mathsf{T}}$*. This system transit from state* $\mathbf{s}_t$ *to state* $\mathbf{s}_{t+1}$ *via the following transition rules*

$$q_{t+1} = \mathrm{MSE}(t)\,, \tag{5.56a}$$

$$\chi_{t+1} = \tau\, C_0(t) \tag{5.56b}$$

where $\mathrm{MSE}(t)$ *and* $C_0(t)$ *are respectively the MSE and impairment-error correlation of the decoupled system given by* $\mathbf{s}_t = [\chi_t, q_t]^{\mathsf{T}}$*. When* $\mathbf{s}_{t+1} = \mathbf{s}_t$*, this system meets its steady state which is the solution to the fixed-point equations of the RS ansatz.*

In the above example, the task of calculating $\mathrm{MSE}(t)$ and $C_0(t)$ can be done directly by Monte-Carlo simulations. In fact, for given χ_t and q_t, the decoupled system is an AWGN channel whose MSE and impairment-error correlation can be calculated via numerical simulations. By this approach, one can avoid analytic derivations for the

[5] Also called *relative entropy*.

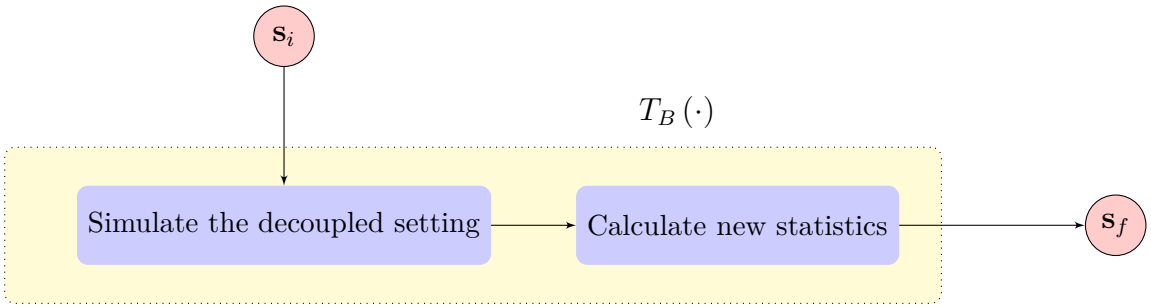

Figure 5.1: Schematic representation of the replica simulator.

replica ansätze. For the general B-RSB ansatz, we refer to this transition system as the *replica simulator*, and define it formally as follows:

Definition 5.7 (Replica simulator of the B-RSB ansatz)**.** *For the B-RSB ansatz for some non-negative integer B and let the vector $\mathbf{s}$ be*

$$\mathbf{s} \coloneqq [\chi, \mu_1, \ldots, \mu_b, p_1, \ldots, p_b, q]\,. \tag{5.57}$$

The entries of $\mathbf{s}$ satisfy the constraints given in Proposition 4.5. Denote the support of $\mathbf{s}$ with $\mathbb{S}_B$. The transition rule

$$T_B(\cdot) : \mathbb{S}_B \mapsto \mathbb{S}_B \tag{5.58}$$

maps the prior state $\mathbf{s}_i \in \mathbb{S}_B$ to the posterior state $\mathbf{s}_f \in \mathbb{S}_B$ in the following way: It realizes the B-RSB decoupled setting via the entries of $\mathbf{s}_i$. It then constructs the entries of $\mathbf{s}_f$ by determining a new set of replica parameters from the statistics of the decoupled system.

The replica simulator of the B-RSB ansatz is then defined as the transition system $\mathsf{Sim}^{\mathsf{R}}[B] \coloneqq (\mathbb{S}_b, T_B(\cdot))$.

A schematic representation of the replica simulator is given in Fig. 5.1. For this transition system, a sequence of states $\{\mathbf{s}_t\}$ is called *process*, if for $t \in \mathbb{Z}^+$

$$\mathbf{s}_{t+1} = T_B(\mathbf{s}_t)\,. \tag{5.59}$$

The state $\mathbf{s}^\star$ is further the *steady state*, if setting $\mathbf{s}_t = \mathbf{s}^\star$ results in $\mathbf{s}_{t+1} = \mathbf{s}^\star$. The solution given by the B-RSB ansatz is hence the steady state of the replica simulator of the B-RSB ansatz which minimizes the free energy function. As a result, the B-RSB solution can be numerically calculated via the Monte-Carlo simulations using the methods developed in the literature of transition systems. It is worth to note that while this approach reduces the complication of numerical analyses, it does not impact the computational complexity.

Following the illustrated approach, the properties of the solution given by RSB ansätze can be studied based on the *state evolution* of the replica simulator. The concept of replica simulator may further clarifies the connection between RSB ansätze and iterative implementation of the RLS method based on the message passing algorithm. Such investigations are left here as a possible future work, since they are out of the scope of this manuscript.

5.6 Bibliographical Notes

The decoupling principle was initially presented for regression problems with linear recovery algorithms, i.e., when $\mathbf{g}_{\mathsf{RLS}}(\boldsymbol{y}|\mathbf{A}) = \mathbf{G}\boldsymbol{y}$ for some $\mathbf{G} \in \mathbb{A}_{\zeta}^{N\times M}$. The property was first observed by Tse and Hanly in [84] where the asymptotic multiuser efficiency of several linear estimators was investigated. Using the asymptotic results, the authors showed that for an i.i.d. channel matrix, the impairment caused by noise and multiuser interference impacts asymptotically similar to an equivalent Gaussian noise term. Inspired by this results, the asymptotic distribution of various output metrics were studied later for several linear estimators; see for example [85,86]. In an independent work, Verdú and Shamai studied the linear minimum mean square error (MMSE) estimator in [87]. The results of this study depicted that the output symbols of the linear MMSE estimator are asymptotically distributed Gaussian conditioned to the input symbols. This result was later justified for a wider class of settings in [88] and extended to a larger class of linear estimators in [89].

When the regression method is linear, the asymptotic characterization mainly deals with random matrix theory [57,58]. The decoupling principle in this case is rigorously

justified by using the known properties of large random matrices and the central limit theorem; see for example the derivations in [90,91]. These tools however fail to justify the decoupling principle for nonlinear methods, such as the generic RLS method. This is due to the fact that in these methods the regression coefficients are derived from the regressands via mappings with nonlinear operations which cannot be marginally factorized for each coefficient.

The initial observations on the decoupling principle of nonlinear regression methods was illustrated by Müller and Gerstacker in [92], where they employed the replica method to calculate the capacity loss caused by separating detection and decoding in a Gaussian channel. The results demonstrated that the additive decoupling of spectral efficiency, reported in [91] for Gaussian channels with Gaussian inputs, also holds for the case with binary inputs. The authors hence conjectured that this decoupling property is generic for spectral efficiency regardless of input distribution and linearity; see [93] for further discussions. This conjecture was later shown to hold in [43] by Guo and Verdú, where they characterized the asymptotic performance of nonlinear MMSE estimators via the replica method. The results depicted that for an i.i.d. channel matrix, the characterization given by the RS ansatz exhibits the decoupling principle in its basic form. Rangan et al. extended this result to nonlinear MAP estimators[6] in [55] using standard large deviations techniques.

Regarding the decoupling property of nonlinear regression methods, the available literature left two questions open:

1. The explicit derivations of decoupled setting for linear regression problems with non-i.i.d. matrices of regressors, and

2. the impact of RSB in regression problems whose corresponding spin glasses exhibit RSB.

Tulino et al. provided a partial answer to the first question in [94]. In this work, the authors investigated the asymptotic performance of MAP-like algorithms when they are used to recover the support of a sparse signal from linear and noisy observations.

[6] Which are mathematically equivalent to the RLS method.

The derivations were based on the RS ansatz and considered a scenario in which samples of a sparse Gaussian signal[7] are measured linearly via a square matrix $\mathbf{V}$, and then the observations are sparsely sampled by a diagonal matrix $\mathbf{B}$ whose diagonal entries are either zero or one. The asymptotic characterization addressed the decoupling property of this setting for a larger class of random measuring matrices $\mathbf{V}$. Although investigations in [94] broadened the matrix ensemble, it cannot be considered as a complete generalization of the decoupling principle stated in [43] and [55], since it restricts the linear regression model to scenarios whose priors are sparse Gaussian prior and whose loads are less than one, i.e., $\alpha \leq 1$. The second problem, i.e., the analysis of decoupling property under RSB, was left open for a long time. The derivations in this chapter give a complete answer to both of these open questions.

5.7 Summary

This chapter has shown the general form of the so-called *decoupling principle* for the generic RLS method. Based on this property, a true regression coefficient and its corresponding recovery given via the RLS method jointly converge in distribution to their counterparts in an *equivalent scalar* linear regression problem with RLS method. This *equivalent scalar* problem has been referred to as the *decoupled setting*. The derivations have shown that the scalar RLS method in the decoupled setting is always of the same form under both RS and RSB. The decoupled regression problem however shows different statistical properties when we use different ansätze for characterization.

It has been shown that under RS, the equivalent regression error term in the decoupled setting is Gaussian and statistically independent of the true regression coefficient. This is consistent with the earlier results in the literature. Nevertheless, when the vector problem is characterized via an RSB ansatz, regression error is not anymore Gaussian and depends on the true regression coefficient. For B-RSB ansatz, the explicit form of the decoupled setting has been derived. Using this setting the concept of replica simulator has been presented in which finding the solution of fixed-point

[7] This means that the signal samples are of the form $x_n b_n$ with x_n and b_n being Gaussian and Bernoulli random variables, respectively.

equations in a particular replica ansatz is interpreted as the problem of finding the *steady state* of a transition system.

Chapter 6

Applications to Sparse Recovery

As indicated several times in previous chapters, one of the most well-known and basic applied problems which is modeled via linear regression is the problem of signal recovery. In this problem, the regressands are observations which have been linearly obtained from signal samples via the regressors. The regressors in this case are often called *sensing bases*. The main objective in this case is to estimate the signal samples from these observations given that we know the sensing bases. In the absence of any prior information on the signal, the most effective approach is to use the LS method, i.e., to minimize the RSS. From Bayesian viewpoint, LS postulates in priori that the signal samples are *uniformly* distributed.

In many practical scenarios of signal recovery, it is known in prior that the signal is *sparse*; see for example [95–101]. This means, we know in priori that a certain fraction of signal samples are zero. Hence, we desire to recover a sparse signal. This is in fact where the terminology *sparse recovery* comes from. The prior information of sparsity makes it theoretically possible to find a unique recovery of the signal, even with an *underdetermined* set of observations, i.e., when the number of observations is less than the number of samples. This means that in this case, we are able to *compress* the signal during the sensing procedure. As a result, sparse recovery is often called *compressive sensing* or *compressed sensing* in the signal processing literature [7, 102, 103].

For sparse recovery, uniform prior is not an effective postulation. The Bayesian framework suggests to regularize the RSS term with a penalty which is proportional to signal sparsity. Hence, most *sparse recovery* algorithms are formulated as an RLS

method. The choice of the regularization term in these algorithms depend on various consideration, e.g., computational complexity or validity of the sparsity model. In this chapter, we consider some well-known sparse recovery algorithms and characterize their performance using the results of Chapters 4 and 5. The generality of the original setting, considered in Chapter 2, enables us to investigate the performance for various sparse signals and sensing matrices. We hence consider two cases of continuous and quantized sparse signals and study their asymptotic characteristics for both random i.i.d. and orthogonal sensing matrices. Our results demonstrate that the computationally intractable algorithm of ℓ_0-norm minimization is not consistently characterized via the RS ansatz, and hence RSB is required for assessing its performance.

6.1 Preliminaries

We start with some basic definitions and formulations in the context of sparse recovery. In this problem, the linear model

$$\boldsymbol{y} = \mathbf{A}\boldsymbol{x}_0 + \boldsymbol{z} \tag{6.1}$$

represents a noisy sampling setting in which the *true signal samples* collected in $\boldsymbol{x}_0$ is linearly measured via *sensing matrix* $\mathbf{A}$. These measurements are corrupted by *noise* which is modeled by the additive term $\boldsymbol{z}$.

The main task in this setting is to recover the signal samples $\boldsymbol{x}_0$ from the measurement vector $\boldsymbol{y}$ with respect to some fidelity constraints. When the measure of fidelity is set to the RSS, signal recovery describes the classic regression problem which is effectively addressed via the LS method[1]. The key difference of sparse recovery is that unlike the classical signal recovery problem, we know in prior that the signal is *sparse*. This means that a certain fraction of samples in $\boldsymbol{x}_0$ are known to be zero[2]. Following the formulation in Chapter 2, the recovery performance is improved by regularizing the LS method via a penalty term which is proportional to sparsity of the signal. In

[1] Detailed discussions are found in Chapter 2.
[2] The support is however not known which makes this problem challenging.

practice, there are various definitions for sparsity. Throughout this chapter, we adopt the following definition:

Definition 6.1 (Sparse signals)**.** *Consider vector* $\boldsymbol{x} \in \mathbb{X}^N$ *whose entries are taken from the support* $\mathbb{X}$ *with* $0 \in \mathbb{X}$*.* $\boldsymbol{x}$ *is said to be sparse, if there exist* $0 \leq \rho < 1$ *such that*

$$\frac{\|\boldsymbol{x}\|_0}{N} \leq \rho. \tag{6.2}$$

The sparsity factor of $\boldsymbol{x}$ *is defined as the minimum value of* ρ *for which the above inequality holds.*

The classical schemes for sparse recovery mainly follow this RLS-based methodology to recover the sparse signal. Although such an approach seems natural from regression points of view, it can be further justified as an algebraic problem. We illustrate this alternative interpretation in the sequel.

6.1.1 An Algebraic View to Sparse Recovery

Consider a *noise-free* sensing setting, i.e., $\boldsymbol{z} \equiv \mathbf{0}$, with continuous signal samples. The true samples in this case are exactly recovered from the observation vector $\boldsymbol{y}$, if the number of observations, i.e., M, equals the signal dimension N, and the sampling matrix $\mathbf{A}$ contains linearly independent rows[3]. It is however desired to further reduce the number of observations in $\boldsymbol{y}$, in order to effectively compress the signal in the sensing stage. By reducing the number of observations, the possible answers to the exact recovery problem increases, and hence the problem is called *underdetermined*. In this case, one can utilize the sparsity of the signal to find the true samples among the available solutions.

To illustrate the latter statement, let $\mathbb{S}$ be the set of all solutions to our underdetermined recovery problem. This means that for the observation vector $\boldsymbol{y}$ and sensing matrix $\mathbf{A}$, $\mathbb{S}$ reads

$$\mathbb{S} = \left\{ \boldsymbol{v} \in \mathbb{R}^N : \ \boldsymbol{y} = \mathbf{A}\boldsymbol{v} \right\} \tag{6.3}$$

[3]Equivalently, we could say in $\mathbf{A}$ is full rank.

From the definition, it is clear that the vector os true signal samples is in $\mathbb{S}$. Knowing that this vector is sparse, i.e.,

$$\|\boldsymbol{x}\|_0 \leq \rho N \tag{6.4}$$

for some $\rho \in [0, 1]$, the true signal samples are given by finding the solution in $\mathbb{S}$ whose ℓ_0-norm is less than ρN. One can equivalently find the vector of true signal samples by solving the following optimization problem:

$$\boldsymbol{x} = \underset{\boldsymbol{v}\in\mathbb{S}}{\operatorname{argmin}} \ \|\boldsymbol{v}\|_0 \,. \tag{6.5}$$

Assuming that the point with ℓ_0-norm less than ρN is unique in $\mathbb{S}$, we have $\boldsymbol{x} \equiv \boldsymbol{x}_0$.

In *noisy* scenarios, the exact recovery is not possible for continuous signals, and one may look for a good estimation of true signal samples. The noise-free approach can hence be extended to this case by letting the set $\mathbb{S}$ contain those vectors whose linear transform lies within a ball of radius ϵ around $\boldsymbol{y}$. This means that

$$\mathbb{S} = \left\{\boldsymbol{v} \in \mathbb{R}^N : \ \|\boldsymbol{y} - \mathbf{A}\boldsymbol{v}\|^2 \leq \epsilon\right\} \tag{6.6}$$

where the value of ϵ is proportional to the noise variance. Consequently, the sparse recovery scheme in the presence of noise reads

$$\boldsymbol{x} = \underset{\boldsymbol{v}\in\mathbb{R}^N}{\operatorname{argmin}} \ \|\boldsymbol{v}\|_0 \qquad \text{subject to } \ \|\boldsymbol{y} - \mathbf{A}\boldsymbol{v}\|^2 \leq \epsilon. \tag{6.7}$$

Invoking the method of Lagrange multipliers, it is then straightforward to show that $\boldsymbol{x}$ is equivalently found by

$$\boldsymbol{x} = \underset{\boldsymbol{v}\in\mathbb{R}^N}{\operatorname{argmin}} \ \|\boldsymbol{v}\|_0 + \psi \|\boldsymbol{y} - \mathbf{A}\boldsymbol{v}\|^2 \tag{6.8}$$

for some properly tuned multiplier ψ. This result recovers the RLS method with a penalty term which is proportional to the ℓ_0-norm, and hence justify the RLS-based approach for recovery.

Although ℓ_0-norm regularization is the most efficient approach for sparse recovery, it is known to be an NP-hard problem[4]. Hence, in practice computationally tractable algorithms such as LASSO are employed. In the following, we give an overview on these algorithms and the effective approaches for implementing them.

6.2 Classical Algorithms for Sparse Recovery

The classical algorithms for sparse recovery are summarized in a special class of generic RLS method, known as ℓ_p-norm minimization schemes, which are introduced and discussed in Chapter 2; see Section 2.3.2. In this class, the regularization term is of the following form

$$u_{\mathrm{v}}(\boldsymbol{v}) = \sum_{n=1}^{N} |v_n|^p \tag{6.9}$$

for some non-negative real p. This penalty is convex when $p \geq 1$. For some choices of p, this method reduces to some well-known algorithms:

- For the special case of $p = 0$, we set $v^0 = 1$ for all $v \neq 0$ and $v^0 = 0$ for $v = 0$. Hence, $u_{\mathrm{v}}(\boldsymbol{v})$ for $p = 0$ recovers the ℓ_0-norm.
- When $p = 1$, the penalty terms reduces to the ℓ_1-norm. This form of the RLS method is called *LASSO*. Tibshirani in his pioneering work [104] showed that by this choice of the penalty, the RLS scheme can address the variable selection task in a tractable way.
- By setting $p = 2$, the RLS method results in a linear recovery scheme. Such a choice of the regularization term does not effectively address the sparsity of the signal, and hence performs poorly for sparse recovery.

Among the above methods, LASSO has received significantly more attention in practical applications. This comes from the fact that this scheme addresses the trade-off between the performance and complexity in a proper manner. On one hand, it

[4]The proof can be followed in [14].

results in a convex optimization problem which can be solved by convex programming, and hence has a tractable computational complexity. On the other hand, it regularizes the so-called *effective sparsity* by penalizing the ℓ_1-norm.

In practice, there are various schemes which address the LASSO methodology for sparse recovery. These schemes mainly differ in their detailed approach to derive the recovered samples, and do not variate in the formulation. An example is the *Basis Pursuit* algorithm which reconstructs samples of the sparse signal in noise-free and noisy scenarios by replacing the ℓ_0-norm with the ℓ_1-norm in (6.5) and (6.7), respectively. This algorithm mainly address the LASSO scheme in an alternative form, and hence its output is equivalent to the LASSO recovery with different tuning parameter λ.

Since the applications of sparse recovery often deal with high dimensional problems, even the polynomial order of complexity imposed by the LASSO scheme is hard to cope in practice. As a result, a rich literature on implementations whose complexity *linearly* grows with the signal dimension have been developed. Before starting our analytic investigations, we shortly mention these algorithms.

6.2.1 Iterative Algorithms for Sparse Recovery

There are roughly two classes of iterative algorithms for sparse recovery:

1. *Basic iterative* algorithms which were developed initially to address the original ℓ_0-norm minimization or its ℓ_1-norm relaxation in an approximated manner. The approximation could follow either a *greedy* formulation or iterative *thresholding*. An example of greedy algorithms is the *orthogonal matching pursuit* which finds the non-zero samples via a stepwise approach. As instances of the latter class, one could consider the iterative *hard* and *soft* thresholding in which the signal samples are reconstructed by iterative linear estimation and entry-wise thresholding. Detailed discussions on these algorithms can be followed in the literature; see for example [14].

2. *AMP-based* algorithms which have been developed later based on the graphical representation of ℓ_p-norm minimization schemes [105–107]. In these algorithms,

the signal samples are reconstructed following the basic thresholding approach; however, the linear estimation in each iteration is updated via an adaptive correction term commonly known as the *Onsager term*.

The basic iterative algorithms were initially developed to address the sparse recovery problem with low computational complexity. These algorithms suffer from poor performance which was initially assumed to be a generic cost for their low complexity. The AMP algorithms were developed later on. These algorithms are shown to recover the performance of the original RLS-based formulation for the recovery in settings with large signal dimensions while imposing linearly growing computational complexity. Hence, they disproved the initial assumption on the performance of iterative algorithms.

6.3 Asymptotic Characterization of Sparse Recovery

Despite the large literature on sparse recovery, there are various analytic questions which are still open. For example, the performance of the RLS-based recovery scheme with ℓ_0-norm regularization is not properly known, even in the large-system limit. Such questions can be answered via the asymptotic characterization of the generic RLS method presented in Chapters 4 and 5. We address this issue in the remaining part of this chapter. To start with analysis, let us first illustrate a stochastic model for a sparse signal.

6.3.1 Stochastic Model for Sparse Signals

In order to investigate the asymptotics of sparse recovery, we need to specify a stochastic model. A sparse signal is stochastically modeled by restricting the prior distribution to be of the following form:

$$\mathrm{p}_0\left(x_0\right) = \left(1-\rho\right)\delta\left(x_0\right) + \rho\,\mathrm{p}_S\left(x_0\right) \tag{6.10}$$

for some distribution $\mathrm{p}_S(\cdot)$ which is *non-singular* at $x_0 = 0$. That means that

$$\int_{0^-}^{0^+} \mathrm{p}_S(x_0)\,\mathrm{d}x_0 = 0. \tag{6.11}$$

By the law of large numbers (LLN), it is observed that (6.10) models the samples of a sparse signal with sparsity factor ρ. To see this point, consider a vector which is distributed i.i.d. according to (6.10). As the number of entries, i.e., N, grows, the strong LLN indicates that

$$\frac{\|\boldsymbol{x}_0\|_0}{N} \xrightarrow{\text{a.s.}} \mathbb{E}\left\{\mathbf{1}\left\{x_0 = 0\right\}\right\} \tag{6.12a}$$

$$= 1 - \int_{0^-}^{0^+} \mathrm{p}_0(x_0)\,\mathrm{d}x_0 = \rho \tag{6.12b}$$

where $\xrightarrow{\text{a.s.}}$ denotes the almost sure convergence. This observation indicates that in the large-system limits, the random samples drawn i.i.d. from this distribution are almost surely sparse with factor ρ.

6.3.2 Performance Measure

The final goal in sparse recovery is to reconstruct the true signal samples with high fidelity. Such a constraint can be evaluated with various measures. The suitable metric depends on the nature of the problem which often follow one of two following distinct scenarios:

1. When the non-zero samples are drawn from a *continuous distribution*, i.e., $\mathbb{X}$ is a continuous subset of $\mathbb{R}$, the exact recovery from noisy measurements is theoretically not possible. Hence, a suitable metric for quantifying the performance in this case is to evaluate the MSE between the true signal samples and the estimated ones. This means that the performance metric in this case reads

$$\mathrm{MSE} = \frac{1}{N}\mathbb{E}\left\{\|\boldsymbol{x} - \boldsymbol{x}_0\|^2\right\} \tag{6.13}$$

where $\boldsymbol{x}_0$ denotes the vector of true signal samples and $\boldsymbol{x}$ represent those calculated via the recovery algorithm. Following the definitions in Section 2.4, this metric denotes the average distortion of the recovery algorithm for the distortion function $\mathsf{d}(x; x_0) = |x - x_0|^2$.

2. For signals whose samples take values from a *discrete* support, the exact recovery is possible even in presence of measurement noise. As a result, and alternative metric for performance evaluation is the SER defined as

$$\mathrm{SER} = \frac{1}{N}\mathbb{E}\left\{\sum_{n=1}^{N} \mathbf{1}\{x_n \neq x_{0n}\}\right\} \tag{6.14a}$$

$$= \frac{1}{N}\mathbb{E}\left\{\|\boldsymbol{x} - \boldsymbol{x}_0\|_0\right\}. \tag{6.14b}$$

By definition, this metric is the average distortion with respect to the distortion function $\mathsf{d}(x; x_0) = \mathbf{1}\{x_n \neq x_{0n}\}$.

6.3.3 Asymptotics via the Decoupling Principle

Our ultimate goal is to determine the asymptotic limit of the performance metric when an RLS-based recovery algorithm is employed for reconstructing a sparse signal. This task is tractably addressed via the decoupling principle. In fact, from Chapter 5 we know that for a given signal and recovery algorithm, the joint distribution of the true and recovered samples is given by the corresponding decoupled setting. The asymptotic performance metric is hence characterized via the expected performance of its decoupled setting. In the sequel, we follow this approach to investigate the performance of several sparse recovery scenarios. Based on the signal model, we divide these scenarios into two cases:

1. *Continuous signals:* This case refers to signals for which $\mathbb{X} = \mathbb{R}$ and the distribution of non-zero entries, i.e., $\mathrm{p}_S(\cdot)$, is an absolute continuous distribution[5].

[5]This means that $\mathrm{p}_S(\cdot)$ is a well-defined function with no impulse term.

2. *Quantized signals:* In this case, the distribution of non-zero entries, i.e., $\mathrm{p}_S(\cdot)$, is absolutely discrete meaning that $\mathrm{p}_S(\cdot)$ is of the following form

$$\mathrm{p}_S(s) = \sum_{q=1}^{Q} w_q \, \delta(s - c_q) \tag{6.15}$$

for some integer Q, where for $q \in [Q]$, $c_q \in \mathbb{R}$ and $w_q \in (0,1)$ satisfying

$$\sum_{q=1}^{Q} w_q = 1. \tag{6.16}$$

For each of these cases, we investigate the performance of standard recovery schemes in the sequel.

6.3.3.1 Recovery of Continuous Sparse Signals

Following the stochastic model for sparsity, the samples of continuous sparse signals can be considered as the multiplication of a continuous random variable and a Bernoulli random variable. In other words, x_{0n} for $n \in [N]$ can be observed as i.i.d. draw of random variable $x_0 = bs$ where s is a continuous random variable distributed with $\mathrm{p}_S(\cdot)$ and $b \sim \mathrm{Bern}(\rho)$. It is worth to remind that in this case, exact recovery is not possible theoretically, and hence the performance of a given recovery algorithm is described via the MSE[6].

From the decoupling principle, the single-letter measurement[7] in this case is

$$\mathrm{y} = \mathrm{x}_0 + \mathrm{z} \tag{6.17}$$

for some noise z, where $\mathrm{x}_0 = \mathrm{bs}$ with $\mathrm{b} \sim \mathrm{Bern}(\rho)$ and $\mathrm{s} \sim \mathrm{p}_S(\mathrm{s})$. The distribution of measurement noise z is moreover specified for different replica ansätze in Chapter 5. We now derive the explicit form of the decoupled recovery scheme[8].

[6] Theoretically, SER = 1 in this case.
[7] This is in fact the decoupled regressand defined in Chapter 5.
[8] This is in fact the decoupled RLS method defined in Definition 5.4.

Recovery Scheme 6.3.3.1.1 (Linear recovery scheme)**.** We start the analysis by considering a linear recovery scheme. The generic RLS method reduces to this scheme, when the regularization term is set to

$$u\left(v\right)=\frac{v^{2}}{2}. \tag{6.18}$$

As mentioned earlier, this scheme exhibits poor performance for sparse recovery, since it does not penalize the LS term effectively with respect to the sparsity constraint. This can be also illustrated via the Bayesian viewpoint given in Section 2.2.1. In fact, the linear recovery scheme is a MAP estimator which postulates a zero-mean and unit-variance Gaussian prior on the signal. Regardless of the explicit expression for $\mathrm{p}_{S}\left(\cdot\right)$, such an assumption on the prior distribution is significantly mismatched when $\rho\neq 0$, and hence results in poor performance.

Substituting the penalty (6.18) into Definition 5.4, the decoupled algorithm is as follows

$$\mathsf{g}_{\mathsf{RLS}}\left(\mathrm{y}|\tau\right)=\frac{\mathrm{y}}{1+\tau}. \tag{6.19}$$

The decoupled setting in this case describes a scalar sensing system with additive noise whose measurement is passed to a *linear* estimator.

Recovery Scheme 6.3.3.1.2 (LASSO)**.** The generic RLS method reduces to the LASSO recovery scheme, if we set

$$u\left(v\right)=\left|v\right|. \tag{6.20}$$

This scheme is known to be the most efficient tractable approach for sparse recovery. In the Bayesian framework, LASSO describes a MAP estimator whose postulated prior distribution Laplace[9] with unit variance. This assumption is known to be a better approximation of the prior distribution of a sparse signal.

[9] Also known as *double exponential* distribution.

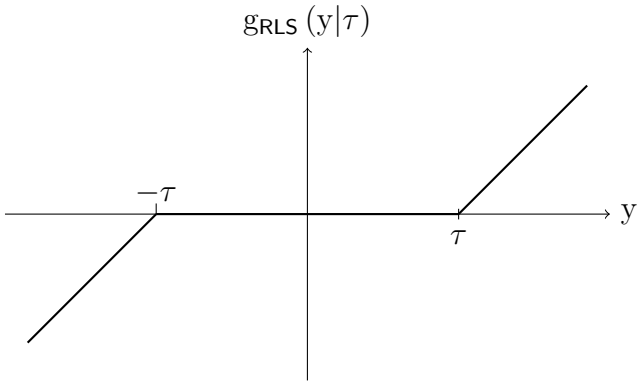

Figure 6.1: Soft-thresholding operator.

The decoupled recovery algorithm in this case is

$$\mathrm{g}_{\mathsf{RLS}}(\mathrm{y}|\tau) = \begin{cases} \mathrm{y} - \tau & \mathrm{y} \geq \tau \\ 0 & |\mathrm{y}| < \tau \\ \mathrm{y} + \tau & \mathrm{y} \leq \tau \end{cases} \tag{6.21}$$

The decoupled LASSO algorithm describes the *soft-thresholding* operator. The input-output characteristic of this this operator is shown in Figure 6.1.

Recovery Scheme 6.3.3.1.3 (ℓ_0-norm minimization)**.** The ℓ_0-norm minimization scheme directly regularizes the LS term with sparsity of the signal by setting

$$u(v) = \mathbf{1}\{v \neq 0\}. \tag{6.22}$$

For this scheme, the decoupled recovery algorithm is

$$\mathrm{g}_{\mathsf{RLS}}(\mathrm{y}|\tau) = \begin{cases} \mathrm{y} & |\mathrm{y}| \geq \sqrt{2\tau} \\ 0 & |\mathrm{y}| < \sqrt{2\tau} \end{cases}. \tag{6.23}$$

The decoupled algorithm in this case describes the *hard-thresholding* operator whose diagram is shown in Figure 6.2.

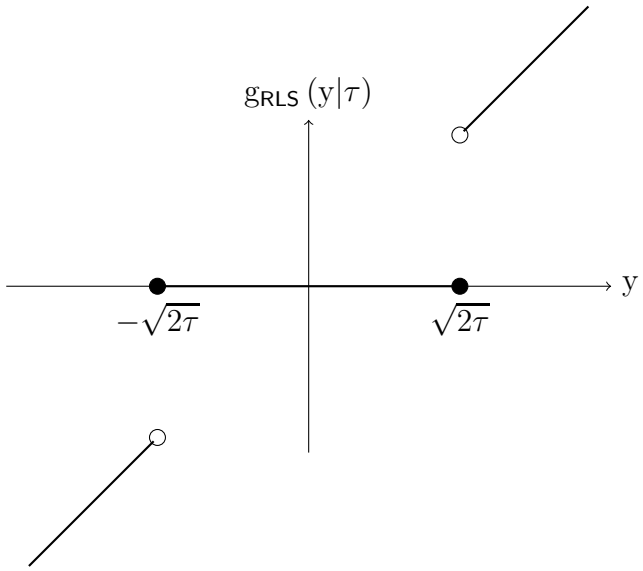

Figure 6.2: Hard-thresholding operator.

6.3.3.2 Quantized signals

Nonzero samples of a quantized signal are taken from a discrete subset of real numbers. Following the notation in (6.15), the support of a quantized sparse signal is

$$\mathbb{X} = \{0, c_1, \ldots, c_Q\}. \tag{6.24}$$

Similar to continuous signals, the samples of this signal can be observed as an i.i.d. draw of $x_0 = bs$ in which $b \sim \text{Bern}(\rho)$ and s is a *non-zero discrete* random variable with distribution $\text{p}_S(s)$.

Regardless of the regularization term, the RLS method for recovery of a quantized signal deals with the NP-hard problem of integer programming. Hence, it is computationally intractable. Note that in this case, by setting the regularization term to

$$u(v) = \begin{cases} -\log(1-\rho) & v = 0 \\ -\log(\rho w_q) & v = c_q \end{cases} \qquad \text{for } q \in [Q] \tag{6.25}$$

and the tuning factor to the noise variance, i.e., $\lambda = \sigma^2$, the RLS method reduces to the matched MAP detector. Recalling that the performance metric in this case is the SER, this detector describes optimal recovery with respect to the considered metric.

To have a tractable recovery algorithm in practice, the original RLS formulation is modified, such that the integer programming is relaxed to a convex optimization problem. A well-known approach in this respect is the so-called *box-LASSO* scheme. In box-LASSO, a *soft estimation* of the signal samples is found via LASSO from the noisy measurements. This algorithm determines the soft estimation tractably by relaxing the signal support to a convex set[10] which includes the discrete set $\mathbb{X}$. Hence, the soft estimation is given by

$$\boldsymbol{x}_{\text{soft}} = \underset{\boldsymbol{v}\in\mathbb{X}_C^N}{\operatorname{argmin}} \ \frac{1}{2\lambda} \left\|\boldsymbol{y} - \mathbf{A}\boldsymbol{v}\right\|^2 + \left\|\boldsymbol{v}\right\|_1 , \tag{6.26}$$

where $\mathbb{X}_C$ is a convex set for which we have $\mathbb{X} \subset \mathbb{X}_C$. The entries of soft estimation are then given to a *decisioning function* $f_{\text{dec}}(\cdot) : \mathbb{X}_C \mapsto \mathbb{X}$ which maps each sample to a symbol in the signal support. An example of decisioning function is a thresholding operator which assigns a value from $\mathbb{X}$ to a softly estimated sample by comparing it with some threshold values. The recovered sample n is hence written as

$$x_n = f_{\text{dec}}\left(x_{\text{soft},n}\right). \tag{6.27}$$

We investigate the asymptotic performance of these two recovery algorithms via the decoupling principle. The single-letter sensing setting for the quantized sparse signals is similar to one given for continuous signals in the previous section. The decoupled algorithm for each of these recovery schemes are moreover given in the sequel.

[10] This set is often set to be the convex hall of $\mathbb{X}$.

Recovery Scheme 6.3.3.2.1 (MAP recovery)**.** By setting the regularization term to be consistent with (6.25), the RLS method reduces to the MAP recovery scheme with matched prior distribution. For such a choice, the decoupled algorithm reads

$$\mathsf{g}_{\mathsf{RLS}}\left(\mathrm{y}|\tau\right) = \begin{cases} 0 & c_{\mathrm{Th}}^{-} \leq \mathrm{y} \leq c_{\mathrm{Th}}^{+} \\ c^{\star}\left(\mathrm{y}|\tau\right) & \text{otherwise} \end{cases} \tag{6.28}$$

where the constants c_{Th}^{-} and c_{Th}^{+} are given by

$$c_{\mathrm{Th}}^{-} = \max_{q \in [Q]^{-}} \frac{c_q}{2} + \frac{\tau}{c_q} \log\left(\frac{1-\rho}{\rho w_q}\right), \tag{6.29a}$$

$$c_{\mathrm{Th}}^{+} = \min_{q \in [Q]^{+}} \frac{c_q}{2} + \frac{\tau}{c_q} \log\left(\frac{1-\rho}{\rho w_q}\right). \tag{6.29b}$$

Here, the notations $[Q]^{-}$ and $[Q]^{+}$ denote

$$[Q]^{-} \coloneqq \{q \in [Q] : c_q < 0\} \tag{6.30a}$$

$$[Q]^{+} \coloneqq \{q \in [Q] : c_q > 0\}. \tag{6.30b}$$

The function $c^{\star}\left(t|\tau\right)$ is further defined as $c^{\star}\left(t|\tau\right) = c_{q^{\star}}$

$$q^{\star} = \operatorname*{argmin}_{q \in [Q]} \frac{1}{2\tau}\left(t - c_q\right)^2 - \log w_q. \tag{6.31}$$

Here, $c^{\star}\left(t|\tau\right)$ represents the decoupled recovery scheme for the optimal detector when[11] $\rho = 1$. The algorithm in (6.28) is hence a hard-thresholding operator which recovers zero when the observation is less than c_{Th}. When the observation passes the threshold, the algorithm switches to the optimal Bayesian detector performing over the non-zero entries in $\mathbb{X}$. As $\rho \uparrow 1$, the threshold tends to $-\infty$, and hence $\mathsf{g}_{\mathsf{RLS}}\left(\mathrm{y}|\tau\right) \to c^{\star}\left(t|\tau\right)$.

Recovery Scheme 6.3.3.2.2 (Box-LASSO)**.** The box-LASSO algorithm first calculates the soft transmission by solving the RLS problem on a relaxed subset $\mathbb{X}_C \supset \mathbb{X}$.

[11] This is the case with sparsity 1, meaning that the signal is not sparse anymore.

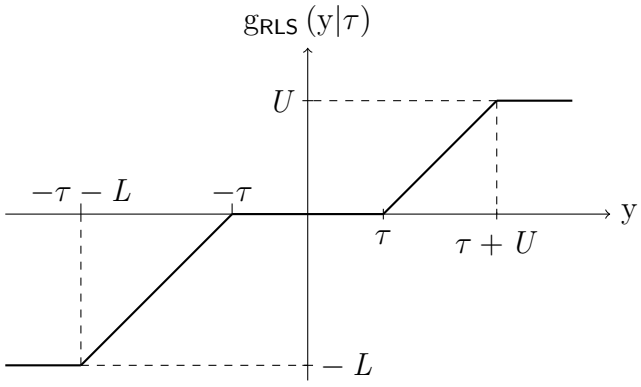

Figure 6.3: Soft-thresholding operator with limited range.

For quantized signals with the support in (6.24), a possible choice is $\mathbb{X}_C = [-L, U]$, where L and U satisfy

$$-L \leq \min_{x \in \mathbb{X}} x \;, \tag{6.32a}$$

$$U \geq \max_{x \in \mathbb{X}} x \;. \tag{6.32b}$$

For such a choice, the decoupled algorithm which calculates the *decoupled soft estimation* reads

$$\mathrm{g}_{\mathsf{RLS}}\left(\mathrm{y}|\tau\right) = \begin{cases} U & \mathrm{y} \geq \tau + U \\ \mathrm{y} - \tau & \tau \leq \mathrm{y} \leq \tau + U \\ 0 & -\tau \leq \mathrm{y} \leq \tau \\ \mathrm{y} + \tau & -\tau - L \leq \mathrm{y} \leq -\tau \\ -L & \mathrm{y} \leq -\tau - L \end{cases} . \tag{6.33}$$

The recovery algorithm in this case is a soft-thresholding operator whose range is restricted to be within $\mathbb{X}_C$. The diagram of this operator is shown in Figure 6.3.

The decoupled recovered sample is given by operating the decisioning function on $\mathrm{g}_{\mathsf{RLS}}(\mathrm{y}|\tau)$. We show this sample by $\mathrm{g}^{\star}(\mathrm{y}|\tau)$ which reads

$$\mathrm{g}^{\star}(\mathrm{y}|\tau) = f_{\mathrm{dec}}\left(\mathrm{g}_{\mathsf{RLS}}(\mathrm{y}|\tau)\right). \tag{6.34}$$

In the sequel, we investigate these recovery algorithms through some numerical simulations.

6.4 Numerical Investigations

To verify our derivations, we now consider some examples and investigate them numerically. Through these examples, we discuss the validity of RS and RSB ansätze under various assumptions, and also illustrate some particular applications of our asymptotic characterizations to the problem of sparse recovery. Before starting the investigations, let us specify the setups which we are studying.

6.4.1 Sensing Matrices

From the literature of sparse recovery, it is well known that structure of the sensing matrix impacts the performance of a recovery algorithm. For deterministically structured matrices, quality of the sensing matrix is often measured in terms of the so-called *coherence* of the matrix or by the concept of *restricted isometry property*[12]. In stochastic models with randomly generated sensing matrices, the effectiveness of the sensing matrix is stated in average via probabilistic tools. There are variety of random sensing matrices which have been studied in this respect in the literature. Throughout the numerical investigations, we consider the two important ensembles of these matrices: random matrices with *i.i.d.* entries, and the so-called random *projector* matrices. The details on each ensemble is given in the sequel.

[12]See [14] and the references therein for detailed discussions on these concepts.

6.4.1.1 i.i.d. Random Matrices

In this case, the entries of $\mathbf{A}$ are drawn i.i.d. from a given distribution. Without loss of generality, we assume that the entries are zero-mean random variables with variance $1/M$. This ensemble is the most primary and also the most discussed case in random matrix theory. For an i.i.d. matrix, regardless of the entry distribution, it is well known that the asymptotic empirical eigenvalue CDF of the Gramian $\mathbf{J} = \mathbf{A}^{\mathsf{T}}\mathbf{A}$ follows the Marcenko-Pastur law which states [57, 58, 108]

$$\mathrm{F}_{\mathbf{J}}(\lambda) = [1-\alpha]^{+}\mathbf{1}\{\lambda > 0\} + \int_{0}^{\lambda} \frac{\sqrt{\alpha - [\alpha(1-u)]^{2}}}{2\pi u}\mathrm{d}u \tag{6.35}$$

where $[x]^{+}$ returns x when x is non-negative and is zero otherwise. Using the definition of R-transform, it is straightforward to show that $\mathrm{R}_{\mathbf{J}}(\cdot)$ reads

$$\mathrm{R}_{\mathbf{J}}(\omega) = \frac{\alpha}{\alpha - \omega}. \tag{6.36}$$

6.4.1.2 Random Projector Matrices

In these matrices, the row vectors are orthogonal. The matrices are also referred to as the *row-orthogonal* matrices. For the sensing matrix $\mathbf{A}$, we consider the case in which the row vectors are normalized by the number of rows and $M \leq N$. Therefore, the outer product $\mathbf{A}\mathbf{A}^{\mathsf{T}}$ reads

$$\mathbf{A}\mathbf{A}^{\mathsf{T}} = \frac{N}{M}\mathbf{I}_{M} = \alpha^{-1}\mathbf{I}_{M}\,. \tag{6.37}$$

Consequently, the Gram matrix $\mathbf{J}$ takes two different eigenvalues: $\lambda = 0$ with multiplicity $N-M$, and $\lambda = \alpha^{-1}$ with multiplicity M. As a result, the asymptotic empirical CDF of the eigenvalues read

$$\mathrm{F}_{\mathbf{J}}(\lambda) = [1-\alpha]\mathbf{1}\{\lambda > 0\} + \alpha\mathbf{1}\left\{\lambda > \alpha^{-1}\right\} \tag{6.38}$$

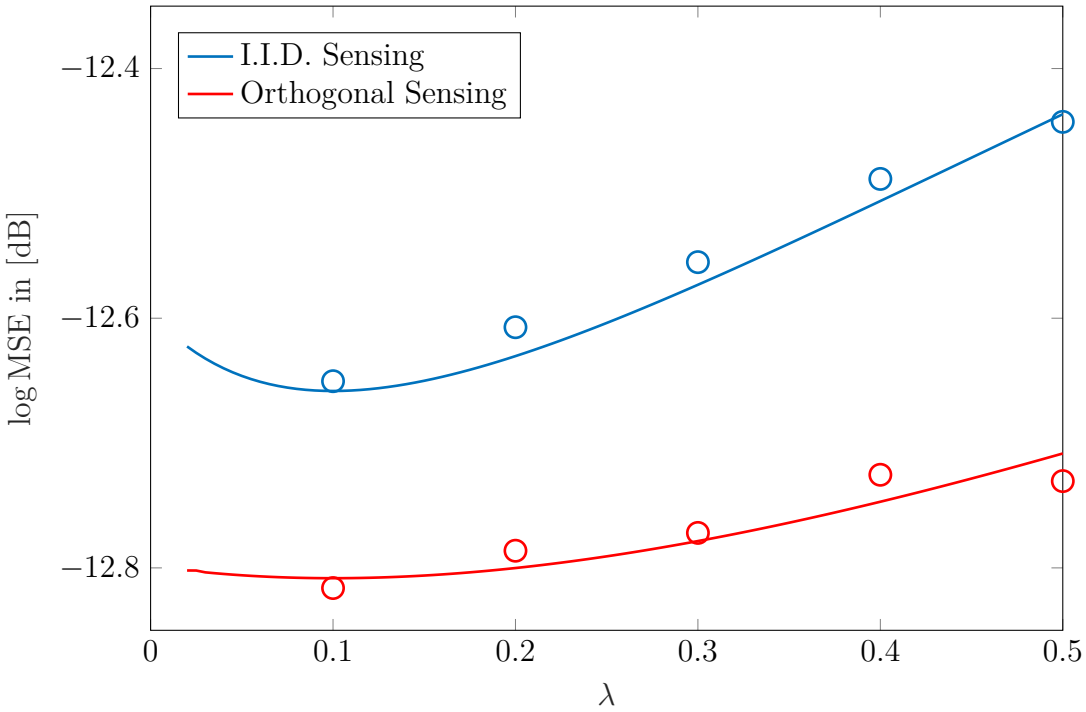

Figure 6.4: Performance of linear recovery for i.i.d. and projector matrices.

which results in the R-transform of the form

$$\mathrm{R}_{\mathbf{J}}(\omega) = \frac{\omega - \alpha + \sqrt{(\omega-\alpha)^2 + 4\alpha^2\omega}}{2\alpha\omega}. \tag{6.39}$$

6.4.2 Results for Continuous Signals

We start the investigations by giving some results for continuous signals. Throughout the simulations, we consider a *sparse-Gaussian* signal whose non-zero entries are distributed Gaussian with zero mean and unit variance, i.e.,

$$\mathrm{p}_S(s) = \frac{1}{\sqrt{2\pi}} \exp\left\{-\frac{s^2}{2}\right\}. \tag{6.40}$$

Figure 6.4 shows the asymptotic MSE achieved via Recovery Scheme 6.3.3.1.1 against tuning factor λ for both i.i.d. and orthogonal sampling. The results are given

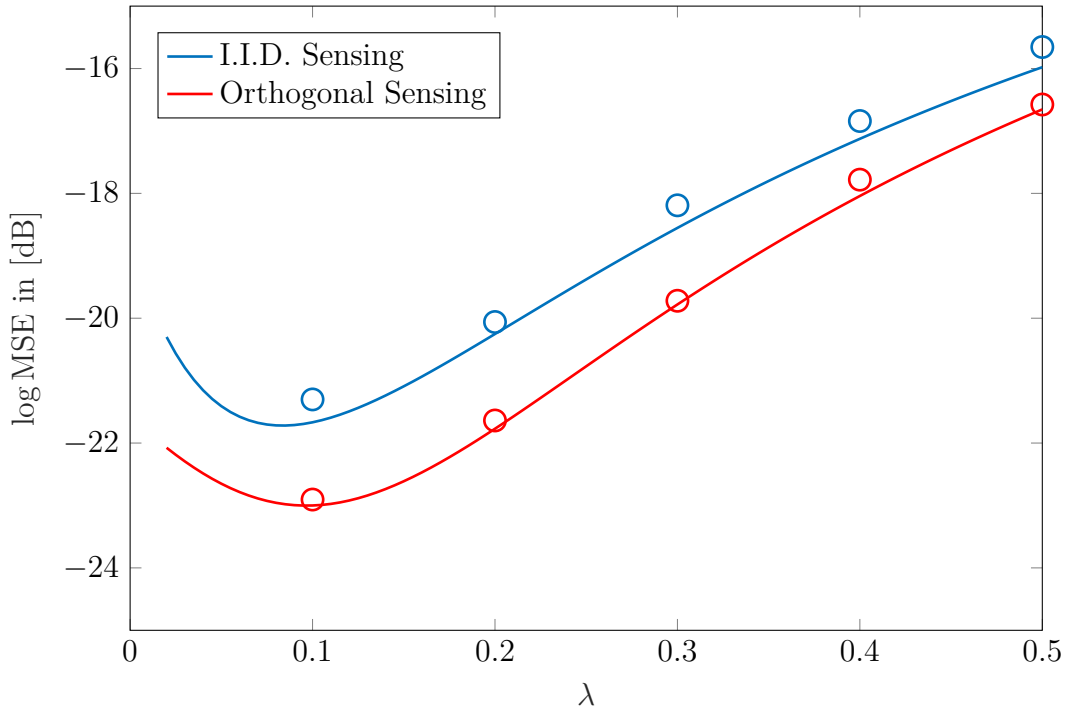

Figure 6.5: Performance of LASSO recovery for i.i.d. and projector matrices.

by the RS ansatz. Here, the sparsity factor is set to $\rho = 0.1$ and the signal-to-noise ratio (SNR), defined as

$$\mathrm{SNR} \coloneqq \frac{\rho}{\sigma^2}, \tag{6.41}$$

is set to $\log \mathrm{SNR} = 10$ decibel (dB). Furthermore, the compression rate defined as

$$R_{\mathrm{c}} \coloneqq \frac{1}{\alpha} \tag{6.42}$$

is considered to be $R_{\mathrm{c}} = 2$.

To validate the RS result, we further run numerical simulations for $N = 300$ signal samples which are indicated by circles in the figure. As the figure depicts, the simulation results closely track the asymptotic characterization via the RS ansatz. This observation indicates the validity of RS for this setting. From the figure we see that orthogonal sampling outperforms i.i.d. sampling in terms of the achievable MSE. This

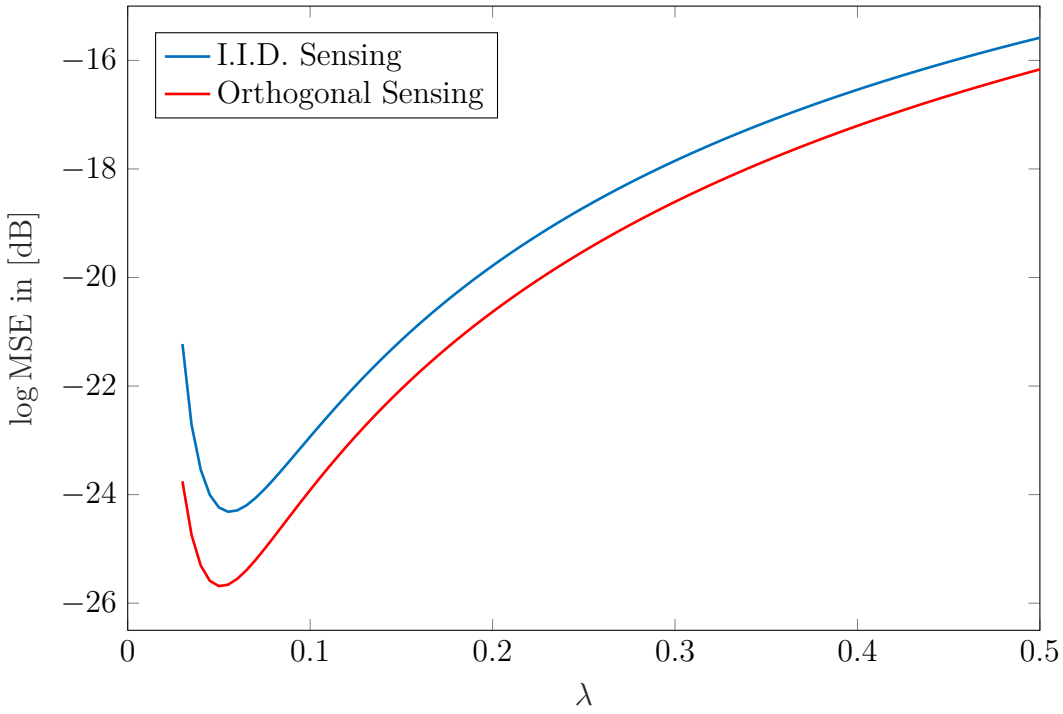

Figure 6.6: Performance of ℓ_0-norm minimization for i.i.d. and projector matrices.

observation is consistent with earlier investigations in literature; see [109]. The figure further demonstrates that the performance of RLS recovery depends notably on the value of tuning factor λ. In fact, some bad choice of λ can significantly degrade the recovery performance.

The similar experiment is performed for the LASSO recovery algorithm, i.e., Recovery Scheme 6.3.3.1.2, whose results is shown in Figure 6.5. Here, the same setting is considered, and the asymptotic performance is sketched by using the RS ansatz. As the figure shows, the LASSO algorithm achieves significantly lower MSE. This follows the fact that linear recovery ignores the sparsity of the signal which degrades notably its performance. Similar to Figure 6.4, the numerical simulations fit closely to the analytic figures given via the RS ansatz. This observation indicate the validity of the RS ansatz in this case.

We further repeat the same experiment for the ℓ_0-norm minimization scheme, i.e., Recovery Scheme 6.3.3.1.3. The results are given in Figure 6.6. Although the curves

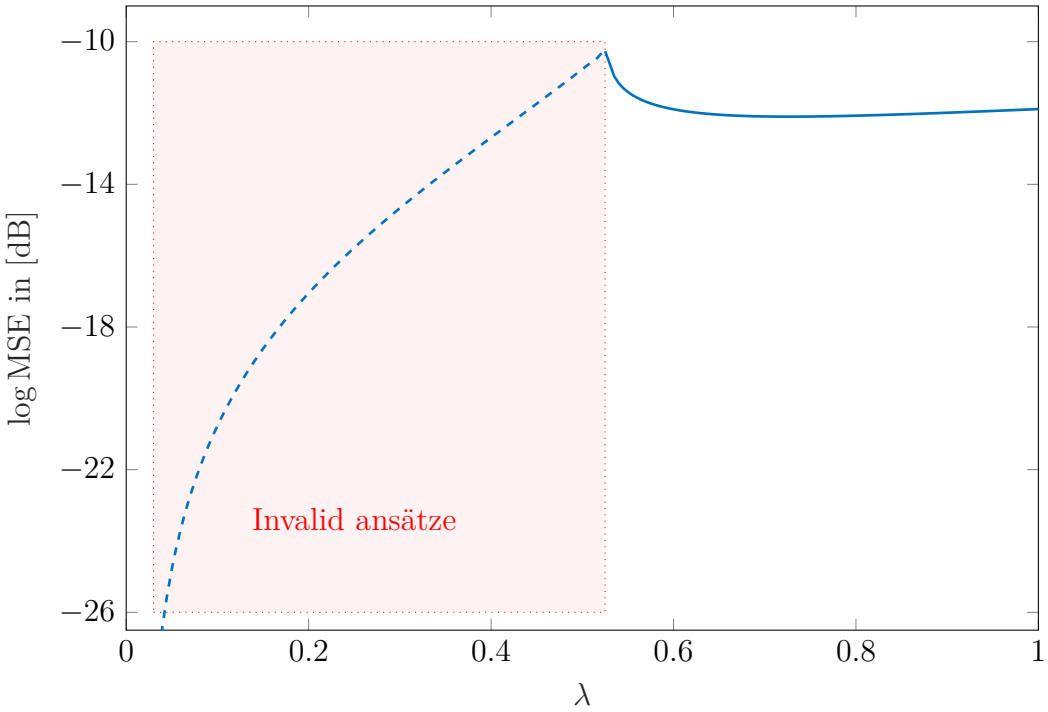

Figure 6.7: RS-prediction of ℓ_0-norm minimization performance for $R_c = 4$.

look consistent with the intuition, numerical validation of the results is not tractable in this case. In fact, numerical simulations are computationally intractable in this case. We hence take an alternative approach: First, we plot the same figure for higher compression rate, namely $R_c = 4$, considering the case with i.i.d. sampling. The result is shown in Figure 6.7 which seems counter-intuitive. Here, the RS ansatz predicts that the MSE achieved by ℓ_0-norm minimization suddenly drops as tuning factor λ tends to zero. By intuition, this result does not seem to be valid. Such an inconsistency has been earlier conjectured in the literature following discussions on the stability of the RS saddle-point for ℓ_0-norm minimization; see for example [75, 77]. We hence conjecture that the sudden drop in Figure 6.7 is due to invalidity of the RS assumption in this setting. To justify our conjecture, we sketch the minimum achievable MSE for different recovery schemes against the compression rate using the RS ansatz. This is given in Figure 6.8. The curves in this figure are plotted as follows:

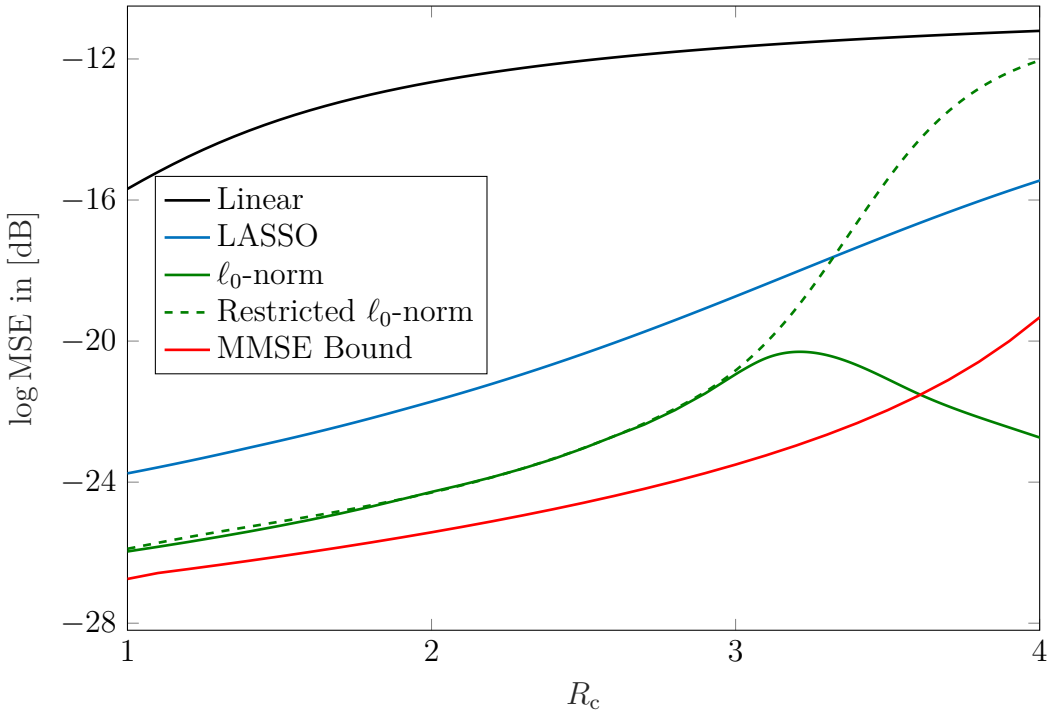

Figure 6.8: Minimum achievable MSE predicted via the RS ansatz.

- The curves for the linear, LASSO and ℓ_0-norm minimization recovery schemes which are shown by solid black, blue and green curves, respectively, are plotted by minimizing numerically the achievable MSE predicted by the RS ansatz with respect to λ in the interval $\lambda \in [0.01, 1]$.

- The dashed green curve shows the RS prediction of the MSE achieved via ℓ_0-norm minimization when we restrict λ to the interval in which the RS ansatz looks *intuitively* consistent. More precisely, we ignore the interval of small tuning factors in which the RS ansatz unexpectedly drops, and minimize the MSE numerically over the remaining interval, e.g., in Figure 6.7 we ignore the red zone.

- The solid red line shows the asymptotic MMSE bound which has been rigorously derived in the literature; see for example [74].

As Figure 6.8 demonstrates the RS prediction of the minimum achievable MSE for ℓ_0-norm minimization recovery violates the MMSE bound. This indicates that our

initial conjecture on the invalidity of the RS ansatz at small values of λ is correct. It is further observed that the restricted curve for ℓ_0-norm minimization recovery violates the curve given for the LASSO scheme. This observation intuitively depicts that in higher compression rates the optimal tuning factor of the ℓ_0-norm minimization scheme with which the minimum MSE is achieved lies within the interval in which the RS ansatz is not valid.

The observed behavior of the recovery schemes can be intuitively justified by former observations in the literature. In fact, it is widely believed that convex optimization problems are asymptotically characterized via the RS ansatz; see for example [64, 73]. In other words, the spin glasses which correspond to optimization problems with convex objective functions and supports are conjectured to exhibit RS. Such a belief is consistent with our results, since both the linear and LASSO recovery schemes are consistently characterized via the RS ansatz. In ℓ_0-norm minimization, however, the RLS scheme deals with a non-convex optimization problem. This issue follows the fact that the regularization term, i.e., the ℓ_0-norm, is a non-convex function. In this case, the corresponding spin glass exhibits RSB. This is clearly observed, as the tuning factor λ tends to zero. Note that by $\lambda \downarrow 0$, the RLS scheme reduces to the following *constrained* ℓ_0-norm minimization problem:

$$\min \|\boldsymbol{v}\|_0 \qquad \text{subject to } \boldsymbol{y} = \mathbf{A}\boldsymbol{v}. \tag{6.43}$$

Since the RS ansatz fails to predict the performance of ℓ_0-norm minimization recovery consistently, we further investigate asymptotic characterization under RSB. Figure 6.9 shows the minimum achievable MSE for the ℓ_0-norm minimization scheme predicted via the one-RSB ansatz. For sake of comparison, we have further plotted the MMSE bound and the curve for LASSO recovery. As the figure shows, unlike the RS ansatz, the one-RSB ansatz is consistent with the bounds.

To check the consistency of the given ansatz, we further sketch the zero-temperature entropy for the RS and one-RSB ansätze against the compression rate in Figure 6.10. As the figure shows, the zero-temperature entropy calculated from the RS ansatz drops significantly as the compression rate grows while the one-RSB entropy remains close to zero in this interval. Such an observation confirms our earlier discussions on the

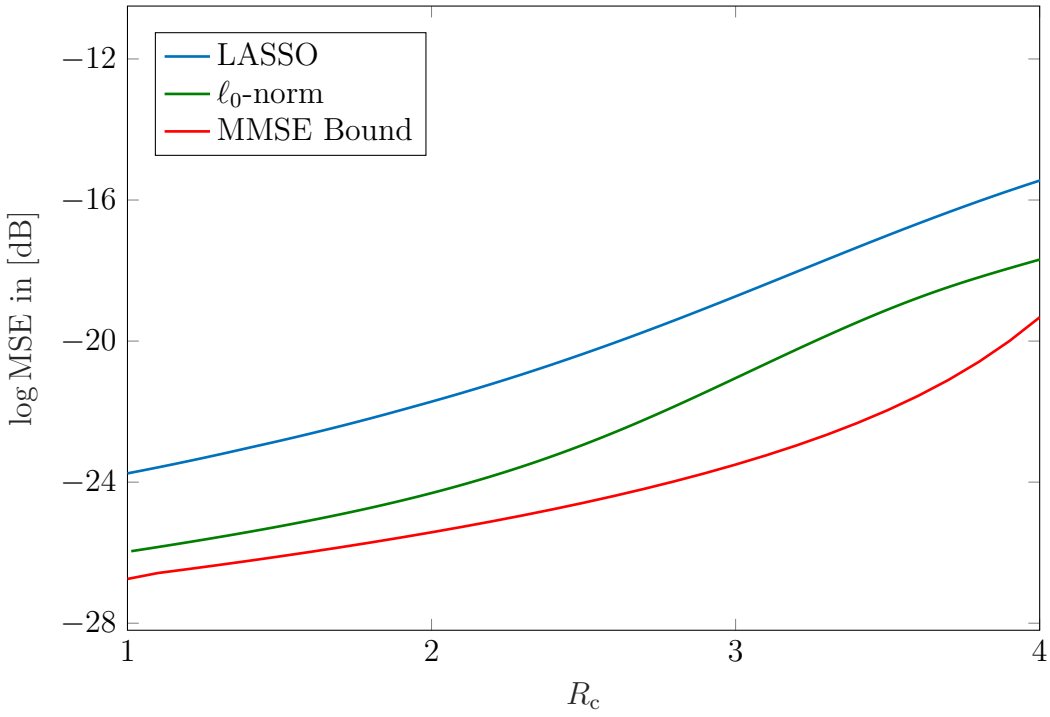

Figure 6.9: Minimum achievable MSE predicted via the one-RSB ansatz.

validity of the RS ansatz. From Figure 6.10, we observe that the zero-temperature entropy for the one-RSB ansatz is also reducing as the compression rate increases. We hence conjecture that the exact performance of ℓ_0-norm minimization recovery is characterized via higher orders of RSB.

6.4.3 Results for Quantized Signals

We now give numerical results for quantized sparse signals. Here, we consider the case in which non-zero samples are uniform bipolar random variables with unit variance. This means that $Q = 2$ and

$$\mathrm{p}_S(s) = \frac{1}{2}\,\delta(s-1) + \frac{1}{2}\,\delta(s+1)\,. \tag{6.44}$$

For investigation, we first consider Recovery Scheme 6.3.3.2.1. Figure 6.11 shows the SER achieved via matched MAP recovery against the compression rate. Here, the

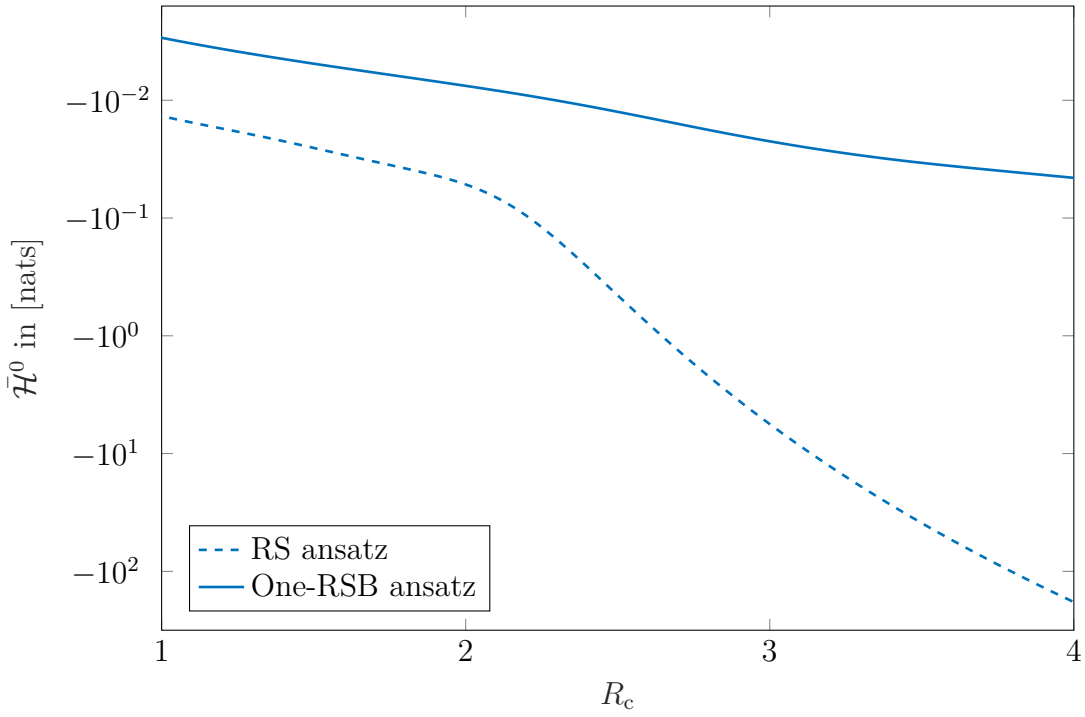

Figure 6.10: Zero-temperature entropy versus compression rate.

SNR is set to $\log \mathrm{SNR} = 5$ dB and the sparsity factor is set to $\rho = 0.1$. The results are given for both i.i.d. and orthogonal sampling. Similar to the ℓ_0-norm minimization scheme for continuous signals, numerical simulation for this scheme is computationally intractable.

As the figure shows, the SER suddenly jumps from some small value to the vicinity of the upper bound[13]

$$\mathrm{SER}_{\mathrm{up}} = 2\rho - \frac{3}{2}\rho^2 = 0.185. \tag{6.45}$$

This is a well-known large-system behavior which is called *phase transition*. Phase transition refers to the sudden change in the property of a thermodynamic system. Such a behavior is also observed in physical systems. The most simple example is the sudden change in the physical shape of water when its temperature passes a critical

[13]This upper bound is calculated by considering the extreme case in which the true signal and its recovery are statistically independent.

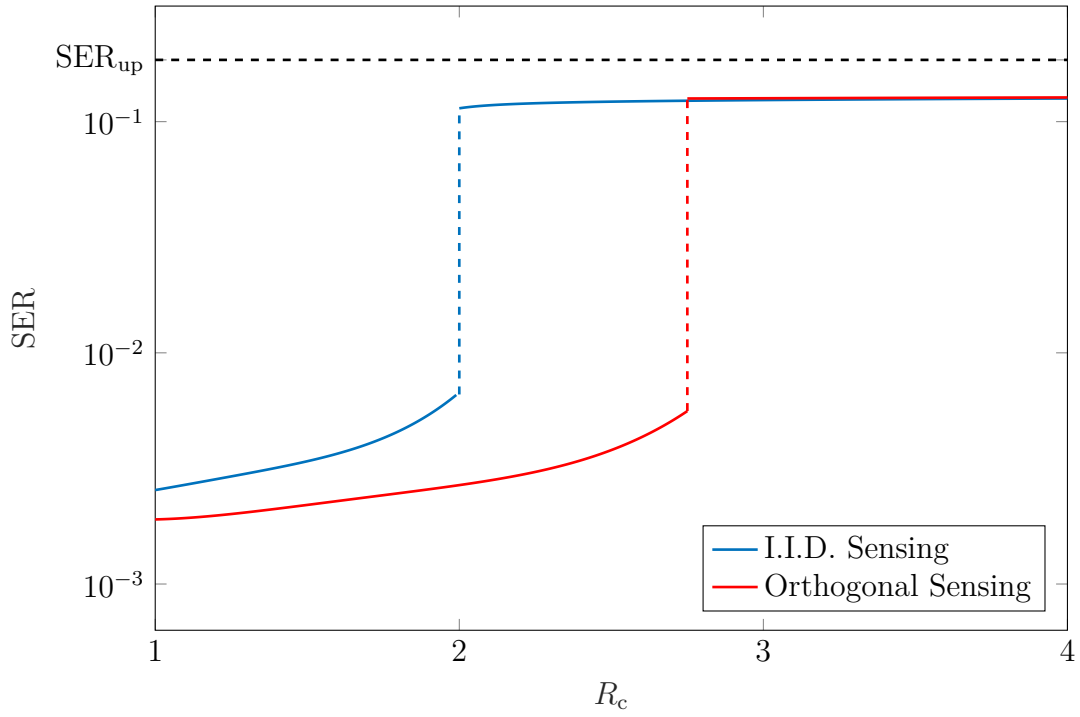

Figure 6.11: SER achieved via matched MAP recovery versus compression rate.

level. This phenomenon has been also seen in various communications system; see for example [40, 110].

From Figure 6.11, it is concluded that in the large system limit by passing a threshold rate, the error probability jumps to the upper bound meaning that the recovered signal is almost independent of the true signal. Similar phenomena are observed in channel and source coding problems. As the figure shows, the threshold rate at which the phase transition happens is larger for orthogonal sensing. This extends our earlier observation to the case of quantized signals, as well.

We now investigate the computationally tractable approach of box-LASSO recovery for the quantized signals. To this end, we consider Recovery Scheme 6.3.3.2.2 with for sparse bipolar signals with sparsity factor $\rho = 0.1$. The SNR is further set to $\log \text{SNR} = 10$ dB. The achievable MSE and SER for this scheme is plotted against the tuning factor for both i.i.d. and orthogonal sensing in Figures 6.12 and 6.13. Here,

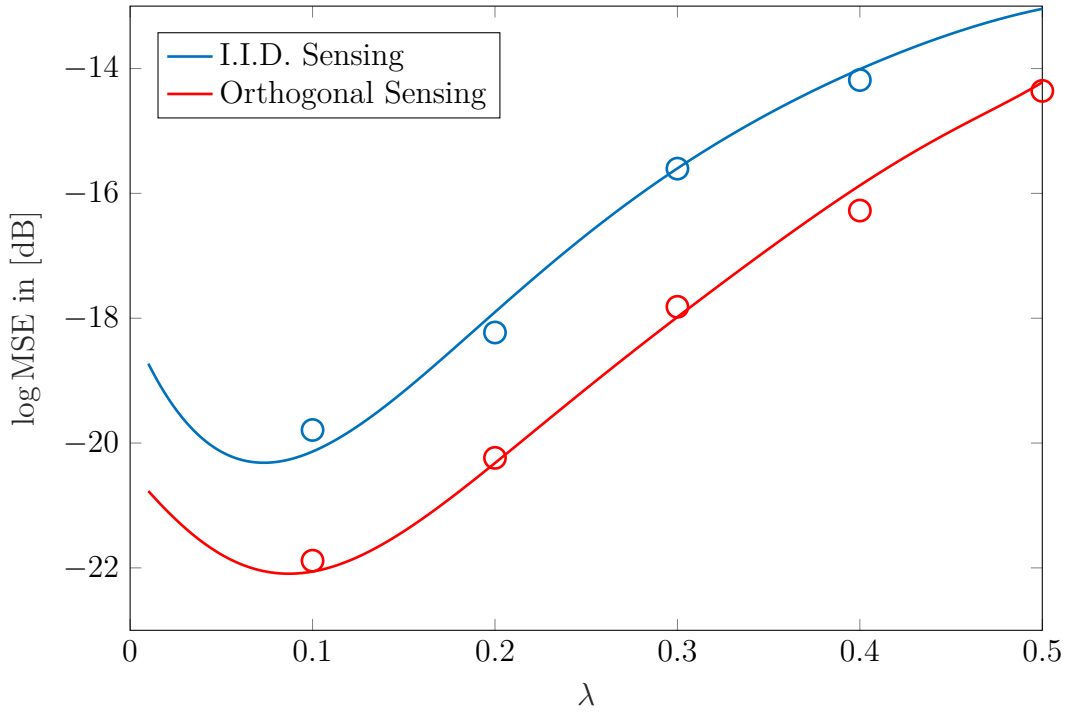

Figure 6.12: MSE achieved via Box LASSO recovery against regularizer λ.

the compression rate is set to $R_c = 2$. The MSE for this setting is defined as the average MSE between the true signal and its soft estimation, i.e.,

$$\mathrm{MSE} = \frac{1}{N}\mathbb{E}\left\{\|\boldsymbol{x}_{\mathrm{soft}} - \boldsymbol{x}_0\|^2\right\}. \tag{6.46}$$

To validate the asymptotic results given by the RS ansatz, we further calculate the average MSE, as well as the SER, for this case by running numerical simulations for $N = 300$ samples. As the figures demonstrate, the numerical results closely track the asymptotic curves derived via the RS ansatz.

As the figure shows, the performance of box-LASSO recovery is remarkably related to its tuning. This is intuitive, as LASSO recovery has shown the similar behavior. It is hence required in practice to tune the recovery algorithm properly. Such a task can be numerically burdensome in several practical scenarios. Using the asymptotic

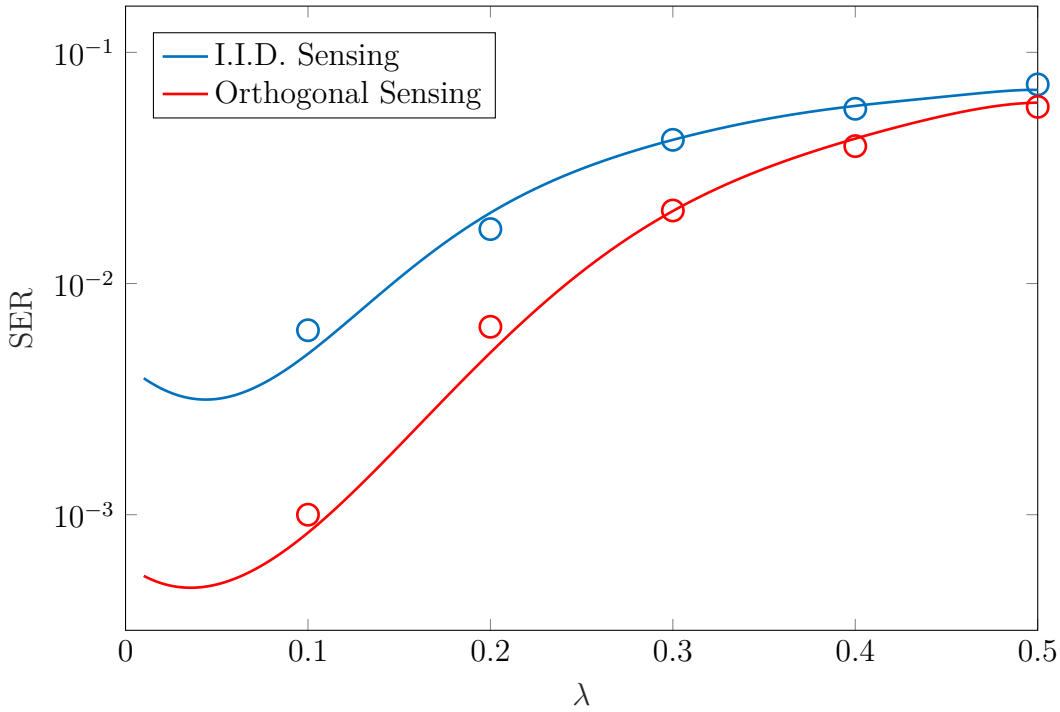

Figure 6.13: SER achieved via Box LASSO recovery against regularizer λ.

result, one address this issue analytically. In fact, one can find the optimal choice for the tuning factor by minimizing the asymptotic performance measure which is given in an analytic form via the replica method. Figure 6.14 shows the achievable SER via the *tuned* box-LASSO algorithm for the same setting, i.e., $\rho = 0.1$ and $\log \mathrm{SNR} = 10$ dB, against the compression rate. Here, the tuning factor at each compression rate is set such that the asymptotic expression for SER determined via the RS ansatz is minimized. Similar to the former cases, orthogonal sensing outperforms i.i.d. sensing. The achievable SER is however higher than the optimal bound determined via matched MAP recovery. This is in fact the price we pay for computational tractability.

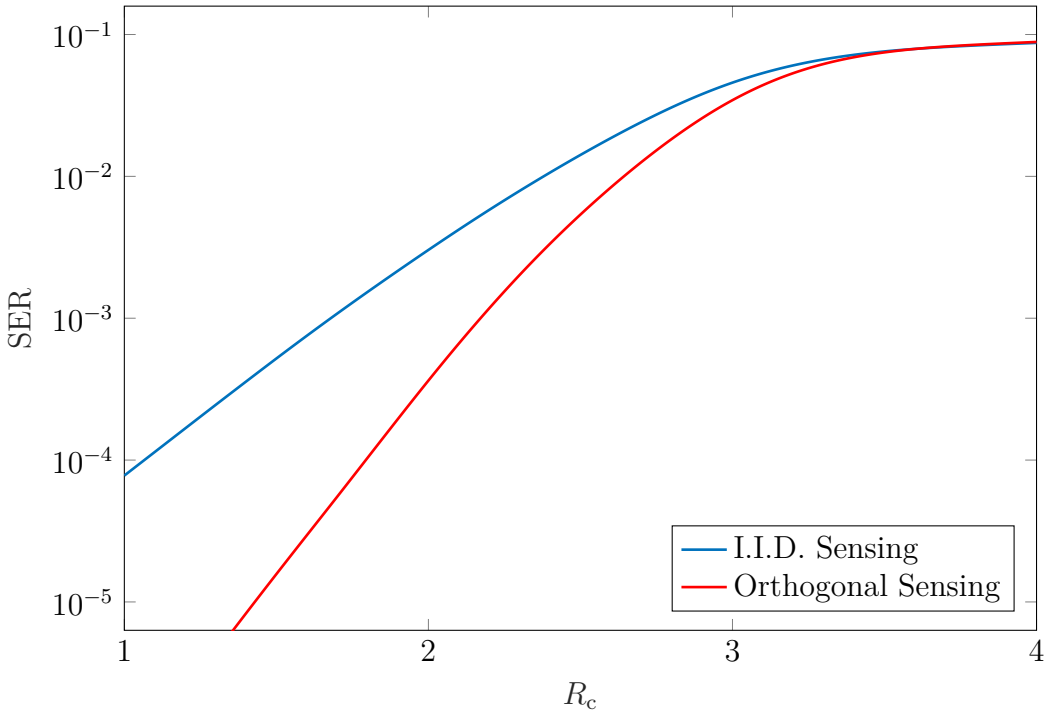

Figure 6.14: SER achieved via tuned box-LASSO.

6.5 Bibliographical Notes

Sparse recovery is considered as an old problem with applications in various contexts; see for example [111–116] and the references therein. As new signal representations such as wavelets, Wilson bases and cosine packets [117–120] started to develop, the problem of sparse recovery received a significant attention in signal processing. This led to vast bodies of work on the theoretical aspects and algorithms, e.g., [121–124]. After the work in [7,102,125,126], sparse recovery has been mostly referred to as *compressed sensing*, *compressive sensing* or *compressive sampling* in the signal processing and information theory literature.

From regression points of view, Tibshirani addressed the problem of sparse recovery in his pioneering work [104], where he introduced the LASSO scheme for joint linear regression and selection. Similar approach was taken by Chen in [127, 128] to find a sparse signal decomposition which led to an alternative formulation based

on ℓ_1-norm minimization known as *basis pursuit*. Following these fundamental formulations, several iterative and greedy algorithms were developed in the literature considering various criteria or deviations from the standard formulations, e.g., designing algorithms for recovery with very low computational complexity or addressing signals with structured sparsity [123, 129–132].

To achieve a desired level of performance with a given sparse recovery algorithm, the sensing matrix is required to satisfy the so-called *restricted isometry property* [133]. This property has been shown to be satisfied with high probability via large random sensing matrices [134]. Following this result along with the high-dimensional nature of sparse recovery applications, the benchmark performance of a recovery scheme is characterized by determining its expected performance for some well-defined large random sensing matrices, e.g. i.i.d. Gaussian matrices. Such a setting is mathematically equivalent to various linear regression models, e.g. multiuser communications [43], with stochastic regressands and regressors. This similarity was considered in a series of papers starting with [46, 55], where the earlier derivations were employed to study sparse recovery. The extension of analyses from the context of multiuser estimation had this disadvantage that the sampling settings were limited to those setups which were consistent with the earlier estimation problems in the literature. Nevertheless, sparse recovery often deals with more generic setups. As a result, a body of work deviated from this approach and directly studied the problem of sparse recovery; see for example [77, 94, 109, 135–137].

Due to computational intractability, earlier studies in the literature often used the replica method to characterize the performance of sparse recovery schemes. Some of these *mathematically non-rigorous* results have been recently shown to be valid by using some alternative tools for analysis. A widely investigated approach is based on the asymptotic analysis of *AMP algorithms*. The AMP algorithms were initially introduced to address iteratively an ℓ_1-norm minimization scheme, such as LASSO and basis pursuit, with low computational complexity [105, 106, 138]. Numerical investigations demonstrated that in settings with large dimensions, the performance is derived in terms of some fixed-points given by *state evolution*, and recovers the asymptotic performance of the ℓ_1-norm minimization schemes [106]. This observation was

a breakthrough, since it showed that the complexity-performance trade-off, initially postulated for iterative schemes [139], does not necessarily hold in high-dimensional problems. The proposed approach was later extended to a large variety of estimation problems including MAP and MMSE estimation; see for example [140, 141]. The initial observations in [106] based on state evolution was later justified rigorously for i.i.d. sub-Gaussian sensing matrices in [142] via the conditioning technique developed in [143]. The study was recently extended to cases with rotationally invariant system matrices in [144, 145]. AMP algorithms have been further shown to achieve the fundamental limits on the required compression rate, e.g., [146, 147], in the asymptotic regime via spatially coupled measurements [148, 149].

From theoretical points of view, the methodology proposed by AMP algorithms and their state evolution provided a justification for validity of several earlier studies based on the replica method. In fact, the results given by the replica method were recovered through state evolution of the corresponding AMP algorithms. A recent example of such results is [52] which invokes this approach along with some other analytical tools to approve the validity of the replica-based prediction for the asymptotic MMSE and mutual information of the sensing setting with i.i.d. Gaussian measurements. Nevertheless, the asymptotic analysis of AMP algorithms is not the only approach for rigorous characterization of sparse recovery. Various alternative approaches have been developed in the literature. For instance, Reeves and Pfister in [74] have recently justified the validity of the RS ansatz for the MMSE bound using a different approach.

6.6 Summary

In this chapter, we have studied the problem of sparse recovery as an application to the asymptotic results derived in Chapters 4 and 5. Using the decoupling property of the generic RLS method, the asymptotic performance of various sparse recovery algorithms have been characterized for both random i.i.d. and orthogonal sensing matrices. The investigations have demonstrated that orthogonal sensing can in general lead to better recovery performance.

For most scenarios, the asymptotic characterizations based on the RS ansatz have been shown to be consistent with the known bounds and numerical simulations for finite dimension. Nevertheless, the RS-predicted performance of ℓ_0-norm minimization has shown to violate the MMSE bound. For this scheme, the characterization has been further given under one step of RSB. The asymptotic MSE predicted via the one-RSB ansatz has been shown to be consistent with the MMSE bound for a larger interval of compression rates.

Chapter 7

Applications to MIMO Precoding

Signal shaping is the dual problem of signal recovery. In this problem a signal with a desired set of properties is to be constructed from a random process. An old example is *pre-emphasis* and *de-emphasis* filtering in analog signal processing in which the information signal is intentionally distorted prior to the input stage of the system and later post-processed at the output stage, such that the output signal-to-noise ratio is improved; see for example [150]. Currently, signal shaping has a variety of applications in communications, digital signal processing and information technology.

An application of signal shaping in recent communication systems is precoding. A *precoder* is mathematically a mapping which assigns a transmit signal to each realization of information symbols intended to be transmitted. The main objective of such *information pre-processing* is to *compensate* the channel impact at the transmit side. By doing so, the signal processing load at receiving terminals significantly reduces. This is a desired feature, since the receiving terminals are often low-power devices in wireless networks.

Theoretically, precoding is possible in any communication system. Nevertheless, this technique has received a great deal of attention in MIMO settings, due to their larger degrees of freedom. In fact, the availability of multiple antennas provides a wider set of possible choices for transmit signals. This results in effectiveness of the precoding technique in these systems. The technique is hence often called *MIMO precoding* in the literature.

There exist various approaches in the literature for designing a precoder. Nevertheless, despite connections to the problem of linear regression, no systematic approach based on the RLS method has been proposed. In this chapter, we develop a generic precoding scheme which addresses a general set of transmit constraints. This scheme interprets MIMO precoding as a linear regression problem and employs the RLS method to solve this problem. Using the asymptotic results in Chapters 4 and 5, we characterize the performance of the proposed scheme in various scenarios.

7.1 Preliminaries

Consider downlink transmission in a multiuser MIMO system with a single transmitter and M user terminals. The transmitter is equipped with an antenna array of size N and the user devices are assumed to be single-antenna, as it is the case in practical scenarios. The transmitter intends to send messages $d_1, \ldots, d_M$ to the corresponding user terminals simultaneously. To this end, it invokes the classic scheme for multiuser communications: It first encodes message d_m for $m \in [M]$ to the sequence $s_m[t]$, where $t \in [T]$ denotes the *discrete* time. The M-dimensional vector of encoded information symbols

$$\boldsymbol{s}[t] \coloneqq \begin{bmatrix} s_1[t] \\ \vdots \\ s_M[t] \end{bmatrix} \tag{7.1}$$

is then mapped into a transmit vector via a deterministic mapping which is referred to as the *precoder*. The output of the precoder is the N-dimensional vector

$$\boldsymbol{x}[t] \coloneqq \begin{bmatrix} x_1[t] \\ \vdots \\ x_N[t] \end{bmatrix} \tag{7.2}$$

whose entry $x_n[t]$ denotes the sample being transmitted in the t-th transmission time interval via the n-th transmit antenna. For a randomly chosen time interval t, we

assume that the entries of $\boldsymbol{s}[t]$ are i.i.d. complex Gaussian random variables with zero mean and unit variance, i.e., $\boldsymbol{s}[t] \sim \mathcal{CN}(\mathbf{0}, \mathbf{I}_M)$.

We assume that the channel experiences frequency-flat fading. This means that the frequency components of the transmit pulses observe almost flat channel response in the frequency domain. It is further assumed that the fading process varies slowly, such that the coherence time interval of the channel comprises multiple transmission time intervals. Consequently, the vector of receive samples in transmission time interval t, denoted by

$$\boldsymbol{y}[t] \coloneqq \begin{bmatrix} y_1[t] \\ \vdots \\ y_M[t] \end{bmatrix}, \tag{7.3}$$

is compactly written as

$$\boldsymbol{y}[t] = \mathbf{H}\,\boldsymbol{x}[t] + \boldsymbol{z}[t]. \tag{7.4}$$

Here, $\mathbf{H} \in \mathbb{C}^{M \times N}$ is contains channel coefficients, and $\boldsymbol{z}[t]$ is AWGN with zero mean and variance σ^2.

The system operates in time division duplexing (TDD) mode, as is the case in most recent MIMO systems with large dimensions. This means that both the uplink and downlink transmissions employ the same frequency channel in this system. As a result, the uplink and downlink channels are *reciprocal*. Following this fact, the user terminals transmit distinct uplink pilot sequences prior to the downlink transmission in the training phase. Using these pilots, the transmitter estimates the uplink channel coefficients, which due to *reciprocity* also describe the downlink channel. Throughout this chapter, we assume that this procedure is performed prior to downlink transmission, and hence the transmitter and user terminals know the channel state information (CSI). For more information on channel estimation techniques in MIMO settings see [151–154] and the references therein.

7.1.1 MIMO Precoding

Mathematically, precoding is a mapping from the M-dimensional space of information symbols to the N-dimensional space of transmit samples. The ultimate goal of this mapping is to construct $\boldsymbol{x}[t]$, such that the user terminals recover the transmitted symbols with minimal post-processing. As a result, precoding often deals with the so-called *channel inversion* problem[1]. In this problem, the transmit symbols are found such that the linear transformation by the channel gives the desired information symbols. In other words, the entries of $\boldsymbol{x}[t]$ are found such that

$$\mathbf{H}\,\boldsymbol{x}[t] = \boldsymbol{s}[t]\,. \tag{7.5}$$

This problem does not necessarily have a solution. The necessary conditions for $\boldsymbol{x}[t]$ to exist depend on the properties of channel matrix $\mathbf{H}$.

In practice, the transmit signal is required to satisfy a set of side constraints. These constraints are imposed to the system either by restricted resources or hardware limitations. A well-known example is the *transmit power* constraint which implies that

$$\|\boldsymbol{x}[t]\|^2 \leq P_{\mathrm{Tr}} \tag{7.6}$$

for some constant P_{Tr}. This limitation is enforced by the fact that the available budget on transmit power is restricted in practice. Another instance is the *per-antenna peak power* constraints which enforces the transmit symbols to fulfill

$$|x_n[t]|^2 \leq P_{\mathrm{Peak}} \tag{7.7}$$

for $n \in [N]$. This constraint restricts the transmit peak power on each antenna element. This limit is often imposed by the characteristics of power amplifiers used in the transmitter.

[1] In an alternative interpretation, precoding design can be observed as an optimization in which the precoder is found, such that a given performance metric is optimized. Nevertheless, this alternative look could ignore the reduction in the processing load at the receive side.

7.2 Precoding via RLS: GLSE Precoding

The MIMO precoding problem can be interpreted as a linear regression model in which the channel matrix includes the set of regressors and the vector of coded information symbols denote the regressands. The transmit symbols represent the regression coefficients which are to be found with respect to the linear model in (7.5). These coefficients are further required to satisfy some side constraints which are imposed on the transmit signal via practical limitations.

Remark 7.1. *Unlike the problem of signal recovery, in this problem the regression model does not have any true regression coefficients. Note that the regressands in* $\boldsymbol{s}[t]$ *are assumed to be i.i.d. Gaussian random variables. Hence, the system model agrees the stochastic model presented in Chapter 2.*

Following the above analogy, MIMO precoding is drectly addressed via the generic RLS method. In fact, one can find the transmit symbols by minimizing the RSS term regularized via a regularization term which penalize the RSS with respect to the signal constraints. Such an approach leads to a generic precoding scheme. We refer to this scheme as *generalized least squares error (GLSE) precoding* and define it formally below:

Definition 7.1 (GLSE precoders)**.** *For a given power control factor* ρ *and the channel matrix* $\mathbf{H}$*, a GLSE precoder maps the vector of coded information symbols* $\boldsymbol{s}$ *into a transmit vector* $\boldsymbol{x}$ *over the precoding support* $\mathbb{X}$ *as*

$$\mathrm{GLSE}\left(\boldsymbol{s}|\rho,\mathbf{H}\right)=\underset{\boldsymbol{v}\in\mathbb{X}^{N}}{\operatorname{argmin}}\ \left\|\mathbf{H}\boldsymbol{v}-\sqrt{\rho}\,\boldsymbol{s}\right\|^{2}+u_{\mathrm{v}}\left(\boldsymbol{v}\right) \tag{7.8}$$

for some penalty $u_{\mathrm{v}}\left(\cdot\right):\mathbb{X}^{N}\mapsto\mathbb{R}$ *which decouples*

$$u_{\mathrm{v}}\left(\boldsymbol{v}\right)=\sum_{n=1}^{N}u\left(v_{n}\right). \tag{7.9}$$

The GLSE precoding scheme finds the transmit samples such that the receive samples after linear coupling by the channel are close to an scaled version of the information symbols. As a result, the receiver mainly deals with the thermal noise which

requires minimal post-processing. The penalty term moreover restricts the transmit samples to fulfill the transmit constraints.

For some choices of penalty and support, the GLSE precoding reduces to a known precoding scheme. The most well-known special case is the so-called *regularized zero-forcing (RZF) precoding* [155] which is deduced from the GLSE scheme by setting $u_{\mathrm{v}}(\boldsymbol{v}) = \lambda \|\boldsymbol{v}\|^2$ and $\mathbb{X} = \mathbb{C}$. RZF is a classical linear technique for MIMO precoding which is widely considered as a benchmark in the literature. We hence introduce it explicitly in the following.

Special Case 7.2.1 (RZF Precoding)**.** By setting $u_{\mathrm{v}}(\boldsymbol{v}) = \lambda \|\boldsymbol{v}\|^2$ and $\mathbb{X} = \mathbb{C}$, the GLSE scheme reduces to RZF precoding in which

$$\boldsymbol{x}[t] = \sqrt{\rho}\, \mathbf{H}^{\mathsf{H}} \left(\mathbf{H}\mathbf{H}^{\mathsf{H}} + \lambda\, \mathbf{I}_M\right)^{-1} \boldsymbol{s}[t]\,. \tag{7.10}$$

Following the RLS-based interpretation, RZF precoding finds the best approximation for the solution of the channel inversion problem among all transmit vectors with restricted transmit power.

There are other particular precoders in the literature which can be deduced from the generic GLSE scheme. For instance, the so-called *per-antenna constant envelope precoder* introduced in [156] is resulted from the GLSE formulation, when we set $u_{\mathrm{v}}(\boldsymbol{v}) = 0$ and

$$\mathbb{X} = \left\{ z \in \mathbb{C} : |z| = \sqrt{P_{\mathrm{C}}} \right\} \tag{7.11}$$

for some positive real P_{C}. This precoder finds the LS solution among those vectors whose entries have always a fixed amplitude. Such a design results in a constant envelope signal on each transmit antenna which let us employ low-cost power amplifiers in practice.

Remark 7.2. *In GLSE precoding, the precoder is a nonlinear function of the data symbols, in general. In other words, a GLSE precoder does not necessarily reduce to a linear function whose slope only depends on the channel matrix. In this sense, GLSE precoding is considered as a so-called symbol-level precoding scheme [157, 158].*

Using the derivations in Chapters 4 and 5, the asymptotic performance of the GLSE scheme is characterized analytically. Such derivations address the performance of this scheme in large MIMO settings known as *massive MIMO* systems [154, 159]. Before we start with the characterization, let us specify the performance metrics used in this chapter, and illustrate some specific applications of GLSE precoding. For sake of brevity, we drop the time index t in the remaining parts of this chapter.

7.2.1 Performance Measures

From the GLSE formulation, we can conclude that the performance of a GLSE precoder is properly quantified via the LSE, defined in Definition 2.1 in Chapter 2. The LSE in this setting is a function of power factor ρ and is given by

$$\mathrm{LSE}_N(\rho) \coloneqq \frac{1}{M}\mathbb{E}\left\{\|\mathbf{H}\boldsymbol{x} - \sqrt{\rho}\,\boldsymbol{s}\|^2\right\}. \tag{7.12}$$

The asymptotic limit of $\mathrm{LSE}_N(\rho)$ is further denoted by $\mathrm{LSE}(\rho)$.

Another metric of performance which is conventional in the context of MIMO systems is the *per-user achievable ergodic rate* which is defined a follows:

Definition 7.2 (Per-user achievable ergodic rate)**.** *Let $\boldsymbol{s} \in \mathbb{C}^M$ denote the vector of information symbols mapped via a GLSE precoder to $\boldsymbol{x} \in \mathbb{X}^N$, and $\boldsymbol{y} \in \mathbb{C}^M$ represent the vector of receive samples. The per-user achievable ergodic rate is then defined as*

$$R_{\mathrm{Erg}} \coloneqq \frac{1}{M}\sum_{m=1}^{M} \mathrm{I}(s_m; y_m|\mathbf{H}) \tag{7.13}$$

where $\mathbf{H}$ denotes the channel matrix.

From information theoretic points of view, this metric determines the average number of information bits per user transferred over the channel assuming that the CSI is known at the transmitter. The direct derivation of R_{Erg} is not trivial, due to the nonlinearity of GLSE precoders. Nevertheless, this metric is bounded from below in the asymptotic regime in terms of the asymptotic LSE as given in the following lemma:

Lemma 7.1. *Consider a sequence of settings with N transmit antennas and $M(N)$ user terminals such that*

$$\lim_{N\uparrow\infty} \frac{M(N)}{N} = \alpha \tag{7.14}$$

is bounded. The per-user achievable ergodic rate R_{Erg} is bounded from below as

$$R_{\mathrm{Erg}} \geq R_{\mathrm{Erg}}^{\mathrm{L}} \tag{7.15}$$

where

$$R_{\mathrm{Erg}}^{\mathrm{L}} \coloneqq \log\left(\frac{\rho}{\sigma^2 + \mathrm{LSE}(\rho)}\right). \tag{7.16}$$

Proof. The proof follows basic information theoretic inequalities and is given in Appendix G. □

7.3 Applications of GLSE Precoding

The generality of the GLSE scheme enables us to consider a large scope of instantaneous signal constraints at the transmit side. Some of these constraints, such as transmit power constraint, are conventional to be addressed at the precoding stage. Some others are however not considered in at the precoder, and are addressed separately via an individual module. Using the GLSE scheme, these constraints are applied directly the precoding stage. This joint approach can lead to performance enhancement. In the sequel, we discuss some particular applications whose performance are later investigated.

7.3.1 Transmit Antenna Selection

As MIMO settings with large dimensions are getting more popular, transmit antenna selection (TAS) is receiving more attention. Using this technique, at each transmission interval some of transmit antennas are turned off, and the downlink transmission is carried out by a subset of antennas. TAS is a classic low-complexity approach to

reduce the overall radio frequency (RF)-cost. Conventionally, TAS is done prior to precoding via a selection algorithm. The transmit signal is then constructed over the selected antennas. Details on TAS, its limits, and conventional algorithms can be followed in [160–163, A14].

For a given performance metric, the optimal TAS approach is to find the subset of antennas which optimize the measure. Nevertheless, this approach leads to an integer programming. Due to computational intractability, suboptimal greedy algorithms are employed in practice. These algorithms pose polynomial computational complexity at the expense of performance degradation; see [164, 165] and [A10] for some particular greedy selection algorithms.

Restricting the number of active transmit antennas is mathematically equivalent to design of an sparse vector with a certain fraction of entries being zero. This means that the sparsity factor of the transmit vector, defined as

$$\eta_N \coloneqq \frac{\|\boldsymbol{x}\|_0}{N}, \tag{7.17}$$

is less than 1. These zero entries represent the passive antennas. We refer to η as the *fraction of active antennas*. From Chapter 6, we know that the optimal penalty in GLSE precoding which restricts η is proportional to the ℓ_0-norm. Such a choice, along with restriction in the transmit power, leads to the following GLSE precoder.

GLSE Precoder 7.3.1.1 (Optimal precoder for TAS)**.** A GLSE precoder whose penalty is

$$u_{\mathrm{v}}(\boldsymbol{v}) = \lambda \|\boldsymbol{v}\|^2 + \lambda_0 \|\boldsymbol{v}\|_0 \tag{7.18}$$

for some real λ and λ_0 jointly selects transmit antennas and restricts the transmit power. For a given fraction of active transmit antennas and transmit power, there exist λ and λ_0 by which the precoder achieves the desired values.

Considering the LSE as the performance metric, this GLSE precoder is the optimal algorithm for joint power control and TAS, since it solves the corresponding constrained optimization problem. Following the earlier discussions on the complexity of

ℓ_0-norm minimization given in Chapter 6, it is concluded that this scheme computationally intractable for moderate and large choices of N. To address this issue, we invoke the LASSO formulation and relax the problem by replacing the ℓ_0-norm with the ℓ_1-norm. Such a relaxation leads to the following GLSE precoder:

GLSE Precoder 7.3.1.2 (LASSO-based precoder for TAS)**.** A GLSE precoder whose penalty is

$$u_{\mathrm{v}}(\boldsymbol{v}) = \lambda \|\boldsymbol{v}\|^2 + \lambda_0 \|\boldsymbol{v}\|_1 \tag{7.19}$$

for some real λ and λ_1 jointly selects transmit antennas and restricts the transmit power. For a given fraction of active transmit antennas and transmit power, there exist λ and λ_1 by which the precoder achieves the desired values.

For convex choices of $\mathbb{X}$, this GLSE precoder solves a convex optimization problem. Hence, it is posed as a generic linear programming.

7.3.2 PAPR Control

The RF-chains used in classical MIMO design are restricted in terms of the peak transmit power. This restriction comes from the nonlinear input-output characteristics of practical power amplifiers. To illustrate this point, a typical input-output diagram of a power amplifier is shown in Figure 7.1. The diagram is plotted following the Saleh's model given in [166] for $\alpha = 2.092$ and $\beta = 1.247$. In this figure, x_{in} and x_{out} denote the input and output sample of the power amplifier, respectively. As it is observed, this amplifier behaves approximately linear up to $\log|x_{\mathrm{in}}| \approx -4.6$ dB. However, for inputs with larger magnitudes, the characteristic is strictly nonlinear. Further models for power amplifiers can be followed in [167–170].

A common metric to evaluate the linearity of a power amplifier is the *input back-off* which is defined as the maximum input power in the linear range divided by the average power. In practice, the expense of a power amplifier is proportional to its linearity characteristics, and hence using amplifiers with high input back-offs results in high RF-cost.

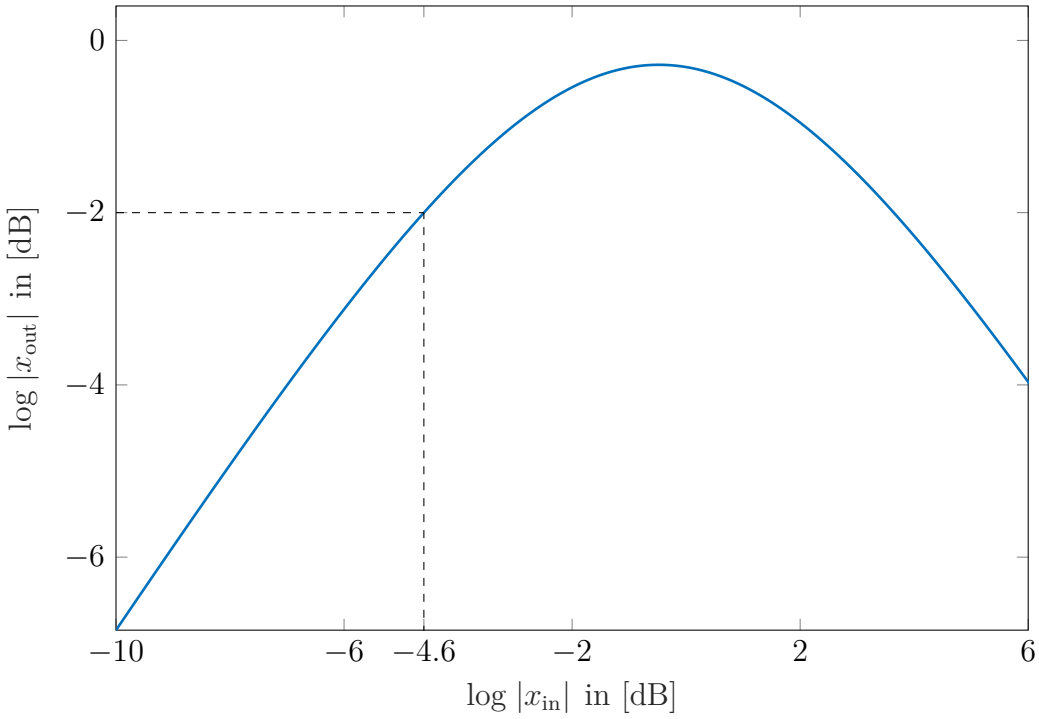

Figure 7.1: The input-output characteristic of a typical power amplifier.

To keep a large MIMO setting cost-efficient, it is desired to use power amplifiers with low input back-offs in the transceiver design. As a result, transmit samples need to have limited PAPR to avoid nonlinear distortion. For the transmit sequence $x_n[t]$ sent over the n-th antenna element, the PAPR is defined as

$$\text{PAPR} = \left(\frac{1}{T}\sum_{t=1}^{T}|x_n[t]|^2\right)^{-1}\left(\max_{t\in[T]}|x_n[t]|^2\right). \tag{7.20}$$

Using GLSE precoding, the PAPR can be restricted by modifying the transmit support, such that the transmit peak power is bounded. This approach leads to the following GLSE precoder:

GLSE Precoder 7.3.2.1 (PAPR-limited precoder)**.** A GLSE precoder whose penalty is

$$u_{\text{v}}(\boldsymbol{v}) = \lambda\|\boldsymbol{v}\|^2, \tag{7.21}$$

for some real λ, and whose support is

$$\mathbb{X} = \left\{ x : |x| \leq \sqrt{P} \right\}. \tag{7.22}$$

for some positive scalar P constructs transmit samples, such that the PAPR on each transmit antenna is restricted. For a given PAPR, there exists λ by which the precoder achieves the desired value.

In this precoder the transmit samples are restricted to lie inside a circle with radius $\sqrt{P}$. This means that the per-antenna peak transmit power is bounded by P. Consequently, one can limit the PAPR by tuning λ, such that the average transmit power is set to the desired one. Further constraints, such as TAS, can be addressed by replacing the penalty with those considered by the precoders in Section 7.3.1.

7.3.3 Transmission via Discrete Constellations

Some recent suggestions for MIMO transmitters have proposed structures whose transmit samples are taken from a discrete constellation set. For instance in the load-modulated single radio frequency (LMSRF) transmitter, introduced and analyzed in [171–173], load modulators are fed by a single RF-chain and construct the transmit constellation. Each load-modulator is equipped with some switches whose configuration specify the transmit sample. As a result the transmit samples are selected from a discrete set whose cardinality is restricted by the total number of transmit states, e.g., for three switches, there are eight possible states. For such transmitters, conventional precoders do not perform effectively. In fact, the majority of the schemes in the literature have continuous precoding supports, and hence to employ them in scenarios with discrete constellation sets, one needs to map the transmit sample on the constellation set by further pre-processing steps. LMSRF transmitters are not the only example with discrete transmit constellation. Another example is a MIMO system with low-resolution digital-to-analog converters where the precoding support is restricted with the output of the digital-to-analog converters. Detailed discussions on these settings can be followed in [174–178]. Unlike the conventional schemes, GLSE

precoding precodes the information symbols directly over the discrete constellation taking into account other desired instantaneous signal constraints.

To have an analytic discussion, let us focus on a particular scenario in which the transmit samples are required to be taken from the K-phase shift keying (PSK) constellation. This means that for $n \in [N]$, we have

$$x_n = \sqrt{P} \exp\left\{ \mathrm{j} \frac{2k\pi}{K} \right\} \tag{7.23}$$

for some positive real P and $k \in [K]$. For this particular case, we can employ the following GLSE precoder to jointly perform TAS and precode over the K-PSK constellation.

GLSE Precoder 7.3.3.1 (K-PSK precoder)**.** A GLSE precoder whose penalty is

$$u_{\mathrm{v}}(\boldsymbol{v}) = \lambda \|\boldsymbol{v}\|^2, \tag{7.24}$$

for some real λ, and whose support is

$$\mathbb{X} = \{0\} \cup \left\{ \sqrt{P} \exp\left\{ \mathrm{j} \frac{2k\pi}{K} \right\} \text{ for } k \in [K] \right\} \tag{7.25}$$

for some positive scalar P jointly selects transmit antennas and constructs transmit samples over a K-PSK constellation. For a given fraction of active transmit antennas, there exists λ by which the precoder achieves the desired value.

This precoder maps the information symbols to a vector whose entries are either taken from an K-PSK constellation or are zero. In general, the number of active transmit antennas is restricted by a penalty which is proportional to the ℓ_0- or ℓ_1-norm. Nevertheless, for the K-PSK constellation, ℓ_2- and ℓ_0-norm are related as

$$\|\boldsymbol{x}\|^2 = P \|\boldsymbol{x}\|_0 . \tag{7.26}$$

This indicates that any restriction on the transmit power limits the number of active antennas. Consequently, TAS can be enforced in this case by the ℓ_2-norm regularization. It is worth to note that the given precoder in its current form deals with

integer programming, and hence is complex. Using approaches such as box relaxation[2] illustrated in Chapter 6, computationally tractable algorithms can be derived for precoding. The derivation of such algorithms is however out of the scope of discussions in this chapter, and is left as a possible direction for future studies.

7.4 Asymptotic Characterization of GLSE Precoding

Using the asymptotic characterization of the generic RLS method, we can analytically investigate the performance of GLSE precoding in the large-system limit. To this end, we derive the asymptotic decoupled setting and determine the asymptotic LSE, asymptotic fraction of active transmit antennas defined as

$$\eta = \lim_{N\uparrow\infty} \eta_N = \lim_{N\uparrow\infty} \frac{\|\boldsymbol{x}\|_0}{N}, \tag{7.27}$$

and the asymptotic average transmit power given by

$$P_{\text{av}} = \lim_{N\uparrow\infty} \frac{\|\boldsymbol{x}\|^2}{N} \tag{7.28}$$

for each of the GLSE precoders proposed in the previous section.

Noting that the regression model has no true coefficients, it is concluded that the decoupled regressand is equal to the effective regression error. This variable denotes the equivalent single-letter representation of the vector of information symbols. To avoid notational confusion, we represent this variable with s and refer to it in this particular application as *decoupled input*. From Chapter 5, we know that this variable is Gaussian when the corresponding spin glass exhibits RS. It however deviates from Gaussian distribution, as RS is broken. We refer to the distribution of s as $\mathsf{p}_{\mathsf{dec}}(\mathrm{s})$ in general.

The decoupled RLS algorithm corresponds to the single-letter effective GLSE precoder which determines a random variable whose marginal distribution describes the marginal distribution of each transmit sample. We hence refer to the decoupled RLS

[2]Remember the box-LASSO algorithm for sparse recovery of quantized signals.

algorithm and its output as the *decoupled GLSE precoder* and the *decoupled transmit sample*. To keep the notation consistent with Chapter 5, we show the former with $\mathsf{g}_{\mathsf{RLS}}(\cdot|\tau)$ and the latter with x. The tuning parameter τ further reads[3]

$$\tau = \frac{1}{\mathrm{R}_{\mathbf{J}}(-\chi)} \tag{7.29}$$

The asymptotic parameters η and P_{av} are further directly derived from the general results in Chapter 4. In fact, η is given as the asymptotic distortion when the distortion function is set to

$$\mathsf{d}(x; x_0) = \mathbf{1}\{x \neq 0\}. \tag{7.30}$$

Moreover, the average transmit power is the asymptotic distortion when we set

$$\mathsf{d}(x; x_0) = |x|^2. \tag{7.31}$$

Following the decoupling result, this means that

$$\eta = \mathbb{E}_{\mathrm{x}}\{\mathbf{1}\{\mathrm{x} \neq 0\}\} = 1 - \Pr\{\mathrm{x} = 0\}, \tag{7.32a}$$

$$P_{\mathrm{av}} = \mathbb{E}_{\mathrm{x}}\left\{|\mathrm{x}|^2\right\}. \tag{7.32b}$$

Finally, the LSE is directly derived from the results in Chapter 4. The exact form of LSE depends on the ansatz. For the RS ansatz, the LSE is of a simple form which reads

$$\mathrm{LSE}(\rho) = \frac{\rho + q}{(1+\chi)^2} \tag{7.33}$$

where (χ, q) denote the solution to the RS fixed-point equations. Detailed derivations are given in the sequel for each proposed GLSE precoder.

[3]Note that the tuning factor of the generic RLS estimator is set to one in the formulation of GLSE precoding.

7.4.1 Optimal GLSE Precoder for TAS

For GLSE Precoder 7.3.1.1, the decoupled GLSE precoder reads

$$\mathrm{g}_{\mathsf{RLS}}\left(\mathrm{s}|\tau\right) = \begin{cases} \dfrac{\mathrm{s}}{1+\tau\lambda} & |\mathrm{s}| \geq t_0 \\ 0 & |\mathrm{s}| < t_0 \end{cases} \tag{7.34}$$

where s is the decoupled input and the threshold t_0 is given by

$$t_0 \coloneqq \sqrt{\tau\lambda_0\left(1+\tau\lambda\right)}. \tag{7.35}$$

The decoupled setting in this case is a hard-thresholding operator whose diagram is shown in Figure 6.2, Chapter 6. The threshold level t_0 is proportional to λ_0. By setting $\lambda_0 = 0$, the threshold reduces to zero, as well. In this case, GLSE Precoder 7.3.1.1 describes RZF precoding.

The fraction of active transmit antennas in this case reads

$$\eta = 1 - \Pr\left\{\mathrm{x} = 0\right\} \tag{7.36a}$$

$$= \Pr\left\{|\mathrm{s}| \geq t_0\right\}. \tag{7.36b}$$

The average transmit power is further calculated as

$$P_{\mathrm{av}} = \mathbb{E}_{\mathrm{x}}\left\{|\mathrm{x}|^2\right\} \tag{7.37a}$$

$$= \left(\frac{1}{1+\tau\lambda}\right)^2 \int_{|\mathrm{s}|\geq t_0} |\mathrm{s}|^2 \, \mathrm{p}_{\mathsf{dec}}\left(\mathrm{s}\right) \mathrm{ds}. \tag{7.37b}$$

7.4.2 LASSO-Based GLSE Precoder for TAS

For GLSE Precoder 7.3.1.2, the decoupled GLSE precoder is given by

$$\mathrm{g}_{\mathsf{RLS}}\left(\mathrm{s}|\tau\right) = \begin{cases} \dfrac{|\mathrm{s}| - t_1}{1+\tau\lambda}\dfrac{\mathrm{s}}{|\mathrm{s}|} & |\mathrm{s}| \geq t_1 \\ 0 & |\mathrm{s}| < t_1 \end{cases} \tag{7.38}$$

where

$$t_1 \coloneqq \frac{\tau\lambda_1}{2}. \tag{7.39}$$

The decoupled precoder in this case is a soft-thresholding operator whose diagram is given in Figure 6.1, in Chapter 6. Similar to GLSE Precoder 7.3.1.1, the threshold level tends to zero when $\lambda_1 = 0$.

The fraction of active transmit antennas for this precoder is given by

$$\eta = 1 - \Pr\{\mathrm{x} = 0\} \tag{7.40a}$$

$$= \Pr\{|\mathrm{s}| \geq t_1\}, \tag{7.40b}$$

and the average transmit power is calculated as

$$P_{\mathrm{av}} = \mathbb{E}_{\mathrm{x}}\left\{|\mathrm{x}|^2\right\} \tag{7.41a}$$

$$= \left(\frac{1}{1+\tau\lambda}\right)^2 \int_{|\mathrm{s}|\geq t_1} \left(|\mathrm{s}| - t_1\right)^2 \mathrm{p}_{\mathsf{dec}}(\mathrm{s})\,\mathrm{ds}. \tag{7.41b}$$

7.4.3 PAPR-Limited GLSE Precoder

The decoupled setting for GLSE Precoder 7.3.2.1 is given by

$$\mathrm{g}_{\mathsf{RLS}}(\mathrm{s}|\tau) = \begin{cases} \dfrac{\mathrm{s}}{|\mathrm{s}|}\sqrt{P} & |\mathrm{s}| \geq t \\ \dfrac{\mathrm{s}}{1+\tau\lambda} & |\mathrm{s}| < t \end{cases} \tag{7.42}$$

where the threshold t is defined as

$$t \coloneqq (1+\tau\lambda)\sqrt{P}. \tag{7.43}$$

The decoupled transmit sample in this case is obtained by clipping. The diagram for the clipping operator is shown in Figure 7.2. Here, the decoupled input s is clipped if the magnitude of s exceeds the threshold t. By doing so, the peak power of the

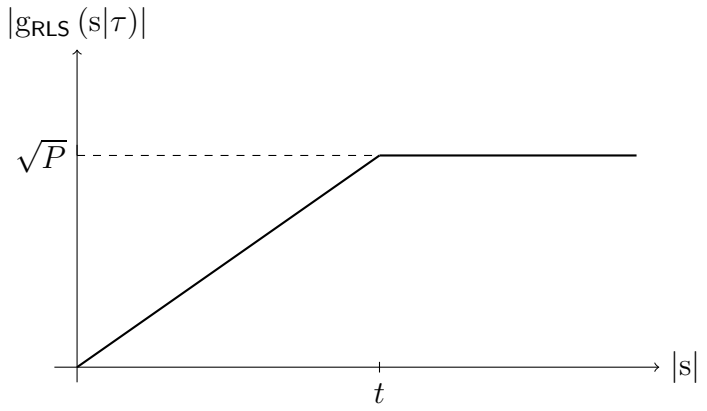

Figure 7.2: Clipping operator.

transmit sample is restricted to P. By sending P to ∞, the precoder reduces to RZF.

The fraction of active transmit antennas for this precoder is always $\eta = 1$, since it does not restrict the umber of active antennas. The average transmit power is further calculated as

$$P_{\mathrm{av}} = \mathbb{E}_{\mathrm{x}}\left\{|\mathrm{x}|^2\right\} \tag{7.44a}$$

$$= \Pr\left\{|\mathrm{s}| \geq t\right\} P + \int_{|\mathrm{s}|<t} |\mathrm{s}|^2 \, \mathrm{p}_{\mathsf{dec}}(\mathrm{s}) \, \mathrm{ds}. \tag{7.44b}$$

7.4.4 K-PSK GLSE Precoder

For the GLSE Precoder 7.3.3.1, the decoupled precoder is

$$\mathrm{g}_{\mathsf{RLS}}(\mathrm{s}|\tau) = \begin{cases} \sqrt{P} \exp\left\{\mathrm{j}\dfrac{2k^\star\pi}{K}\right\} & |\mathrm{s}| \geq t_K \\ 0 & |\mathrm{s}| < t_K \end{cases} \tag{7.45}$$

where the threshold t_K is defined as

$$t_K \coloneqq \frac{\sqrt{P}\,(1+\tau\lambda)}{2\,\Theta\left(k^\star|\lhd\mathrm{s}\right)} \tag{7.46}$$

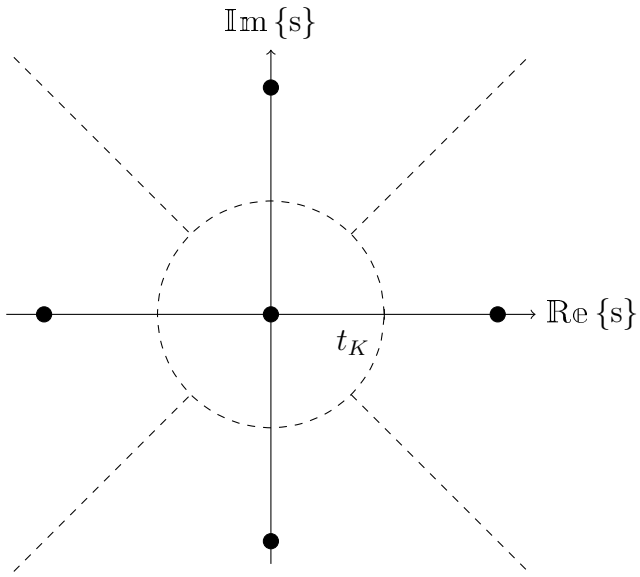

Figure 7.3: 5-level hard-thresholding operator for QPSK constellation.

for

$$k^\star \coloneqq \underset{k\in[K]}{\operatorname{argmax}}\ \Theta\left(k|\sphericalangle \mathrm{s}\right) \tag{7.47}$$

with

$$\Theta\left(k|\theta\right) \coloneqq \cos\left(\frac{2k\pi}{K} - \theta\right). \tag{7.48}$$

The decoupled precoder in this case describes a $(K+1)$-level hard-thresholding operator in which the magnitude of the decoupled input is first compared to t_K, and then, its non-zero output is mapped to a K-PSK symbol whose phase is closest to $\sphericalangle \mathrm{s}$. This operator is shown for the quadrature PSK (QPSK) constellation, i.e., $K = 4$, in Figure 7.3. The solid points in the diagram denote the QPSK constellation points and the origin which represent the possible choices for x. The dashed lines moreover specify the thresholding areas. When the decoupled input lies in a certain area, the corresponding point is taken as the decoupled transmit sample.

The fraction of active transmit antennas for this precoder is given by

$$\eta = 1 - \Pr\{\mathrm{x} = 0\} \tag{7.49a}$$

$$= \Pr\{|\mathrm{s}| \geq t_K\}. \tag{7.49b}$$

Note that in this case, by growth of λ, the threshold t_K increases, and thus, the fraction of active transmit antennas reduces. Hence, η in practice is tuned by λ. The average transmit power is further determined as

$$P_{\mathrm{av}} = \mathbb{E}_{\mathrm{x}}\left\{|\mathrm{x}|^2\right\} \tag{7.50a}$$

$$= \Pr\{|\mathrm{s}| \geq t\}\, P = \eta P. \tag{7.50b}$$

7.5 Numerical Investigations

We now investigate the performance of GLSE precoding numerically. To this end, we consider some examples of the special GLSE precoders studied in the last section and compare their performance to the benchmark. Before presenting the results, let us first specify the channel model.

7.5.1 Channel Model

The stochastic model considered for the matrix of regressors encloses the wide class of unitarily invariant channel matrices. Hence, the performance of these GLSE precoders can be studied for various fading models. For sake of analytical tractability, we consider a standard i.i.d. flat Rayleigh fading model whose channel matrix is decomposed as

$$\mathbf{H} = \mathbf{D}^{1/2}\mathbf{G}. \tag{7.51}$$

Here,

- $\mathbf{G} \in \mathbb{C}^{M \times N}$ contains i.i.d. zero-mean complex Gaussian entries whose variance is $1/N$. This matrix models the multipath effect in the channel.
- $\mathbf{D} \in \mathbb{C}^{M \times M}$ is a diagonal matrix, i.e.,

$$\mathbf{D} = \mathrm{diag}\left\{[D_1, \ldots, D_M]\right\} \tag{7.52}$$

  with D_m being a non-negative real variable. $\mathbf{D}$ describes the path-loss and shadowing. The diagonal entries of $\mathbf{D}$ are modeled as i.i.d. random variables whose mean values depend on the network topology. We denote the limiting empirical cumulative distribution of $\{D_1, \ldots, D_M\}$ by $\mathrm{F}^{\mathsf{snr}}(\cdot)$.

For asymptotic characterization, the R-transform of the Gramian $\mathbf{J} = \mathbf{H}^{\mathsf{H}}\mathbf{H}$ is required. For the considered model, one notes that $\mathbf{D}^{\mathsf{H}} = \mathbf{D}$ and writes

$$\mathbf{J} = \mathbf{G}^{\mathsf{H}}\mathbf{D}\mathbf{G}. \tag{7.53}$$

For $\mathbf{D} = \mathbf{I}_M$, the asymptotic distribution $\mathrm{F}_{\mathbf{J}}$ follows the Marčenko-Pastur law[4], and hence the R-transform is given by

$$\mathrm{R}_{\mathbf{J}}(\omega) = \frac{\alpha}{1-\omega}. \tag{7.54}$$

When $\mathbf{D} \neq \mathbf{I}_M$, one can use the Silverstein-Bai result in [179][5] which leads to

$$\mathrm{R}_{\mathbf{J}}(\omega) = \alpha \int \frac{D}{1 - D\omega} \mathrm{dF}^{\mathsf{snr}}(D). \tag{7.55}$$

For sake of brevity, we assume $\mathbf{D} = \mathbf{I}_M$ throughout the investigations. The derivations straightforwardly extend to cases with $\mathbf{D} \neq \mathbf{I}_M$, by substituting (7.55) into the derivations.

[4]Check [57, 58] or Chapter 6 for detailed discussions.
[5]See also [57, Section 3.2.2].

7.5.2 Tuning Strategy

To satisfy a desired set of constraints the tuning parameters in the GLSE precoder, e.g., λ and λ_0 in GLSE Precoder 7.3.1.1, need to be tuned. For this aim, we take the following approach: We fix the desired values and solve the fixed-point equations in terms of the tuning parameters.

To make this strategy clear, let us consider GLSE Precoder 7.3.1.1. In this precoder, we need to specify λ and λ_0, such that the transmit power and the fraction of active transmit antennas are set to some desired values. Noting that η and P_{av} are both derived in terms of λ and λ_0, we set η and P_{av} to the desired values and derive λ and λ_0 in terms of them. We then replace these tuned parameters into the fixed-point equation in the replica ansatz to derive the asymptotic LSE. For other precoders, we follow th same approach.

7.5.3 Results for Optimal GLSE Precoder for TAS

In Figure 7.4, the asymptotic LSE is sketched against the inverse load, i.e., $\alpha^{-1} = N/M$, for multiple asymptotic fractions of active antennas. Here, the tuning factors λ and λ_0 are tuned such that $P_{\text{av}} = 0.5$, and the power control factor is set to $\rho = 1$. The results are determined from the RS ansatz.

To compare the performance of the GLSE precoder with the benchmark, we consider the following well-known TAS algorithm:

Algorithm 7.5.1. *Assume that L antennas are to be selected out of N antennas available at the transmitter. Given the channel matrix $\mathbf{H}$, the transmit antennas are selected whose channel gains are the L largest: Let $\mathbf{h}_n \in \mathbb{C}^M$ denote the n-th column of $\mathbf{H}$ which corresponds to transmit antenna n. We define $\{i_1, \ldots, i_N\}$ to be a permutation of $[N]$ for which*

$$\|\mathbf{h}_{i_1}\| \geq \ldots \geq \|\mathbf{h}_{i_N}\| . \tag{7.56}$$

In this case, the algorithm selects the L transmit antennas which correspond to $\{i_1, \ldots, i_L\}$.

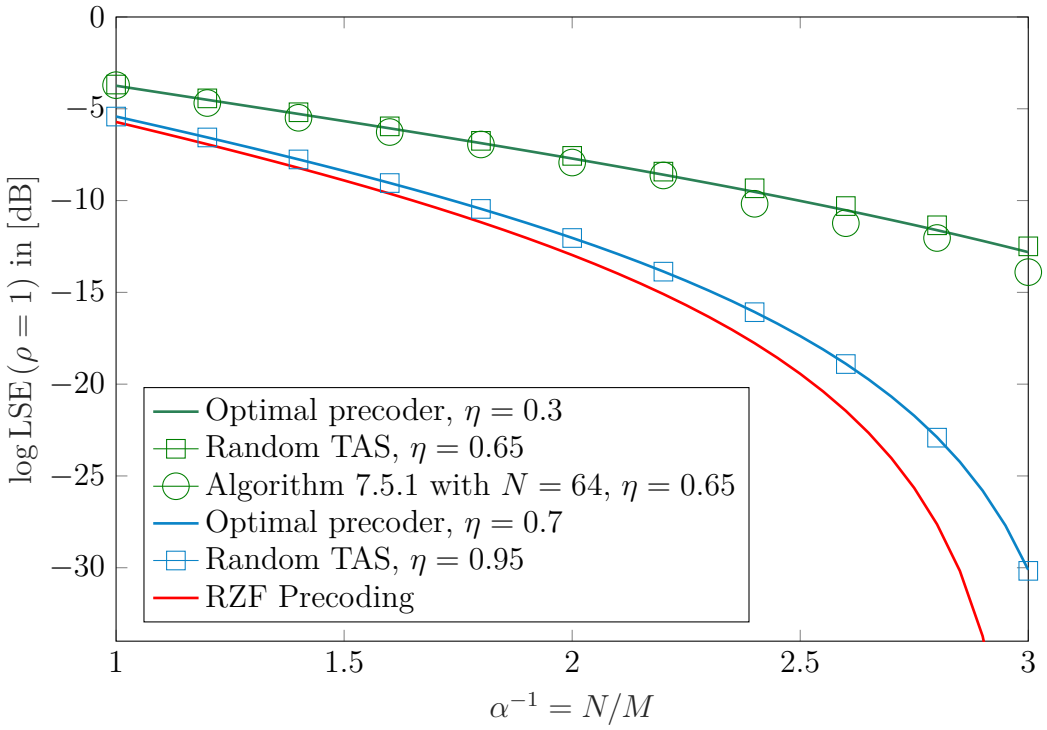

Figure 7.4: Asymptotic LSE versus inverse load for GLSE Precoder 7.3.1.1.

For large number of antennas, Algorithm 7.5.1 performs close to random selection. This is observed in Figure 7.4 where the algorithm is run for $N = 64$ antennas. We hence characterize Algorithm 7.5.1 in the large-system limit considering the asymptotics of random TAS. By random selection, we mean that the transmitter selects the subset of active antennas randomly and precodes the coded information symbols over the selected antennas via RZF precoding, i.e., $\lambda_0 = 0$.

As Figure 7.4 depicts, for a given constraint on η, the GLSE precoder significantly outperforms RZF precoding with random TAS. To quantify the gain, we sketch the LSE for random TAS with different fraction of active transmit antennas, such that the achieved LSE by both the approaches are the same. The numerical investigations show that the performance of the GLSE precoder with $\eta = 0.3$ is tracked by random TAS when $\eta = 0.65$ of antennas are set active. Therefore, the optimal GLSE precoder for TAS employs around $0.35N$ less active antennas than random TAS. This means 54% of reduction in the number of active antennas. The difference between the fraction of

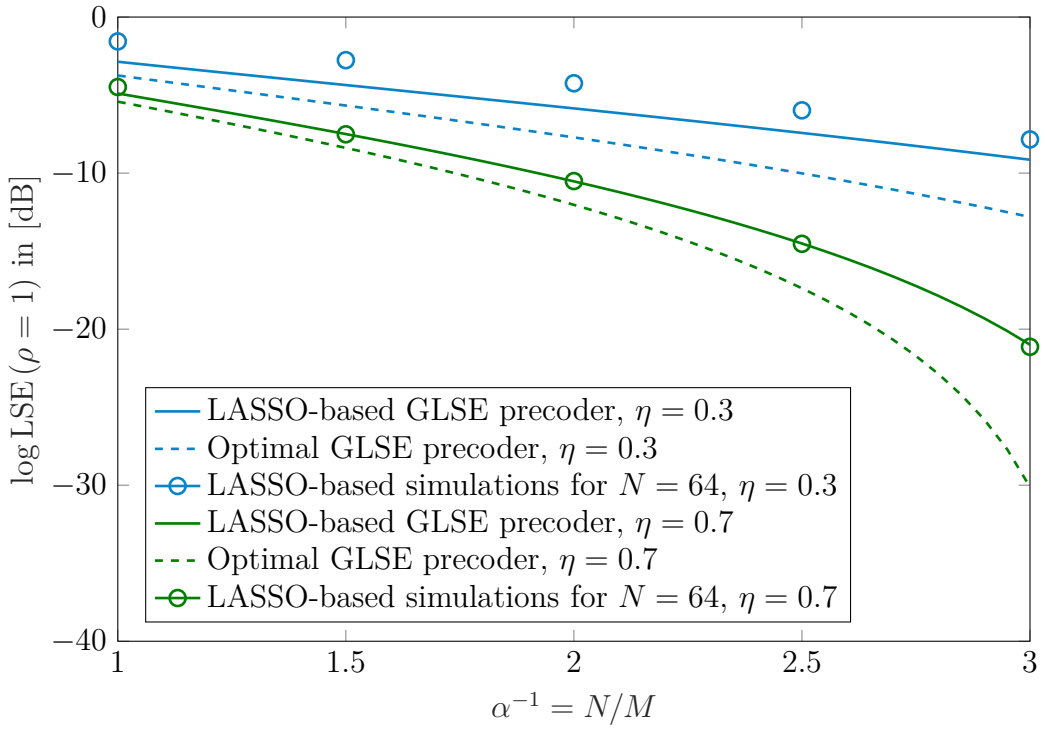

Figure 7.5: Comparison between the optimal and LASSO-based GLSE precoders.

active antennas reduces to 0.25 when $\eta = 0.7$ in the optimal precoder. Note that this significant gain is achieved at the expense of high computational complexity, since the optimal precoder deals with an NP-hard problem.

7.5.4 Results for LASSO-Based GLSE Precoder for TAS

We now sketch the asymptotic LSE achieved via the GLSE Precoder 7.3.1.2 against the inverse load. The results are shown in Figure 7.5. Here, we set $P_{\text{av}} = 0.5$ and $\rho = 1$. λ and λ_1 are further tuned, such that the given constraints on the transmit power and fraction of active antennas are fulfilled.

For sake of comparison, we further sketch the result for the optimal GLSE precoder. The results show degradation in the performance which follows the fact that the GLSE precoder in this case employs the suboptimal LASSO algorithm for TAS. To validate the result given via the replica method, we further determine the distortion of the

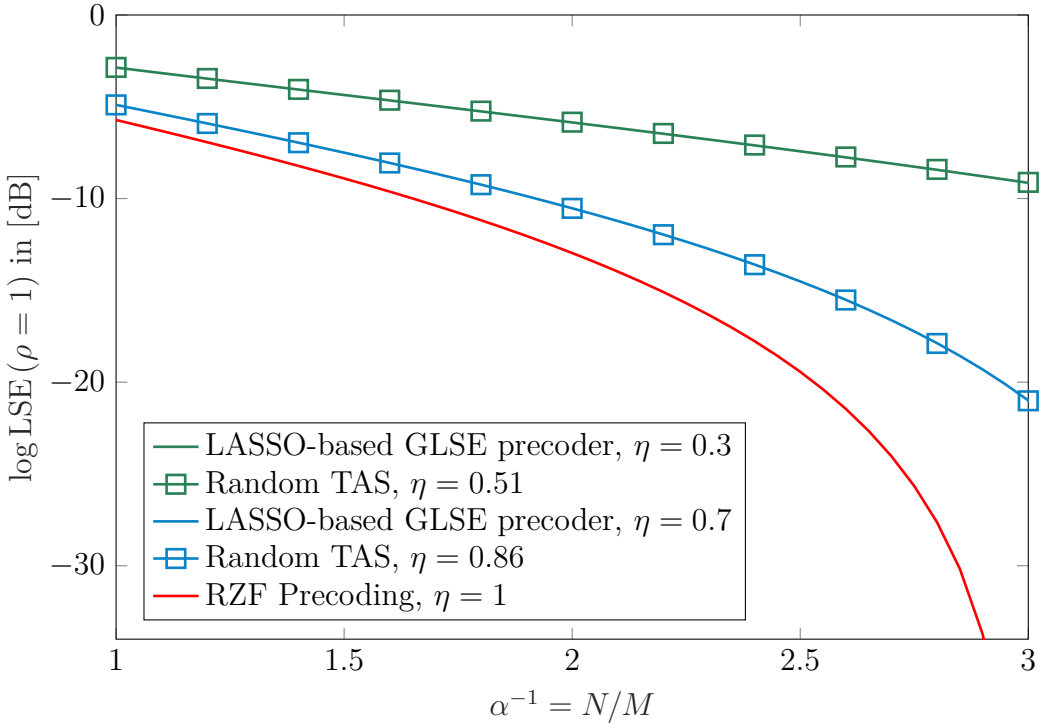

Figure 7.6: Comparing the LASSO-based GLSE precoders to the benchmark.

precoder numerically using CVX [180, 181]. The simulations are given for the same setting with $N = 64$ transmit antennas. λ and λ_1 are further set to those values determined by tuning the asymptotic results. The results demonstrate that the LSE achieved by finite dimensions accurately match the asymptotic LSE. The accurate consistency of the results further validates the tuning strategy, and indicates that the large-system results can be employed to tune GLSE precoders in finite dimensions.

To quantify the gain achieved by the LASSO-based GLSE precoder compared to the benchmark scheme, we have fit the LSE curves achieved by GLSE Precoder 7.3.1.2 to those given by random TAS with different η in Figure 7.6. As it is observed, the performance of GLSE precoder at $\eta = 0.3$ is tracked via random TAS with $\eta = 0.51$. This means that by using computationally tractable GLSE precoding based on LASSO, $0.21N$ less active antennas are required compared to random TAS. Recalling that this gain is $0.35N$ for optimal TAS, we conclude that $0.14N$ less antennas are saved, in this case. Nevertheless, we still get a significant enhancement compared to the benchmark.

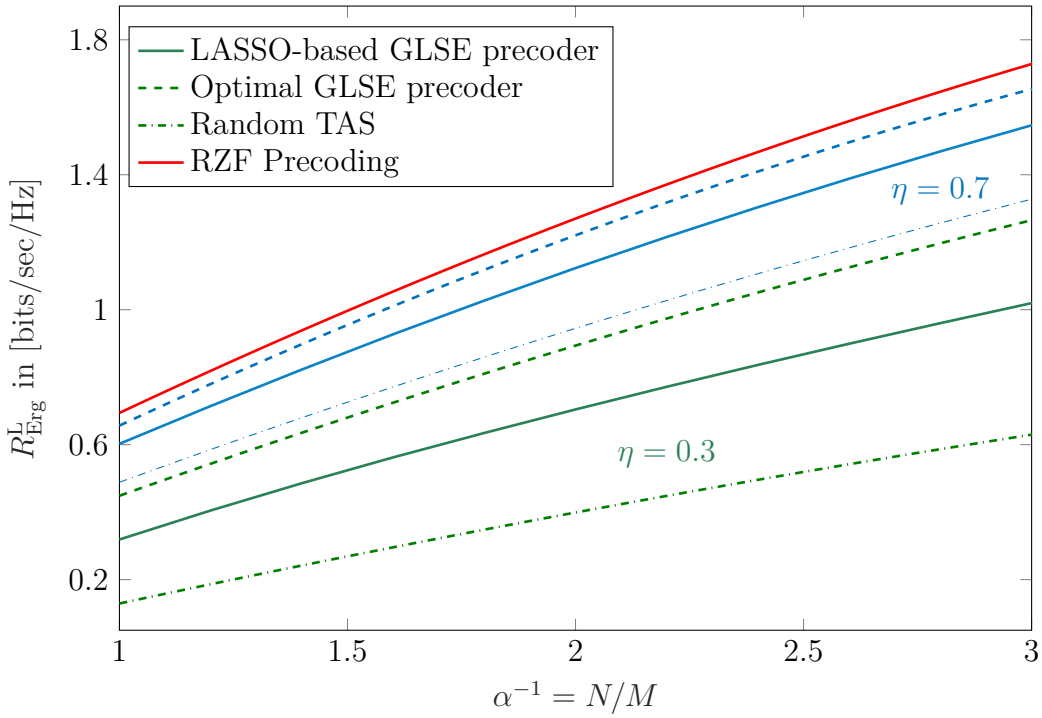

Figure 7.7: Lower bound on the achievable rate via GLSE precoding for TAS.

The lower bound on the per-user achievable ergodic rate is plotted against the inverse load in Figure 7.7 for both the optimal and LASSO-based GLSE precoders. The bound is calculated from the asymptotic LSE following Lemma 7.1. The plots in green shows the bound for $\eta = 0.3$ and the blue curves correspond to $\eta = 0.7$. In this figure, the noise power is set to $\sigma^2 = 0.5$ and the bound is optimized over ρ numerically. For sake of comparison, this bound is further plotted for RZF precoding and random TAS.

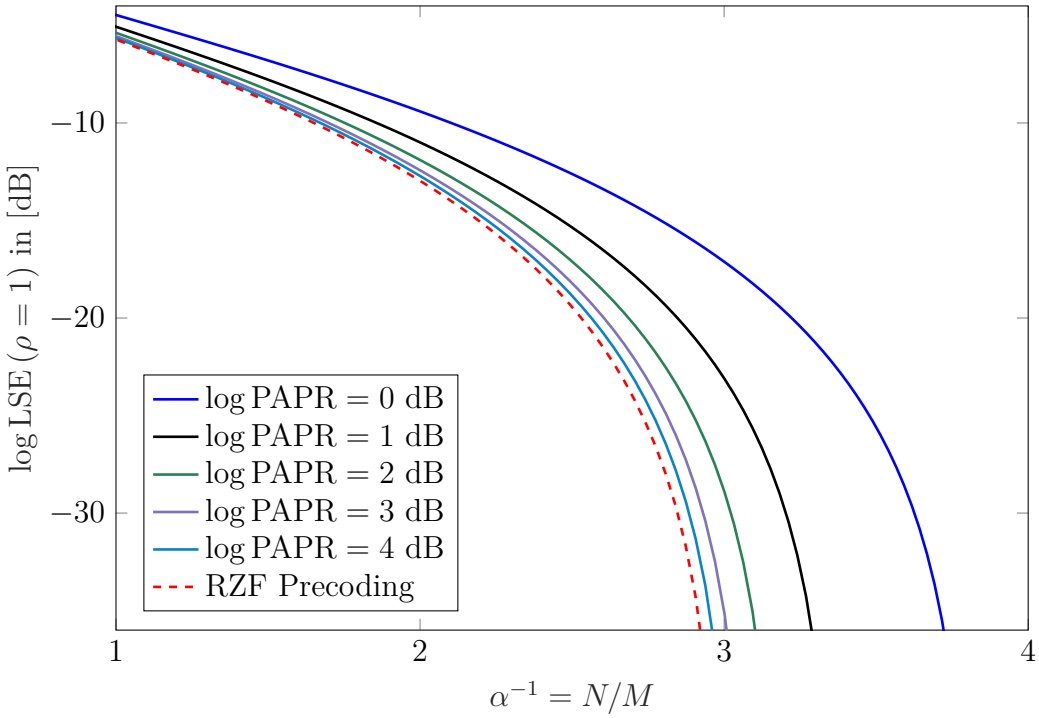

Figure 7.8: Performance of the PAPR-limited GLSE Precoder.

7.5.5 Results for PAPR-Limited GLSE Precoder

Figure 7.8 shows the variation of asymptotic LSE with respect to the inverse load for the GLSE Precoder 7.3.2.1 considering various limits on the PAPR. For these curves, the peak power is restricted to $P = 1$, and the tunable parameter λ is tuned such that

$$\text{PAPR} = \frac{P}{P_{\text{av}}} \tag{7.57}$$

is set to the desired value. The results are given for power control factor $\rho = 1$, and are derived using the RS ansatz.

As the benchmark, the curve for RZF precoding is further shown. This case can be theoretically considered as the limiting case for which PAPR $\uparrow \infty$. The figure demonstrates the trade-off between the achievable LSE and the PAPR. As it is observed, by restricting the PAPR, a desired level of LSE is achieved via a larger transmit array. In the most extreme case of constant envelope transmission, i.e.,

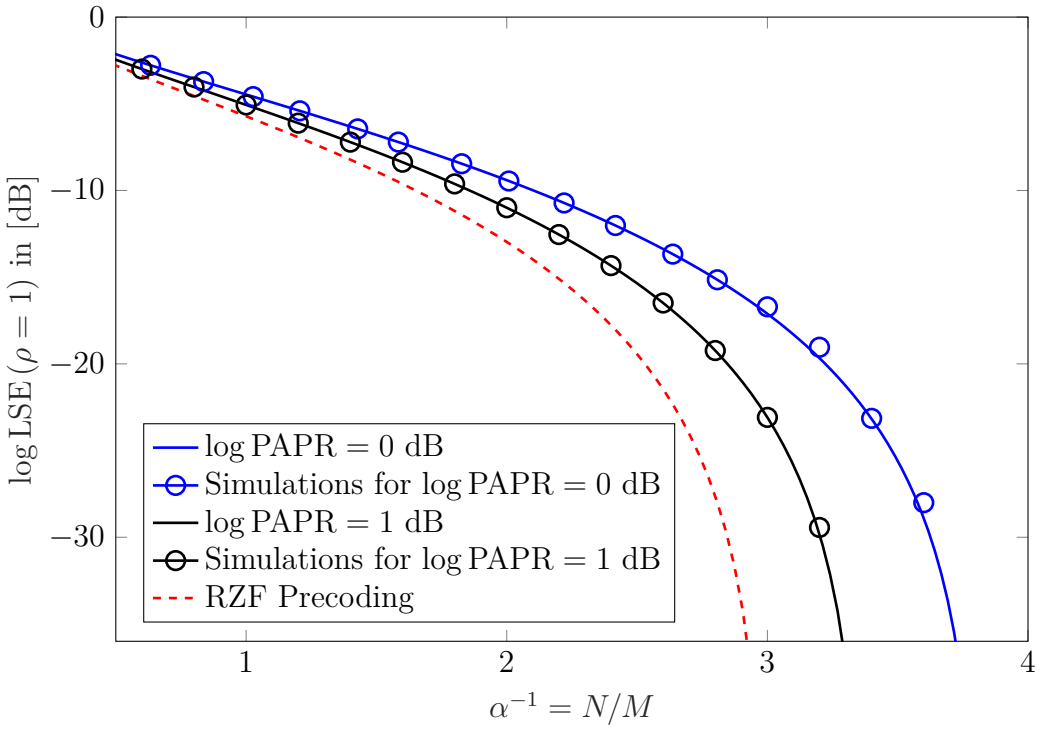

Figure 7.9: Simulation results for the PAPR-limited GLSE Precoder.

log PAPR = 0 dB, this gap is about 0.68 antennas per user for log LSE = −20 dB. Nevertheless, the degradation becomes almost negligible at log PAPR = 4 dB which is a practically feasible value. This indicates that using GLSE precoding, a relatively small PAPR can be achieved at sufficiently low performance degradation.

To validate the asymptotic result, we further derive the average LSE via simulations. This is shown in Figure 7.9. The simulation results are given for $M = 200$ users. To tune the precoder, we use the asymptotic characterization. The simulation results are then derived by directly solving the RLS minimization via MATLAB and calculating the average LSE. As the figure depicts, the simulations are consistently tracking the RS ansatz. This observation supports the validity of the RS solution, as well as the effectiveness of our tuning strategy.

The lower bound on the achievable ergodic rate is further shown in Figure 7.10 for larger interval of inverse loads. Given the RZF precoding, at $R^{\mathrm{L}}_{\mathrm{Erg}} = 3$ bits/sec/Hz

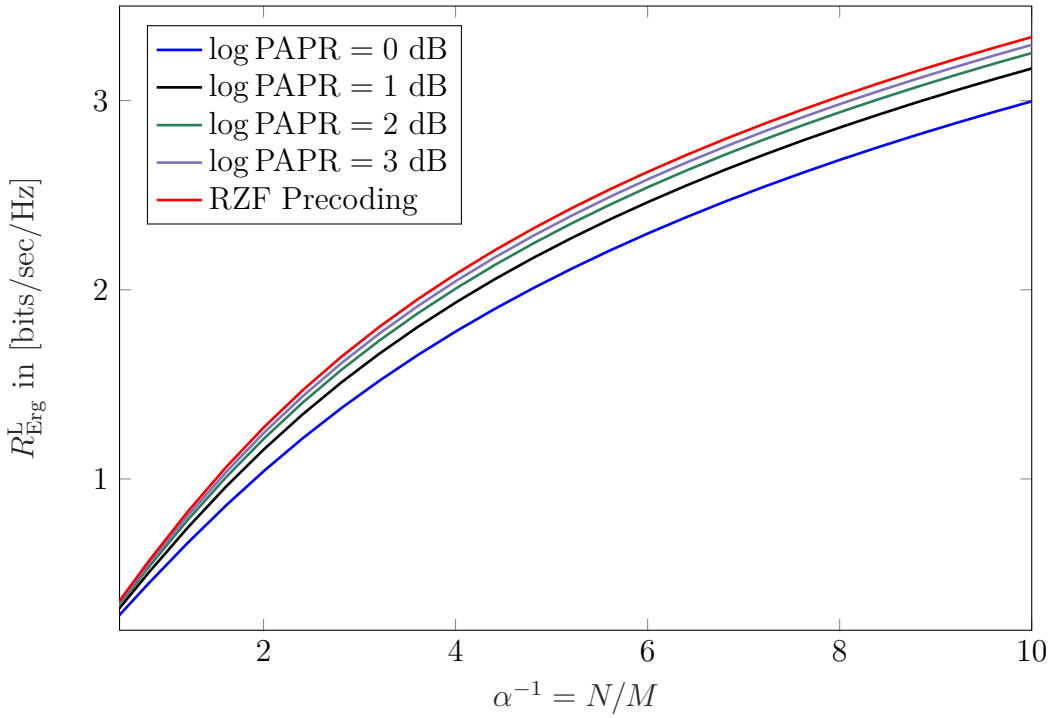

Figure 7.10: Lower bound on the achievable rate via PAPR-limited GLSE Precoding.

we need approximately two more antennas per user to achieve the same performance via constant envelope precoding.

7.5.6 Results for K-PSK GLSE Precoder

To investigate the K-PSK GLSE precoder numerically, we consider the two particular cases of $K = 2$, i.e., binary PSK (BPSK), and $K = 4$, i.e., QPSK constellation. When $K = 2$, the decoupled setting of GLSE Precoder 7.3.3.1 reduces to

$$\mathrm{g}_{\mathsf{RLS}}\left(\mathrm{s}|\tau\right) = \sqrt{P}\exp\left\{\mathrm{j}\frac{2k^{\star}\pi}{K}\right\} T\left(\mathbb{R}\mathrm{e}\left\{\mathrm{s}\right\}|\tau\right), \tag{7.58}$$

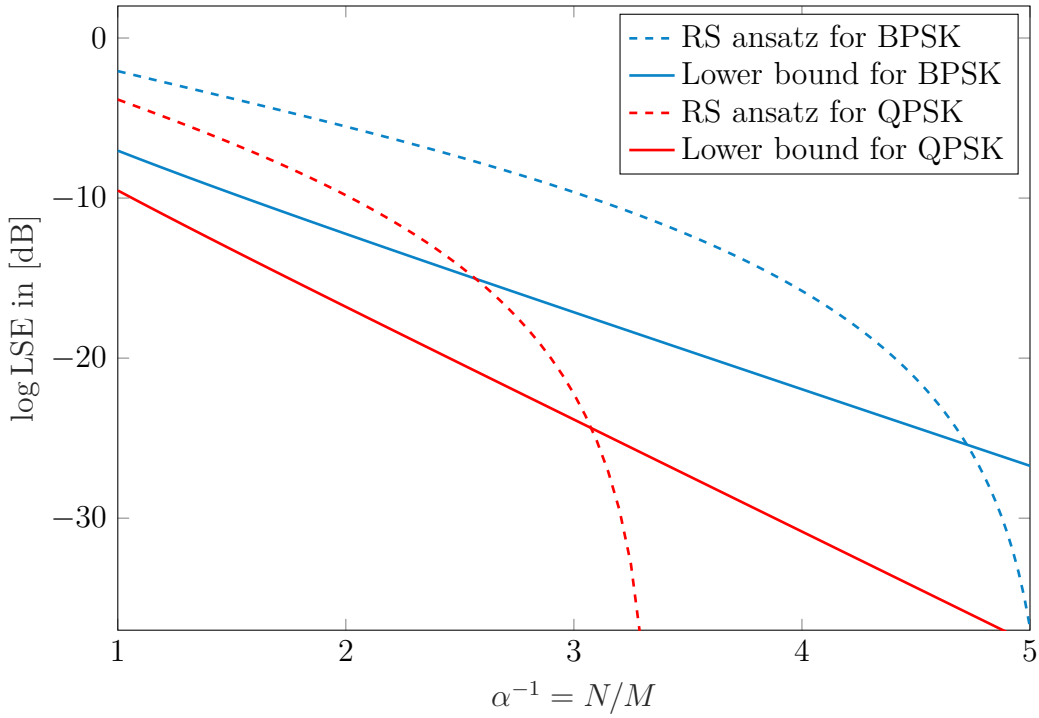

Figure 7.11: Asymptotic LSE given by the RS ansatz for K-PSK constellations.

where $k^\star$ is defined in (7.47), and the real-valued thresholding function $T(\cdot|\tau)$ is given by

$$T(u|\tau) \coloneqq \mathbf{1}\left\{|u| \geq \frac{1+\tau\lambda}{2}\sqrt{P}\right\}. \tag{7.59}$$

For $K = 4$, the decoupled precoder reads

$$\mathsf{g}_{\mathsf{RLS}}(\mathrm{s}|\tau) = \sqrt{P}\exp\left\{\mathrm{j}\frac{2k^\star\pi}{K}\right\} T(\mathbb{R}\mathrm{e}\{\mathrm{s}\}|\tau)\, T(\mathbb{I}\mathrm{m}\{\mathrm{s}\}|\tau). \tag{7.60}$$

Considering these decoupled settings, we first employ the RS ansatz and sketch the asymptotic LSE for both the BPSK and QPSK constellations in Figure 7.11 against the inverse load. The figure is plotted for envelope power $P = 1$ and power factor $\rho = 1$ where the parameter λ is tuned such that $\eta = 0.4$.

The validation of the result in this case is not tractable, since the GLSE precoder deals with an integer programming. We hence derive a rigorous lower bound on the asymptotic LSE and compare it with the solution given by the RS ansatz.

Lemma 7.2. *Let entries of the channel matrix be distributed i.i.d. Gaussian with zero-mean and variance* $1/N$*. For given peak power* P*, power factor* ρ*, load* α *and fraction of active transmit antennas* η*, the asymptotic LSE of GLSE Precoder 7.3.3.1 is bounded from below by* $\mathcal{L}_0$ *which satisfies the following fixed-point equation:*

$$\frac{\alpha \mathcal{L}_0}{\rho + \eta P} = \log\left(1 + K\right) + \alpha \left(1 + \log \frac{\mathcal{L}_0}{\rho + \eta P}\right). \tag{7.61}$$

Proof. See Appendix H. □

The lower bound in Lemma 7.2 is further sketched in Figure. 7.11 for both the understudy cases. Compared this lower bound to the asymptotic LSE given by the RS ansatz, it is observed that the RS solution is consistent with the lower-bounded only for small inverse loads and starts to violate the bound as the inverse load increases. This observation indicates that the RS the solution to the saddle-point equation does not exhibit the symmetry assumed by the RS primary assumptions. As a result, one needs to break this symmetry to assess a more accurate approximation of the asymptotic LSE for a larger range of loads.

For the sake of further investigations, we focus on the BPSK scenario and plot the asymptotic LSE given after one step of RSB against the inverse load in Figure 7.12. The figure is sketched for the same parameters considered in Figure 7.11 and is swept over a larger range of inverse loads. In this figure, we observe that the one-step RSB ansatz gives a solution which remains above the lower bound for a larger range of inverse loads. Noting that the RS and one-step RSB solutions are sufficiently close for $\alpha^{-1} < 3.5$, one could intuitively predicts that the given solution for this range is a very accurate approximation of the exact LSE[6]. Nevertheless, similar to the RS ansatz, the solution of the one-step RSB ansatz violates the rigorous lower bound at $\alpha^{-1} \approx 7.9$. This means that for larger values of α^{-1}, more steps of RSB are required,

[6]Note that this observation is not a rigorous proof.

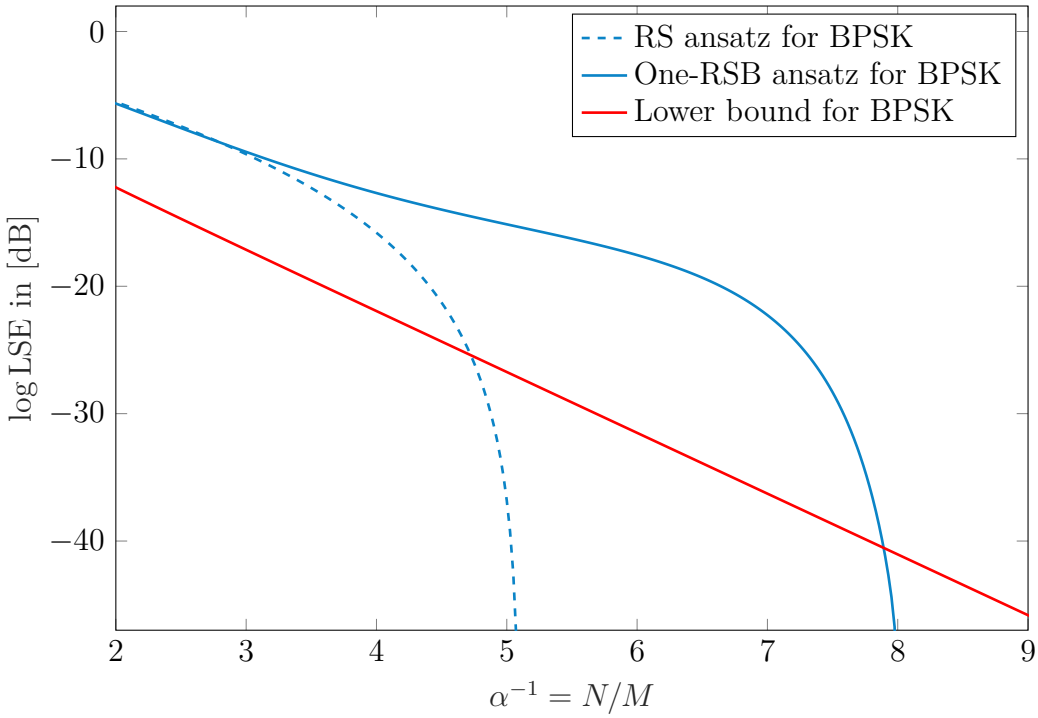

Figure 7.12: Asymptotic LSE given by one step of RSB for the BPSK constellation.

in order to assess the asymptotic LSE accurately. The solution might be given by the full RSB ansatz, i.e., with infinitely large number of breaking steps, or with a finite number of breaking steps $B > 1$.

7.6 Bibliographical Notes

By early developments in design of arrays with multiple antennas various communication settings with multiple transmit and receive antennas were proposed [182, 183]. These proposals brought significant attention to the concept of MIMO communications resulting in a rich analytic and algorithmic literature [184–198]. Although the analysis of large MIMO systems started early in parallel with the studies on MIMO communications, e.g., [44, 45, 199–202], they remained mostly as theoretical results, due to implementational intractability. The technological and theoretical progresses in millimeter wave communications indicated that shifting to this spectrum is prac-

tically feasible in a near future [203–207]. Such a conclusion led to a great deal of interest in *massive MIMO* architectures in the recent years [154, 159, 208–213].

Since early investigations on MIMO communications, the concept of MIMO precoding[7] was considered in the literature [190, 214–217], due to the limited computational capacity and power supply of user devices. The conventional approaches for MIMO precoding are *fully digital*. These approaches are roughly divided into two classes of *linear* and *nonlinear* schemes. Examples of linear techniques are maximum ratio transmission, zero-forcing and the RZF [155] scheme. The main characteristic of these schemes is their low computational complexity which is achieved at the expense of limited performance gains. By spending higher computational capacity, superior performance gains can be achieved via nonlinear techniques such as Tomlinson-Harashima [218–220] and nonlinear vector perturbation [221].

Due to high RF costs, the implementation of conventional precoders is considered intractable in several MIMO scenarios. As a result, various techniques were proposed in the literature which try to address this implementational issue in an effective manner. A primary technique is TAS in which the transmission is done through a subset of transmit antennas; see [163, 164, 222–227] and [A10, A15, A16] for some analysis and algorithms. Using TAS, the number of active transmit antennas is limited, and hence the number of required RF chains reduces. This leads to a reduced RF cost making the implementation of the transmitter tractable. Conventional designs for TAS propose a separate selecting module prior to the precoder which selects a suitable subset of antennas. MIMO precoding is then done over the selected antennas digitally. Another approach is the so-called *spatial modulation* [228–233]. Similar to TAS, the transmission in this case is carried out through a subset of antennas. However, in this technique the antenna selection procedure is done directly based on the realization of transmit data. For a given sequence of information symbols, the spatial modulator first selects a subset of antennas whose index corresponds to first block of the sequence. The remained part of the symbols is then transmitted via a digital precoder over the selected antennas. A detailed comparison between spatial modulation and TAS can be followed in [A17].

[7] Also called *signal shaping* or *pre-distorting*.

An alternative solution to the high RF cost of digital precoding in massive MIMO settings was given by the introduction of hybrid analog-digital precoding [234–239]. In this technique, the information symbols are first precoded over a restricted number of active transmit antennas via a digital precoding scheme. The digitally precoded signal is then mapped to a signal of higher dimension via a network of analog phase shifters.

7.7 Summary

This chapter has studied another application of RLS in information theory. The RLS method has been employed to address the problem of MIMO precoding. By interpreting precoding as a linear regression problem, we have designed a generic precoding scheme, referred to as GLSE precoding, which addresses a large variety of constraints on the downlink transmit signal in a multiuser MIMO setting. Using the asymptotic results derived in Chapters 4 and 5, the performance of the proposed scheme has been characterized in the large-system limit.

To address a few applications, we have investigated some particular special forms of the GLSE scheme, namely precoders which select a limited number of active antennas, precoders with restricted transmit PAPR, and a class of precoders whose transmit signal samples belong to a discrete constellation. For various forms of GLSE precoding, the asymptotic results based on the RS ansatz has shown consistency with numerical simulations or available bounds in the literature. The large-system performance of these precoders has further depicted a significant gain compared to the benchmark. For the particular case of precoding over discrete constellations, the asymptotic LSE given by the RS ansatz has shown to violate rigorous lower-bounds for small channel loads. For this case, the investigations under RSB have shown to be consistent with the lower-bound for a wider interval of channel loads.

Chapter 8

Conclusions and Future Work

Statistical mechanics provides a large scope of useful analytic tools which enable us to study high-dimensional data processing algorithms. Following this approach, the generic RLS method for linear regression is asymptotically characterized via the replica method. Similar to various other analytic tools from statistical mechanics, the replica method lacks rigorous justifications in some particular parts. Nevertheless, it provides analytically tractable lines for asymptotic characterization. The characterizations are used to investigate the performance of well-known sparse recovery algorithms. To illustrate another possible application of the results, the problem of MIMO precoding is interpreted as linear regression and addressed via the RLS method. The performance of the RLS-based scheme is investigated via the asymptotic results and compared to the benchmark.

The results of this study clarify the *efficiency* of statistical mechanical approaches for analysis of *applied* high-dimensional problems and provided a *systematic approach* to derive the asymptotic characteristics of a communication system via the replica method. The work further enlightens the applications of the RLS method in communications and signal processing. In this chapter, we give some final remarks and illustrate possible directions for future work.

8.1 Concluding Points

The characterization of the generic RLS method in this dissertation has been given for a generic replica correlation matrix which includes the RS ansatz as well as its broken versions. For various examples, the asymptotic characterization given under RS is highly consistent with tractable large-system simulations and available analytic bounds. Nevertheless, there exist some particular examples, such as RLS with ℓ_0-norm regularization, in which the RS ansatz tracks the asymptotic behavior only for a restricted set of configurations and leads to invalid results as the system parameters exceed these restrictions. This restricted set widens as the characterization is given by the broken RS structure with one step of braking. This observation agrees with earlier results in the literature, and hence strengthens this conjecture that the major points, such as *replica continuity*, in which the replica method lacks mathematical proof do not impose any inconsistency on the characterization.

The investigations further demonstrate that the earlier form of the decoupling principle is not *generic*. It is in fact a valid conclusion only for those settings whose corresponding spin glass exhibits RS. As the replica correlation matrix at the saddle point violates this symmetry, i.e., when it is characterized via an RSB ansatz, effective regression error in the decoupled setting is non-Gaussian and statistically depends on the true regression coefficient. The distribution of this error term, unlike the Gaussian distribution, shows asymmetry.

The numerical investigations further depict that the specific forms of RLS method which deal with *convex* optimization problems, e.g., LASSO, are perfectly characterized via the RS ansatz. This result is in harmony with the well-known belief in the literature which indicates that convex optimization problems do not exhibit RSB. It is however concluded from the literature and the derivations in this thesis that there exists *no injective relation* between convexity and RS. This statement is simply understood by considering the results for ℓ_0-norm scheme derived in Chapter 6 and the earlier investigations on MMSE estimation; see for example [74, 240]. Although both the problems deal with non-convex optimizations, the former exhibits RSB and the latter does not. This observation implies that the *various non-convex* problems do not require RSB for asymptotic characterization. We conjecture that these non-convex

problems contain a form of *hidden convexity* which appears in the large-system limit due to *marginalization*, e.g., several Bayesian estimators. There is however no clear proof for this statement, and hence we leave it as a conjecture.

The asymptotic analyses given in this treatise have been used to investigate two various applications, namely sparse recovery and MIMO precoding. Although the derivations are mainly theoretical, they are practically useful in two major respects:

1. For various particular examples, such as sparse recovery via ℓ_0-norm minimization and precoding over discrete constellations, the asymptotic performance is not tractably evaluated. The computational complexity is further growing exponentially with the dimension which makes the numerical investigation practically infeasible. For these scenarios, the asymptotic derivations can provide useful bounds on the performance, specially when the scheme of interest is considered to be *optimal*. In other words, although the derivations based on the replica method only describe the performance in the large-system limit and does not specify the output of the scheme, e.g., the estimated signal, it demonstrates the optimal achievable performance. The result can hence be used as a *reference* with which the benchmark performance is compared.

2. The asymptotic characterization further provides an efficient approach for tuning the benchmark forms of the RLS method. To illustrate this point, consider the LASSO scheme. As illustrated, the performance of this scheme depends on the choice of tuning factor. In practice, adaptive strategies are used for tuning. These strategies invoke some iterative algorithms and find the tuning factor such that the performance meets a local extrema. For some applications such as MIMO precoding, the adaptive approaches introduce further computational loads to the system. Following the fact that the asymptotic characterization closely tracks the finite-dimensional performance for practical dimensions, one could use the results to find the optimal tuning factor analytically. Such an approach can lead to lower computational loads in those applications of RLS scheme in which the tuning factor is updated periodically.

Applications of the generic RLS method is not limited to what presented in this dissertation, since linear regression model describes a wide set of applied problems.

By taking the similar approach as in Chapter 7, several problems are modeled as linear regression, and an effective solution to them can be determined via RLS. For these applications, the results of this treatise provide large-system characterization which can be used for the two major use cases illustrated above.

8.2 Future Work

The study of this thesis can be pursued in various respects. In the sequel, we briefly discuss some directions for the future work.

8.2.1 Investigating Further Applications

As indicated in the concluding remarks, various problems in communications and signal processing are consistent with the linear regression model. Examples of such problems are the linear inverse problem with multiple measurement vectors (MMV) [241], dictionary learning [13], matrix completion [242, 243], pattern recognition [244, 245] and data mining [246]. Although most of these problems are known for decades, their applications have received a great deal of attention lately following the recent improvements in the computational capacity of processing modules. In this respect, the derivations in this dissertation can be employed to investigate the asymptotic performance of RLS-based algorithms in these topics.

8.2.2 Linear Regression with Non-identical Prior Model

Throughout the investigations in this treatise, the postulated distribution of true regression coefficients have been considered to be i.i.d.. This is a typical assumption which holds in many applications of linear regression. There are however some particular examples in which the statistical model is not consistently described with such priors. The most relevant example is the problem of *structured* sparse recovery [132, 247]. This problem aims to address the same task as in standard sparse recovery. The key difference in this case is that the true signal is not only sparse, but also is known to be drawn from a certain *structure*. An instance of such structure is

block sparsity in which signal samples are grouped into distinct *sparse* subsets with *different* sparsity factors. Such structured priors are not precisely modeled via an i.i.d. distribution, and hence the asymptotic derivations in this study does not characterize the performance of RLS-based schemes in these cases. In this respect, a possible direction for future work is to extend the formulations in this thesis to models with *non-identical* prior distributions. The work in this direction is currently ongoing and some prior results have been published in [A13, A26].

8.2.3 Distributed Linear Regression Problems

The basic linear regression model considered in this treatise addresses *centralized* applications. For instance, in the example of signal recovery, the model describes a setting in which a signal is sampled at a *single* sampling center and then recovered by a recovery algorithm. Nevertheless, many applied problems in communications have a *distributed* nature. A well-known example of such problems is *distributed compressive sensing* in which multiple *statistically dependent* sparse signals are sampled at distinct terminals. The recovery is then performed at a single *data-fusion center*, where the observations of all the terminals are collected [248, 249]. A naive approach for recovery is to use multiple algorithms in parallel, each recovering a distinct signal from its corresponding measurements. From Slepian-Wolf theorem, it is known that this approach is not effective and could impose significant degradation on the performance, since it ignores the dependency among the signals; see [250, Chapter 10]. Bayesian inference suggests that we employ a *joint* RLS-based recovery scheme whose regularization term is a *coupled* function of signal samples.

Following the similar approach as the one taken in this thesis, the asymptotic performance of the RLS method can be further investigated in *distributed* forms of linear regression. Such study clarifies the efficiency of optimal joint recovery schemes and demonstrates the level of degradation when the dependency among terminals is ignored. Some initial investigations in this direction have been given in [A12].

8.2.4 Developing AMP Algorithms for MIMO Precoding

For many forms of the RLS method, iterative algorithms have been developed which *approximate* the recovered regression coefficients with low computational complexity. For a long time, it was believed that the low complexity of these algorithms comes at the expense of *poor* approximations. The development of AMP-based algorithms demonstrated that this trade-off is *not generic*. In high-dimensional problems, AMP has shown to perform RLS-based recovery accurately within a fixed number of iterations. The complexity of AMP-based algorithms in each iteration grows linearly with the dimension. These two key features have brought a great deal of attention to AMP in recent years. For many high-dimensional applications of linear regression in signal processing, AMP-based algorithms are considered as the most effective approach; see for example [47, 52, 138, 148] and the references therein.

The AMP methodology, used to address signal processing problems, can be further extended to other applications of RLS. An example of such applications is the GLSE framework proposed in Chapter 7 for MIMO precoding. Our investigations demonstrate that for various transmission constraints, the GLSE scheme outperforms its conventional counterpart approaches significantly. It is however known that even for the convex forms of GLSE, the computational complexity is higher than the benchmark. In this respect, an interesting direction for future work is to develop AMP algorithms for various forms of the GLSE precoding scheme. Such algorithms enjoy both the performance enhancement and low complexity features. Some initial studies in this direction have been started, and the results have been published in [A11, A21].

Appendix A

Derivation of the General Ansatz

As discussed in Chapter 3, the main task for deriving the replica ansatz is to calculate the moments function $f_{\mathcal{Z}}(t)$. To this end, we start from the formulation in Chapter 3: Using replica continuity conjecture, $f_{\mathcal{Z}}(t)$ has been given in (3.75d) as

$$f_{\mathcal{Z}}(t) \coloneqq \mathbb{E}\left\{\sum_{\{\boldsymbol{v}_a\}} \exp\left\{\sum_{a=1}^{t} -\beta\mathcal{E}\left(\boldsymbol{v}_a|\boldsymbol{y},\mathbf{A}\right) + h\psi_{\mathrm{v}}\left(\boldsymbol{v}_a|\boldsymbol{x}_0\right)\right\}\right\} \tag{A.1}$$

where we use notation $\{\boldsymbol{v}_a\}$ to denote

$$\{\boldsymbol{v}_1,\ldots,\boldsymbol{v}_t\} \in \prod_{a=1}^{t} \mathbb{X}^N. \tag{A.2}$$

Moreover, modification term $\psi_{\mathrm{v}}(\boldsymbol{v}|\boldsymbol{x}_0)$ is of the form

$$\psi_{\mathrm{v}}\left(\boldsymbol{v}|\boldsymbol{x}_0\right) = \sum_{w\in\mathbb{W}} \psi\left(v_w|x_{0w}\right) \tag{A.3}$$

for some scalar function $\psi(\cdot|\cdot)$ and $\mathbb{W} \subseteq [N]$. As shown in Chapter 3, depending on the choice of $\psi(\cdot|\cdot)$, this modification term determines the asymptotic distortion or the asymptotic LSE.

A.1 Derivation of the Expectation

Starting from (A.1), the expectation is written as

$$f_{\mathcal{Z}}(t) = \mathbb{E}_{\boldsymbol{x}_0}\left\{\mathbb{E}_{\mathbf{A}}\left\{\mathbb{E}_{\boldsymbol{z}}\left\{\sum_{\{\boldsymbol{v}_a\}}\exp\left\{\sum_{a=1}^{t}-\beta\mathcal{E}\left(\boldsymbol{v}_a|\boldsymbol{y},\mathbf{A}\right)+h\psi_{\mathrm{v}}\left(\boldsymbol{v}_a|\boldsymbol{x}_0\right)\right\}\right\}\right\}\right\} \tag{A.4}$$

where the factorization comes from the fact that $\boldsymbol{z}$, $\mathbf{A}$ and $\boldsymbol{x}_0$ are statistically independent. We first take the expectation with respect to $\boldsymbol{z}$ invoking the stochastic model of the regression error in Section 2.1.1.

A.1.1 Averaging over Regression Error

Using Gaussian integration, we have

$$f_{\mathcal{Z}}(t) = C_0(\beta,t)\,\mathbb{E}\left\{\sum_{\{\boldsymbol{v}_a\}}\exp\left\{E\left(\{\boldsymbol{v}_a\}|\boldsymbol{x}_0,\beta,h,t\right)-\beta\sum_{a,b=1}^{t}\tilde{\boldsymbol{v}}_a^{\mathsf{H}}\mathbf{J}\tilde{\boldsymbol{v}}_b i_{ab}(\beta,t)\right\}\right\}. \tag{A.5}$$

In (A.5), for $a\in[t]$

$$\tilde{\boldsymbol{v}}_a = \boldsymbol{x}_0 - \boldsymbol{v}_a \tag{A.6}$$

is the a-th unbiased replica[1]. $\mathbf{J}$ is the Gramian of regressors matrix $\mathbf{A}$, i.e.

$$\mathbf{J} = \mathbf{A}^{\mathsf{H}}\mathbf{A} \tag{A.7}$$

and satisfies the properties stated in Chapter 2. The indication operator $i_{ab}(\beta,t)$ is moreover defined as

$$i_{ab}(\beta,t) \coloneqq \frac{\zeta}{2\lambda}\left[\mathbf{1}\{a=b\}-\frac{\beta\sigma^2}{\lambda+t\beta\sigma^2}\right] \tag{A.8}$$

[1] We call it unbiased, since it expresses the deviation of $\boldsymbol{v}_a$ from the true coefficients.

where σ^2 denotes the variance of the regression error. Finally, the functions $C_0(\beta, t)$ and $E(\{\boldsymbol{v}_a\}|\boldsymbol{x}_0, \beta, h, t)$ are given by

$$C_0(\beta, t) \coloneqq \left(\frac{\lambda}{\lambda + t\beta\sigma^2}\right)^{\frac{\zeta}{2}M} \tag{A.9a}$$

$$E(\{\boldsymbol{v}_a\}|\boldsymbol{x}_0, \beta, h, t) \coloneqq \sum_{a=1}^{t} -\beta u_{\mathrm{v}}(\boldsymbol{v}_a) + h\psi_{\mathrm{v}}(\boldsymbol{v}_a|\boldsymbol{x}_0). \tag{A.9b}$$

For sake of brevity, we drop the arguments β, h and t in $E(\{\boldsymbol{v}_a\}|\boldsymbol{x}_0, \beta, h, t)$ in the sequel and denote it as $E(\{\boldsymbol{v}_a\}|\boldsymbol{x}_0)$.

Remark A.1. *While defining the corresponding spin glass, the Hamiltonian could be defined as*

$$\mathcal{E}_{\mathrm{new}}(\boldsymbol{v}_a|\boldsymbol{y}, \mathbf{A}) = \mathcal{E}(\boldsymbol{v}_a|\boldsymbol{y}, \mathbf{A}) - \frac{\zeta}{2\lambda}\|\boldsymbol{z}\|^2. \tag{A.10}$$

This modified Hamiltonian does not impact the relation between the spin glass and the generic RLS method, since the modification term is not a function of optimization variable $\boldsymbol{v}$. In this case, starting from (A.4)*, the moments function finds the same form as in* (A.5) *with*

$$C_{0,\mathrm{new}}(\beta, t) = 1, \tag{A.11a}$$

$$i_{ab}^{\mathrm{new}}(\beta, t) = \frac{\zeta}{2\lambda}\left[\mathbf{1}\{a = b\} - \frac{\sigma^2}{\lambda}\beta\right]. \tag{A.11b}$$

Such a modification just simplifies the derivations and results in a same result as the limits are taken.

A.1.2 Averaging over Regressors

We now define the random variable

$$f_{\mathcal{Z}}(t|\boldsymbol{x}_0) \coloneqq \mathbb{E}_{\mathbf{A}}\left\{\sum_{\{\boldsymbol{v}_a\}} \exp\left\{E(\{\boldsymbol{v}_a\}|\boldsymbol{x}_0) - \beta\sum_{a,b=1}^{t} \tilde{\boldsymbol{v}}_a^{\mathsf{H}}\mathbf{J}\tilde{\boldsymbol{v}}_b i_{ab}(\beta, t)\right\}\right\}. \tag{A.12}$$

which is randomized by $\boldsymbol{x}_0$. The moments function is hence given as

$$f_{\mathcal{Z}}(t) = C_0(\beta, t)\, \mathbb{E}\left\{ f_{\mathcal{Z}}(t|\boldsymbol{x}_0) \right\}. \tag{A.13}$$

We later on show that for almost all realizations of the source vector, $f_{\mathcal{Z}}(t|\boldsymbol{x}_0)$ converges to a deterministic value, and thus the expectation with respect to $\boldsymbol{x}_0$ can be dropped. To determine $f_{\mathcal{Z}}(t|\boldsymbol{x}_0)$, we rewrite

$$f_{\mathcal{Z}}(t|\boldsymbol{x}_0) = \sum_{\{\boldsymbol{v}_a\}} \mathbb{E}_{\mathbf{J}} \left\{ \exp\left\{ -\beta N \mathrm{tr}\left\{ \mathbf{JG} \right\} \right\} \right\} \exp\left\{ E\left(\{\boldsymbol{v}_a\} | \boldsymbol{x}_0 \right) \right\}, \tag{A.14}$$

where $\mathbf{G} \in \mathbb{A}_{\zeta}^{N \times N}$ is defined as

$$\mathbf{G} \coloneqq \frac{1}{N} \sum_{a,b=1}^{t} \tilde{\boldsymbol{v}}_b \tilde{\boldsymbol{v}}_a^{\mathsf{H}} i_{a,b}(\beta, t) \tag{A.15}$$

and the expectation variable is changed to $\mathbf{J}$.

Considering the stochastic model of the regressors in Chapter 2, we know that Gramian matrix $\mathbf{J}$ has the eigendecomposition $\mathbf{J} = \mathbf{UDU}^{\mathsf{H}}$ with following properties:

1. $\mathbf{D}$ is a diagonal matrix whose empirical diagonal distribution converges to $\mathrm{F}_{\mathbf{J}}(\lambda)$.
2. $\mathbf{U}$ is distributed with a Haar probability measure over group $\mathbb{O}_N^{\zeta}$, where

$$\mathbb{O}_N^{\zeta} = \begin{cases} \mathbb{O}_N & \zeta = 1 \\ \mathbb{U}_N & \zeta = 2 \end{cases} \tag{A.16}$$

with $\mathbb{O}_N$ and $\mathbb{U}_N$ being orthogonal and unitary groups of size N, respectively.

Hence, the term $\mathbb{E}_{\mathbf{J}} \left\{ \exp\left\{ -\beta N \mathrm{tr}\left\{ \mathbf{JG} \right\} \right\} \right\}$ in (A.14) is expressed as

$$\mathbb{E}_{\mathbf{J}} \left\{ \exp\left\{ -\beta N \mathrm{tr}\left\{ \mathbf{JG} \right\} \right\} \right\} = \int_{\mathbb{O}_N^{\zeta}} \exp\left\{ N \mathrm{tr}\left\{ \mathbf{U}^{\mathsf{H}} (-\beta \mathbf{G}) \mathbf{UD} \right\} \right\} \mathrm{d}\mu_N^{\zeta}(\mathbf{U}) \tag{A.17}$$

where μ_N^{ζ} denotes a Haar measure over $\mathbb{O}_N^{\zeta}$. The right hand side of (A.17) describes a spherical integral which is often referred to in the literature as "Harish-Chandra" or

"Itzykson-Zuber" integral. The integral has been extensively studied in the physics and mathematics literature, see for example [251], [252] and [253]. A brief discussion on the spherical integral and its closed form solution has been given in Appendix E.

From Theorems 1.2 and 1.7 in [59], we can state that if[2]

$$\operatorname{rank}(\mathbf{G}) = \mathcal{O}\left(\sqrt{N}\right), \tag{A.18}$$

then,

$$\mathbb{E}_{\mathbf{J}}\left\{\exp\left\{-\beta N \operatorname{tr}\left\{\mathbf{JG}\right\}\right\}\right\} \doteq \exp\left\{-N\left[\sum_{n=1}^{N}\int_{0}^{\beta\lambda_n^{\mathbf{G}}} \mathrm{R}_{\mathbf{J}}(-\frac{2}{\zeta}\omega)\mathrm{d}\omega\right]\right\} \tag{A.19}$$

where $\lambda_n^{\mathbf{G}}$ for $n \in [N]$ denotes the n-th eigenvalue of $\mathbf{G}$ defined in (A.15). In order to utilize (A.19), we need to check the rank condition.

Lemma A.1. *Considering* $\mathbf{G}$ *to be defined as in* (A.15)*,* (A.18) *holds.*

Proof. First, we rewrite $\mathbf{G}$ as

$$\mathbf{G} = \frac{\zeta}{2\lambda N}\left[\sum_{a=1}^{t}\tilde{\boldsymbol{v}}_a\tilde{\boldsymbol{v}}_a^{\mathsf{H}} - \frac{\beta\sigma^2}{\lambda + t\beta\sigma^2}\left(\sum_{a=1}^{t}\tilde{\boldsymbol{v}}_a\right)\left(\sum_{b=1}^{t}\tilde{\boldsymbol{v}}_b^{\mathsf{H}}\right)\right] \tag{A.20a}$$

$$= \frac{\zeta}{2\lambda N}\tilde{\mathbf{V}}\left(\mathbf{I}_m - \frac{\beta\sigma^2}{\lambda + t\beta\sigma^2}\mathbf{1}_m\right)\tilde{\mathbf{V}}^{\mathsf{H}} \tag{A.20b}$$

where we define

$$\tilde{\mathbf{V}} = [\tilde{\boldsymbol{v}}_1, \ldots, \tilde{\boldsymbol{v}}_t] \tag{A.21}$$

Noting that $\tilde{\mathbf{V}} \in \mathbb{A}_{\zeta}^{N\times t}$, it is observed from (A.20b) that $\mathbf{G}$ could be, at most, of rank t. Considering replica continuity conjecture, $f_{\mathcal{Z}}(t)$ analytically continues to the real

[2] $\mathcal{O}(\cdot)$ indicates the growth order with respect to composition, i.e., $\lim_{n\uparrow\infty} \mathcal{O}(f(n))/f(n) = \mathsf{K} < \infty$.

axis, and the limit with respect to t is taken in a right neighborhood of $t_0 = 0$. Hence, for all values of N there exists a constant $K \in \mathbb{R}^+$, such that $t \leq K$. Consequently,

$$\lim_{N\uparrow\infty} \frac{\operatorname{rank}(\mathbf{G})}{\sqrt{N}} \leq \lim_{N\uparrow\infty} \frac{t}{\sqrt{N}} \leq \lim_{N\uparrow\infty} \frac{K}{\sqrt{N}} = 0 \tag{A.22}$$

which concludes that $\operatorname{rank}(\mathbf{G}) = \mathcal{O}\left(\sqrt{N}\right)$. □

Lemma A.1 ensures that (A.18) always holds, and thus, the asymptotic equivalence in (A.19) can be employed to determine the expectation. Noting the fact that $\mathbf{G}$ has only t non-zero eigenvalues, we write

$$\mathbb{E}_{\mathbf{J}}\left\{\exp\left\{-\beta N \operatorname{tr}\left\{\mathbf{J}\mathbf{G}\right\}\right\}\right\} \doteq \exp\left\{-N\mathcal{G}\left(\mathbf{T}\mathbf{Q}^{\mathrm{v}}\left(\{\boldsymbol{v}_a\}\,|\boldsymbol{x}_0\right)\right) + \epsilon_N\right\} \tag{A.23}$$

where $\epsilon_N \to 0$ as $N \uparrow \infty$, function $\mathcal{G}(\cdot)$ is defined as

$$\mathcal{G}(\mathbf{M}) \coloneqq \int_0^{\beta} \operatorname{tr}\left\{\mathbf{M}\mathrm{R}_{\mathbf{J}}(-\frac{2}{\zeta}\mathbf{M}\omega)\right\} \mathrm{d}\omega \tag{A.24}$$

for some $\mathbf{M} \in \mathbb{A}_{\zeta}^{t\times t}$, and $\mathbf{T} \in \mathbb{R}^{t\times t}$ is a deterministic matrix given by

$$\mathbf{T} \coloneqq \frac{\zeta}{2\lambda}\left[\mathbf{I}_t - \frac{\beta\sigma^2}{\lambda + t\beta\sigma^2}\mathbf{1}_t\right]. \tag{A.25}$$

Matrix $\mathbf{Q}^{\mathrm{v}}\left(\{\boldsymbol{v}_a\}\,|\boldsymbol{x}_0\right) \in \mathbb{A}_{\zeta}^{t\times t}$ in (A.23) is moreover defined as

$$\mathbf{Q}^{\mathrm{v}}\left(\{\boldsymbol{v}_a\}\,|\boldsymbol{x}_0\right) = \frac{1}{N}\tilde{\mathbf{V}}^{\mathsf{H}}\tilde{\mathbf{V}}. \tag{A.26}$$

and determines *correlations* among the biased replicas. It is worth to note that

$$\left[\mathbf{Q}^{\mathrm{v}}\left(\{\boldsymbol{v}_a\}\,|\boldsymbol{x}_0\right)\right]_{ab} = \frac{1}{N}\tilde{\boldsymbol{v}}_a^{\mathsf{H}}\tilde{\boldsymbol{v}}_b = \left[\mathbf{Q}^{\mathrm{v}}\left(\{\boldsymbol{v}_a\}\,|\boldsymbol{x}_0\right)\right]_{ba}^{*} \tag{A.27}$$

which indicates that the correlation matrix is Hermitian symmetric.

Remark A.2. *Note that although* $\mathbf{Q}^{\mathrm{v}}\left(\{\boldsymbol{v}_a\}\,|\boldsymbol{x}_0\right)$ *is symmetric,* $\mathbf{T}\mathbf{Q}^{\mathrm{v}}\left(\{\boldsymbol{v}_a\}\,|\boldsymbol{x}_0\right)$ *is not a symmetric matrix, in general; however, due to the symmetry of* $\mathbf{G}$*, the eigenvalues*

of $\mathbf{TQ}^{\mathrm{v}}\left(\{\boldsymbol{v}_a\}\,|\boldsymbol{x}_0\right)$ *are real, and therefore, the sequence of integrals over the real axis in* (A.23) *exists for all indices.*

By substituting (A.23) in (A.14), $f_{\mathcal{Z}}\left(t|\boldsymbol{x}_0\right)$ is given by

$$f_{\mathcal{Z}}\left(t|\boldsymbol{x}_0\right)=\sum_{\{\boldsymbol{v}_a\}}\exp\left\{-N\mathcal{G}\left(\mathbf{TQ}^{\mathrm{v}}\left(\{\boldsymbol{v}_a\}\,|\boldsymbol{x}_0\right)\right)+E\left(\{\boldsymbol{v}_a\}\,|\boldsymbol{x}_0\right)+\epsilon_N\right\} \tag{A.28}$$

To determine the sum in (A.28), we split the space of all replicas into subshells defined by the correlation matrices in which all the replicas within each subshell have the same correlation matrix. More precisely, for a given $\boldsymbol{x}_0$, the subshell of matrix $\mathbf{Q}$ is

$$\mathbb{S}(\mathbf{Q})=\left\{\boldsymbol{v}_1,\ldots,\boldsymbol{v}_t|\left(\boldsymbol{x}-\boldsymbol{v}_a\right)^{\mathsf{H}}\left(\boldsymbol{x}-\boldsymbol{v}_b\right)=Nq_{ab}\right\} \tag{A.29}$$

with $q_{ab}=[\mathbf{Q}]_{ab}$. The sum is first determined over each subshell individually, and then, the results are summed over all the subshells. Noting that the correlation matrix shows Hermitian symmetry, it is conclude that each subshell is fully characterized via the upper diagonal entries of the correlation matrix. Hence,

$$f_{\mathcal{Z}}\left(t|\boldsymbol{x}_0\right)=\int\exp\left\{-N\mathcal{G}\left(\mathbf{TQ}\right)+\epsilon_N\right\}\exp\left\{N\mathcal{I}\left(\mathbf{Q}|\boldsymbol{x}_0\right)\right\}\mathrm{d}\mathbf{Q} \tag{A.30}$$

where the integral is taken over $\mathbb{A}_{\zeta}^{\frac{t(t+1)}{2}\times 1}$ with

$$\mathrm{d}\mathbf{Q}\coloneqq\prod_{a=1}^{t}\prod_{b=a+1}^{t}\mathrm{d}q_{ab}. \tag{A.31}$$

The term $\exp\left\{N\mathcal{I}\left(\mathbf{Q}\right)\right\}$ in (A.30) is defined as

$$\exp\left\{N\mathcal{I}\left(\mathbf{Q}|\boldsymbol{x}_0\right)\right\}\coloneqq\sum_{\{\boldsymbol{v}_a\}}\delta\left(\mathbf{Q}^{\mathrm{v}}\left(\{\boldsymbol{v}_a\}\,|\boldsymbol{x}_0\right)-\mathbf{Q}\right)\exp\left\{E\left(\{\boldsymbol{v}_a\}\,|\boldsymbol{x}_0\right)\right\} \tag{A.32}$$

where the Dirac impulse function with matrix argument is given by

$$\delta\left(\mathbf{Q}^{\mathrm{v}}\left(\{\boldsymbol{v}_a\}\,|\boldsymbol{x}_0\right)-\mathbf{Q}\right)\coloneqq\prod_{a=1}^{t}\prod_{b=a+1}^{t}\delta\left(\tilde{\boldsymbol{v}}_a^{\mathsf{H}}\tilde{\boldsymbol{v}}_b-Nq_{ab}\right). \tag{A.33}$$

Considering the definition of subshell $\mathbb{S}(\mathbf{Q})$, the term $\exp\{N\mathcal{I}(\mathbf{Q}|\boldsymbol{x}_0)\}$ is interpreted as a density measure on the set of all subshells. Therefore, the right hand side of (A.30) can be observed as the first order moment of $\exp\{-N\mathcal{G}(\mathbf{TQ}) + \epsilon_N\}$ determined with respect to density function $\exp\{N\mathcal{I}(\mathbf{Q}|\boldsymbol{x}_0)\}$. In the following, we derive this density term explicitly in an analytic form.

A.1.3 Deriving the Density Term

We start derivations by representing the Dirac impulse function via its inverse Laplace transform. To this end, let us denote entry $q_{ab} \in \mathbb{A}_\zeta$

$$q_{ab} = q_{ab}^I + \mathrm{j}q_{ab}^Q \tag{A.34}$$

which equivalently indicates that

$$q_{ba} = q_{ab}^I - \mathrm{j}q_{ab}^Q. \tag{A.35}$$

It is worth to indicate that for $\zeta = 1$, i.e. $\mathbb{A}_\zeta = \mathbb{R}$, we have $q_{ab}^Q = 0$ for $a, b \in [t]$. Moreover, for $a \in [t]$, $q_{aa}^Q = 0$.

Noting that the Laplace transform of Dirac impulse is one, for $a \in [t]$, we have

$$\delta_{aa} \coloneqq \delta\left(\|\tilde{\boldsymbol{v}}_a\|^2 - Nq_{aa}\right) \tag{A.36a}$$

$$= \frac{1}{2\pi\mathrm{j}} \int_{\mathbb{J}} \exp\left\{s_{aa}\left(\|\tilde{\boldsymbol{v}}_a\|^2 - Nq_{aa}\right)\right\} \mathrm{d}s_{aa} \tag{A.36b}$$

where s_{aa} is a complex frequency, and the integral is taken over

$$\mathbb{J} = (C - \mathrm{j}\infty, C + \mathrm{j}\infty) \tag{A.37}$$

for some constant $C \in \mathbb{R}$. For $a \neq b$, we moreover have

$$\delta_{ab} \coloneqq \delta\left(\tilde{\boldsymbol{v}}_a^{\mathsf{H}}\tilde{\boldsymbol{v}}_b - Nq_{ab}\right) \tag{A.38a}$$

$$= \delta\left(\mathbb{R}\mathrm{e}\left\{\tilde{\boldsymbol{v}}_a^{\mathsf{H}}\tilde{\boldsymbol{v}}_b\right\} - Nq_{ab}^{I}\right)\left[\delta\left(\mathbb{I}\mathrm{m}\left\{\tilde{\boldsymbol{v}}_a^{\mathsf{H}}\tilde{\boldsymbol{v}}_b\right\} - Nq_{ab}^{Q}\right)\right]^{\zeta-1}, \tag{A.38b}$$

where we define

$$\left[\delta\left(x\right)\right]^{0} \coloneqq 1 \tag{A.39}$$

for $x \in \mathbb{R}$. Using the inverse Laplace transform, δ_{ab} reads

$$\delta_{ab} = \frac{1}{(2\pi\mathrm{j})^{\zeta}} \int\limits_{\mathbb{J}^{\zeta}} \exp\left\{P_{ab}\left(s_{ab}^{I}, s_{ab}^{Q}\right)\right\} \mathrm{d}s_{ab}^{I}\left[\mathrm{d}s_{ab}^{Q}\right]^{\zeta-1} \tag{A.40}$$

where we define for $a \neq b$ the exponent function

$$P_{ab}\left(s_{ab}^{I}, s_{ab}^{Q}\right) \coloneqq \begin{cases} s_{ab}^{I}\left(\mathbb{R}\mathrm{e}\left\{\tilde{\boldsymbol{v}}_a^{\mathsf{H}}\tilde{\boldsymbol{v}}_b\right\} - Nq_{ab}^{I}\right) & \zeta = 1 \\ s_{ab}^{I}\left(\mathbb{R}\mathrm{e}\left\{\tilde{\boldsymbol{v}}_a^{\mathsf{H}}\tilde{\boldsymbol{v}}_b\right\} - Nq_{ab}^{I}\right) + s_{ab}^{Q}\left(\mathbb{I}\mathrm{m}\left\{\tilde{\boldsymbol{v}}_a^{\mathsf{H}}\tilde{\boldsymbol{v}}_b\right\} - Nq_{ab}^{Q}\right) & \zeta = 2 \end{cases} \tag{A.41}$$

for some complex frequencies s_{ab}^{I} and s_{ab}^{Q}. We now define the frequency domain correlation matrix $\mathbf{S}$, whose entries $s_{ab} = [\mathbf{S}]_{ab}$ read

$$s_{ab} = \begin{cases} s_{aa} & a = b \\ \frac{1}{2}\left(s_{ab}^{I} - \mathrm{j}s_{ab}^{Q}\right) & b > a \\ \frac{1}{2}\left(s_{ba}^{I} + \mathrm{j}s_{ba}^{Q}\right) & b < a \end{cases}. \tag{A.42}$$

By this definition, $P_{ab}\left(s_{ab}^{I}, s_{ab}^{Q}\right)$ is reformulated as

$$P_{ab}\left(s_{ab}^{I}, s_{ab}^{Q}\right) = s_{ab}\left(\tilde{\boldsymbol{v}}_a^{\mathsf{H}}\tilde{\boldsymbol{v}}_b - Nq_{ab}\right) + s_{ba}\left(\tilde{\boldsymbol{v}}_b^{\mathsf{H}}\tilde{\boldsymbol{v}}_a - Nq_{ba}\right) \tag{A.43}$$

Substituting into (A.33), one can write

$$\delta\left(\mathbf{Q}^{\mathrm{v}}\left(\{\boldsymbol{v}_a\}\,|\boldsymbol{x}_0\right) - \mathbf{Q}\right) = \int\limits_{\mathbb{J}^{\varphi}} \exp\left\{\sum_{a=1}^{t} s_{aa}\left(\left\|\tilde{\boldsymbol{v}}_a\right\|^2 - Nq_{aa}\right)\right. \tag{A.44a}$$

$$+\sum_{b=a+1}^{t} s_{ab}\left(\tilde{\boldsymbol{v}}_a^{\mathsf{H}}\tilde{\boldsymbol{v}}_b - Nq_{ab}\right) + s_{ba}\left(\tilde{\boldsymbol{v}}_b^{\mathsf{H}}\tilde{\boldsymbol{v}}_a - Nq_{ba}\right)\Bigg\}\,\mathrm{d}\mathbf{S}$$

$$= \int_{\mathbb{J}^{\varphi}} \exp\left\{-N\mathrm{tr}\left\{\mathbf{S}^{\mathsf{T}}\mathbf{Q}\right\} + \sum_{a,b=1}^{t} s_{ab}\tilde{\boldsymbol{v}}_a^{\mathsf{H}}\tilde{\boldsymbol{v}}_b\right\}\mathrm{d}\mathbf{S} \tag{A.44b}$$

where $\mathrm{d}\mathbf{S}$ is defined as

$$\mathrm{d}\mathbf{S} \coloneqq \prod_{a=1}^{t}\left[\frac{\mathrm{d}s_{aa}}{2\pi\mathrm{j}}\prod_{b=a+1}^{t}\frac{\mathrm{d}s_{ab}^{I}\left[\mathrm{d}s_{ab}^{Q}\right]^{\zeta-1}}{(2\pi\mathrm{j})^{\zeta}}\right] \tag{A.45}$$

and

$$\varphi = \zeta\frac{t^2}{2} + t - \zeta\frac{t}{2}. \tag{A.46}$$

Consequently, the density term reads

$$\exp\left\{N\mathcal{I}\left(\mathbf{Q}|\boldsymbol{x}_0\right)\right\} = \int\sum_{\{\boldsymbol{v}_a\}}\exp\left\{-N\mathrm{tr}\left\{\mathbf{S}^{\mathsf{T}}\mathbf{Q}\right\} + \sum_{a,b=1}^{t} s_{ab}\tilde{\boldsymbol{v}}_a^{\mathsf{H}}\tilde{\boldsymbol{v}}_b + E\left(\{\boldsymbol{v}_a\}\,|\boldsymbol{x}_0\right)\right\}\mathrm{d}\mathbf{S} \tag{A.47a}$$

$$= \int \exp\left\{-N\mathrm{tr}\left\{\mathbf{S}^{\mathsf{T}}\mathbf{Q}\right\} + N\mathcal{M}\left(\mathbf{S}|\boldsymbol{x}_0\right)\right\}\mathrm{d}\mathbf{S} \tag{A.47b}$$

with $\mathcal{M}(\mathbf{S})$ being defined as

$$\mathcal{M}\left(\mathbf{S}|\boldsymbol{x}_0\right) = \frac{1}{N}\log\sum_{\{\boldsymbol{v}_a\}}\exp\left\{\sum_{a,b=1}^{t} s_{ab}\tilde{\boldsymbol{v}}_a^{\mathsf{H}}\tilde{\boldsymbol{v}}_b + E\left(\{\boldsymbol{v}_a\}\,|\boldsymbol{x}_0\right)\right\}. \tag{A.48}$$

Considering (A.47b), the density term reads

$$\exp\left\{N\mathcal{I}\left(\mathbf{Q}|\boldsymbol{x}_0\right)\right\} = \int\exp\left\{N\mathcal{I}_N\left(\mathbf{Q},\mathbf{S}|\boldsymbol{x}_0\right)\right\}\mathrm{d}\mathbf{S} \tag{A.49}$$

where

$$\mathcal{I}_N\left(\mathbf{Q},\mathbf{S}|\boldsymbol{x}_0\right) \coloneqq \mathcal{M}\left(\mathbf{S}|\boldsymbol{x}_0\right) - \operatorname{tr}\left\{\mathbf{S}^{\mathsf{T}}\mathbf{Q}\right\}. \tag{A.50}$$

From (A.49), $\exp\left\{N\mathcal{I}\left(\mathbf{Q}|\boldsymbol{x}_0\right)\right\}$ is interpreted as a marginalization of the joint density $\exp\left\{N\mathcal{I}_N\left(\mathbf{Q},\mathbf{S}|\boldsymbol{x}_0\right)\right\}$ over $\mathbf{S}$. The exponent term $\mathcal{I}_N\left(\mathbf{Q},\mathbf{S}|\boldsymbol{x}_0\right)$ depends on N. This implies that $\mathcal{I}\left(\mathbf{Q}\right)$ is in general a function of N. Nevertheless, our analysis considers the regime in which the system dimension is significantly large. For this regime, we show that this dependency vanishes.

The dependency of $\mathcal{I}_N\left(\mathbf{Q},\mathbf{S}|\boldsymbol{x}_0\right)$ on N comes through $\mathcal{M}\left(\mathbf{S}|\boldsymbol{x}_0\right)$ which is random. Lemma A.2 shows that, as N grows large, this term converges to a deterministic term which does not depend on the system dimension. The derivation follows the law of large numbers and the decoupling nature of functions $u_{\mathrm{v}}(\cdot)$ and $\psi_{\mathrm{v}}\left(\cdot|\cdot\right)$.

Lemma A.2. *Let modification term $\psi_{\mathrm{v}}\left(\cdot|\cdot\right)$ be summed over $\mathbb{W} \subset [N]$ whose cardinality when $N > N_0$ reads*

$$\frac{|\mathbb{W}|}{N} = \eta \tag{A.51}$$

for some integer N_0. Then, as $N \uparrow \infty$, $\mathcal{M}\left(\mathbf{S}|\boldsymbol{x}_0\right)$ converges to

$$\begin{aligned}\mathcal{M}_{\mathrm{asy}}\left(\mathbf{S}\right) \coloneqq \eta\, \mathbb{E}\left\{\log \sum_{\mathbf{v}\in\mathbb{X}^t} \exp\left\{\left(\mathbf{x}-\mathbf{v}\right)^{\mathsf{H}}\mathbf{S}\left(\mathbf{x}-\mathbf{v}\right) - \beta u_{\mathrm{v}}\left(\mathbf{v}\right) + h\psi_{\mathrm{v}}\left(\mathbf{v}|\mathbf{x}\right)\right\}\right\} \\ + \left(1-\eta\right)\mathbb{E}\left\{\log \sum_{\mathbf{v}\in\mathbb{X}^t} \exp\left\{\left(\mathbf{x}-\mathbf{v}\right)^{\mathsf{H}}\mathbf{S}\left(\mathbf{x}-\mathbf{v}\right) - \beta u_{\mathrm{v}}\left(\mathbf{v}\right)\right\}\right\}\end{aligned} \tag{A.52}$$

where $\mathbf{x} = x_0\mathbf{1}_{t\times 1}$ with $x_0 \sim \mathrm{p}\left(x_0\right)$.

Proof. We start with expanding $E\left(\{\boldsymbol{v}_a\}|\boldsymbol{x}_0\right)$ as

$$E\left(\{\boldsymbol{v}_a\}|\boldsymbol{x}_0\right) = \sum_{a=1}^{t} -\beta u_{\mathrm{v}}\left(\boldsymbol{v}_a\right) + h\psi_{\mathrm{v}}\left(\boldsymbol{v}_a|\boldsymbol{x}_0\right) \tag{A.53a}$$

$$= \sum_{n=1}^{N} \sum_{a=1}^{t} -\beta u\left(v_{an}\right) + h w_n \psi\left(v_{an} | x_{0n}\right) \tag{A.53b}$$

$$= \sum_{n=1}^{N} -\beta u_{\mathrm{v}}\left(\mathbf{v}_n\right) + h w_n \psi_{\mathrm{v}}\left(\mathbf{v}_n | \mathbf{x}_n\right) \tag{A.53c}$$

$$= \sum_{n=1}^{N} E\left(\mathbf{v}_n | \mathbf{x}_n, w_n\right) \tag{A.53d}$$

where coefficient w_n for $n \in [N]$ reads

$$w_n = \begin{cases} 0 & \text{if } n \notin \mathbb{W} \\ 1 & \text{if } n \in \mathbb{W} \end{cases} \tag{A.54}$$

and $\mathbf{v}_n, \mathbf{x}_n \in \mathbb{X}^t$ are given by

$$\mathbf{v}_n = \left[v_{1n}, \ldots, v_{tn}\right]^{\mathsf{T}} \tag{A.55a}$$

$$\mathbf{x}_n = x_{0n} \mathbf{1}_{t \times 1}. \tag{A.55b}$$

Furthermore, with standard matrix expansion, we have

$$\sum_{a,b=1}^{t} s_{ab} \tilde{\boldsymbol{v}}_a^{\mathsf{H}} \tilde{\boldsymbol{v}}_b = \sum_{a,b=1}^{t} \sum_{n=1}^{N} \left(x_{0n} - v_{an}\right)^* s_{ab} \left(x_{0n} - v_{bn}\right) \tag{A.56a}$$

$$= \sum_{n=1}^{N} \left(\mathbf{x}_n - \mathbf{v}_n\right)^{\mathsf{H}} \mathbf{S} \left(\mathbf{x}_n - \mathbf{v}_n\right). \tag{A.56b}$$

Substituting in (A.48), we have

$$\mathcal{M}\left(\mathbf{S} | \boldsymbol{x}_0\right) = \frac{1}{N} \log \sum_{\{\boldsymbol{v}_a\}} \exp \left\{ \sum_{a,b=1}^{t} s_{ab} \tilde{\boldsymbol{v}}_a^{\mathsf{H}} \tilde{\boldsymbol{v}}_b + E\left(\{\boldsymbol{v}_a\} | \boldsymbol{x}_0\right) \right\} \tag{A.57a}$$

$$= \frac{1}{N} \log \sum_{\{\boldsymbol{v}_a\}} \exp \left\{ \sum_{n=1}^{N} \left(\mathbf{x}_n - \mathbf{v}_n\right)^{\mathsf{H}} \mathbf{S} \left(\mathbf{x}_n - \mathbf{v}_n\right) + E\left(\mathbf{v}_n | \mathbf{x}_n, w_n\right) \right\} \tag{A.57b}$$

$$= \frac{1}{N} \log \prod_{n=1}^{N} \sum_{\mathbf{v}_n \in \mathbb{X}^t} \exp\left\{ (\mathbf{x}_n - \mathbf{v}_n)^{\mathsf{H}} \mathbf{S} (\mathbf{x}_n - \mathbf{v}_n) + E(\mathbf{v}_n | \mathbf{x}_n, w_n) \right\} \quad \text{(A.57c)}$$

$$= \frac{1}{N} \sum_{n=1}^{N} \log \sum_{\mathbf{v}_n \in \mathbb{X}^t} \exp\left\{ (\mathbf{x}_n - \mathbf{v}_n)^{\mathsf{H}} \mathbf{S} (\mathbf{x}_n - \mathbf{v}_n) + E(\mathbf{v}_n | \mathbf{x}_n, w_n) \right\}. \quad \text{(A.57d)}$$

At this step, let us define functions $E_w^{\mathcal{M}}(\cdot)$ for $w \in \{0, 1\}$ as

$$E_w^{\mathcal{M}}(x, \mathbf{S}) \coloneqq \log \sum_{\mathbf{v} \in \mathbb{X}^t} \exp\left\{ (x\mathbf{1}_{t\times 1} - \mathbf{v})^{\mathsf{H}} \mathbf{S} (x\mathbf{1}_{t\times 1} - \mathbf{v}) + E(\mathbf{v} | x\mathbf{1}_{t\times 1}, w) \right\}. \quad \text{(A.58)}$$

Consequently, (A.57d) is rewritten as

$$\mathcal{M}(\mathbf{S} | \boldsymbol{x}_0) = \frac{1}{N} \left(\sum_{n \in \mathbb{W}} E_1^{\mathcal{M}}(x_{0n}, \mathbf{S}) + \sum_{n \in \mathbb{W}^{\mathrm{C}}} E_0^{\mathcal{M}}(x_{0n}, \mathbf{S}) \right) \quad \text{(A.59)}$$

where $\mathbb{W}^{\mathrm{C}} = [N] - \mathbb{W}$. As $\boldsymbol{x}_0$ is modeled as an i.i.d. random sequence, we can conclude that the sequences

$$\left\{ E_1^{\mathcal{M}}(x_{0n}, \mathbf{S}) : n \in \mathbb{W} \right\} \quad \text{(A.60a)}$$

$$\left\{ E_0^{\mathcal{M}}(x_{0n}, \mathbf{S}) : n \in \mathbb{W}^{\mathrm{C}} \right\} \quad \text{(A.60b)}$$

are i.i.d. sequences, as well. Hence, using the law of large number, we have

$$\frac{1}{N} \sum_{n \in \mathbb{W}} E_1^{\mathcal{M}}(x_0, \mathbf{S}) \to \eta \, \mathbb{E}\left\{ E_1^{\mathcal{M}}(x_{0n}, \mathbf{S}) \right\} \quad \text{(A.61a)}$$

$$\frac{1}{N} \sum_{n \in \mathbb{W}^{\mathrm{C}}} E_0^{\mathcal{M}}(x_{0n}, \mathbf{S}) \to (1 - \eta) \, \mathbb{E}\left\{ E_0^{\mathcal{M}}(x_0, \mathbf{S}) \right\} \quad \text{(A.61b)}$$

where $x_0 \sim \mathrm{p}(x_0)$. Consequently, we can asymptotically say that

$$\mathcal{M}(\mathbf{S} | \boldsymbol{x}_0) \to \mathcal{M}_{\mathrm{asy}}(\mathbf{S}) \quad \text{(A.62)}$$

where $\mathcal{M}_{\mathrm{asy}}(\mathbf{S})$ is given in (A.52). □

Remark A.3. *Considering Lemma A.2, it indicates that $e^{n\mathcal{I}(\mathbf{Q})}$ for a given correlation matrix $\mathbf{Q}$ converges to a deterministic term as N grows large. This equivalently states that for almost any given realization of true regression coefficients, the replica correlation matrix converges to its expectation.*

Using Lemma A.2, the density term in the asymptotic regime is written as

$$\exp\left\{N\mathcal{I}\left(\mathbf{Q}|\boldsymbol{x}_0\right)\right\} = \int \exp\left\{N\mathcal{M}_{\text{asy}}\left(\mathbf{S}\right) - N\text{tr}\left\{\mathbf{S}^{\mathsf{T}}\mathbf{Q}\right\}\right\} \mathrm{d}\mathbf{S} \tag{A.63}$$

which does not depend on a given realization of $\boldsymbol{x}_0$. Hence, for large N, we have

$$f_{\mathcal{Z}}\left(t\right) \overset{\star}{=} C_0\left(\beta, t\right) f_{\mathcal{Z}}\left(t|\boldsymbol{x}_0\right) \tag{A.64a}$$

$$= C_0\left(\beta, t\right) \int \exp\left\{-N\mathcal{G}\left(\mathbf{TQ}\right) + \epsilon_N\right\} \exp\left\{N\mathcal{I}\left(\mathbf{Q}|\boldsymbol{x}_0\right)\right\} \mathrm{d}\mathbf{Q} \tag{A.64b}$$

$$= C_0\left(\beta, t\right) \int \exp\left\{-NE_{\mathcal{Z}}\left(\mathbf{Q}, \mathbf{S}\right) + \epsilon_N\right\} \mathrm{d}\mathbf{Q}\mathrm{d}\mathbf{S} \tag{A.64c}$$

where $\star$ comes from the fact that $\exp\left\{N\mathcal{I}\left(\mathbf{Q}|\boldsymbol{x}_0\right)\right\}$ does not depend on $\boldsymbol{x}_0$ as N grows large, and

$$E_{\mathcal{Z}}\left(\mathbf{Q}, \mathbf{S}\right) \coloneqq \mathcal{G}\left(\mathbf{TQ}\right) + \text{tr}\left\{\mathbf{S}^{\mathsf{T}}\mathbf{Q}\right\} - \mathcal{M}_{\text{asy}}\left(\mathbf{S}\right). \tag{A.65}$$

A.2 Asymptotic Limits via the Saddle-point Method

Following the discussion in Chapter 3, the next step of analysis is to derive the modified free energy in the thermodynamic limit, i.e., $N \uparrow \infty$, from moments function. From (3.73b), we know that

$$\bar{\mathcal{F}}\left(\beta, h\right) = \lim_{N\uparrow\infty} \lim_{t\downarrow 0} -\frac{1}{\beta N t} \log f_{\mathcal{Z}}\left(t\right). \tag{A.66}$$

Taking the limits in the respective order is challenging, as function $f_{\mathcal{Z}}\left(t\right)$ is represented in a compact analytic form in the asymptotic regime. It is hence assumed that the

limits with respect to N and t are exchangeable. This is a common assumption in the literature which is taken along with replica continuity. By this assumption, we have

$$\bar{\mathcal{F}}(\beta,h) = \lim_{t\downarrow 0}\lim_{N\uparrow\infty} -\frac{1}{\beta N t}\log f_{\mathcal{Z}}(t) \tag{A.67a}$$

$$= \lim_{t\downarrow 0}\lim_{N\uparrow\infty} -\frac{1}{\beta N t}\log C_0(\beta,t)\int \exp\left\{-NE_{\mathcal{Z}}(\mathbf{Q},\mathbf{S})+\epsilon_N\right\}\mathrm{d}\mathbf{Q}\mathrm{d}\mathbf{S} \tag{A.67b}$$

$$= \lim_{t\downarrow 0}\lim_{N\uparrow\infty} \frac{\zeta M}{2\beta N t}\log\left(1+\frac{t\beta\sigma^2}{\lambda}\right)$$

$$- \lim_{t\downarrow 0}\lim_{N\uparrow\infty} \frac{1}{\beta N t}\log\int \exp\left\{-NE_{\mathcal{Z}}(\mathbf{Q},\mathbf{S})+\epsilon_N\right\}\mathrm{d}\mathbf{Q}\mathrm{d}\mathbf{S} \tag{A.67c}$$

$$= \frac{\zeta\alpha\sigma^2}{2\lambda} - \lim_{t\downarrow 0}\lim_{N\uparrow\infty} \frac{1}{\beta N t}\log\int \exp\left\{-NE_{\mathcal{Z}}(\mathbf{Q},\mathbf{S})+\epsilon_N\right\}\mathrm{d}\mathbf{Q}\mathrm{d}\mathbf{S}. \tag{A.67d}$$

Denoting that $E_{\mathcal{Z}}(\mathbf{Q},\mathbf{S})$ satisfies the large deviation property, we employ the saddle point method, illustrated in Lemma 3.1, to evaluate the limit with respect to N in the right hand side of (A.67d). This means that we can write

$$\lim_{N\uparrow\infty}\frac{1}{N}\log\int \exp\left\{-NE_{\mathcal{Z}}(\mathbf{Q},\mathbf{S})+\epsilon_N\right\}\mathrm{d}\mathbf{Q}\mathrm{d}\mathbf{S} = -E_{\mathcal{Z}}(\mathbf{Q}^\star,\mathbf{S}^\star) - \frac{\epsilon_N}{N} \tag{A.68}$$

$$= -E_{\mathcal{Z}}(\mathbf{Q}^\star,\mathbf{S}^\star) \tag{A.69}$$

where $(\mathbf{Q}^\star,\mathbf{S}^\star)$ is the saddle point of the exponent function. Substituting into (A.67d), we can conclude that

$$\bar{\mathcal{F}}(\beta,h) = \frac{\zeta\alpha\sigma^2}{2\lambda} + \lim_{t\downarrow 0}\frac{1}{\beta t}E_{\mathcal{Z}}(\mathbf{Q}^\star,\mathbf{S}^\star). \tag{A.70}$$

The saddle point is found by letting derivatives of the exponent function equal to zero. Using the standard definition

$$\left[\frac{\partial}{\partial\mathbf{M}}\right]_{ab} \coloneqq \frac{\partial}{\partial[\mathbf{M}]_{ab}}, \tag{A.71}$$

the saddle point is given by the solving fixed point equations

$$\frac{\partial}{\partial \mathbf{Q}} E_{\mathcal{Z}}\left(\mathbf{Q},\mathbf{S}\right)|_{(\mathbf{Q}^{\star},\mathbf{S}^{\star})} = \frac{\partial}{\partial \mathbf{Q}}\left[\mathcal{G}\left(\mathbf{TQ}\right) + \mathrm{tr}\left\{\mathbf{S}^{\mathsf{T}}\mathbf{Q}\right\} - \mathcal{M}_{\mathrm{asy}}\left(\mathbf{S}\right)\right] = 0 \tag{A.72a}$$

$$\frac{\partial}{\partial \mathbf{S}} E_{\mathcal{Z}}\left(\mathbf{Q},\mathbf{S}\right)|_{(\mathbf{Q}^{\star},\mathbf{S}^{\star})} = \frac{\partial}{\partial \mathbf{S}}\left[\mathcal{G}\left(\mathbf{TQ}\right) + \mathrm{tr}\left\{\mathbf{S}^{\mathsf{T}}\mathbf{Q}\right\} - \mathcal{M}_{\mathrm{asy}}\left(\mathbf{S}\right)\right] = 0. \tag{A.72b}$$

(A.72a) reduces to

$$\mathbf{S}^{\star} = -\beta\mathbf{T}\mathrm{R}_{\mathbf{J}}(-\frac{2}{\zeta}\beta\mathbf{T}\mathbf{Q}^{\star}). \tag{A.73}$$

Noting that the replica correlation matrix does not depend on the dummy variable h, the fixed point (A.72b) can be written for any choice of h. Hence, by setting $h = 0$, (A.72b) reads[3]

$$\mathbf{Q}^{\star} = \mathbb{E}\left\{\sum_{\mathbf{v}\in\mathbb{X}^t} \frac{\left(\mathbf{x}-\mathbf{v}\right)\left(\mathbf{x}-\mathbf{v}\right)^{\mathsf{H}} \exp\left\{\left(\mathbf{x}-\mathbf{v}\right)^{\mathsf{H}}\mathbf{S}^{\star}\left(\mathbf{x}-\mathbf{v}\right) - \beta u_{\mathrm{v}}\left(\mathbf{v}\right)\right\}}{\sum\limits_{\mathbf{v}\in\mathbb{X}^t} \exp\left\{\left(\mathbf{x}-\mathbf{v}\right)^{\mathsf{H}}\mathbf{S}^{\star}\left(\mathbf{x}-\mathbf{v}\right) - \beta u_{\mathrm{v}}\left(\mathbf{v}\right)\right\}}\right\}. \tag{A.74}$$

By substituting (A.73) into (A.74), the fixed point equations are written compactly as

$$\mathbf{Q}^{\star} = \mathbb{E}_{\mathbf{x}}\left\{\sum_{\mathbf{v}\in\mathbb{X}^t} \left(\mathbf{x}-\mathbf{v}\right)\left(\mathbf{x}-\mathbf{v}\right)^{\mathsf{H}} \mathrm{p}_{\beta}^{\mathsf{R}}\left(\mathbf{v}|\mathbf{x}\right)\right\} \tag{A.75a}$$

$$= \mathbb{E}_{\mathbf{x},\mathbf{v}}\left\{\left(\mathbf{x}-\mathbf{v}\right)\left(\mathbf{x}-\mathbf{v}\right)^{\mathsf{H}}\right\}, \tag{A.75b}$$

where we define random variable $\mathbf{v}$, depend on $\mathbf{x}$, with conditional distribution

$$\mathrm{p}_{\beta}^{\mathsf{R}}\left(\mathbf{v}|\mathbf{x}\right) \coloneqq \frac{\exp\left\{-\beta\mathcal{E}^{\mathsf{R}}\left(\mathbf{v}|\mathbf{x}\right)\right\}}{\mathcal{Z}^{\mathsf{R}}\left(\beta|\mathbf{x}\right)}. \tag{A.76}$$

[3] Although this statement rigorously follows the formulation in Chapter 3, one may not see it directly at this point. In that case, one could assume that $\mathbf{Q}^{\star}$ is a function of h and by taking the derivative with respect to h show that $\partial\mathbf{Q}^{\star}/\partial h = 0$ which concludes our initial statement.

Here, the exponent function $\mathcal{E}^{\mathsf{R}}(\mathbf{v}|\mathbf{x})$ is

$$\mathcal{E}^{\mathsf{R}}(\mathbf{v}|\mathbf{x}) = (\mathbf{x}-\mathbf{v})^{\mathsf{H}}\mathbf{T}\mathrm{R}_{\mathbf{J}}(-\frac{2}{\zeta}\beta\mathbf{T}\mathbf{Q}^{\star})(\mathbf{x}-\mathbf{v}) + u_{\mathrm{v}}(\mathbf{v}), \tag{A.77}$$

and the normalization factor is given by $\mathcal{Z}^{\mathsf{R}}(\beta|\mathbf{x}) \coloneqq \mathcal{Z}^{\mathsf{R}}(\beta, 0|\mathbf{x})$ with

$$\mathcal{Z}^{\mathsf{R}}(\beta, h|\mathbf{x}) \coloneqq \sum_{\mathbf{v}\in\mathbb{X}^t} \exp\left\{-\beta\mathcal{E}^{\mathsf{R}}(\mathbf{v}|\mathbf{x}) + h\psi_{\mathrm{v}}(\mathbf{v}|\mathbf{x})\right\}. \tag{A.78}$$

Substituting into (A.70), the modified free energy reads

$$\bar{\mathcal{F}}(\beta, h) = \frac{\zeta\alpha\sigma^2}{2\lambda} + \lim_{t\downarrow 0}\frac{1}{\beta t}E_{\mathcal{Z}}(\mathbf{Q}^{\star}, \mathbf{S}^{\star}) \tag{A.79a}$$

$$= \frac{\zeta\alpha\sigma^2}{2\lambda} + \lim_{t\downarrow 0}\frac{1}{\beta t}\left[\int_0^{\beta}\mathrm{tr}\left\{\mathbf{T}\mathbf{Q}^{\star}\mathrm{R}_{\mathbf{J}}(-\frac{2}{\zeta}\mathbf{T}\mathbf{Q}^{\star}\omega)\right\}\mathrm{d}\omega - \beta\mathrm{tr}\left\{\mathbf{Q}^{\star\mathsf{T}}\mathbf{T}\mathrm{R}_{\mathbf{J}}(-\frac{2}{\zeta}\beta\mathbf{T}\mathbf{Q}^{\star})\right\}\right.$$
$$\left. -\mathbb{E}\left\{(1-\eta)\log\mathcal{Z}^{\mathsf{R}}(\beta|\mathbf{x}) + \eta\log\mathcal{Z}^{\mathsf{R}}(\beta, h|\mathbf{x})\right\}\right] \tag{A.79b}$$

$$= \frac{\zeta\alpha\sigma^2}{2\lambda} + \lim_{t\downarrow 0}\left[\Delta E(\beta, t) + (1-\eta)\mathcal{F}^{\mathsf{R}}(\beta, t) + \eta\mathcal{F}^{\mathsf{R}}(\beta, h, t)\right] \tag{A.79c}$$

where we define

$$\Delta E(\beta, t) \coloneqq \frac{1}{t}\int_0^1 \mathrm{tr}\left\{\mathbf{T}\mathbf{Q}^{\star}\mathrm{R}_{\mathbf{J}}(-\frac{2}{\zeta}\beta\mathbf{T}\mathbf{Q}^{\star}\omega)\right\}\mathrm{d}\omega - \frac{1}{t}\mathrm{tr}\left\{\mathbf{Q}^{\star\mathsf{T}}\mathbf{T}\mathrm{R}_{\mathbf{J}}(-\frac{2}{\zeta}\beta\mathbf{T}\mathbf{Q}^{\star})\right\}, \tag{A.80}$$

and $\mathcal{F}^{\mathsf{R}}(\beta, t) \coloneqq \mathcal{F}^{\mathsf{R}}(\beta, 0, t)$ with

$$\mathcal{F}^{\mathsf{R}}(\beta, h, t) \coloneqq -\frac{1}{\beta t}\mathbb{E}\left\{\log\mathcal{Z}^{\mathsf{R}}(\beta, h|\mathbf{x})\right\}. \tag{A.81}$$

From (A.79c), it is instantly concluded that

$$\bar{\mathcal{F}}(\beta) = \frac{\zeta\alpha\sigma^2}{2\lambda} + \lim_{t\downarrow 0}\left[\Delta E(\beta, t) + \mathcal{F}^{\mathsf{R}}(\beta, t)\right]. \tag{A.82}$$

A.2.1 Derivation of Macroscopic Parameters

From discussions in Chapter 3, we know that all macroscopic parameters are directly derived from the modified free energy function. Following Property 2 in Section 3.2.1, the asymptotic distortion reads

$$D_{\mathsf{RLS}}^{\mathbb{W}} = -\lim_{\beta\uparrow\infty} \beta \frac{\partial}{\partial h} \bar{\mathcal{F}}\left(\beta, h\right)|_{h=0} \tag{A.83}$$

when the modification function is

$$\psi\left(v_w|x_{0w}\right) \coloneqq \frac{N}{|\mathbb{W}|}\, \mathsf{d}\left(v_w; x_{0w}\right) \tag{A.84a}$$

$$= \frac{1}{\eta}\, \mathsf{d}\left(v_w; x_{0w}\right) \tag{A.84b}$$

Substituting (A.79c) into (A.83), we have

$$D_{\mathsf{RLS}}^{\mathbb{W}} = -\lim_{\beta\uparrow\infty} \lim_{t\downarrow 0} \beta\eta \frac{\partial}{\partial h} \mathcal{F}^{\mathsf{R}}\left(\beta, h, t\right)|_{h=0} \tag{A.85a}$$

$$= \lim_{\beta\uparrow\infty} \lim_{t\downarrow 0} \frac{\eta}{t} \mathbb{E}\left\{ \sum_{\mathbf{v}\in\mathbb{X}^t} \frac{\psi_{\mathrm{v}}\left(\mathbf{v}|\mathbf{x}\right) \exp\left\{-\beta \mathcal{E}^{\mathsf{R}}\left(\mathbf{v}|\mathbf{x}\right)\right\}}{\mathcal{Z}^{\mathsf{R}}\left(\beta, 0|\mathbf{x}\right)} \right\} \tag{A.85b}$$

$$= \lim_{\beta\uparrow\infty} \lim_{t\downarrow 0} \mathbb{E}\left\{ \frac{1}{t} \sum_{a=1}^{t} \mathsf{d}\left(\mathrm{v}_a; x_0\right) \right\} \tag{A.85c}$$

$$= \lim_{\beta\uparrow\infty} \lim_{t\downarrow 0} D^{\mathsf{R}}\left(\beta, t\right) \tag{A.85d}$$

where

$$D^{\mathsf{R}}\left(\beta, t\right) = \frac{1}{t} \mathbb{E}\left\{ \sum_{a=1}^{t} \mathsf{d}\left(\mathrm{v}_a, x_0\right) \right\}. \tag{A.86}$$

For asymptotic LSE, we moreover have

$$\mathrm{LSE}_{\mathsf{RLS}} = \frac{2\lambda}{\zeta\alpha} \left[\lim_{\beta\uparrow\infty} \frac{\partial}{\partial\beta} \beta \bar{\mathcal{F}}\left(\beta, 0\right) - \bar{\psi} \right]. \tag{A.87}$$

when the modification function is

$$\psi\left(v_w|x_{0w}\right) = u\left(v_w\right). \tag{A.88}$$

Using the derived term for the free energy, we have

$$\frac{\partial}{\partial\beta}\beta\bar{\mathcal{F}}\left(\beta,0\right) = \frac{\zeta\alpha\sigma^2}{2\lambda} + \frac{\partial}{\partial\beta}\beta\lim_{t\downarrow 0}\left[\Delta E\left(\beta,t\right) + \mathcal{F}^{\mathsf{R}}\left(\beta,t\right)\right] \tag{A.89a}$$

$$= \frac{\zeta\alpha\sigma^2}{2\lambda} + \frac{\partial}{\partial\beta}\left[\beta\Delta E\left(\beta\right) + \beta\mathcal{F}^{\mathsf{R}}\left(\beta\right)\right] \tag{A.89b}$$

where we define

$$\beta\Delta E\left(\beta\right) = \lim_{t\downarrow 0}\Delta E\left(\beta,t\right) \tag{A.90a}$$

$$\mathcal{F}^{\mathsf{R}}\left(\beta\right) = \lim_{t\downarrow 0}\mathcal{F}^{\mathsf{R}}\left(\beta,t\right) \tag{A.90b}$$

$\bar{\psi}$ is furthermore given by

$$\bar{\psi} = -\lim_{\beta\uparrow\infty}\beta\frac{\partial}{\partial h}\bar{\mathcal{F}}\left(\beta,h\right)|_{h=0} \tag{A.91a}$$

$$= \lim_{\beta\uparrow\infty}\lim_{t\downarrow 0}\mathbb{E}\left\{\frac{1}{t}\sum_{a=1}^{t}u\left(\mathrm{v}_a\right)\right\} \tag{A.91b}$$

$$= \lim_{\beta\uparrow\infty}\lim_{t\downarrow 0}\frac{1}{t}\mathbb{E}\left\{u_{\mathrm{v}}(\mathbf{v})\right\}. \tag{A.91c}$$

Hence, the asymptotic LSE reduces to

$$\mathrm{LSE}_{\mathsf{RLS}} = \frac{2\lambda}{\zeta\alpha}\lim_{\beta\uparrow\infty}\left[\frac{\zeta\alpha\sigma^2}{2\lambda} + \frac{\partial}{\partial\beta}\beta\Delta E\left(\beta\right) + \frac{\partial}{\partial\beta}\beta\mathcal{F}^{\mathsf{R}}\left(\beta\right) - \lim_{t\downarrow 0}\frac{1}{t}\mathbb{E}\left\{u_{\mathrm{v}}(\mathbf{v})\right\}\right] \tag{A.92a}$$

$$= \sigma^2 + \frac{2\lambda}{\zeta\alpha}\lim_{\beta\uparrow\infty}\left[\frac{\partial}{\partial\beta}\beta\Delta E\left(\beta\right) + L\left(\beta\right)\right] \tag{A.92b}$$

where

$$L(\beta) \coloneqq \frac{\partial}{\partial \beta} \beta \mathcal{F}^{\mathsf{R}}(\beta) - \lim_{t \downarrow 0} \frac{1}{t} \mathbb{E}\left\{u_{\mathrm{v}}(\mathbf{v})\right\} \tag{A.93}$$

The macroscopic parameters along with the fixed-point equation in (A.75b) conclude Proposition 4.1.

Appendix B

Derivation of the RS Ansatz

RS assumes that the correlation matrix is written as

$$\mathbf{Q} = \frac{\chi}{\beta}\mathbf{I}_t + q\mathbf{1}_t \tag{B.1}$$

for some non-negative real χ and q. Hence, the RS ansatz is derived by substituting this $\mathbf{Q}$ into the generic ansatz given by Proposition 4.1.

B.1 Limiting Free Energy

We start derivations by considering Definition 4.3 and determining the Hamiltonian of the spin glass of replicas for the RS structure. To this end, let us define

$$\mathbf{R} \coloneqq \mathbf{T}\mathrm{R}_{\mathbf{J}}(-\frac{2}{\zeta}\beta\mathbf{T}\mathbf{Q}) \tag{B.2}$$

where $\mathbf{T}$ is given in (4.9). In Appendix F, it is shown that for a generic RSB structure, which also includes RS, $\mathbf{R}$ and $\mathbf{Q}$ have same structures. Hence, one can write

$$\mathbf{R} = e\ \mathbf{I}_t - \frac{\beta\zeta f^2}{2}\ \mathbf{1}_t, \tag{B.3}$$

for some real f and e which are functions of χ and q. The investigations in Appendix F show that all RSB structures span a same eigensubspace. This implies that the eigendecompositions of $\mathbf{Q}$, $\mathbf{T}$ and $\mathbf{R}$ read[1]

$$\mathbf{Q} = \mathbf{V}\mathbf{D}^{\mathrm{Q}}\mathbf{V}^{\mathsf{T}} \tag{B.4a}$$

$$\mathbf{T} = \mathbf{V}\mathbf{D}^{\mathrm{T}}\mathbf{V}^{\mathsf{T}} \tag{B.4b}$$

$$\mathbf{R} = \mathbf{V}\mathbf{D}^{\mathrm{R}}\mathbf{V}^{\mathsf{T}} \tag{B.4c}$$

for a common $\mathbf{V} \in \mathbb{R}^{t\times t}$, where $\mathbf{D}^{\mathrm{Q}}$, $\mathbf{D}^{\mathrm{T}}$ and $\mathbf{D}^{\mathrm{R}}$ are the diagonal matrices of eigenvalues. Substituting in (B.2), we have

$$\mathbf{D}^{\mathrm{R}} = \mathbf{D}^{\mathrm{T}}\mathrm{R}_{\mathbf{J}}(-\frac{2}{\zeta}\beta\mathbf{D}^{\mathrm{T}}\mathbf{D}^{\mathrm{Q}}) \tag{B.5}$$

which equivalently states that for $a \in [t]$

$$\lambda_a^{\mathbf{R}} = \lambda_a^{\mathbf{T}}\mathrm{R}_{\mathbf{J}}(-\frac{2}{\zeta}\beta\lambda_a^{\mathbf{T}}\lambda_a^{\mathbf{Q}}) \tag{B.6}$$

with $\lambda_a^{\mathbf{R}}$, $\lambda_a^{\mathbf{Q}}$ and $\lambda_a^{\mathbf{T}}$ being the eigenvalues of $\mathbf{R}$, $\mathbf{Q}$ and $\mathbf{T}$ which correspond to the ath column of $\mathbf{V}$. The matrices $\mathbf{Q}$, $\mathbf{R}$ and $\mathbf{R}$ have two different eigenvalues, namely

$$\lambda_1^{\mathbf{Q}} = \frac{\chi}{\beta} + tq \tag{B.7a}$$

$$\lambda_1^{\mathbf{T}} = \frac{\zeta}{2\left(\lambda + t\beta\sigma^2\right)} \tag{B.7b}$$

$$\lambda_1^{\mathbf{R}} = e - t\beta\frac{\zeta f^2}{2} \tag{B.7c}$$

which occur with multiplicity 1, and

$$\lambda_2^{\mathbf{Q}} = \frac{\chi}{\beta} \tag{B.8a}$$

[1]Note that $\mathbf{Q}$, $\mathbf{T}$ and $\mathbf{R}$ are real-valued full-rank and symmetric matrices.

$$\lambda_2^{\mathbf{T}} = \frac{\zeta}{2\lambda} \tag{B.8b}$$

$$\lambda_2^{\mathbf{R}} = e \tag{B.8c}$$

which occur with multiplicity $t-1$. Substituting in (B.6) and taking the limit when $t \downarrow 0$, e and f are found as

$$e = \frac{\zeta}{2\lambda} \mathrm{R}_{\mathbf{J}}(-\frac{\chi}{\lambda}), \tag{B.9a}$$

$$f^2 = \frac{1}{\lambda^2} \frac{\partial}{\partial \chi} \left\{ \left[\chi\sigma^2 - q\lambda \right] \mathrm{R}_{\mathbf{J}}(-\frac{\chi}{\lambda}) \right\}. \tag{B.9b}$$

To pursue derivations, we rewrite the Hamiltonian using (B.3)

$$\mathcal{E}^{\mathsf{R}}(\mathbf{v}|\mathbf{x}) = e \left\| \mathbf{x} - \mathbf{v} \right\|^2 - \beta \frac{\zeta f^2}{2} \mathrm{tr} \left\{ (\mathbf{x} - \mathbf{v}) (\mathbf{x} - \mathbf{v})^{\mathsf{H}} \mathbf{1}_t \right\} + u_{\mathrm{v}}(\mathbf{v}) \tag{B.10a}$$

$$= e \left\| \mathbf{x} - \mathbf{v} \right\|^2 - \beta \frac{\zeta f^2}{2} \left\| \mathbf{1}_{1\times t} (\mathbf{x} - \mathbf{v}) \right\|^2 + u_{\mathrm{v}}(\mathbf{v}) \tag{B.10b}$$

Thus, the partition function $\mathcal{Z}^{\mathsf{R}}(\beta|\mathbf{x})$ is given by

$$\mathcal{Z}^{\mathsf{R}}(\beta|\mathbf{x}) = \sum_{\mathbf{v}\in\mathbb{X}^t} \exp \left\{ -\beta e \left\| \mathbf{x} - \mathbf{v} \right\|^2 + \beta^2 \frac{\zeta f^2}{2} \left\| \mathbf{1}_{1\times t} (\mathbf{x} - \mathbf{v}) \right\|^2 - \beta u_{\mathrm{v}}(\mathbf{v}) \right\}. \tag{B.11}$$

Using the Gaussian integral, we have[2]

$$\exp \left\{ \beta^2 \frac{\zeta f^2}{2} \left| \mathbf{1}_{1\times t} (\mathbf{x} - \mathbf{v}) \right|^2 \right\} = \int \exp \left\{ -\beta \zeta f \sum_{a=1}^{t} \mathbb{R}\mathrm{e} \left\{ (\mathrm{x}_a - \mathrm{v}_a) z^* \right\} \right\} \mathrm{D}^{\zeta} z \tag{B.12}$$

which concludes that the partition function reads

$$\mathcal{Z}^{\mathsf{R}}(\beta|\mathbf{x}) = \int \left[\sum_{v\in\mathbb{X}} \exp \left\{ -\beta \mathcal{E}^{\mathrm{RS}}(v|z, x_0) \right\} \right]^t \mathrm{D}^{\zeta} z \tag{B.13}$$

[2]It is worth to recall that $\mathrm{D}^{\zeta} z = \phi^{\zeta}(z)\, \mathrm{d}z$ where $\phi^{\zeta}(z)$ denotes the density function of $\mathcal{N}^{\zeta}(0, 1)$.

where we use the fact that $\mathrm{x}_a = x_0$ for $a \in [t]$ and define

$$\mathcal{E}^{\mathrm{RS}}(v|z, x_0) = e\,|x_0 - v|^2 + \zeta f\,\mathbb{Re}\left\{(x_0 - v)\,z^*\right\} + u(v)\,. \tag{B.14}$$

The parameters of the spin glass of replicas are then determined using the partition function. Starting with the free energy, we have

$$\mathcal{F}^{\mathsf{R}}(\beta, t) = -\frac{1}{\beta t}\,\mathbb{E}\left\{\log \mathcal{Z}^{\mathsf{R}}(\beta|\mathbf{x})\right\} \tag{B.15}$$

$$= -\frac{1}{\beta t}\,\mathbb{E}\left\{\log \int \left[\sum_{v\in\mathbb{X}} \exp\left\{-\beta \mathcal{E}^{\mathrm{RS}}(v|z, x_0)\right\}\right]^t \mathrm{D}^{\zeta} z\right\}. \tag{B.16}$$

Noting that $\int \mathrm{D}^{\zeta} z$ takes expectation over a Gaussian distribution, one can use the Riesz equality, in Lemma 3.2, and conclude that when t varies in a vicinity of 0

$$\mathcal{F}^{\mathsf{R}}(\beta, t) = -\frac{1}{\beta}\mathbb{E}\left\{\int \log \sum_{v\in\mathbb{X}} \exp\left\{-\beta \mathcal{E}^{\mathrm{RS}}(v|z, x_0)\right\} \mathrm{D}^{\zeta} z\right\} + \epsilon_t \tag{B.17}$$

where ϵ_t tends to 0 as $t \downarrow 0$ and the expectation is taken over $x_0 \sim \mathrm{p}_0(x_0)$. By taking the limit $t \downarrow 0$, the free energy function reads

$$\mathcal{F}^{\mathsf{R}}(\beta) \coloneqq \lim_{t\downarrow 0} \mathcal{F}^{\mathsf{R}}(\beta, t) \tag{B.18a}$$

$$= -\frac{1}{\beta}\mathbb{E}\left\{\int \log \sum_{v\in\mathbb{X}} \exp\left\{-\beta \mathcal{E}^{\mathrm{RS}}(v|z, x_0)\right\} \mathrm{D}^{\zeta} z\right\} \tag{B.18b}$$

B.2 Fixed-point Equations

As the next step, we intend to derive RS fixed-point equations which specify χ and q. By determining the conditional distribution $\mathrm{p}^{\mathsf{R}}_{\beta}(\mathbf{v}|\mathbf{x})$ and substituting into the generic fixed-point equation in (4.10), the following fixed point equations are determined

$$\left(\frac{\chi}{\beta} + q\right) t = \mathbb{E}\left\{\sum_{\mathbf{v}\in\mathbb{X}^t} \|\mathbf{x} - \mathbf{v}\|^2\ \ \mathrm{p}^{\mathsf{R}}_{\beta}(\mathbf{v}|\mathbf{x})\right\}, \tag{B.19a}$$

$$\left(\frac{\chi}{\beta}+tq\right)t=\mathbb{E}\left\{\sum_{\mathbf{v}\in\mathbb{X}^t}\mathrm{tr}\left\{(\mathbf{x}-\mathbf{v})\,(\mathbf{x}-\mathbf{v})^{\mathsf{H}}\,\mathbf{1}_m\right\}\;\mathrm{p}_\beta^{\mathsf{R}}\left(\mathbf{v}|\mathbf{x}\right)\right\}. \tag{B.19b}$$

where (B.19a) and (B.19b) are found by taking the trace and sum over all entries of the both sides of (4.10), respectively. One can directly evaluate the right hand sides of (B.19a) and (B.19b); however, considering (B.11), it is straightforward to show that

$$\mathbb{E}\left\{\sum_{\mathbf{v}\in\mathbb{X}^t}\left\|\mathbf{x}-\mathbf{v}\right\|^2\mathrm{p}_\beta^{\mathsf{R}}\left(\mathbf{v}|\mathbf{x}\right)\right\}=t\frac{\partial}{\partial e}\mathcal{F}^{\mathsf{R}}\left(\beta,t\right), \tag{B.20a}$$

$$\mathbb{E}\left\{\sum_{\mathbf{v}\in\mathbb{X}^t}\mathrm{tr}\left\{(\mathbf{x}-\mathbf{v})(\mathbf{x}-\mathbf{v})^{\mathsf{T}}\mathbf{1}_m\right\}\mathrm{p}_\beta^{\mathsf{R}}\left(\mathbf{v}|\mathbf{x}\right)\right\}=-\frac{t}{\beta\zeta f}\frac{\partial}{\partial f}\mathcal{F}^{\mathsf{R}}\left(\beta,t\right). \tag{B.20b}$$

Hence, by substituting the free energy function in (B.17) into the fixed-point equations, we have

$$\frac{\chi}{\beta}+q=\frac{\partial}{\partial e}\mathcal{F}^{\mathsf{R}}\left(\beta,t\right) \tag{B.21a}$$

$$=\mathbb{E}\left\{\int\sum_{v\in\mathbb{X}}\frac{\left|v-x_0\right|^2\exp\left\{-\beta\mathcal{E}^{\mathrm{RS}}\left(v|z,x_0\right)\right\}}{\sum\limits_{v\in\mathbb{X}}\exp\left\{-\beta\mathcal{E}^{\mathrm{RS}}\left(v|z,x_0\right)\right\}}\,\mathrm{D}^{\zeta}z\right\} \tag{B.21b}$$

$$\frac{\chi}{\beta}+tq=-\frac{1}{\beta\zeta f}\frac{\partial}{\partial f}\mathcal{F}^{\mathsf{R}}\left(\beta,t\right) \tag{B.21c}$$

$$=\frac{1}{\beta f}\mathbb{E}\left\{\int\sum_{v\in\mathbb{X}}\frac{\mathbb{R}\mathrm{e}\left\{\left(v-x_0\right)z^*\right\}\exp\left\{-\beta\mathcal{E}^{\mathrm{RS}}\left(v|z,x_0\right)\right\}}{\sum\limits_{v\in\mathbb{X}}\exp\left\{-\beta\mathcal{E}^{\mathrm{RS}}\left(v|z,x_0\right)\right\}}\,\mathrm{D}^{\zeta}z\right\}. \tag{B.21d}$$

By taking the limit $t\downarrow 0$, the fixed-point equations finally read

$$\frac{\chi}{\beta}+q=\mathbb{E}\left\{\int\sum_{v\in\mathbb{X}}\frac{\left|v-x_0\right|^2\exp\left\{-\beta\mathcal{E}^{\mathrm{RS}}\left(v|z,x_0\right)\right\}}{\sum\limits_{v\in\mathbb{X}}\exp\left\{-\beta\mathcal{E}^{\mathrm{RS}}\left(v|z,x_0\right)\right\}}\,\mathrm{D}^{\zeta}z\right\} \tag{B.22a}$$

$$\chi = \frac{1}{f}\mathbb{E}\left\{\int \sum_{v\in\mathbb{X}} \frac{\mathbb{R}\mathrm{e}\left\{(v-x_0)\,z^*\right\}\exp\left\{-\beta\mathcal{E}^{\mathrm{RS}}\left(v|z,x_0\right)\right\}}{\sum\limits_{v\in\mathbb{X}}\exp\left\{-\beta\mathcal{E}^{\mathrm{RS}}\left(v|z,x_0\right)\right\}}\,\mathrm{D}^{\zeta}z\right\} \tag{B.22b}$$

with f and e defined in (B.9a) and (B.9b).

B.2.1 Zero-temperature Limit

The fixed-point equations should be solved in zero temperature where the asymptotics of RLS is characterized. Therefore, we take the limit of $\beta\uparrow\infty$. For this purpose, we note that density measure

$$\mathrm{p}_{\beta}^{\mathrm{RS}}\left(v|z,x_0\right) = \frac{\exp\left\{-\beta\mathcal{E}^{\mathrm{RS}}\left(v|z,x_0\right)\right\}}{\sum\limits_{v\in\mathbb{X}}\exp\left\{-\beta\mathcal{E}^{\mathrm{RS}}\left(v|z,x_0\right)\right\}} \tag{B.23}$$

satisfies the large deviations property. Hence, using Lemma 3.1, we can write

$$q = \mathbb{E}\left\{\int \left|v^{\star}\left(z,x_0\right)-x_0\right|^2\mathrm{D}^{\zeta}z\right\} \tag{B.24a}$$

$$\chi = \frac{1}{f}\mathbb{E}\left\{\int \mathbb{R}\mathrm{e}\left\{\left(v^{\star}\left(z,x_0\right)-x_0\right)z^*\right\}\mathrm{D}^{\zeta}z\right\} \tag{B.24b}$$

where

$$v^{\star}\left(z,x_0\right) \coloneqq \underset{v\in\mathbb{X}}{\operatorname{argmin}}\ \mathcal{E}^{\mathrm{RS}}\left(v|z,x_0\right) \tag{B.25a}$$

$$= \underset{v\in\mathbb{X}}{\operatorname{argmin}}\ e\left|x_0+\frac{\zeta f}{2e}\,z-v\right|^2+u\left(v\right) \tag{B.25b}$$

$$= \underset{v\in\mathbb{X}}{\operatorname{argmin}}\ \frac{\zeta}{2\tau}\left|x_0+\theta_0\,z-v\right|^2+u\left(v\right) \tag{B.25c}$$

with τ and θ_0 being

$$\tau = \frac{\zeta}{2e} = \left[\mathrm{R}_{\mathbf{J}}(-\frac{\chi}{\lambda})\right]^{-1}\lambda, \tag{B.26a}$$

$$\theta_0^2 = \left(\frac{\zeta f}{2e}\right)^2 = \left[\mathrm{R}_{\mathbf{J}}(-\frac{\chi}{\lambda})\right]^{-2} \frac{\partial}{\partial \chi}\left[\left(\sigma^2\chi - \lambda q\right)\mathrm{R}_{\mathbf{J}}(-\frac{\chi}{\lambda})\right]. \tag{B.26b}$$

B.3 Macroscopic Parameters

We now derive the macroscopic parameters of the corresponding spin glass under RS which characterize the asymptotic performance of RLS.

B.3.1 Asymptotic Distortion

To determine the asymptotic distortion, we start by deriving the average distortion of replicas, i.e.

$$D^{\mathsf{R}}(\beta, t) = \frac{1}{t}\mathbb{E}\left\{\sum_{a=1}^{t} \mathsf{d}\left(\mathrm{v}_a, x\right)\right\}. \tag{B.27}$$

The expectation in (B.27) is calculated by invoking the averaging trick which modifies the Hamiltonian as

$$\mathcal{E}^{\mathsf{R}}(\mathbf{v}, h|\mathbf{x}) \coloneqq \mathcal{E}^{\mathsf{R}}(\mathbf{v}|\mathbf{x}) - \frac{h}{\beta}\sum_{a=1}^{t} \mathsf{d}\left(\mathrm{v}_a; x_0\right). \tag{B.28}$$

In this case, the modified free energy $\mathcal{F}^{\mathsf{R}}(\beta, h)$, in the limit of $t \downarrow 0$, reads[3]

$$\mathcal{F}^{\mathsf{R}}(\beta, h) = -\frac{1}{\beta}\mathbb{E}\left\{\int \log \sum_{v\in\mathbb{X}} \exp\left\{-\beta\mathcal{E}^{\mathrm{RS}}(v|x_0) + h\ \mathsf{d}\left(v; x_0\right)\right\}\mathrm{D}^{\zeta}z\right\}. \tag{B.29}$$

Consequently, the limiting average distortion of replicas is given by

$$\lim_{t\downarrow 0} D^{\mathsf{R}}(\beta, t) = -\beta\frac{\partial}{\partial h}\mathcal{F}^{\mathsf{R}}(\beta, h)\,|_{h=0} \tag{B.30a}$$

[3]Note that in this case, the free energy is directly derived from (B.17) by considering $u_{\mathrm{new}}(v) = u(v) - h/\beta\mathsf{d}\left(v; x_0\right)$ as the penalty function.

$$= \mathbb{E}\left\{ \int \sum_{v\in\mathbb{X}} \frac{\mathsf{d}\left(v;x_0\right)\exp\left\{-\beta\mathcal{E}^{\mathrm{RS}}\left(v|x_0\right)\right\}}{\sum\limits_{v\in\mathbb{X}}\exp\left\{-\beta\mathcal{E}^{\mathrm{RS}}\left(v|x_0\right)\right\}}\mathrm{D}^{\zeta}z \right\}. \tag{B.30b}$$

Finally, the asymptotic distortion is given by

$$D^{\mathbb{W}}_{\mathsf{RLS}} = \lim_{\beta\uparrow\infty}\lim_{t\downarrow 0} D^{\mathsf{R}}\left(\beta,t\right) \tag{B.31a}$$

$$= \mathbb{E}\left\{ \int \mathsf{d}\left(v^{\star}\left(z,x_0\right);x_0\right)\mathrm{D}^{\zeta}z \right\} \tag{B.31b}$$

with $v^{\star}\left(z,x_0\right)$ being defined in (B.25c).

B.3.2 Energy Difference

To derive the energy difference function, i.e. $\Delta E\left(\beta\right)$, we start with (4.19). Hence,

$$\Delta E\left(\beta\right) \coloneqq \lim_{t\downarrow 0}\frac{1}{t}\left[\int_0^1 \mathrm{tr}\left\{\mathbf{TQ}\mathrm{R}_{\mathbf{J}}(-\frac{2}{\zeta}\beta\omega\mathbf{TQ})\right\}\,\mathrm{d}\omega - \mathrm{tr}\left\{\mathbf{Q}^{\mathsf{T}}\mathbf{R}\right\}\right] \tag{B.32a}$$

$$= \frac{\zeta}{2\lambda}\int_0^1 T\left(\beta,\omega\right)\mathrm{d}\omega - \frac{\chi}{\beta}e - qe + \frac{\zeta\chi}{2}f^2 \tag{B.32b}$$

$$\overset{\star}{=} \frac{\zeta}{2\lambda}\left[\int_0^1 T\left(\beta,\omega\right)\mathrm{d}\omega - T_0\left(\beta\right)\right] \tag{B.32c}$$

where we define

$$T\left(\beta,\omega\right) \coloneqq \frac{\chi}{\beta}\mathrm{R}_{\mathbf{J}}(-\frac{\chi}{\lambda}\omega) + \left(q - \frac{\chi}{\lambda}\sigma^2\right)\frac{\partial}{\partial\omega}\omega\mathrm{R}_{\mathbf{J}}(-\frac{\chi}{\lambda}\omega) \tag{B.33a}$$

$$T_0\left(\beta\right) \coloneqq \left[\frac{\chi}{\beta}+q\right]\mathrm{R}_{\mathbf{J}}(-\frac{\chi}{\lambda}) + \frac{\chi}{\lambda}\frac{\partial}{\partial\chi}\left(q\lambda-\chi\sigma^2\right)\mathrm{R}_{\mathbf{J}}(-\frac{\chi}{\lambda}), \tag{B.33b}$$

and $\star$ follows the identities in (B.9a) and (B.9b).

B.3.3 Asymptotic LSE

The asymptotic LSE is given by (4.21) in Proposition 4.1 as

$$\mathrm{LSE}_{\mathsf{RLS}} = \sigma^2 + \frac{2\lambda}{\zeta\alpha} \lim_{\beta\uparrow\infty} \left[L\left(\beta\right) + \frac{\partial}{\partial\beta}\beta\Delta E\left(\beta\right) \right]. \tag{B.34}$$

We thus need to determine function $L\left(\beta\right)$. To this end, we start from definition in (4.22) which states that

$$L\left(\beta\right) = \frac{\partial}{\partial\beta}\beta\mathcal{F}^{\mathsf{R}}\left(\beta\right) - \lim_{t\downarrow 0}\frac{1}{t}\mathbb{E}\left\{u_{\mathrm{v}}(\mathbf{v})\right\}. \tag{B.35}$$

Noting that

$$\lim_{t\downarrow 0}\frac{1}{t}\mathbb{E}\left\{u_{\mathrm{v}}(\mathbf{v})\right\} = -\beta\frac{\partial}{\partial h}\mathcal{F}^{\mathsf{R}}\left(\beta,h\right)|_{h=0} \tag{B.36}$$

when $\mathsf{d}\left(v;x_0\right) = u\left(v\right)$, we have

$$L\left(\beta\right) = \frac{\partial}{\partial\beta}\beta\mathcal{F}^{\mathsf{R}}\left(\beta\right) + \beta\frac{\partial}{\partial h}\mathcal{F}^{\mathsf{R}}\left(\beta,h\right)|_{h=0} \tag{B.37a}$$

$$= e\,\mathbb{E}\left\{\int \sum_{v\in\mathbb{X}} \frac{\left|x_0 - v\right|^2 \exp\left\{-\beta\mathcal{E}^{\mathrm{RS}}\left(v|z,x_0\right)\right\}}{\sum\limits_{v\in\mathbb{X}}\exp\left\{-\beta\mathcal{E}^{\mathrm{RS}}\left(v|z,x_0\right)\right\}}\mathrm{D}^{\zeta}z\right\}$$

$$+\,\zeta f\,\mathbb{E}\left\{\int \sum_{v\in\mathbb{X}} \frac{\mathbb{R}\mathrm{e}\left\{\left(x_0 - v\right)z^*\right\}\exp\left\{-\beta\mathcal{E}^{\mathrm{RS}}\left(v|z,x_0\right)\right\}}{\sum\limits_{v\in\mathbb{X}}\exp\left\{-\beta\mathcal{E}^{\mathrm{RS}}\left(v|z,x_0\right)\right\}}\mathrm{D}^{\zeta}z\right\} \tag{B.37b}$$

$$\overset{\star}{=} e\left[\frac{\chi}{\beta} + q\right] - \zeta f^2\chi \tag{B.37c}$$

$$\overset{\dagger}{=} \frac{\zeta}{2\lambda}\left[T_0\left(\beta\right) + \frac{\chi}{\lambda}\frac{\partial}{\partial\chi}\left(q\lambda - \chi\sigma^2\right)\mathrm{R}_{\mathbf{J}}(-\frac{\chi}{\lambda})\right] \tag{B.37d}$$

where $\star$ follows (B.22a) and (B.22b), $\dagger$ is concluded from (B.9a) and (B.9b). Substituting into (4.21), we finally conclude that

$$\mathrm{LSE}_{\mathsf{RLS}} = \sigma^2 + \frac{2\lambda}{\zeta\alpha} \lim_{\beta\uparrow\infty} \left[L(\beta) + \frac{\partial}{\partial\beta} \beta \Delta E(\beta) \right] \tag{B.38a}$$

$$= \sigma^2 + \frac{1}{\alpha} \lim_{\beta\uparrow\infty} \left[\frac{\chi}{\beta} \mathrm{R}_{\mathbf{J}}(-\frac{\chi}{\lambda}\omega) + G(\chi) + \chi G'(\chi) \right] \tag{B.38b}$$

$$= \sigma^2 + \alpha^{-1} R'_{\mathrm{LSE}}(\chi) \tag{B.38c}$$

where we define function $G(\cdot)$ as

$$G(\chi) \coloneqq \left[q - \frac{\chi}{\lambda}\sigma^2 \right] \mathrm{R}_{\mathbf{J}}(-\frac{\chi}{\lambda}), \tag{B.39}$$

and $R_{\mathrm{LSE}}(\cdot)$ as

$$R_{\mathrm{LSE}}(\chi) \coloneqq \chi G(\chi). \tag{B.40}$$

B.3.4 Zero-temperature Free Energy

The free energy of the corresponding spin glass at inverse temperature β is given in terms of the energy difference function and $\mathcal{F}^{\mathsf{R}}(\beta)$ as

$$\bar{\mathcal{F}}(\beta) = \frac{\zeta\alpha\sigma^2}{2\lambda} + \Delta E(\beta) + \mathcal{F}^{\mathsf{R}}(\beta) \tag{B.41a}$$

$$= \frac{\zeta}{2\lambda} \left[\alpha\sigma^2 + \int_0^1 T(\beta,\omega)\,\mathrm{d}\omega - T_0(\beta) \right] + \mathcal{F}^{\mathsf{R}}(\beta). \tag{B.41b}$$

Using Lemma 3.1, we can write

$$\lim_{\beta\uparrow\infty} \mathcal{F}^{\mathsf{R}}(\beta) = \mathbb{E}\left\{ \int \mathcal{E}^{\mathrm{RS}}(v^\star(z,x_0)\,|z,x_0)\,\mathrm{D}^\zeta z \right\} \tag{B.42a}$$

$$= \frac{\zeta}{2\tau} \left[\mathbb{E}\left\{ \int |x_0 + \theta_0\, z - v^\star(z,x_0)|^2 + u(v^\star(z,x_0))\,\mathrm{D}^\zeta z \right\} - \theta_0^2 \right] \tag{B.42b}$$

Moreover, we have

$$\lim_{\beta\uparrow\infty}\left[\int_0^1 T\left(\beta,\omega\right)\mathrm{d}\omega - T_0\left(\beta\right)\right] = G\left(\chi\right) - \chi G'\left(\chi\right) - q\mathrm{R}_{\mathbf{J}}(-\frac{\chi}{\lambda}). \tag{B.43}$$

Therefore, the free energy of the corresponding spin glass at zero temperature under RS reads

$$\bar{\mathcal{F}}_{\mathrm{RS}}^{0} = \Delta\mathcal{F}_{\mathrm{RS}} + \frac{\zeta}{2\tau}\left[\mathbb{E}\left\{\int \left|x_0 + \theta_0\, z - v^{\star}\left(z, x_0\right)\right|^2 + u\left(v^{\star}\left(z, x_0\right)\right)\mathrm{D}^{\zeta}z\right\} - \theta_0^2\right] \tag{B.44}$$

with $\Delta\mathcal{F}_{\mathrm{RS}}$ being

$$\Delta\mathcal{F}_{\mathrm{RS}} \coloneqq \frac{\zeta}{2\lambda}\left[\alpha\sigma^2 + G\left(\chi\right) - \chi G'\left(\chi\right) - q\mathrm{R}_{\mathbf{J}}(-\frac{\chi}{\lambda})\right]. \tag{B.45}$$

This concludes Proposition 4.2.

Appendix C

Derivation of the One-RSB Ansatz

With a single step of RSB, the replica correlation matrix is of the form

$$\mathbf{Q} = \frac{\chi}{\beta}\,\mathbf{I}_t + p\,\mathbf{I}_{\frac{t\beta}{\mu}} \otimes \mathbf{1}_{\frac{\mu}{\beta}} + q\,\mathbf{1}_t, \tag{C.1}$$

for some non-negative real χ, p, q, and μ. In the sequel, we derive the one-RSB ansatz by considering this structure in the general replica ansatz.

C.1 Limiting Free Energy

We start the analysis by determining the Hamiltonian of the spin glass of replicas. Our analysis takes same steps as in Appendix B. To this end, we first define

$$\mathbf{R} \coloneqq \mathbf{T}\mathrm{R}_{\mathbf{J}}(-\frac{2}{\zeta}\beta\mathbf{T}\mathbf{Q}) \tag{C.2}$$

Following the discussion in Appendix F, we can conclude that $\mathbf{R}$ is of the form

$$\mathbf{R} = e\mathbf{I}_t - \beta\,\frac{\zeta g^2}{2}\,\mathbf{I}_{\frac{t\beta}{\mu}} \otimes \mathbf{1}_{\frac{\mu}{\beta}} - \beta\,\frac{\zeta f^2}{2}\,\mathbf{1}_t \tag{C.3}$$

for some real e, g and f. Noting that

$$\mathbf{Q} = \mathbf{V}\mathbf{D}^{\mathrm{Q}}\mathbf{V}^{\mathsf{T}} \tag{C.4a}$$

$$\mathbf{T} = \mathbf{V}\mathbf{D}^{\mathrm{T}}\mathbf{V}^{\mathsf{T}} \tag{C.4b}$$

$$\mathbf{R} = \mathbf{V}\mathbf{D}^{\mathrm{R}}\mathbf{V}^{\mathsf{T}} \tag{C.4c}$$

for the diagonal matrices $\mathbf{D}^{\mathrm{Q}}$, $\mathbf{D}^{\mathrm{T}}$ and $\mathbf{D}^{\mathrm{R}}$, the scalars e, g and f can be found in terms of χ, p and q using (C.2).

Considering the one-RSB structure, there are three different sets of corresponding eigenvalues for $\mathbf{Q}$, $\mathbf{T}$ and $\mathbf{R}$, namely

$$\lambda_1^{\mathbf{Q}} = \frac{\chi + \mu p}{\beta} + tq \tag{C.5a}$$

$$\lambda_1^{\mathbf{T}} = \frac{\zeta}{2\left(\lambda + t\beta\sigma^2\right)} \tag{C.5b}$$

$$\lambda_1^{\mathbf{R}} = e - \mu\frac{\zeta g^2}{2} - t\beta\frac{\zeta f^2}{2} \tag{C.5c}$$

with multiplicity 1,

$$\lambda_2^{\mathbf{Q}} = \frac{\chi + \mu p}{\beta} \tag{C.6a}$$

$$\lambda_2^{\mathbf{T}} = \frac{\zeta}{2\lambda} \tag{C.6b}$$

$$\lambda_2^{\mathbf{R}} = e - \mu\frac{\zeta g^2}{2} \tag{C.6c}$$

with multiplicity $t\beta/\mu - 1$, and

$$\lambda_3^{\mathbf{Q}} = \frac{\chi}{\beta} \tag{C.7a}$$

$$\lambda_3^{\mathbf{T}} = \frac{\zeta}{2\lambda} \tag{C.7b}$$

$$\lambda_3^{\mathbf{R}} = e \tag{C.7c}$$

with multiplicity $t - t\beta/\mu$. By substituting into (C.2) and taking the limit $t \downarrow 0$, e, g and f are given as

$$e = \frac{\zeta}{2\lambda} \mathrm{R}_{\mathbf{J}}(-\frac{\chi}{\lambda}), \tag{C.8a}$$

$$g^2 = \frac{1}{\lambda\mu} \left[\mathrm{R}_{\mathbf{J}}(-\frac{\chi}{\lambda}) - \mathrm{R}_{\mathbf{J}}(-\frac{\tilde{\chi}}{\lambda}) \right], \tag{C.8b}$$

$$f^2 = \frac{1}{\lambda^2} \frac{\partial}{\partial \tilde{\chi}} \left\{ \left[\tilde{\chi}\sigma^2 - \lambda q \right] \mathrm{R}_{\mathbf{J}}(-\frac{\tilde{\chi}}{\lambda}) \right\}, \tag{C.8c}$$

where we define $\tilde{\chi} \coloneqq \chi + \mu p$, for sake of compactness.

The Hamiltonian of the spin glass of replicas is derived by substituting (C.3) into Definition 4.3. This concludes

$$\mathcal{E}^{\mathsf{R}}(\mathbf{v}|\mathbf{x}) = e \left\| \mathbf{x} - \mathbf{v} \right\|^2 - \beta \frac{\zeta g^2}{2} \left\langle \mathbf{x} - \mathbf{v} \right\rangle_{\frac{\mu}{\beta}} - \beta \frac{\zeta f^2}{2} \left\langle \mathbf{x} - \mathbf{v} \right\rangle_t + u\left(\mathbf{v}\right) \tag{C.9}$$

where we define the notation

$$\left\langle \mathbf{v} \right\rangle_u \coloneqq \mathrm{tr} \left\{ \mathbf{v}\mathbf{v}^{\mathsf{H}} \mathbf{I}_{\frac{t}{u}} \otimes \mathbf{1}_u \right\} \tag{C.10}$$

for sake of brevity. The partition function is then determined as in (4.12). Substituting into (4.12) and using the equalities

$$\exp\left\{ \beta^2 \frac{\zeta f^2}{2} \left\langle \mathbf{x} - \mathbf{v} \right\rangle_t \right\} = \int \exp\left\{ -\beta\zeta f \sum_{a=1}^{t} \mathbb{R}\mathrm{e}\left\{ \left(x_0 - \mathrm{v}_a \right) z_0^* \right\} \right\} \mathrm{D}^{\zeta} z_0, \tag{C.11a}$$

$$\exp\left\{ \beta^2 \frac{\zeta g^2}{2} \left\langle \mathbf{x} - \mathbf{v} \right\rangle_{\frac{\mu}{\beta}} \right\} = \prod_{k=0}^{\Xi} \int \exp\left\{ -\beta\zeta g \sum_{a=\rho_k+1}^{\rho_{k+1}} \mathbb{R}\mathrm{e}\left\{ \left(x_0 - \mathrm{v}_a \right) z_1^* \right\} \right\} \mathrm{D}^{\zeta} z_1, \tag{C.11b}$$

with $\rho_k \coloneqq k\mu/\beta$ and $\Xi \coloneqq t\beta/\mu$, the partition function is found as

$$\mathcal{Z}^{\mathsf{R}}\left(\beta|\mathbf{x}\right) = \int \left[\int \left[\sum_{v \in \mathbb{X}} \exp\left\{ -\beta \mathcal{E}_1^{\mathrm{RSB}}\left(v|z_0, z_1, x_0\right) \right\} \right]^{\frac{\mu}{\beta}} \mathrm{D}^{\zeta} z_1 \right]^{\frac{t\beta}{\mu}} \mathrm{D}^{\zeta} z_0 \tag{C.12}$$

where we define single-letter Hamiltonian $\mathcal{E}_1^{\mathrm{RSB}}(v|z_0,z_1,x_0)$ as

$$\mathcal{E}_1^{\mathrm{RSB}}(v|z_0,z_1,x_0) \coloneqq e\,|x-v|^2 + \zeta\mathbb{R}\mathrm{e}\left\{(fz_0+gz_1)^*(x-v)\right\} + u(v)\,. \tag{C.13}$$

Consequently, the free energy of the spin glass of replicas reads

$$\mathcal{F}^{\mathsf{R}}(\beta,t) = -\frac{1}{\beta t}\mathbb{E}\left\{\log\int\left[\int\left[\sum_{v\in\mathbb{X}}\exp\left\{-\beta\mathcal{E}_1^{\mathrm{RSB}}(v|z_0,z_1,x_0)\right\}\right]^{\frac{\mu}{\beta}}\mathrm{D}^{\zeta}z_1\right]^{\frac{t\beta}{\mu}}\mathrm{D}^{\zeta}z_0\right\} \tag{C.14}$$

which following Lemma 3.2 as $t\downarrow 0$, reduces to

$$\mathcal{F}^{\mathsf{R}}(\beta) = \lim_{t\downarrow 0}\mathcal{F}^{\mathsf{R}}(\beta,t) \tag{C.15}$$

$$= -\frac{1}{\mu}\mathbb{E}\left\{\int\log\left(\int\left[\sum_{v\in\mathbb{X}}\exp\left\{-\beta\mathcal{E}_1^{\mathrm{RSB}}(v|z_0,z_1,x_0)\right\}\right]^{\frac{\mu}{\beta}}\mathrm{D}^{\zeta}z_1\right)\mathrm{D}^{\zeta}z_0\right\}. \tag{C.16}$$

C.2 Fixed-point Equations

Under one-step of RSB, the generic fixed-point equation in (4.10) reduces to a system of nonlinear equations in terms of χ, q, p and μ. To derive these equations, we sum over different blocks of the matrices on both sides of (4.10). In this case, we have

$$\left[\frac{\chi}{\beta}+q+p\right]t = \mathbb{E}_{\mathbf{x}}\left\{\sum_{\mathbf{v}\in\mathbb{X}^t}\|\mathbf{x}-\mathbf{v}\|^2\,\mathrm{p}_\beta^{\mathsf{R}}(\mathbf{v}|\mathbf{x})\right\}, \tag{C.17a}$$

$$\left[\frac{\chi}{\beta}+\frac{\mu p}{\beta}+\frac{\mu q}{\beta}\right]t = \mathbb{E}_{\mathbf{x}}\left\{\mathbf{x}\sum_{\mathbf{v}\in\mathbb{X}^t}\langle\mathbf{x}-\mathbf{v}\rangle_{\frac{\mu}{\beta}}\,\mathrm{p}_\beta^{\mathsf{R}}(\mathbf{v}|\mathbf{x})\right\}, \tag{C.17b}$$

$$\left[\frac{\chi}{\beta}+\frac{\mu p}{\beta}+tq\right]t = \mathbb{E}_{\mathbf{x}}\left\{\mathbf{x}\sum_{\mathbf{v}\in\mathbb{X}^t}\langle\mathbf{x}-\mathbf{v}\rangle_{t}\,\mathrm{p}_\beta^{\mathsf{R}}(\mathbf{v}|\mathbf{x})\right\}, \tag{C.17c}$$

where (C.17a), (C.17b) and (C.17c) are determined by taking the trace, sum over the diagonal blocks and sum over all the entries on both sides of (4.10), respectively. To evaluate the right hand sides of (C.17a)-(C.17c), we note that

$$\mathbb{E}_{\mathbf{x}}\left\{\sum_{\mathbf{v}\in\mathbb{X}^t}\|\mathbf{x}-\mathbf{v}\|^2\,\mathrm{p}_\beta^{\mathsf{R}}\left(\mathbf{v}|\mathbf{x}\right)\right\}=t\frac{\partial}{\partial e}\mathcal{F}^{\mathsf{R}}\left(\beta,t\right), \tag{C.18a}$$

$$\mathbb{E}_{\mathbf{x}}\left\{\mathbf{x}\sum_{\mathbf{v}\in\mathbb{X}^t}\langle\mathbf{x}-\mathbf{v}\rangle_{\frac{\mu}{\beta}}\,\mathrm{p}_\beta^{\mathsf{R}}\left(\mathbf{v}|\mathbf{x}\right)\right\}=-\frac{t}{\beta\zeta g}\frac{\partial}{\partial g}\mathcal{F}^{\mathsf{R}}\left(\beta,t\right), \tag{C.18b}$$

$$\mathbb{E}_{\mathbf{x}}\left\{\mathbf{x}\sum_{\mathbf{v}\in\mathbb{X}^t}\langle\mathbf{x}-\mathbf{v}\rangle_{t}\,\mathrm{p}_\beta^{\mathsf{R}}\left(\mathbf{v}|\mathbf{x}\right)\right\}=-\frac{t}{\beta\zeta f}\frac{\partial}{\partial f}\mathcal{F}^{\mathsf{R}}\left(\beta,t\right). \tag{C.18c}$$

Hence by substituting into (C.17a)-(C.17c) and taking the limit $t\downarrow 0$, the fixed-point equations read

$$\frac{\chi}{\beta}+q+p=\mathbb{E}\left\{\int\sum_{v\in\mathbb{X}}|v-x_0|^2\,\mathrm{p}_\beta^{\mathrm{RSB}}\left(v|z_0,z_1,x_0\right)\,\bar{\Lambda}_\beta\left(z_0,z_1|x_0\right)\,\mathrm{D}^\zeta z_1\,\mathrm{D}^\zeta z_0\right\} \tag{C.19a}$$

$$\tilde{\chi}+\mu q=\frac{1}{g}\mathbb{E}\left\{\int\sum_{v\in\mathbb{X}}\mathbb{R}\mathrm{e}\left\{\left(v-x_0\right)z_1^*\right\}\mathrm{p}_\beta^{\mathrm{RSB}}\left(v|z_0,z_1,x_0\right)\times\right.$$

$$\left.\bar{\Lambda}_\beta\left(z_0,z_1|x_0\right)\mathrm{D}^\zeta z_1\mathrm{D}^\zeta z_0\right\} \tag{C.19b}$$

$$\tilde{\chi}=\frac{1}{f}\mathbb{E}\left\{\int\sum_{v\in\mathbb{X}}\mathbb{R}\mathrm{e}\left\{\left(v-x_0\right)z_0^*\right\}\mathrm{p}_\beta^{\mathrm{RSB}}\left(v|z_0,z_1,x_0\right)\bar{\Lambda}_\beta\left(z_0,z_1|x_0\right)\mathrm{D}^\zeta z_1\mathrm{D}^\zeta z_0\right\} \tag{C.19c}$$

where g and f are given in (C.8b) and (C.8c), respectively, and we define

$$\mathrm{p}_\beta^{\mathrm{RSB}}\left(v|z_0,z_1,x_0\right)\coloneqq\frac{\exp\left\{-\beta\mathcal{E}_1^{\mathrm{RSB}}\left(v|z_0,z_1,x_0\right)\right\}}{\sum_{v\in\mathbb{X}}\exp\left\{-\beta\mathcal{E}_1^{\mathrm{RSB}}\left(v|z_0,z_1,x_0\right)\right\}} \tag{C.20}$$

and

$$\bar{\Lambda}_\beta\left(z_0, z_1|x_0\right) \coloneqq \frac{\Lambda_\beta\left(z_0, z_1|x_0\right)}{\int \Lambda_\beta\left(z_0, z_1|x_0\right) \mathrm{D}^\zeta z_1} \tag{C.21}$$

with $\Lambda_\beta\left(z_0, z_1|x_0\right)$ being

$$\Lambda_\beta\left(z_0, z_1|x_0\right) \coloneqq \left[\sum_{v\in\mathbb{X}} \exp\left\{-\beta\mathcal{E}_1^{\mathrm{RSB}}\left(v|z_0, z_1, x_0\right)\right\}\right]^{\frac{\mu}{\beta}}. \tag{C.22}$$

The fixed-point equations in (C.19a)-(C.19c), specify χ, p and q for a given μ. Noting that the free energy of the system in minimized at saddle-point, μ is found such that the free energy function is minimized over all realizations of one-RSB structure. We derive this fixed-point equation, later in Section C.3.

C.2.1 Zero-temperature Limit

Lemma 3.1 indicates that as the temperature tends to zero, i.e. $\beta \uparrow \infty$,

$$\sum_{v\in\mathbb{X}} \exp\left\{-\beta\mathcal{E}_1^{\mathrm{RSB}}\left(v|z_0, z_1, x_0\right)\right\} \doteq \exp\left\{-\beta\mathcal{E}_1^{\mathrm{RSB}}\left(v^\star\left(z_0, z_1, x_0\right)|z_0, z_1, x_0\right)\right\} \tag{C.23}$$

where

$$v^\star\left(z_0, z_1, x_0\right) \coloneqq \operatorname*{argmin}_{v\in\mathbb{X}}\ \mathcal{E}_1^{\mathrm{RSB}}\left(v|z_0, z_1, x_0\right) \tag{C.24a}$$

$$= \operatorname*{argmin}_{v\in\mathbb{X}}\ e\left|x_0 + \frac{\zeta f}{2e}\, z_0 + \frac{\zeta g}{2e}\, z_1 - v\right|^2 + u\left(v\right) \tag{C.24b}$$

$$= \operatorname*{argmin}_{v\in\mathbb{X}}\ \frac{\zeta}{2\tau}\left|x_0 + \theta_0\, z_0 + \theta_1\, z_1 - v\right|^2 + u\left(v\right) \tag{C.24c}$$

with τ, θ_0 and θ_1 being

$$\tau = \frac{\zeta}{2e} = \left[\mathrm{R}_{\mathbf{J}}(-\frac{\chi}{\lambda})\right]^{-1}\lambda, \tag{C.25a}$$

$$\theta_0^2 = \left(\frac{\zeta f}{2e}\right)^2 = \left[\mathrm{R}_{\mathbf{J}}(-\frac{\chi}{\lambda})\right]^{-2} \frac{\partial}{\partial \tilde{\chi}} \left[\left[\tilde{\chi}\sigma^2 - \lambda q\right] \mathrm{R}_{\mathbf{J}}(-\frac{\tilde{\chi}}{\lambda})\right], \tag{C.25b}$$

$$\theta_1^2 = \left(\frac{\zeta g}{2e}\right)^2 = \left[\mathrm{R}_{\mathbf{J}}(-\frac{\chi}{\lambda})\right]^{-2} \frac{\lambda}{\mu} \left[\mathrm{R}_{\mathbf{J}}(-\frac{\chi}{\lambda}) - \mathrm{R}_{\mathbf{J}}(-\frac{\tilde{\chi}}{\lambda})\right]. \tag{C.25c}$$

This implies that in the large-system limit $\bar{\Lambda}_\beta\left(z_0, z_1|x_0\right)$ converges to

$$\bar{\Lambda}\left(z_0, z_1|x_0\right) \coloneqq \frac{\Lambda\left(z_0, z_1|x_0\right)}{\int \Lambda\left(z_0, z_1|x_0\right) \mathrm{D}^\zeta z_1}, \tag{C.26}$$

where

$$\Lambda\left(z_0, z_1|x_0\right) \coloneqq \exp\left\{-\mu\, \mathcal{E}_1^{\mathrm{RSB}}\left(v^\star\left(z_0, z_1, x_0\right)|z_0, z_1, x_0\right)\right\}. \tag{C.27}$$

Consequently, the fixed point equations, for a given μ, in the zero-temperature limit read

$$q + p = \mathbb{E}\left\{\int \left|v^\star\left(z_0, z_1, x_0\right) - x_0\right|^2 \bar{\Lambda}\left(z_0, z_1|x_0\right)\, \mathrm{D}^\zeta z_1\, \mathrm{D}^\zeta z_0\right\}, \tag{C.28a}$$

$$\tilde{\chi} + \mu q = \frac{1}{g}\, \mathbb{E}\left\{\int \mathbb{Re}\left\{\left(v^\star\left(z_0, z_1, x_0\right) - x_0\right) z_1^*\right\} \bar{\Lambda}\left(z_0, z_1|x_0\right)\, \mathrm{D}^\zeta z_1 \mathrm{D}^\zeta z_0\right\}, \tag{C.28b}$$

$$\tilde{\chi} = \frac{1}{f}\, \mathbb{E}\left\{\int \mathbb{Re}\left\{\left(v^\star\left(z_0, z_1, x_0\right) - x_0\right) z_0^*\right\} \bar{\Lambda}\left(z_0, z_1|x_0\right)\, \mathrm{D}^\zeta z_1\, \mathrm{D}^\zeta z_0\right\}. \tag{C.28c}$$

C.3 Macroscopic Parameters

We now derive the macroscopic parameters of the corresponding spin glass which characterize the asymptotic performance of the generic RLS method.

C.3.1 Asymptotic Distortion

The asymptotic distortion of RLS is given by the zero-temperature limit of the replicas' average distortion when $t \downarrow 0$. To derive the limit of replicas' average distortion, we use the averaging trick. To this end, we modify the Hamiltonian as

$$\mathcal{E}^{\mathsf{R}}\left(\mathbf{v}, h|\mathbf{x}\right) \coloneqq \mathcal{E}^{\mathsf{R}}\left(\mathbf{v}|\mathbf{x}\right) - \frac{h}{\beta}\sum_{a=1}^{t}\mathsf{d}\left(\mathrm{v}_a; x_0\right). \tag{C.29}$$

The modified free energy in this case is given by replacing $u\left(\cdot\right)$ with $u\left(\cdot\right) - h/\beta\mathsf{d}\left(\cdot; x_0\right)$ in (C.16). In this case, the limiting modified energy reads

$$\begin{aligned}\mathcal{F}^{\mathsf{R}}\left(\beta, h\right) = -\frac{1}{\mu}\mathbb{E}\Bigg\{\int \log\Bigg[\int\Bigg[\sum_{v\in\mathbb{X}}\exp\Big\{-\beta\mathcal{E}_1^{\mathrm{RSB}}\left(v|z_0, z_1, x_0\right) \\ + \ h\mathsf{d}\left(v; x_0\right)\Big\}\Bigg]^{\frac{\mu}{\beta}}\mathrm{D}^{\zeta}z_1\Bigg]\mathrm{D}^{\zeta}z_0\Bigg\}\end{aligned} \tag{C.30}$$

and the limiting average distortion of replicas is derived as

$$\lim_{t\downarrow 0} D^{\mathsf{R}}\left(\beta, t\right) = -\beta\frac{\partial}{\partial h}\mathcal{F}^{\mathsf{R}}\left(\beta, h\right)|_{h=0} \tag{C.31a}$$

$$= \mathbb{E}\left\{\int\sum_{v\in\mathbb{X}}\mathsf{d}\left(v; x_0\right)\mathrm{p}_{\beta}^{\mathrm{RSB}}\left(v|z_0, z_1, x_0\right)\bar{\Lambda}_{\beta}\left(z_0, z_1|x_0\right)\ \mathrm{D}^{\zeta}z_1\ \mathrm{D}^{\zeta}z_0\right\}. \tag{C.31b}$$

By taking the zero-temperature limit,m we can finally conclude that

$$D_{\mathsf{RLS}}^{\mathbb{W}} = \mathbb{E}\left\{\int\mathsf{d}\left(v^{\star}\left(z_0, z_1, x_0\right); x_0\right)\bar{\Lambda}\left(z_0, z_1|x_0\right)\ \mathrm{D}^{\zeta}z_1\ \mathrm{D}^{\zeta}z\right\} \tag{C.32a}$$

with $v^{\star}\left(z_0, z_1, x_0\right)$ being defined in (C.24c).

C.3.2 Energy Difference

Starting from (4.19), the energy difference function reads

$$\Delta E\left(\beta\right) \coloneqq \lim_{t\downarrow 0} \frac{1}{t}\left[\int_0^1 \operatorname{tr}\left\{\mathbf{TQ}\mathrm{R}_{\mathbf{J}}(-\frac{2}{\zeta}\beta\omega\mathbf{TQ})\right\}\,\mathrm{d}\omega - \operatorname{tr}\left\{\mathbf{Q}^{\mathsf{T}}\mathbf{R}\right\}\right] \tag{C.33a}$$

$$= \frac{\zeta}{2\lambda}\left[\int_0^1 T\left(\beta,\omega\right)\mathrm{d}\omega - T_0\left(\beta\right)\right] \tag{C.33b}$$

where we define

$$T\left(\beta,\omega\right) \coloneqq \left[\frac{\chi}{\beta}+p\right]\mathrm{R}_{\mathbf{J}}(-\frac{\chi}{\lambda}\omega) + \left(q-\frac{\tilde{\chi}}{\lambda}\sigma^2\right)\frac{\partial}{\partial\omega}\omega\mathrm{R}_{\mathbf{J}}(-\frac{\tilde{\chi}}{\lambda}\omega) + \frac{\tilde{\chi}}{\mu}\Delta\mathrm{R}\left(\omega\right) \tag{C.34a}$$

$$T_0\left(\beta\right) \coloneqq \left[\frac{\chi}{\beta}+p+q\right]\mathrm{R}_{\mathbf{J}}(-\frac{\chi}{\lambda}) + \left[\frac{\tilde{\chi}}{\mu}+q\right]\Delta\mathrm{R}\left(1\right) + \tilde{\chi}G'\left(\tilde{\chi}\right), \tag{C.34b}$$

with $\Delta\mathrm{R}\left(\cdot\right)$ being

$$\Delta\mathrm{R}\left(\omega\right) = \mathrm{R}_{\mathbf{J}}(-\frac{\tilde{\chi}}{\lambda}\omega) - \mathrm{R}_{\mathbf{J}}(-\frac{\chi}{\lambda}\omega) \tag{C.35}$$

and

$$G\left(\omega\right) \coloneqq \left[q-\frac{\sigma^2}{\lambda}\omega\right]\mathrm{R}_{\mathbf{J}}(-\frac{\omega}{\lambda}). \tag{C.36}$$

Using the energy difference function, we can derive the free energy of the corresponding spin glass.

C.3.3 Breaking Block Size

As indicated earlier, the fixed-point equations are derived for a given block size parameter μ. This parameter is moreover set, such that the specified one-RSB structure minimizes the free energy at the fixed-point equation. We hence need to derive the

free energy of the corresponding spin glass at inverse temperature β, first. To this end, we use Proposition 4.1 and write

$$\bar{\mathcal{F}}\left(\beta\right) = \frac{\zeta\alpha\sigma^2}{2\lambda} + \Delta E\left(\beta\right) + \mathcal{F}^{\mathsf{R}}\left(\beta\right). \tag{C.37}$$

Substituting the energy difference function into (C.37), we have

$$\bar{\mathcal{F}}\left(\beta\right) = \frac{\zeta}{2\lambda}\left[\alpha\sigma^2 + \int_0^1 T\left(\beta,\omega\right)\mathrm{d}\omega - T_0\left(\beta\right)\right] + \mathcal{F}^{\mathsf{R}}\left(\beta\right). \tag{C.38}$$

$\bar{\mathcal{F}}\left(\beta\right)$ is a function of the breaking parameter μ along with some other parameters which have not been indicated explicitly in the argument for sake of compactness. At the saddle point, we need

$$\frac{\partial}{\partial\mu}\bar{\mathcal{F}}\left(\beta\right) = 0. \tag{C.39}$$

This results in

$$\frac{\zeta}{2\lambda}\left[\frac{p}{\mu}\mathrm{R}_{\mathbf{J}}(-\frac{\chi}{\lambda}) + \lambda q g^2 - \frac{1}{\mu^2}\int_{\chi}^{\tilde{\chi}}\mathrm{R}_{\mathbf{J}}(-\frac{\omega}{\lambda})\mathrm{d}\omega\right] = \frac{1}{\mu}\mathcal{F}^{\mathsf{R}}\left(\beta\right) + \mathrm{LR}\left(\mu,\beta\right) \tag{C.40}$$

where

$$\mathrm{LR}\left(\mu,\beta\right) \coloneqq \frac{1}{\mu^2}\mathbb{E}\left\{\int \bar{\Lambda}_{\beta}\left(z_0,z_1|x_0\right)\log\Lambda_{\beta}\left(z_0,z_1|x_0\right)\mathrm{D}^{\zeta}z_1\,\mathrm{D}^{\zeta}z_0\right\}. \tag{C.41}$$

At zero temperature, this fixed-point reduces to

$$\frac{\zeta}{2\lambda}\left[\frac{p}{\mu}\mathrm{R}_{\mathbf{J}}(-\frac{\chi}{\lambda}) + \lambda q g^2 - \frac{1}{\mu^2}\int_{\chi}^{\tilde{\chi}}\mathrm{R}_{\mathbf{J}}(-\frac{\omega}{\lambda})\mathrm{d}\omega\right] = \frac{1}{\mu}\lim_{\beta\uparrow\infty}\mathcal{F}^{\mathsf{R}}\left(\beta\right) + \mathrm{LR}\left(\mu\right) \tag{C.42}$$

with $\mathrm{LR}\left(\mu\right)$ being

$$\mathrm{LR}\left(\mu\right) \coloneqq \lim_{\beta\uparrow\infty}\mathrm{LR}\left(\mu,\beta\right) \tag{C.43a}$$

$$= -\frac{1}{\mu}\mathbb{E}\left\{\int \mathcal{E}_1^{\mathrm{RSB}}\left(v^{\star}\left(z_0,z_1,x_0\right)|z_0,z_1,x_0\right)\bar{\Lambda}\left(z_0,z_1\right)\mathrm{D}^{\zeta}z_1\,\mathrm{D}^{\zeta}z_0\right\}. \tag{C.43b}$$

Noting that

$$\lim_{\beta\uparrow\infty}\mathcal{F}^{\mathsf{R}}\left(\beta\right)=-\frac{1}{\mu}\mathbb{E}\left\{\int\log\int\Lambda\left(z_0,z_1|x_0\right)\mathrm{D}^{\zeta}z_1\mathrm{D}^{\zeta}z_0\right\},\tag{C.44}$$

The fixed-point equation finally reads

$$\frac{\zeta}{2\lambda}\left[\frac{p}{\mu}\mathrm{R}_{\mathbf{J}}(-\frac{\chi}{\lambda})+\lambda qg^2-\frac{1}{\mu^2}\int_{\chi}^{\tilde{\chi}}\mathrm{R}_{\mathbf{J}}(-\frac{\omega}{\lambda})\mathrm{d}\omega\right]=\frac{1}{\mu^2}\,\mathrm{Div}\left(\mu\right)\tag{C.45}$$

where $\mathrm{Div}\left(\mu\right)$ the zero-temperature limit of $\mathrm{Div}\left(\mu,\beta\right)$, defined as

$$\mathrm{Div}\left(\mu,\beta\right)\coloneqq\mathbb{E}\left\{\int\bar{\Lambda}_{\beta}\left(z_0,z_1|x_0\right)\log\bar{\Lambda}_{\beta}\left(z_0,z_1|x_0\right)\,\mathrm{D}^{\zeta}z_1\,\mathrm{D}^{\zeta}z_0\right\},\tag{C.46}$$

and reads

$$\mathrm{Div}\left(\mu\right)\coloneqq\lim_{\beta\uparrow\infty}\mathrm{Div}\left(\mu,\beta\right)\tag{C.47a}$$

$$=\mathbb{E}\left\{\int\bar{\Lambda}\left(z_0,z_1|x_0\right)\log\bar{\Lambda}\left(z_0,z_1|x_0\right)\,\mathrm{D}^{\zeta}z_1\,\mathrm{D}^{\zeta}z_0\right\}.\tag{C.47b}$$

The fixed-point equation in (C.45) along with (C.28a)-(C.28c) specifies the parameters in the one-RSB structure.

C.3.4 Asymptotic LSE

In order to derive the asymptotic LSE, given in (4.21), we need to determine $L\left(\beta\right)$ which is defined as

$$L\left(\beta\right)=\frac{\partial}{\partial\beta}\beta\mathcal{F}^{\mathsf{R}}\left(\beta\right)-\lim_{t\downarrow0}\frac{1}{t}\mathbb{E}\left\{u_{\mathrm{v}}(\mathbf{v})\right\}.\tag{C.48}$$

By setting $\mathsf{d}\left(v;x_0\right)=u\left(v\right)$ in (C.30), we have

$$\lim_{t\downarrow0}\frac{1}{t}\mathbb{E}\left\{u_{\mathrm{v}}(\mathbf{v})\right\}=-\beta\frac{\partial}{\partial h}\mathcal{F}^{\mathsf{R}}\left(\beta,h\right)|_{h=0}.\tag{C.49}$$

Hence, $L(\beta)$ reads

$$L(\beta) = \frac{\partial}{\partial\beta}\beta\mathcal{F}^{\mathsf{R}}(\beta) + \beta\frac{\partial}{\partial h}\mathcal{F}^{\mathsf{R}}(\beta,h)\,|_{h=0} \tag{C.50a}$$

$$= \frac{1}{\mu}\,\mathrm{Div}(\mu,\beta) + e\,\mathbb{E}\left\{\int\sum_{v\in\mathbb{X}}|x_0-v|^2\,\mathrm{p}_\beta^{\mathrm{RSB}}(v|z_0,z_1,x_0)\;\bar{\Lambda}_\beta(z_0,z_1)\;\mathrm{D}^\zeta z_1\,\mathrm{D}^\zeta z_0\right\}$$

$$+\,\zeta g\,\mathbb{E}\left\{\int\sum_{v\in\mathbb{X}}\mathbb{R}\mathrm{e}\left\{(x_0-v)\,z_1^*\right\}\mathrm{p}_\beta^{\mathrm{RSB}}(v|z_0,z_1,x_0)\;\bar{\Lambda}_\beta(z_0,z_1)\;\mathrm{D}^\zeta z_1\,\mathrm{D}^\zeta z_0\right\}$$

$$+\,\zeta f\,\mathbb{E}\left\{\int\sum_{v\in\mathbb{X}}\mathbb{R}\mathrm{e}\left\{(x_0-v)\,z_0^*\right\}\mathrm{p}_\beta^{\mathrm{RSB}}(v|z_0,z_1,x_0)\;\bar{\Lambda}_\beta(z_0,z_1)\;\mathrm{D}^\zeta z_1\,\mathrm{D}^\zeta z_0\right\} \tag{C.50b}$$

$$\overset{\star}{=} \frac{1}{\mu}\,\mathrm{Div}(\mu,\beta) + e\left[\frac{\chi}{\beta}+p+q\right] - \zeta g^2\,(\tilde{\chi}+\mu q) - \zeta f^2\tilde{\chi} \tag{C.50c}$$

$$= \frac{1}{\mu}\,\mathrm{Div}(\mu,\beta) + \frac{\zeta}{2\lambda}\left[T_0(\beta) + \left(\frac{\tilde{\chi}}{\mu}+q\right)\Delta\mathrm{R}(1) + \tilde{\chi}G'(\tilde{\chi})\right] \tag{C.50d}$$

where $\star$ follows (C.19a)-(C.19c). Substituting into (4.21) and using the identity in (C.45), we have

$$\mathrm{LSE}_{\mathsf{RLS}} = \sigma^2 + \frac{2\lambda}{\zeta\alpha}\lim_{\beta\uparrow\infty}\left[L(\beta) + \frac{\partial}{\partial\beta}\beta\Delta E(\beta)\right] \tag{C.51a}$$

$$= \sigma^2 + \frac{1}{\alpha}\lim_{\beta\uparrow\infty}\left[\frac{\chi}{\beta}\mathrm{R}_{\mathbf{J}}(-\frac{\chi}{\lambda}\omega) + \frac{\partial}{\partial\chi}\chi G(\chi) + D_{\mathrm{R}}(\tilde{\chi},\chi)\right] \tag{C.51b}$$

$$= \sigma^2 + \alpha^{-1}\left[R'_{\mathrm{LSE}}(\chi) + \frac{1}{\mu}L_{\mathrm{R}}\right] \tag{C.51c}$$

where L_{R} is defined as

$$L_{\mathrm{R}} \coloneqq \tilde{\chi}\mathrm{R}_{\mathbf{J}}(-\frac{\tilde{\chi}}{\lambda}) - \chi\mathrm{R}_{\mathbf{J}}(-\frac{\chi}{\lambda}), \tag{C.52}$$

and $R_{\mathrm{LSE}}(\omega) \coloneqq \omega G(\omega)$.

C.3.5 Zero-temperature Free Energy

The zero-temperature free energy is obtained by taking the limit of $\beta \uparrow \infty$ in (C.38). To this end, we note that

$$\lim_{\beta\uparrow\infty} \Delta E\left(\beta\right) = \frac{\zeta}{2\lambda}\left[G\left(\tilde{\chi}\right) - \tilde{\chi}G'\left(\tilde{\chi}\right) - q\mathrm{R}_{\mathbf{J}}(-\frac{\tilde{\chi}}{\lambda}) + \frac{1}{\mu}\int_{\chi}^{\tilde{\chi}} \mathrm{R}_{\mathbf{J}}(-\frac{\omega}{\lambda})\mathrm{d}\omega - \frac{L_{\mathrm{R}}}{\mu}\right]. \quad \text{(C.53)}$$

The zero-temperature limit of $\mathcal{F}^{\mathsf{R}}\left(\beta\right)$ is moreover given by (C.44). Hence,the free energy of the corresponding spin glass at zero temperature under one-RSB reads

$$\bar{\mathcal{F}}^{0(1)}_{\mathrm{RSB}} = \Delta\mathcal{F}^{(1)}_{\mathrm{RSB}} + \frac{1}{\mu}\left[\Delta L^{(1)}_{\mathrm{R}} - \mathbb{E}\left\{\int \log \int \Lambda\left(z_0, z_1|x_0\right)\mathrm{D}^{\zeta}z_1\mathrm{D}^{\zeta}z_0\right\}\right], \quad \text{(C.54)}$$

with $\Delta\mathcal{F}^{(1)}_{\mathrm{RSB}}$ and $\Delta L^{(1)}_{\mathrm{R}}$ being

$$\Delta\mathcal{F}^{(1)}_{\mathrm{RSB}} \coloneqq \frac{\zeta}{2\lambda}\left[\alpha\sigma^2 + G\left(\tilde{\chi}\right) - \tilde{\chi}G'\left(\tilde{\chi}\right) - q\mathrm{R}_{\mathbf{J}}(-\frac{\tilde{\chi}}{\lambda})\right], \quad \text{(C.55a)}$$

$$\Delta L^{(1)}_{\mathrm{R}} \coloneqq \int_{\chi}^{\tilde{\chi}} \mathrm{R}_{\mathbf{J}}(-\frac{\omega}{\lambda})\mathrm{d}\omega - L_{\mathrm{R}}. \quad \text{(C.55b)}$$

This concludes Proposition 4.4.

Appendix D

Extension to Higher Breaking Steps

We extend the derivations in Appendix C to a case with an arbitrary number of breaking steps. With B steps of RSB, the replica correlation matrix is of the form

$$\mathbf{Q} = \frac{\chi}{\beta}\,\mathbf{I}_t + \sum_{b=1}^{B} p_b\,\mathbf{I}_{\frac{t\beta}{\mu_b}} \otimes \mathbf{1}_{\frac{\mu_b}{\beta}} + q\mathbf{1}_t \tag{D.1}$$

for some χ, $\{p_b\}$, $\{\mu_b\}$ and q. We assume that for $b \in [B-1]$, the fraction

$$\vartheta_b \coloneqq \frac{\mu_{b+1}}{\mu_b} \tag{D.2}$$

is a non-negative integer.

D.1 Limiting Free Energy

Similar to Appendices B and C, we define the frequency domain correlation matrix

$$\mathbf{R} \coloneqq \mathbf{T}\mathrm{R}_{\mathbf{J}}(-\frac{2}{\zeta}\beta\mathbf{T}\mathbf{Q}) \tag{D.3}$$

for $\mathbf{T}$ defined in (4.9). Appendix F indicates that $\mathbf{R}$ is of the following form:

$$\mathbf{R} = e\,\mathbf{I}_t - \beta\sum_{b=1}^{B}\frac{\zeta g_b^2}{2}\mathbf{I}_{\frac{t\beta}{\mu_b}} \otimes \mathbf{1}_{\frac{\mu_b}{\beta}} - \beta\frac{\zeta f^2}{2}\mathbf{1}_t \tag{D.4}$$

for some real e, $\{g_b\}$ and f.

Following the discussions in Appendix F, there exist diagonal matrices $\mathbf{D}^{\mathrm{Q}}$, $\mathbf{D}^{\mathrm{T}}$ and $\mathbf{D}^{\mathrm{R}}$, and orthogonal matrix $\mathbf{V}$, with which we can decompose $\mathbf{Q}$, $\mathbf{T}$ and $\mathbf{R}$ as

$$\mathbf{Q} = \mathbf{V}\mathbf{D}^{\mathrm{Q}}\mathbf{V}^{\mathsf{T}} \tag{D.5a}$$

$$\mathbf{T} = \mathbf{V}\mathbf{D}^{\mathrm{T}}\mathbf{V}^{\mathsf{T}} \tag{D.5b}$$

$$\mathbf{R} = \mathbf{V}\mathbf{D}^{\mathrm{R}}\mathbf{V}^{\mathsf{T}}. \tag{D.5c}$$

Hence, e, $\{g_b\}$ and f are found in terms of χ, $\{p_b\}$, $\{\mu_b\}$ and q by setting

$$\lambda_a^{\mathbf{R}} = \lambda_a^{\mathbf{T}} \mathrm{R}_{\mathbf{J}}(-\frac{2}{\zeta}\beta\lambda_a^{\mathbf{T}}\lambda_a^{\mathbf{Q}}) \tag{D.6}$$

for $a \in [t]$, where $\lambda_a^{\mathbf{Q}}$, $\lambda_a^{\mathbf{T}}$ and $\lambda_a^{\mathbf{R}}$ denote the a-th diagonal entry of $\mathbf{D}^{\mathrm{Q}}$, $\mathbf{D}^{\mathrm{T}}$ and $\mathbf{D}^{\mathrm{R}}$, or alternatively, the a-th corresponding eigenvalue of $\mathbf{Q}$, $\mathbf{T}$ and $\mathbf{R}$, respectively.

With the constraint in (D.2) holding, $\mathbf{Q}$, $\mathbf{T}$ and $\mathbf{R}$ have $B+2$ different corresponding eigenvalues; namely,

$$\lambda_1^{\mathbf{Q}} = \frac{\chi}{\beta} + \frac{1}{\beta}\sum_{b=1}^{B}\mu_b p_b + tq \tag{D.7a}$$

$$\lambda_1^{\mathbf{T}} = \frac{\zeta}{2\left(\lambda + t\beta\sigma^2\right)} \tag{D.7b}$$

$$\lambda_1^{\mathbf{R}} = e - \frac{\zeta}{2}\sum_{b=1}^{B}\mu_b g_b^2 - t\beta\frac{\zeta f^2}{2} \tag{D.7c}$$

with multiplicity 1,

$$\lambda_2^{\mathbf{Q}} = \frac{\chi}{\beta} + \frac{1}{\beta}\sum_{b=1}^{B}\mu_b p_b \tag{D.8a}$$

$$\lambda_2^{\mathbf{T}} = \frac{\zeta}{2\lambda} \tag{D.8b}$$

$$\lambda_2^{\mathbf{R}} = e - \frac{\zeta}{2}\sum_{b=1}^{B}\mu_b g_b^2 \tag{D.8c}$$

with multiplicity $t\beta\mu_B^{-1} - 1$,

$$\lambda_{b+2}^{\mathbf{Q}} = \frac{\chi}{\beta} + \frac{1}{\beta}\sum_{\kappa=1}^{b}\mu_\kappa p_\kappa \tag{D.9a}$$

$$\lambda_{b+2}^{\mathbf{T}} = \frac{\zeta}{2\lambda} \tag{D.9b}$$

$$\lambda_{b+2}^{\mathbf{R}} = e - \frac{\zeta}{2}\sum_{\kappa=1}^{b}\mu_\kappa g_\kappa^2 \tag{D.9c}$$

with multiplicity $t\beta\left(\mu_b^{-1} - \mu_{b+1}^{-1}\right)$ for $b \in [B-1]$, and

$$\lambda_{B+2}^{\mathbf{Q}} = \frac{\chi}{\beta} \tag{D.10a}$$

$$\lambda_{B+2}^{\mathbf{T}} = \frac{\zeta}{2\lambda} \tag{D.10b}$$

$$\lambda_{B+2}^{\mathbf{R}} = e \tag{D.10c}$$

with multiplicity $t - t\beta\mu_1^{-1}$. Substituting in (D.6), e, f and $\{g_b\}$ for $b \in [B]$ are derived in terms of χ, q, $\{p_b\}$ and $\{\mu_b\}$ as

$$e = \frac{\zeta}{2\lambda}\mathrm{R}_{\mathbf{J}}(-\frac{\chi}{\lambda}), \tag{D.11a}$$

$$g_b^2 = \frac{1}{\lambda\mu_b}\left[\mathrm{R}_{\mathbf{J}}(-\frac{\tilde{\chi}_{b-1}}{\lambda}) - \mathrm{R}_{\mathbf{J}}(-\frac{\tilde{\chi}_b}{\lambda})\right], \tag{D.11b}$$

$$f^2 = \frac{1}{\lambda^2}\frac{\partial}{\partial\tilde{\chi}_B}\left\{\left[\tilde{\chi}_B\sigma^2 - \lambda q\right]\mathrm{R}_{\mathbf{J}}(-\frac{\tilde{\chi}_B}{\lambda})\right\}. \tag{D.11c}$$

where we define $\tilde{\chi}_0 \coloneqq \chi$ and

$$\tilde{\chi}_b \coloneqq \chi + \sum_{\kappa=1}^{b}\mu_\kappa p_\kappa \tag{D.12}$$

for $b \in [B]$.

Substituting into the definition, the Hamiltonian of the spin glass of replicas reads

$$\mathcal{E}^{\mathsf{R}}(\mathbf{v}|\mathbf{x}) = e\left\|\mathbf{x}-\mathbf{v}\right\|^2 - \beta\sum_{b=1}^{B}\frac{\zeta g_b^2}{2}\left\langle \mathbf{x}-\mathbf{v}\right\rangle_{\frac{\mu_b}{\beta}} - \beta\frac{\zeta f^2}{2}\left\langle \mathbf{x}-\mathbf{v}\right\rangle_t + u(\mathbf{v}) \tag{D.13}$$

where we use the notation

$$\left\langle \mathbf{v}\right\rangle_u \coloneqq \operatorname{tr}\left\{\mathbf{v}\mathbf{v}^{\mathsf{H}}\mathbf{I}_{\substack{t\\u}}\otimes\mathbf{1}_u\right\}, \tag{D.14}$$

defined in Appendix C. Using the identities

$$\exp\left\{\frac{\beta^2 f^2}{2}\left\langle \mathbf{x}-\mathbf{v}\right\rangle_t\right\} = \int\exp\left\{-\beta\zeta f\sum_{a=1}^{t}\mathbb{Re}\left\{(x-\mathrm{v}_a)\,z_0^*\right\}\right\}\mathrm{D}^{\zeta}z_0, \tag{D.15a}$$

$$\exp\left\{\beta^2\frac{\zeta g_b^2}{2}\left\langle \mathbf{x}-\mathbf{v}\right\rangle_{\frac{\mu_b}{\beta}}\right\} = \prod_{k=0}^{\Xi_b}\int\exp\left\{-\beta\zeta g_b\sum_{a=\rho_k^b+1}^{\rho_{k+1}^b}\mathbb{Re}\left\{(x_0-\mathrm{v}_a)\,z_b^*\right\}\right\}\mathrm{D}^{\zeta}z_b, \tag{D.15b}$$

with $\rho_k^b = k\mu_b/\beta$ and $\Xi_b = t\beta/\mu_\kappa$, the partition function finally reads

$$\mathcal{Z}^{\mathsf{R}}(\beta|\mathbf{x}) = \int\left[\bigwedge_{b=1}^{B-1}\int\left[\int\left[\sum_{v\in\mathbb{X}}\exp\left\{-\beta\mathcal{E}_B^{\mathrm{RSB}}(v|\{z_b\},x_0)\right\}\right]^{\frac{\mu_1}{\beta}}\mathrm{D}^{\zeta}z_1\right]^{\frac{\mu_{b+1}}{\mu_b}}\mathrm{D}^{\zeta}z_b\right]^{\frac{t\beta}{\mu_B}}\mathrm{D}^{\zeta}z_0, \tag{D.16}$$

where $\{z_b\} \coloneqq \{z_0,\ldots,z_B\}$, and the notation $\bigwedge$ is defined as

$$\bigwedge_{b=1}^{B}\int\mathrm{F}\left(\{z_b\}\right)^{\xi_b}\mathrm{D}z_b \coloneqq \int\left[\cdots\int\left[\int\mathrm{F}\left(\{z_b\}\right)^{\xi_1}\mathrm{D}^{\zeta}z_1\right]^{\xi_2}\mathrm{D}^{\zeta}z_2\cdots\right]^{\xi_B}\mathrm{D}z_B. \tag{D.17}$$

The single-letter Hamiltonian is further defined as

$$\mathcal{E}_B^{\mathrm{RSB}}(v|\{z_b\},x_0) \coloneqq e\left|x-v\right|^2 + \zeta\mathbb{Re}\left\{\left(fz_0+\sum_{b=1}^{B}g_b z_b\right)^*(x-v)\right\} + u(v). \tag{D.18}$$

Substituting into the definition and using Lemma 3.2, the limiting free energy reads

$$\mathcal{F}^{\mathsf{R}}(\beta) = \lim_{t\downarrow 0} \mathcal{F}^{\mathsf{R}}(\beta, t) \tag{D.19a}$$

$$= -\frac{1}{\mu_B}\mathbb{E}\left\{\int \log\left(\bigwedge_{b=1}^{B}\int\left[\sum_{v\in\mathbb{X}}\exp\left\{-\beta\mathcal{E}_B^{\mathrm{RSB}}\left(v\middle|\left\{z_b\right\}, x_0\right)\right\}\right]^{\frac{\mu_b}{\mu_{b-1}}}\mathrm{D}^{\zeta}z_b\right)\mathrm{D}^{\zeta}z_0\right\} \tag{D.19b}$$

where we define $\mu_0 = \beta$ for sake of compactness.

D.2 Fixed-point Equations

To find the fixed-point equations, we start with taking trace and sum over all the entries from both sides of (4.10) which concludes that

$$\left[\frac{\chi}{\beta} + \sum_{b=1}^{B} p_\kappa + q\right] t = \mathbb{E}_{\mathbf{x}}\left\{\sum_{\mathbf{v}\in\mathbb{X}^t}\left\|\mathbf{x}-\mathbf{v}\right\|^2 \mathrm{p}_\beta^{\mathsf{R}}(\mathbf{v}|\mathbf{x})\right\}, \tag{D.20a}$$

$$\left[\frac{\tilde{\chi}_B}{\beta} + tq\right] t = \mathbb{E}_{\mathbf{x}}\left\{\mathbf{x}\sum_{\mathbf{v}\in\mathbb{X}^t}\left\langle\mathbf{x}-\mathbf{v}\right\rangle_t \mathrm{p}_\beta^{\mathsf{R}}(\mathbf{v}|\mathbf{x})\right\}. \tag{D.20b}$$

By taking sum over all the entries in the diagonal block of size μ_b/β for $b \in [B]$, we further have

$$\left[\frac{\tilde{\chi}_{b-1}}{\beta} + \frac{\mu_b}{\beta}\left(\sum_{\kappa=b}^{B} p_\kappa + q\right)\right] t = \mathbb{E}_{\mathbf{x}}\left\{\mathbf{x}\sum_{\mathbf{v}\in\mathbb{X}^t}\left\langle\mathbf{x}-\mathbf{v}\right\rangle_{\frac{\mu_b}{\beta}} \mathrm{p}_\beta^{\mathsf{R}}(\mathbf{v}|\mathbf{x})\right\}, \tag{D.21}$$

The right hand sides of (D.20a)-(D.21) are evaluated using the identities

$$\mathbb{E}_{\mathbf{x}}\left\{\sum_{\mathbf{v}\in\mathbb{X}^t}\left\|\mathbf{x}-\mathbf{v}\right\|^2 \mathrm{p}_\beta^{\mathsf{R}}(\mathbf{v}|\mathbf{x})\right\} = t\frac{\partial}{\partial e}\mathcal{F}^{\mathsf{R}}(\beta, t), \tag{D.22a}$$

$$\mathbb{E}_{\mathbf{x}}\left\{\mathbf{x}\sum_{\mathbf{v}\in\mathbb{X}^t}\left\langle\mathbf{x}-\mathbf{v}\right\rangle_{\frac{\mu}{\beta}} \mathrm{p}_\beta^{\mathsf{R}}(\mathbf{v}|\mathbf{x})\right\} = -\frac{t}{\beta\zeta g_b}\frac{\partial}{\partial g_b}\mathcal{F}^{\mathsf{R}}(\beta, t), \tag{D.22b}$$

$$\mathbb{E}_{\mathbf{x}}\left\{\mathbf{x}\sum_{\mathbf{v}\in\mathbb{X}^t}\langle\mathbf{x}-\mathbf{v}\rangle_t\,\mathrm{p}_\beta^{\mathsf{R}}\left(\mathbf{v}|\mathbf{x}\right)\right\}=-\frac{t}{\beta\zeta f}\frac{\partial}{\partial f}\mathcal{F}^{\mathsf{R}}\left(\beta,t\right). \tag{D.22c}$$

This concludes that

$$\frac{\chi}{\beta}+\sum_{b=1}^{B}p_b+q=\mathbb{E}\left\{\int\sum_{v\in\mathbb{X}}\left|v-x_0\right|^2\mathrm{p}_\beta^{\mathrm{RSB}}\left(v,\{z_b\}\,|x_0\right)\prod_{b=0}^{B}\mathrm{D}^\zeta z_b\right\} \tag{D.23a}$$

$$\tilde{\chi}_b=\frac{1}{f}\mathbb{E}\left\{\int\sum_{v\in\mathbb{X}}\mathbb{R}\mathrm{e}\left\{\left(v-x_0\right)z_0^*\right\}\mathrm{p}_\beta^{\mathrm{RSB}}\left(v,\{z_b\}\,|x_0\right)\prod_{b=0}^{B}\mathrm{D}^\zeta z_b\right\}, \tag{D.23b}$$

and

$$\tilde{\chi}_{b-1}+\mu_b\left(\sum_{\kappa=b}^{B}p_\kappa+q\right)=\frac{1}{g_b}\mathbb{E}\left\{\int\sum_{v\in\mathbb{X}}\mathbb{R}\mathrm{e}\left\{\left(v-x_0\right)z_b^*\right\}\mathrm{p}_\beta^{\mathrm{RSB}}\left(v,\{z_b\}\,|x_0\right)\prod_{b=0}^{B}\mathrm{D}^\zeta z_b\right\} \tag{D.24}$$

for $b\in[B]$, where we define the joint distribution

$$\mathrm{p}_\beta^{\mathrm{RSB}}\left(v,\{z_b\}\,|x_0\right)\coloneqq\mathrm{p}_\beta^{\mathrm{RSB}}\left(v|\,\{z_b\}\,,x_0\right)\prod_{b=1}^{B}\bar{\Lambda}_\beta^{(b)}\left(\{z_\kappa\}_{\kappa=b}^{B}|x_0\right) \tag{D.25}$$

with the conditional distributions

$$\mathrm{p}_\beta^{\mathrm{RSB}}\left(v|\,\{z_b\}\,,x_0\right)\coloneqq\frac{\exp\left\{-\beta\mathcal{E}_B^{\mathrm{RSB}}\left(v|\,\{z_b\}\,,x_0\right)\right\}}{\sum_{v\in\mathbb{X}}\exp\left\{-\beta\mathcal{E}_B^{\mathrm{RSB}}\left(v|\,\{z_b\}\,,x_0\right)\right\}} \tag{D.26}$$

and

$$\bar{\Lambda}_\beta^{(b)}\left(\{z_\kappa\}_{\kappa=b}^{B},z_0|x_0\right)\coloneqq\frac{\Lambda_\beta^{(b)}\left(\{z_\kappa\}_{\kappa=b}^{B},z_0|x_0\right)}{\int\Lambda_\beta^{(b)}\left(\{z_\kappa\}_{\kappa=b}^{B},z_0|x_0\right)\mathrm{D}^\zeta z_b}. \tag{D.27}$$

The function $\Lambda_\beta^{(1)}\left(\{z_b\},z_0|x_0\right)$ is further defined as

$$\Lambda_\beta^{(1)}\left(\{z_b\},z_0|x_0\right)\coloneqq\left[\sum_{v\in\mathbb{X}}\exp\left\{-\beta\mathcal{E}_B^{\mathrm{RSB}}\left(v|\,\{z_b\}\,,x_0\right)\right\}\right]^{\frac{\mu_1}{\beta}}, \tag{D.28}$$

and $\Lambda_\beta^{(b)}\left(\{z_\kappa\}_{\kappa=b}^{B}, z_0|x_0\right)$, for $b \geq 2$, are recursively calculated as

$$\Lambda_\beta^{(b)}\left(\{z_\kappa\}_{\kappa=b}^{B}, z_0|x_0\right) \coloneqq \left[\int \Lambda_\beta^{(b-1)}\left(\{z_\kappa\}_{\kappa=b-1}^{B}, z_0|x_0\right) \mathrm{D}^{\zeta} z_{b-1}\right]^{\frac{\mu_b}{\mu_{b-1}}}. \tag{D.29}$$

Similar to the one-RSB ansatz, the fixed-point equations here are derived for a given set of block sizes, i.e. $\{\mu_b\}$. The block sizes are later found by minimizing the free energy.

D.2.1 Zero-temperature Limit

As the temperature converges to zero, the conditional distribution $\mathrm{p}_\beta^{\mathrm{RSB}}\left(v|\left\{z_b\right\}, x_0\right)$ tends to an impulse function at

$$v^\star\left(\left\{z_b\right\}, x_0\right) \coloneqq \underset{v\in\mathbb{X}}{\operatorname{argmin}}\ \mathcal{E}_B^{\mathrm{RSB}}\left(v|\left\{z_b\right\}, x_0\right) \tag{D.30a}$$

$$= \underset{v\in\mathbb{X}}{\operatorname{argmin}}\ e\left|x_0 + \frac{\zeta}{2e}\left(f z_0 + \sum_{b=1}^{B} g_b z_b\right) - v\right|^2 + u\left(v\right) \tag{D.30b}$$

$$= \underset{v\in\mathbb{X}}{\operatorname{argmin}}\ \frac{\zeta}{2\tau}\left|x_0 + \sum_{b=0}^{B} \theta_b\, z_b - v\right|^2 + u\left(v\right) \tag{D.30c}$$

where

$$\tau = \frac{\zeta}{2e} = \left[\mathrm{R}_{\mathbf{J}}(-\frac{\chi}{\lambda})\right]^{-1}\lambda, \tag{D.31}$$

and θ_b, for $b \in [0:B]$, is defined as

$$\theta_0^2 = \left(\frac{\zeta f}{2e}\right)^2 = \left[\mathrm{R}_{\mathbf{J}}(-\frac{\chi}{\lambda})\right]^{-2}\frac{\partial}{\partial\tilde{\chi}_B}\left[\left[\tilde{\chi}_B\sigma^2 - \lambda q\right]\mathrm{R}_{\mathbf{J}}(-\frac{\tilde{\chi}_B}{\lambda})\right], \tag{D.32a}$$

$$\theta_b^2 = \left(\frac{\zeta g_b}{2e}\right)^2 = \left[\mathrm{R}_{\mathbf{J}}(-\frac{\chi}{\lambda})\right]^{-2}\frac{\lambda}{\mu}\left[\mathrm{R}_{\mathbf{J}}(-\frac{\tilde{\chi}_{b-1}}{\lambda}) - \mathrm{R}_{\mathbf{J}}(-\frac{\tilde{\chi}_b}{\lambda})\right]. \tag{D.32b}$$

Consequently, the function $\Lambda_{\beta}^{(1)}\left(\{z_b\}, z_0|x_0\right)$ converges to

$$\Lambda^{(1)}\left(\{z_b\}, z_0|x_0\right) \coloneqq \exp\left\{-\mu_1 \mathcal{E}_B^{\mathrm{RSB}}\left(v^\star\left(\{z_b\}, x_0\right) | \{z_b\}, x_0\right)\right\} \tag{D.33}$$

and the higher order functions are recursively determined as

$$\Lambda^{(b)}\left(\{z_\kappa\}_{\kappa=b}^{B}, z_0|x_0\right) \coloneqq \left[\int \Lambda^{(b-1)}\left(\{z_\kappa\}_{\kappa=b-1}^{B}, z_0|x_0\right) \mathrm{D}^\zeta z_{b-1}\right]^{\frac{\mu_b}{\mu_{b-1}}}. \tag{D.34}$$

The normalized terms are then given by

$$\bar{\Lambda}^{(b)}\left(\{z_\kappa\}_{\kappa=b}^{B}, z_0|x_0\right) \coloneqq \frac{\Lambda^{(b)}\left(\{z_\kappa\}_{\kappa=b}^{B}, z_0|x_0\right)}{\int \Lambda^{(b)}\left(\{z_\kappa\}_{\kappa=b}^{B}, z_0|x_0\right) \mathrm{D}^\zeta z_b}. \tag{D.35}$$

Substituting into the fixed-point equations, we have

$$\sum_{b=1}^{B} p_b + q = \mathbb{E}\left\{\int \left|v^\star\left(\{z_b\}, x_0\right) - x_0\right|^2 \mathrm{D}^\zeta \mathrm{F}_{\mathrm{RSB}}\left(\{z_b\}|x_0\right)\right\}, \tag{D.36a}$$

$$\tilde{\chi}_B = \frac{1}{f}\mathbb{E}\left\{\int \mathbb{R}\mathrm{e}\left\{\left(v^\star\left(\{z_b\}, x_0\right) - x_0\right) z_0^*\right\} \mathrm{D}^\zeta \mathrm{F}_{\mathrm{RSB}}\left(\{z_b\}|x_0\right)\right\}. \tag{D.36b}$$

and

$$\tilde{\chi}_{b-1} + \mu_b\left(\sum_{\kappa=b}^{B} p_\kappa + q\right) = \frac{1}{g_b}\mathbb{E}\left\{\int \mathbb{R}\mathrm{e}\left\{\left(v^\star\left(\{z_b\}, x_0\right) - x_0\right) z_b^*\right\} \mathrm{D}^\zeta \mathrm{F}_{\mathrm{RSB}}\left(\{z_b\}|x_0\right)\right\}, \tag{D.37}$$

for $b \in [B]$, where we define

$$\mathrm{D}^\zeta \mathrm{F}_{\mathrm{RSB}}\left(\{z_b\}|x_0\right) \coloneqq \prod_{b=1}^{B} \bar{\Lambda}^{(b)}\left(\{z_\kappa\}_{\kappa=b}^{B}, z_0|x_0\right) \mathrm{D}^\zeta z_b \, \mathrm{D}^\zeta z_0 \,. \tag{D.38}$$

D.3 Macroscopic Parameters

We now derive the macroscopic parameters of the spin glass of replicas which characterize the asymptotics of the generic RLS method.

D.3.1 Asymptotic Distortion

Following the standard averaging trick, we determine the free energy for the modified Hamiltonian

$$\mathcal{E}^{\mathsf{R}}\left(\mathbf{v}, h|\mathbf{x}\right) \coloneqq \mathcal{E}^{\mathsf{R}}\left(\mathbf{v}|\mathbf{x}\right) - \frac{h}{\beta}\sum_{a=1}^{t}\mathsf{d}\left(\mathrm{v}_a; x_0\right). \tag{D.39}$$

The free energy in this case is derived by (D.19b) when $u\left(v\right)$ is replaced with $u\left(v\right) - h\mathsf{d}\left(v; x_0\right)/\beta$ in (F.7). Doing so, the modified free energy is given by

$$\begin{aligned}\mathcal{F}^{\mathsf{R}}\left(\beta, h\right) = -\frac{1}{\mu_B}\mathbb{E}\Bigg\{\int \log\Bigg(\bigwedge_{b=1}^{B}\int\Bigg[\sum_{v\in\mathbb{X}}\exp\Big\{-\beta\mathcal{E}_B^{\mathrm{RSB}}\left(v|\left\{z_b\right\}, x_0\right) \\ + h\,\mathsf{d}\left(v; x_0\right)\Big\}\Bigg]^{\frac{\mu_b}{\mu_{b-1}}}\mathrm{D}^{\zeta}z_b\Bigg)\mathrm{D}^{\zeta}z_0\Bigg\}.\end{aligned} \tag{D.40}$$

Hence, the limit of average distortion reads

$$\lim_{t\downarrow 0} D^{\mathsf{R}}\left(\beta, t\right) = -\beta\frac{\partial}{\partial h}\mathcal{F}^{\mathsf{R}}\left(\beta, h\right)|_{h=0} \tag{D.41a}$$

$$= \mathbb{E}\left\{\int\sum_{v\in\mathbb{X}}\mathsf{d}\left(v; x_0\right)\mathrm{p}_{\beta}^{\mathrm{RSB}}\left(v, \left\{z_b\right\}|x_0\right)\prod_{b=0}^{B}\mathrm{D}^{\zeta}z_b\right\} \tag{D.41b}$$

with $\mathrm{p}_{\beta}^{\mathrm{RSB}}\left(v, \left\{z_b\right\}|x_0\right)$ being defined in (D.25). As the temperature tends to zero, the average distortion converges to

$$D_{\mathsf{RLS}}^{\mathbb{W}} = \mathbb{E}\left\{\int\mathsf{d}\left(v^{\star}\left(\left\{z_b\right\}, x_0\right); x_0\right)\mathrm{D}^{\zeta}\mathrm{F}_{\mathrm{RSB}}\left(\left\{z_b\right\}|x_0\right)\right\} \tag{D.42a}$$

which characterize the asymptotic distortion of the generic RLS method.

D.3.2 Energy Difference

The next macroscopic parameter to be calculated is the energy difference which for a generic replica correlation matrix $\mathbf{Q}$ is defined as

$$\Delta E\left(\beta\right) \coloneqq \lim_{t\downarrow 0}\frac{1}{t}\left[\int_0^1 \mathrm{tr}\left\{\mathbf{TQ}\mathrm{R}_{\mathbf{J}}(-\frac{2}{\zeta}\beta\omega\mathbf{TQ})\right\}\,\mathrm{d}\omega - \mathrm{tr}\left\{\mathbf{Q}^{\mathsf{T}}\mathbf{R}\right\}\right] \tag{D.43a}$$

$$= \frac{\zeta}{2\lambda}\left[\int_0^1 T\left(\beta,\omega\right)\mathrm{d}\omega - T_0\left(\beta\right)\right] \tag{D.43b}$$

where we have

$$T\left(\beta,\omega\right) \coloneqq \frac{\chi}{\beta}\mathrm{R}_{\mathbf{J}}(-\frac{\chi}{\lambda}\omega) + \left(q - \frac{\tilde{\chi}_B}{\lambda}\sigma^2\right)\frac{\partial}{\partial\omega}\omega\mathrm{R}_{\mathbf{J}}(-\frac{\tilde{\chi}_B}{\lambda}\omega) + \sum_{b=1}^{B}\frac{1}{\mu_b}\Delta\mathrm{R}_b\left(\omega\right) \tag{D.44a}$$

$$T_0\left(\beta\right) \coloneqq \frac{\chi}{\beta}\mathrm{R}_{\mathbf{J}}(-\frac{\chi}{\lambda}) + \sum_{b=1}^{B}\frac{1}{\mu_b}\Delta\mathrm{R}_b\left(1\right) + q\mathrm{R}_{\mathbf{J}}(-\frac{\tilde{\chi}_B}{\lambda}) + \tilde{\chi}_B G'\left(\tilde{\chi}_B\right), \tag{D.44b}$$

with $\Delta\mathrm{R}_b\left(\cdot\right)$ being

$$\Delta\mathrm{R}_b\left(\omega\right) \coloneqq \tilde{\chi}_b\mathrm{R}_{\mathbf{J}}(-\frac{\tilde{\chi}_b}{\lambda}\omega) - \tilde{\chi}_{b-1}\mathrm{R}_{\mathbf{J}}(-\frac{\tilde{\chi}_{b-1}}{\lambda}\omega) \tag{D.45}$$

and

$$G\left(\omega\right) \coloneqq \left[q - \frac{\sigma^2}{\lambda}\omega\right]\mathrm{R}_{\mathbf{J}}(-\frac{\omega}{\lambda}). \tag{D.46}$$

D.3.3 Breaking Block Sizes

The braking block sizes, i.e. μ_b for $b \in [B]$, are specified by minimizing the free energy over all the possible choices. Using the results of the previous sections, the free energy of the corresponding spin glass at a given inverse temperature β is given by

$$\bar{\mathcal{F}}\left(\beta\right) = \frac{\zeta\alpha\sigma^2}{2\lambda} + \Delta E\left(\beta\right) + \mathcal{F}^{\mathsf{R}}\left(\beta\right) \tag{D.47a}$$

$$= \frac{\zeta}{2\lambda}\left[\alpha\sigma^2 + \int_0^1 T\left(\beta,\omega\right)\mathrm{d}\omega - T_0\left(\beta\right)\right] + \mathcal{F}^{\mathsf{R}}\left(\beta\right). \tag{D.47b}$$

$\Delta E\left(\beta\right)$ and $\mathcal{F}^{\mathsf{R}}\left(\beta\right)$ in the right hand side of (D.47b) depend in the choice of $\{\mu_b\}$. We hence denote these terms with $\Delta E\left(\{\mu_b\},\beta\right)$ and $\mathcal{F}^{\mathsf{R}}\left(\{\mu_b\},\beta\right)$ to indicate this dependency. The block sizes are then set to $\mu_b = \mathrm{SP}_b\left(\beta\right)$, where

$$\{\mathrm{SP}_b\left(\beta\right)\} \coloneqq \underset{\{\omega_b\}\in\mathbb{R}^{+B}}{\operatorname{argmin}} \Delta E\left(\{\omega_b\},\beta\right) + \mathcal{F}^{\mathsf{R}}\left(\{\omega_b\},\beta\right) \tag{D.48}$$

for $b \in [B]$.

D.3.4 Asymptotic LSE

From the generic replica ansatz, we know that the asymptotic LSE reads

$$\mathrm{LSE}_{\mathsf{RLS}} = \sigma^2 + \frac{2\lambda}{\zeta\alpha}\lim_{\beta\uparrow\infty}\left[L\left(\beta\right) + \frac{\partial}{\partial\beta}\beta\Delta E\left(\beta\right)\right] \tag{D.49}$$

From the definition, $L\left(\beta\right)$ is given by

$$L\left(\beta\right) = \frac{\partial}{\partial\beta}\beta\mathcal{F}^{\mathsf{R}}\left(\beta\right) - \lim_{t\downarrow 0}\frac{1}{t}\mathbb{E}\left\{u_{\mathrm{v}}(\mathbf{v})\right\} \tag{D.50a}$$

$$= \frac{\partial}{\partial\beta}\beta\mathcal{F}^{\mathsf{R}}\left(\beta\right) + \beta\frac{\partial}{\partial h}\mathcal{F}^{\mathsf{R}}\left(\beta,h\right)|_{h=0} \tag{D.50b}$$

when we set $\mathsf{d}\left(v;x_0\right) = u\left(v\right)$ in (D.42a). Consequently, we have

$$\begin{aligned}\lim_{\beta\uparrow\infty} L\left(\beta\right) = {}& \frac{\mathrm{Div}\left(\{\mu_b\}\right)}{\mu_B} + e\,\mathbb{E}\left\{\int \left|x_0 - v^\star\left(\{z_b\},x_0\right)\right|^2 \mathrm{D}^{\zeta}\mathrm{F}_{\mathrm{RSB}}\left(\{z_b\}\,|x_0\right)\right\} \\ & + \zeta\sum_{b=1}^{B} g_b\,\mathbb{E}\left\{\int \mathbb{R}\mathrm{e}\left\{\left(x_0 - v^\star\left(\{z_b\},x_0\right)\right) z_b^*\right\} \mathrm{D}^{\zeta}\mathrm{F}_{\mathrm{RSB}}\left(\{z_b\}\,|x_0\right)\right\} \\ & + \zeta f\,\mathbb{E}\left\{\int \mathbb{R}\mathrm{e}\left\{\left(x_0 - v^\star\left(\{z_b\},x_0\right)\right) z_0^*\right\} \mathrm{D}^{\zeta}\mathrm{F}_{\mathrm{RSB}}\left(\{z_b\}\,|x_0\right)\right\}\end{aligned} \tag{D.51a}$$

$$\overset{\star}{=} \mathrm{Div}\left(\{\mu_b\}\right) + e\left[\sum_{b=1}^{B} p_b + q\right] - \zeta\sum_{b=1}^{B} g_b^2\left(\tilde{\chi}_{b-1} + \mu_b\sum_{\kappa=b}^{B} p_\kappa + \mu_b q\right) - \zeta f^2\tilde{\chi}_B \tag{D.51b}$$

$$\stackrel{\dagger}{=} \mathrm{Div}\left(\{\mu_b\}\right) - \frac{\zeta}{2\lambda}\left[\left(\sum_{b=1}^{B} p_b + q\right)\mathrm{R}_{\mathbf{J}}(-\frac{\chi}{\lambda}) - 2\tilde{\chi}_B G'\left(\tilde{\chi}_B\right) - 2\sum_{b=1}^{B}\frac{\Delta \mathrm{R}_b\left(1\right)}{\mu_b}\right]. \quad \text{(D.51c)}$$

where $\star$ follows the fixed-point equations, $\dagger$ comes from (D.11a)-(D.11c) and $\mathrm{Div}\left(\cdot\right)$ is defined as

$$\mathrm{Div}\left(\{\mu_b\}\right) \coloneqq \frac{1}{\mu_B}\mathbb{E}\left\{\int \log \Pi\left(\{z_b\}\,|x_0\right) \mathrm{D}^{\zeta}\mathrm{F}_{\mathrm{RSB}}\left(\{z_b\}\,|x_0\right)\right\}, \quad \text{(D.52)}$$

with $\Pi\left(\cdot\right)$ being

$$\Pi\left(\{z_b\}\,|x_0\right) \coloneqq \frac{\exp\left\{-\mu_B \mathcal{E}_B^{\mathrm{RSB}}\left(v^{\star}\left(\{z_b\}, x_0\right)|\,\{z_b\}, x_0\right)\right\}}{\int \Lambda^{(B)}\left(z_B, z_0|x_0\right)\mathrm{D}^{\zeta} z_B}. \quad \text{(D.53)}$$

Following the recursive definition of $\Lambda^{(b)}\left(\{z_\kappa\}_b^B\,|x_0\right)$, we can show that

$$\Pi\left(\{z_b\}\,|x_0\right) = \prod_{b=1}^{B}\left[\bar{\Lambda}^{(b)}\left(\{z_\kappa\}_b^B, z_0|x_0\right)\right]^{\frac{\mu_B}{\mu_b}}. \quad \text{(D.54)}$$

Hence, $\mathrm{Div}\left(\cdot\right)$ reduces to

$$\mathrm{Div}\left(\{\mu_b\}\right) = \frac{1}{\mu_B}\mathbb{E}\left\{\int\left(\sum_{b=1}^{B}\frac{\mu_B}{\mu_b}\log\bar{\Lambda}^{(b)}\left(\{z_\kappa\}_b^B, z_0|x_0\right)\right)\mathrm{D}^{\zeta}\mathrm{F}_{\mathrm{RSB}}\left(\{z_b\}\,|x_0\right)\right\} \quad \text{(D.55a)}$$

$$= \sum_{b=1}^{B}\frac{1}{\mu_b}\mathbb{E}\left\{\int \log\tilde{\Lambda}^{(b)}\left(\{z_\kappa\}_b^B, z_0|x_0\right)\mathrm{D}^{\zeta}\mathrm{F}_{\mathrm{RSB}}\left(\{z_b\}\,|x_0\right)\right\}. \quad \text{(D.55b)}$$

Defining the sequence of functions

$$\mathrm{Div}_b\left(\{\mu_b\}\right) \coloneqq \mathbb{E}\left\{\int \log\bar{\Lambda}^{(b)}\left(\{z_\kappa\}_b^B, z_0|x_0\right)\mathrm{D}^{\zeta}\mathrm{F}_{\mathrm{RSB}}\left(\{z_b\}\,|x_0\right)\right\} \quad \text{(D.56)}$$

for $b \in [B]$, $\mathrm{Div}\left(\cdot\right)$ is finally given as

$$\mathrm{Div}\left(\{\mu_b\}\right) = \sum_{b=1}^{B}\frac{1}{\mu_b}\mathrm{Div}_b\left(\{\mu_b\}\right). \quad \text{(D.57)}$$

For the second term, we have

$$\lim_{\beta\uparrow\infty}\frac{\partial}{\partial\beta}\beta\Delta E\left(\beta\right)=\frac{\zeta}{2\lambda}\left[G\left(\tilde{\chi}_B\right)-\tilde{\chi}_B G'\left(\tilde{\chi}_B\right)-q\mathrm{R}_{\mathbf{J}}(-\frac{\tilde{\chi}_B}{\lambda})\right.$$
$$\left.+\sum_{b=1}^{B}\frac{1}{\mu_b}\int_0^1\left(\Delta\mathrm{R}_b\left(\omega\right)-\Delta\mathrm{R}_b\left(1\right)\right)\mathrm{d}\omega\right]. \tag{D.58}$$

This concludes that

$$\mathrm{LSE}_{\mathsf{RLS}}=\sigma^2+\frac{2\lambda}{\zeta\alpha}\lim_{\beta\uparrow\infty}\left[L\left(\beta\right)+\frac{\partial}{\partial\beta}\beta\Delta E\left(\beta\right)\right] \tag{D.59a}$$

$$=\sigma^2+\frac{1}{\alpha}\left[R'_{\mathrm{LSE}}\left(\tilde{\chi}_B\right)+\sum_{b=1}^{B}\frac{1}{\mu_b}L_{\mathrm{R},b}+L_{\mathrm{R},0}\right] \tag{D.59b}$$

where $L_{\mathrm{R},b}$ for $b\in[B]$ is defined as

$$L_{\mathrm{R},b}\coloneqq\frac{2\lambda}{\zeta}\mathrm{Div}\left(\{\mu_b\}\right)+\Delta\mathrm{R}_b\left(1\right)+\int\Delta\mathrm{R}_b\left(\omega\right)\mathrm{d}\omega, \tag{D.60}$$

$L_{\mathrm{R},0}$ reads

$$L_{\mathrm{R},0}\coloneqq-q\mathrm{R}_{\mathbf{J}}(-\frac{\tilde{\chi}_B}{\lambda})-\left(\sum_{b=1}^{B}p_b+q\right)\mathrm{R}_{\mathbf{J}}(-\frac{\chi}{\lambda}), \tag{D.61}$$

and $R_{\mathrm{LSE}}\left(\omega\right)\coloneqq\omega G\left(\omega\right)$. Note that by setting $B=1$ and using the identity (C.45), the result in (D.59b) reduces to the one given by one-RSB solution.

D.3.5 Zero-temperature Free Energy

As the corresponding spin glass freezes, the free energy, given in (D.47b), converges to

$$\bar{\mathcal{F}}_{\mathrm{RSB}}^{0(B)}=\Delta\mathcal{F}_{\mathrm{RSB}}^{(B)}+\sum_{b=1}^{B}\frac{1}{\mu_b}\Delta L_{\mathrm{R}}^{(b)}-\frac{1}{\mu_B}\mathbb{E}\left\{\int\log\int\Lambda^{(B)}\left(z_B,z_0|x_0\right)\mathrm{D}^{\zeta}z_B\mathrm{D}^{\zeta}z_0\right\}. \tag{D.62}$$

where $\Delta\mathcal{F}_{\mathrm{RSB}}^{(B)}$ and $\Delta L_{\mathrm{R}}^{(B)}$ are given by

$$\Delta\mathcal{F}_{\mathrm{RSB}}^{(B)} \coloneqq \frac{\zeta}{2\lambda}\left[\alpha\sigma^2 + G\left(\tilde{\chi}_B\right) - \tilde{\chi}_B G'\left(\tilde{\chi}_B\right) - q\mathrm{R}_{\mathbf{J}}(-\frac{\tilde{\chi}_B}{\lambda})\right], \tag{D.63a}$$

$$\Delta L_{\mathrm{R}}^{(b)} \coloneqq \frac{\zeta}{2\lambda}\int_0^1 \left(\Delta\mathrm{R}_b\left(\omega\right) - \Delta\mathrm{R}_b\left(1\right)\right)\mathrm{d}\omega. \tag{D.63b}$$

This concludes Proposition 4.5.

Appendix E

Asymptotics of Spherical Integrals

We start with defining the spherical integral:

Definition E.1 (Spherical integral)**.** *Let μ_N^ζ be the Haar measure on the orthogonal group $\mathbb{O}_N$ for $\zeta = 1$, and on the unitary group $\mathbb{U}_N$ for $\zeta = 2$. For $\mathbf{G}_N, \mathbf{D}_N \in \mathbb{A}_\zeta^{N\times N}$, the integral of the form*

$$\mathcal{I}_N^\zeta(\mathbf{G}_N, \mathbf{D}_N) \coloneqq \int \exp\left\{N\mathrm{tr}\left\{\mathbf{U}\mathbf{G}_N\mathbf{U}^\dagger\mathbf{D}_N\right\}\right\} \mathrm{d}\mu_N^\zeta(\mathbf{U}), \tag{E.1}$$

is called a spherical integral.

The spherical integral has been extensively studied. In physics literature, it is often called *Harish-Chandra* or *Itzykson-Zuber* integral. In several problems, the asymptotic value of a spherical integral is of interest. As a result, its asymptotic properties have been widely investigated.

In [253], the asymptotics of spherical integrals investigated when $\mathbf{G}_N$ and $\mathbf{D}_N$ have N distinct eigenvalues with converging densities of states, and under some assumptions, a closed form formula was given. Nevertheless, the final formula is too complicated and hard to employ. Guionnet et al. showed later in [59] that for a low-rank $\mathbf{G}_N$, the derived asymptotics is represented explicitly in terms of the R-transform corresponding to the asymptotic eigenvalue distribution of $\mathbf{D}_N$.

Considering the replica analysis, the latter results in [59] are applicable, since the number of replicas are considered small by the replica continuity assumption. In [59, Theorem 1.2], it is shown that for rank-one $\mathbf{G}_N$, when the density of state of $\mathbf{D}_N$

asymptotically converges to deterministic CDF $\mathrm{F}_{\mathbf{D}}$ with compact and finite length support, the spherical integral asymptotically is given in terms of R-transform $\mathrm{R}_{\mathbf{D}}(\cdot)$ as

$$\lim_{N\uparrow\infty} \frac{1}{N} \log \mathcal{I}_N^{\zeta} \left(\mathbf{G}_N, \mathbf{D}_N\right) = \int_0^{\theta} \mathrm{R}_{\mathbf{D}} \left(\frac{2\omega}{\zeta}\right) \mathrm{d}\omega, \tag{E.2}$$

in which θ denotes the single nonzero eigenvalue of $\mathbf{G}_N$.

[59, Theorem 1.7] further indicates when $\mathrm{rank}\left(\mathbf{G}_N\right) = \mathcal{O}\left(\sqrt{N}\right)$, under the same assumption as in [59, Theorem 1.2], the spherical integral asymptotically factorizes into product of rank-one integrals. This means that in this case

$$\lim_{N\uparrow\infty} \frac{1}{N} \log \mathcal{I}_N^{\zeta} \left(\mathbf{G}_N, \mathbf{D}_N\right) = \sum_{i=1}^{t} \int_0^{\theta_i} \mathrm{R}_{\mathbf{D}} \left(\frac{2\omega}{\zeta}\right) \mathrm{d}\omega, \tag{E.3}$$

where $\{\theta_i\}$ for $i \in [t]$ with $t < N$ denotes the set of nonzero eigenvalues of $\mathbf{G}_N$, and $t = \mathrm{rank}(\mathbf{G}_n)$.

Appendix F

Notes on RSB Correlation Matrix

Consider the spin glass of replicas defined in Definition 4.3. The Hamiltonian of this spin glass can be written as

$$\mathcal{E}^{\mathsf{R}}(\mathbf{v}|\mathbf{x}) = (\mathbf{x}-\mathbf{v})^{\mathsf{H}}\mathbf{R}(\mathbf{x}-\mathbf{v}) + u(\mathbf{v}). \tag{F.1}$$

where matrix $\mathbf{R}$ reads

$$\mathbf{R} \coloneqq \mathbf{T}\mathrm{R}_{\mathbf{J}}(-\frac{2}{\zeta}\beta\mathbf{T}\mathbf{Q}). \tag{F.2}$$

We refer to $\mathbf{R}$ as the *frequency domain replica correlation matrix*. In the sequel, we show that when $\mathbf{Q}$ is structured with B steps of RS, including the RS case for $b=0$, the frequency domain correlation matrix has the same structure as $\mathbf{Q}$ with different scalar coefficients.

Let the correlation matrix be of the form

$$\mathbf{Q} = q_0\mathbf{I}_t + \sum_{b=1}^{B} q_b\mathbf{I}_{\frac{t}{\xi_b}} \otimes \mathbf{1}_{\xi_b} + q_{B+1}\mathbf{1}_t \tag{F.3}$$

for some integer B, where $q_0, q_{B+1} \neq 0$. (F.3) represents the B-RSB structure as well as RS structures by setting the coefficients correspondingly. Substituting $\mathbf{T}$ from (4.9), $\mathbf{TQ}$ reads

$$\mathbf{TQ} = \frac{\zeta}{2\lambda}\left[\mathbf{Q} - \frac{\beta\sigma^2}{\lambda + t\beta\sigma^2}\mathbf{1}_t\mathbf{Q}\right]. \tag{F.4}$$

Let $\mathbf{Q} = \mathbf{V}\mathbf{D}^{\mathrm{Q}}\mathbf{V}^{\mathsf{T}}$ be the eigendecomposition of $\mathbf{Q}$. Noting that $\mathbf{1}_{t\times 1}$ is an eigenvector of $\mathbf{Q}$, we have

$$\mathbf{1}_t = \mathbf{1}_{t\times 1}\mathbf{1}_{t\times 1}^{\mathsf{T}} = \mathbf{V}\mathbf{D}^{1}\mathbf{V}^{\mathsf{T}} \tag{F.5}$$

where $\mathbf{D}^1$ is a diagonal matrix in which all the diagonal entries expect the entry corresponding to the eigenvector $\mathbf{1}_{t\times 1}$ are zero. As a result, (F.4) reduces to

$$\mathbf{TQ} = \frac{1}{2\lambda}\mathbf{V}\left[\mathbf{D}^{\mathrm{Q}} - \frac{\beta\sigma^2}{\lambda + t\beta\sigma^2}\mathbf{D}^{1}\mathbf{D}^{\mathrm{Q}}\right]\mathbf{V}^{\mathsf{T}} \tag{F.6}$$

which states that $\mathbf{TQ}$ and $\mathbf{Q}$ span the same eigenspace. The eigenvalues of $\mathbf{TQ}$ and $\mathbf{Q}$ are also distributed with the same frequencies: As the eigenvalue corresponding to $\mathbf{1}_{t\times 1}$ occurs with multiplicity 1, the second term on the right hand side of (F.4) does not change the distribution of eigenvalues and only changes the eigenvalue corresponding to $\mathbf{1}_{t\times 1}$. This concludes that $\mathbf{TQ}$ is represented with the same form as in (F.3), with only the scalar coefficients being different.

To extend the scope of the analysis to $\mathbf{R}$, we note that the function $\mathrm{R}_{\mathbf{J}}(\cdot)$ is strictly increasing for any $\mathrm{F}_{\mathbf{J}}$ different from the single mass point CDF[1] [64, Appendix E]. As a result, the density of state remains unchanged, and hence,

$$\mathbf{R} = r_0\mathbf{I}_t + \sum_{b=1}^{B} r_b\mathbf{I}_{\frac{t}{\xi_b}} \otimes \mathbf{1}_{\xi_b} + r_{B+1}\mathbf{1}_t. \tag{F.7}$$

for some real $\{r_b\}$.

In the case that $\mathrm{F}_{\mathbf{J}}$ is the single mass point CDF, the R-transform becomes a constant function which results in $\mathrm{R}_{\mathbf{J}}(-2\beta\mathbf{TQ}) = K\mathbf{I}_t$ for some constant K. Therefore, $\mathbf{R} = K\mathbf{T}$ which is again of the form (F.7) in which $r_b = 0$ for $b \in [1 : B]$. This concludes that $\mathbf{R}$ has the same structure as $\mathbf{Q}$ for any $\mathrm{F}_{\mathbf{J}}$.

[1] In the single mass point CDF, we have $\mathrm{F}_{\mathbf{J}}(\lambda) = \mathbf{1}\{\lambda \geq K\}$ for some real constant K.

Appendix G

Bounding Per-User Ergodic Rate

In this appendix, we prove Lemma 7.1 in Chapter 7. We start the derivations by defining the random variable $w_m(\mathbf{H})$ as

$$w_m(\mathbf{H}) \coloneqq [\mathbf{H}\boldsymbol{x}]_m - \sqrt{\rho}\, s_m \tag{G.1}$$

for some $\rho > 0$ and $m \in [M]$. Here, $[\mathbf{H}\boldsymbol{x}]_m$ denotes the m-th entry of the vector $\mathbf{H}\boldsymbol{x}$. As the result, the symbol received by user terminal m is given by

$$y_m = \sqrt{\rho}\, s_m + w_m(\mathbf{H}) + z_m. \tag{G.2}$$

By definition, the achievable ergodic rate of user m reads

$$R_m = \mathrm{I}(y_m; s_m|\mathbf{H}) \tag{G.3a}$$

$$= \mathrm{h}(s_k|\mathbf{H}) - \mathrm{h}(s_k|y_k, \mathbf{H}). \tag{G.3b}$$

Using the identity

$$\mathrm{h}(s_m|y_m, \mathbf{H}) = \mathrm{h}\left(s_m - \frac{y_m}{\sqrt{\rho}}|y_m, \mathbf{H}\right), \tag{G.4}$$

one concludes that

$$R_m = \mathrm{h}(s_m|\mathbf{H}) - \mathrm{h}\left(\frac{w_m(\mathbf{H}) + z_m}{\sqrt{\rho}}|y_m, \mathbf{H}\right) \tag{G.5a}$$

$$\overset{\dagger}{\geq} \mathrm{h}\left(s_m\right) - \mathrm{h}\left(\frac{w_m\left(\mathbf{H}\right) + z_m}{\sqrt{\rho}} | \mathbf{H}\right) \tag{G.5b}$$

where † is concluded due to the facts that s_m is independent of $\mathbf{H}$ and $\mathrm{h}\left(x|y\right) \leq \mathrm{h}\left(x\right)$. Noting that $w_m\left(\mathbf{H}\right)$ and z_m are independent, we have

$$\mathrm{h}\left(\frac{w_m\left(\mathbf{H}\right) + z_m}{\sqrt{\rho}} | \mathbf{H}\right) \leq \mathrm{h}\left(\frac{w_m\left(\mathbf{H}\right) + z_m}{\sqrt{\rho}}\right) \tag{G.6a}$$

$$\overset{\star}{\leq} \log\left(\pi e \, \frac{\sigma^2 + \psi_m}{\rho}\right) \tag{G.6b}$$

where we define ψ_m to be the variance of $w_m\left(\mathbf{H}\right)$. The equality in $\star$ holds when $w_m\left(\mathbf{H}\right)$ is Gaussian. Since $s_m \sim \mathcal{CN}\left(0, 1\right)$, the achievable ergodic rate for user m is bounded from below as

$$R_m \geq \log\left(\frac{\rho}{\sigma^2 + \psi_m}\right). \tag{G.7}$$

By substituting in (7.13), one derives the following bound on the achievable ergodic rate per user

$$R_{\mathrm{Erg}} \geq \frac{1}{M} \sum_{m=1}^{M} \log\left(\frac{\rho}{\sigma^2 + \psi_m}\right) \tag{G.8}$$

Using Jensen's inequality, we have

$$\frac{1}{M} \sum_{m=1}^{M} \log\left(\frac{\rho}{\sigma^2 + \psi_m}\right) \geq \log\left(\frac{\rho}{\sigma^2 + \dfrac{1}{M} \displaystyle\sum_{m=1}^{M} \psi_m}\right). \tag{G.9}$$

The inequality is tight when ψ_m is constant in m. By definition, we have

$$\mathrm{LSE}_N\left(\rho\right) \coloneqq \frac{1}{M} \mathbb{E}\left\{\left\|\mathbf{H}\boldsymbol{x} - \sqrt{\rho}\, \boldsymbol{s}\right\|^2\right\} \tag{G.10a}$$

$$= \frac{1}{M} \sum_{m=1}^{M} \mathbb{E}\left\{ |w_m(\mathbf{H})|^2 \right\} \tag{G.10b}$$

$$= \frac{1}{M} \sum_{m=1}^{M} \psi_m. \tag{G.10c}$$

Substituting into (G.9), we finally have

$$R_{\text{Erg}} \geq \log\left(\frac{\rho}{\sigma^2 + \text{LSE}_N(\rho)} \right) \tag{G.11}$$

which as N grows large concludes the lower bound in Lemma 7.1.

Appendix H

Proof of Lemma 7.2

In this appendix, we justify Lemma 7.2 which gives a lower bound on the achievable LSE for K-PSK transmission.

To start with the proof, consider an i.i.d. flat Rayleigh fading channel whose channel matrix is $\mathbf{H}$ and assume that the entries of $\boldsymbol{x}$ are either zero or K-PSK, as assumed in GLSE Precoder 7.3.3.1. Let the fraction of active transmit antennas be η and denote their amplitude by $\sqrt{P}$. Define the random variable

$$D(\boldsymbol{x}) \coloneqq \frac{1}{M} \|\mathbf{H}\boldsymbol{x} - \sqrt{\rho}\boldsymbol{s}\|^2 \tag{H.1}$$

whose expectation evaluates the LSE, and $q_{\min}$ to be

$$q_{\min} = \Pr\left\{\min_{\boldsymbol{x}} D(\boldsymbol{x}) \leq \mathcal{L}_0\right\}. \tag{H.2}$$

Using the union bound, we have

$$q_{\min} = \Pr\left\{\cup_{\boldsymbol{x}} D(\boldsymbol{x}) \leq \mathcal{L}_0\right\} \tag{H.3a}$$

$$\leq \sum_{\boldsymbol{x}} \Pr\left\{D(\boldsymbol{x}) \leq \mathcal{L}_0\right\}. \tag{H.3b}$$

To determine the upper bound in (H.3b), we first calculate the asymptotic distribution of $D(\boldsymbol{x})$. For a given vector $\boldsymbol{x}$, the entry $[\mathbf{H}\boldsymbol{x}]_m$ for $m \in [M]$ reads

$$[\mathbf{H}\boldsymbol{x}]_m = \sum_{n=1}^{N} x_n [\mathbf{H}]_{m,n} \tag{H.4}$$

which is the sum of ηN independent complex Gaussian random variables. The weighting coefficients in this sum, i.e., x_n with $n \in [N]$ for which $x_n \neq 0$, are complex scalars whose amplitudes equal to $\sqrt{P}$. Noting that $[\mathbf{H}]_{m,n} \sim \mathcal{CN}(0, 1/N)$, we conclude that $[\mathbf{H}\boldsymbol{x}]_m$ is a zero-mean complex Gaussian random variable with variance

$$\mathbb{E}\left\{|[\mathbf{H}\boldsymbol{x}]_m|^2\right\} = \sum_{n=1}^{N} |x_n|^2 = \eta P. \tag{H.5}$$

As a result, in the asymptotic regime

$$[\mathbf{H}\boldsymbol{x}]_m - \sqrt{\rho} s_m \sim \mathcal{CN}(0, \rho + \eta P). \tag{H.6}$$

Hence, $D(\boldsymbol{x})$ is asymptotically distributed with [254]

$$f(d) = \frac{M^M d^{M-1}}{(\rho + \eta P)^M (M-1)!} \exp\left\{-\frac{Md}{\rho + \eta P}\right\}. \tag{H.7}$$

Substituting into (H.3b), $q_{\min}$ is bounded as

$$q_{\min} \leq |\mathbb{X}|^N \int_0^{\mathcal{L}_0} f(d)\, \mathrm{d}d \tag{H.8a}$$

$$= (1+K)^N \int_0^{\mathcal{L}_0} f(d)\, \mathrm{d}d. \tag{H.8b}$$

Noting that $f(d)$ is an increasing function within the vicinity of zero, and using the inequality

$$(M-1)! \geq \sqrt{2\pi} (M-1)^{M-0.5} \exp\{-M+1\} \tag{H.9}$$

given in [255], one can further write

$$q_{\min} \leq (1+K)^N \frac{M^M \mathcal{L}_0^{M-1} \exp\{M-1\}}{\sqrt{2\pi}(\rho+\eta P)^M (M-1)^{M-0.5}} \exp\left\{-\frac{M\mathcal{L}_0}{\rho+\eta P}\right\}. \tag{H.10}$$

Since logarithm is an increasing function, we further have

$$\log q_{\min} \leq M\left[1 - \frac{\mathcal{L}_0}{\rho+\eta P} + \frac{1}{\alpha}\log(1+K) + \log\frac{\mathcal{L}_0}{\rho+\eta P}\right] + \epsilon_M \tag{H.11}$$

where $\epsilon_M \downarrow 0$ as $M \uparrow \infty$.

To make sure that the asymptotic LSE is bounded from below by $\mathcal{L}_0$, we need the probability $q_{\min}$ tend to zero as M and N grow large. This holds if

$$1 - \frac{\mathcal{L}_0}{\rho+\eta P} + \frac{1}{\alpha}\log(1+K) + \log\frac{\mathcal{L}_0}{\rho+\eta P} < 0. \tag{H.12}$$

Hence, for any $\mathcal{L}_0$ which satisfy (H.12) the asymptotic distortion is greater than $\mathcal{L}_0$. The lower bound in Lemma 7.2 is found by choosing the maximum value of $\mathcal{L}_0$ which satisfies (H.12). This value is given by replacing the inequality with equality.

Glossary

Abbreviations

AWGN	additive white Gaussian noise
AMP	approximate message passing
CSI	channel state information
CDMA	code division multiple accsess
CDF	cumulative distribution function
dB	decibel
GLSE	generalized least squares error
i.i.d.	independent and identically distributed
LLN	law of large numbers
LASSO	least absolute shrinkage and selection operator
LS	least squares
LSE	least squares error
LMSRF	load-modulated single radio frequency
MPM	marginal posterior mode
ML	maximum likelihood
MAP	maximum-a-posteriori
MSE	mean squared error
MMSE	minimum mean square error
MMV	multiple measurement vectors
MIMO	multiple-input multiple-output
NP	nondeterministic polynomial time
PAPR	peak-to-average power ratio
PSK	phase shift keying
PDF	probability density function
PMF	probability mass function
RF	radio frequency
REM	random energy model
RLS	regularized least squares
RZF	regularized zero-forcing
RS	replica symmetry
RSB	replica symmetry breaking

RSS	residual sum of squares
SNR	signal-to-noise ratio
SER	symbol error rate
TDD	time division duplexing
TAS	transmit antenna selection

Operators

$\lvert\cdot\rvert$	absolute value of a number or cardinality of a set
$\lfloor\cdot\rfloor$	floor function mapping a real number to the largest smaller or equal integer
$\lceil\cdot\rceil$	ceiling function mapping a real number to the smallest larger or equal integer
$\log(\cdot)$	natural logarithm
$\exp\{\cdot\}$	exponential function
$\int(\cdot)\,\mathrm{D}^{\zeta}z$	integral over $\mathbb{A}_\zeta$ with respect to the Gaussian measure where $\mathbb{A}_1$ and $\mathbb{A}_2$ respectively denote the real axis and the complex plane
$[n]$	set of consecutive integers $\{1,\ldots,n\}$ for positive integer n
$[m:n]$	set of consecutive integers $\{m,\ldots,n\}$ for integers $m \leq n$
$\mathbf{1}\{\cdot\}$	indicator function which returns 1 if its argument holds and 0 otherwise
$(\cdot)^*$	conjugate of a complex number, vector or matrix
$\mathbb{Re}\{s\}$	real part of complex number s
$\mathbb{Im}\{s\}$	imaginary part of complex number s
$\lVert\cdot\rVert$	Euclidean norm
$\lVert\cdot\rVert_p$	ℓ_p-norm where $p \geq 1$
$\lVert\boldsymbol{x}\rVert_0$	ℓ_0-norm of $\boldsymbol{x}$ which counts the number of non-zero entires in $\boldsymbol{x}$
$\langle\boldsymbol{x}\rangle_u$	trace of matrix $\boldsymbol{x}\boldsymbol{x}^{\mathsf{H}}\mathbf{I}_{N/u} \otimes \mathbf{1}_u$ where $\boldsymbol{x}$ is an $N \times 1$ vector
$\mathbf{A}^{\mathsf{T}}$	transpose of matrix $\mathbf{A}$
$\mathbf{A}^{\mathsf{H}}$	transposed conjugate of matrix $\mathbf{A}$
$[\mathbf{A}]_{ij}$	entry in the i-th row and j-th column of matrix $\mathbf{A}$
$\mathrm{tr}\{\cdot\}$	trace of a matrix
$\det\lvert\cdot\rvert$	determinant of a matrix

$\mathrm{diag}\left\{\boldsymbol{x}\right\}$	$M \times M$ diagonal matrix whose diagonal is given by the entries of $\boldsymbol{x}$
$\mathbb{E}\left\{\cdot\right\}$	expectation with respect to all random variables involved
$\mathbb{E}_x\left\{\cdot\right\}$	expectation with respect to random variable x
$\Pr\left\{A\right\}$	probability of event A
$D_{\mathsf{KL}}\left(\mathrm{p}_x \| \mathrm{q}_x\right)$	Kullback-Leibler divergence between distributions p_x and q_x
$\mathbf{I}\left(x;y\right)$	mutual information between random variables x and y
$\mathbf{H}\left(x\right)$	entropy of discrete random variable x
$\mathrm{h}\left(x\right)$	differential entropy of continuous random variable x

Symbols

$\mathbf{a}$	bold lower-case letters denote vectors
$\mathbf{A}$	bold upper-case letters denote matrices
$\mathbb{A}$	blackboard bold upper-case letters denote sets
$\mathbf{1}_{K\times 1}$	a $K \times 1$ vector whose elements are all ones
$\mathbf{1}_K$	a $K \times K$ matrix whose elements are all ones
$\mathbf{I}_K$	a $K \times K$ identity matrix
$\mathbb{N}$	set of natural numbers
$\mathbb{Z}$	set of integer numbers
$\mathbb{R}$	set of real numbers
$\mathbb{R}^+$	set of positive real numbers
$\mathbb{R}_0^+$	set of non-negative real numbers
$\mathbb{C}$	complex plane
$\mathbb{A}_\zeta$	universal representation for set of scalars which represents the set of real numbers if $\zeta = 1$ and the complex plane if $\zeta = 2$
$\mathbb{O}_N$	orthogonal group of size N
$\mathbb{U}_N$	unitary group of size N
$\mathbb{O}_N^\zeta$	universal representation of orthogonal groups which returns $\mathbb{O}_N$ for $\zeta = 1$ and $\mathbb{U}_N$ for $\zeta = 2$
$\mathbb{S}\left(\mathbf{Q}\right)$	subshell of all replicas with correlation matrix $\mathbf{Q}$
$\mathrm{p}_x\left(\cdot\right)$	probability density or mass function of random variable x

$\mathrm{F}_x(\cdot)$	cumulative density function of random variable x
$\mathrm{F}_{\mathbf{J}}^N(\lambda)$	cumulative density of states for $N \times N$ matrix $\mathbf{J}$
$\mathrm{G}_x(\cdot)$	Stieltjes transform of $\mathrm{F}_x(\cdot)$
$\mathrm{R}_x(\cdot)$	R-transform of $\mathrm{F}_x(\cdot)$
$\mathrm{R}_{\mathbf{A}}(\cdot)$	R-transform of the asymptotic density of state of matrix $\mathbf{A}$
$\mathcal{N}(\boldsymbol{\mu}, \mathbf{R})$	real-valued Gaussian distribution with mean $\boldsymbol{\mu}$ and covariance matrix $\mathbf{R}$
$\mathcal{CN}(\boldsymbol{\mu}, \mathbf{R})$	complex-valued Gaussian distribution with mean $\boldsymbol{\mu}$ and covariance matrix $\mathbf{R}$
$\mathcal{N}^{\zeta}(\boldsymbol{\mu}, \mathbf{R})$	universal representation of Gaussian distribution which denotes $\mathcal{N}(\boldsymbol{\mu}, \mathbf{R})$ for $\zeta = 1$ and $\mathcal{CN}(\boldsymbol{\mu}, \mathbf{R})$ for $\zeta = 2$
$\Delta(\boldsymbol{x}\|\mathbb{D}, \boldsymbol{y})$	residual sum of squares of linear regression with regression coefficients $\boldsymbol{x}$, regressors in $\mathbb{D}$ and regressands $\boldsymbol{y}$
$\Delta_{\mathrm{R}}(\boldsymbol{x}\|\mathbb{D}, \boldsymbol{y})$	regularized residual sum of squares of linear regression with regression coefficients $\boldsymbol{x}$, regressors in $\mathbb{D}$ and regressands $\boldsymbol{y}$
$\mathsf{g}_{\mathsf{RLS}}(\boldsymbol{y}\|\mathbf{A})$	regularized least squares algorithm which calculates the regression coefficients of the linear model with vector of regressands $\boldsymbol{y}$ and matrix of regressors $\mathbf{A}$
$\mathrm{LSE}_N\{\mathbf{g}\}$	least squares error achieved by regression method $\mathbf{g}(\cdot\|\cdot)$ for a problem with dimension N
$\mathrm{LSE}_{\mathsf{RLS}}$	asymptotic least squares error of the regularized least squares method
$\mathsf{d}(\cdot;\cdot)$	distortion function
$D_N^{\mathbb{W}}\{\mathbf{g}\}$	distortion with respect to a given distortion function which is achieved by regression method $\mathbf{g}(\cdot\|\cdot)$ for a problem with dimension N and is averaged over $\mathbb{W}(N) \subseteq [N]$
$D_{\mathsf{RLS}}^{\mathbb{W}}$	asymptotic distortion of the regularized least squares method averaged over the limit of $\mathbb{W}(N)$
$\mathcal{E}(\cdot)$	Hamiltonian of a thermodynamic system
$\mathcal{E}(\cdot\|\Omega)$	Hamiltonian of a spin glass with quenched randomizer Ω
$\mathcal{H}_N(\cdot)$	normalized entropy of a thermodynamic system with N particles

$\mathcal{H}_N(\cdot\|\Omega)$	normalized entropy of an N-particle spin glass with quenched randomizer Ω
$\mathcal{F}_N(\cdot)$	normalized free energy of a thermodynamic system with N articles
$\mathcal{F}_N(\cdot\|\Omega)$	normalized free energy of an N-particle spin glass with quenched randomizer Ω
$\bar{\mathcal{F}}_N(\cdot)$	expectation of normalized free energy of an N-particle spin glass with respect to its quenched randomizer
$\bar{\mathcal{F}}(\cdot)$	asymptotic expectation of normalized free energy of a spin glass
$\mathcal{Z}_N(\cdot)$	partition function of a thermodynamic system with N articles
$\mathcal{Z}_N(\cdot\|\Omega)$	partition function of an N-particle spin glass with quenched randomizer Ω
R_{Erg}	per-user achievable ergodic rate
R_{c}	compression rate
$a(x) \doteq b(x)$	$a(x)$ and $b(x)$ are asymptotically equivalent in exponential scale
$\xrightarrow{\text{a.s.}}$	almost sure convergence
$\delta(\cdot)$	Dirac impulse function
$\mathcal{O}(\cdot)$	growth order: big O notation
$\otimes$	Kronecker product
μ_N^{ζ}	Haar measure on $\mathbb{O}_N^{\zeta}$
$\mathcal{I}_N^{\zeta}(\cdot,\cdot)$	spherical integral with respect to Haar measure μ_N^{ζ}

Author's Publications

[A1] A. Bereyhi, R. R. Müller, and H. Schulz-Baldes, "Statistical mechanics of MAP estimation: General replica ansatz," *IEEE Transations on Information Theory*, vol. 65, no. 12, pp. 7896–7934, August 2019.

[A2] A. Bereyhi, R. R. Müller, and H. Schulz-Baldes, "Replica symmetry breaking in compressive sensing," *Proc. IEEE Information Theory and Applications Workshop (ITA)*, pp. 1–7, February 2017, San Diego, CA, USA.

[A3] A. Bereyhi, R. Müller, and H. Schulz-Baldes, "RSB decoupling property of MAP estimators," *Proc. IEEE Information Theory Workshop (ITW)*, pp. 379–383, October 2016, Cambridge, UK.

[A4] A. Bereyhi, S. Asaad, B. Gäde, and R. R. Müller, "RLS-based detection for massive spatial modulation MIMO," *Proc. IEEE International Symposium on Information Theory (ISIT)*, pp. 1167–1171, July 2019, Paris, France.

[A5] A. Bereyhi, M. A. Sedaghat, R. R. Müller, and G. Fischer, "GLSE precoders for massive MIMO systems: Analysis and applications," *IEEE Transactions on Wireless Communications*, vol. 18, no. 9, pp. 4450–4465, September 2019.

[A6] A. Bereyhi, M. A. Sedaghat, and R. R. Müller, "Asymptotics of nonlinear LSE precoders with applications to transmit antenna selection," *Proc. IEEE International Symposium on Information Theory (ISIT)*, pp. 81–85, June 2017, Aachen, Germany.

[A7] A. Bereyhi, M. A. Sedaghat, S. Asaad, and R. Müller, "Nonlinear precoders for massive MIMO systems with general constraints," *Proc. VDE 21st Interna-*

tional ITG Workshop on Smart Antennas (WSA), pp. 1–8, March 2017, Berlin, Germany.

[A8] M. A. Sedaghat, A. Bereyhi, and R. Müller, "A new class of nonlinear precoders for hardware efficient massive MIMO systems," *Proc. IEEE International Conference on Communications (ICC)*, July 2017, Paris, France.

[A9] M. A. Sedaghat, A. Bereyhi, and R. R. Müller, "Least square error precoders for massive MIMO with signal constraints: Fundamental limits," *IEEE Transactions on Wireless Communications*, vol. 17, no. 1, pp. 667–679, January 2018.

[A10] A. Bereyhi, S. Asaad, and R. R. Müller, "Stepwise transmit antenna selection in downlink massive multiuser MIMO," *Proc. VDE 22nd International ITG Workshop on Smart Antennas (WSA)*, 2018, Bochum, Germany.

[A11] A. Bereyhi, M. A. Sedaghat, and R. R. Müller, "Precoding via approximate message passing with instantaneous signal constraints," *Proc. International Zurich Seminar on Information and Communication (IZS)*, pp. 128–132, February 2018, Zürich, Switzerland.

[A12] A. Bereyhi, S. Haghighatshoar, and R. R. Müller, "Theoretical bounds on MAP estimation in distributed sensing networks," *Proc. IEEE International Symposium on Information Theory (ISIT)*, June 2018, Vail, CO, USA.

[A13] A. Bereyhi and R. R. Müller, "Maximum-a-posteriori signal recovery with prior information: Applications to compressive sensing," *Proc. IEEE International Conference on Acoustics, Speech and Signal Processing (ICASSP)*, pp. 4494–4498, April 2018, Calgary, AB, Canada.

[A14] S. Asaad, A. Bereyhi, R. R. Müller, R. F. Schaefer, and A. M. Rabiei, "Optimal number of transmit antennas for secrecy enhancement in massive MIMOME channels," *Proc. IEEE Global Communications Conference (GLOBECOM)*, 2017, Singapore, Singapore.

[A15] S. Asaad, A. Bereyhi, R. R. Müller, and A. M. Rabiei, "Asymptotics of transmit antenna selection: Impact of multiple receive antennas," *Proc. IEEE International Conference on Communications (ICC)*, pp. 1–6, July 2017, Paris, France.

[A16] S. Asaad, A. Bereyhi, A. M. Rabiei, R. R. Müller, and R. F. Schaefer, "Optimal transmit antenna selection for massive MIMO wiretap channels," *IEEE Journal on Selected Areas in Communications*, vol. 36, no. 4, pp. 817–828, April 2018.

[A17] B. Gäde, A. Bereyhi, S. Asaad, and R. R. Müller, "A fair comparison between spatial modulation and antenna selection in massive MIMO systems," *Proc. VDE 23rd International ITG Workshop on Smart Antennas (WSA)*, pp. 1–6, April 2019, Vienna, Austria.

[A18] A. Bereyhi, S. Asaad, R. R. Müller, R. F. Schaefer, and A. M. Rabiei, "On robustness of massive MIMO systems against passive eavesdropping under antenna selection," *Proc. IEEE Global Communications Conference (GLOBECOM)*, pp. 1–7, December 2018, Abu Dhabi, United Arab Emirates.

[A19] A. Bereyhi, S. Asaad, R. F. Schaefer, and R. R. Müller, "Iterative antenna selection for secrecy enhancement in massive MIMO wiretap channels," pp. 1–5, June 2018, Kalamata, Greece.

[A20] S. Asaad, A. Bereyhi, M. A. Sedaghat, R. Müller, and A. M. Rabiei, "Asymptotic performance analysis of spatially reconfigurable antenna arrays," in *Proc. VDE 21st International ITG Workshop on Smart Antennas (WSA)*. VDE, March 2017, Berlin, Germany, pp. 1–6.

[A21] A. Bereyhi, S. Asaad, R. R. Müller, and S. Chatzinotas, "RLS precoding for massive MIMO systems with nonlinear front-end," *Proc. IEEE 20th International Workshop on Signal Processing Advances in Wireless Communications (SPAWC)*, 2019, Cannes, France.

[A22] R. R. Müller, A. Bereyhi, and C. F. Mecklenbräuker, "Oversampled adaptive sensing with random projections: Analysis and algorithmic approaches," *Proc.*

IEEE International Symposium on Signal Processing and Information Technology (ISSPIT), pp. 336–341, December 2018, Louisville, KY, USA.

[A23] R. R. Müller, A. Bereyhi, and C. Mecklenbräuker, "Oversampled adaptive sensing," *Proc. Information Theory and Applications Workshop (ITA)*, pp. 1–7, February 2018, San Diego, CA, USA.

[A24] V. Schram, A. Bereyhi, J.-N. Zaech, R. R. Müller, and W. H. Gerstacker, "Approximate message passing for indoor THz channel estimation," *Proc. 3rd International Balkan Conference on Communications and Networking*, June 2019, Skopje, North Macedonia.

[A25] B. Gäde, M. Amon, A. Bereyhi, G. Fischer, and R. R. Müller, "Outphasing elements for hybrid analogue digital beamforming and single-RF MIMO," *Proc. IEEE International Conference on Acoustics, Speech and Signal Processing (ICASSP)*, pp. 7839–7843, May 2019, Brighton, UK.

[A26] A. Bereyhi, M. A. Sedaghat, and R. R. Müller, "RLS recovery with asymmetric penalty: Fundamental limits and algorithmic approaches," *Proc. 2nd International Balkan Conference on Communications and Networking*, June 2018, Podgorica, Montenegro.

[A27] A. Bereyhi, V. Jamali, , R. R. Müller, G. F. R. Schober, and A. M. Tulino, "PAPR-limited precoding in massive MIMO systems with reflect- and transmit-array antennas," *Proc. Asilomar Conference on Signals, Systems, and Computers (to be appeared)*, November 2019, Pacific Grove, CA, USA.

[A28] S. Asaad, A. Bereyhi, R. R. Müller, and R. F. Schaefer, "Secure regularized zero forcing for multiuser MIMOME channels," *Proc. Asilomar Conference on Signals, Systems, and Computers (to be appeared)*, November 2019, Pacific Grove, CA, USA.

[A29] S. Asaad, A. Bereyhi, R. R. Müller, and R. F. Schaefer, "Joint user selection and precoding in multiuser MIMO systems via group LASSO," *Proc. IEEE In-*

ternational Symposium on Personal, Indoor and Mobile Radio Communications (PIMRC), September 2019, Istanbul, Turkey.

Bibliography

[1] R. H. Myers, *Classical and modern regression with applications*, 2nd ed. Duxbury Advanced Series in Statistics and Decision Sciences, Duxbury Classic Series, Duxbury Press Belmont, USA, 1990, vol. 2.

[2] J. Neter, M. H. Kutner, C. J. Nachtsheim, and W. Wasserman, *Applied linear statistical models*, 5th ed. McGraw-Hill, Irwin, USA, 2004, vol. 4.

[3] S. Weisberg, *Applied linear regression*, 3rd ed. Wiley Series in Probability and Statistics, John Wiley & Sons, New Jersey, USA, 2005, vol. 528.

[4] T. P. Ryan, *Modern regression methods*, 2nd ed. Wiley Series in Probability and Statistics, John Wiley & Sons, New Jersey, USA, 2009, vol. 655.

[5] D. C. Montgomery, E. A. Peck, and G. G. Vining, *Introduction to linear regression analysis*, 5th ed. John Wiley & Sons, New Jersey, USA, 2012, vol. Wiley Series in Probability and Statistics; 821.

[6] G. A. Seber and A. J. Lee, *Linear regression analysis*, 2nd ed. John Wiley & Sons, New Jersey, USA, 2012, vol. Wiley Series in Probability and Statistics; 329.

[7] D. L. Donoho, "Compressed sensing," *IEEE Transactions on Information Theory*, vol. 52, no. 4, pp. 1289–1306, 2006.

[8] T. Richardson and R. Urbanke, *Modern coding theory*. Cambridge University Press, Cambridge, UK, 2008.

[9] S. M. Kay, *Fundamentals of statistical Signal Processing: Estimation theory*. Upper Saddle River, Prentice Hall PTR, New Jersey, USA, 1993, vol. 1.

[10] ——, *Fundamentals of statistical signal processing: Detection theory.* Upper Saddle River, Prentice Hall PTR, New Jersey, USA, 2009, vol. 2.

[11] A. J. Viterbi, *CDMA: Principles of spread spectrum communication.* Addison-Wesley Wireless Communications Series, Addison Wesley Longman Publishing Co., Inc., USA, 1995.

[12] M. Vu and A. Paulraj, "MIMO wireless linear precoding," *IEEE Signal Processing Magazine*, vol. 24, no. 5, pp. 86–105, September 2007.

[13] I. Tosic and P. Frossard, "Dictionary learning: What is the right representation for my signal?" *IEEE Signal Processing Magazine*, vol. 28.

[14] S. Foucart and H. Rauhut, *A mathematical introduction to compressive sensing.* Birkhäuser, New York, USA, 2013, vol. 1, no. 3.

[15] L. Pastur and M. Shcherbina, "Absence of self-averaging of the order parameter in the Sherrington-Kirkpatrick model," *Journal of Statistical Physics*, vol. 62, no. 1-2, pp. 1–19, 1991.

[16] F. Guerra and F. L. Toninelli, "The thermodynamic limit in mean field spin glass models," *Communications in Mathematical Physics*, vol. 230, no. 1, pp. 71–79, 2002.

[17] ——, "The infinite volume limit in generalized mean field disordered models," *arXiv preprint cond-mat/0208579*, 2002.

[18] S. B. Korada and N. Macris, "Tight bounds on the capacity of binary input random CDMA systems," *IEEE Transactions on Information Theory*, vol. 56, no. 11, pp. 5590–5613, 2010.

[19] A. Dembo and O. Zeitouni, *Large deviations techniques and applications*, corrected printing of the 1998 edition ed. Stochastic Modelling and Applied Probability, Springer-Verlag, New York, USA, 2009, vol. 38.

[20] F. Riesz, "Sur les valeurs moyennes des fonctions," *Journal of the London Mathematical Society*, vol. 1, no. 2, pp. 120–121, 1930.

[21] J. Shore and R. Johnson, "Axiomatic derivation of the principle of maximum entropy and the principle of minimum cross-entropy," *IEEE Transactions on Information Theory*, vol. 26, no. 1, pp. 26–37, 1980.

[22] E. T. Jaynes, "Information theory and statistical mechanics," *Physical review*, vol. 106, no. 4, p. 620, 1957.

[23] ——, "Information theory and statistical mechanics. II," *Physical review*, vol. 108, no. 2, p. 171, 1957.

[24] R. Baierlein, *Atoms and information theory: An introduction to statistical mechanics*. W. H. Freeman, San Francisco, USA, 1971.

[25] N. Merhav, "A statistical-mechanical view on source coding: physical compression and data compression," *Journal of Statistical Mechanics: Theory and Experiment*, vol. 2011, no. 01, p. P01029, 2011.

[26] H. Nishimori, *Statistical physics of spin glasses and information processing: an introduction*. Oxford University Press, UK, 2001, no. 111.

[27] B. Derrida, "Random-energy model: Limit of a family of disordered models," *Physical Review Letters*, vol. 45, no. 2, p. 79, 1980.

[28] ——, "Random-energy model: An exactly solvable model of disordered systems," *Physical Review B*, vol. 24, no. 5, p. 2613, 1981.

[29] D. Sherrington and S. Kirkpatrick, "Solvable model of a spin-glass," *Physical Review Letters*, vol. 35, no. 26, pp. 1792–1796, 1975.

[30] S. Kirkpatrick and D. Sherrington, "Infinite-ranged models of spin-glasses," *Physical Review B*, vol. 17, no. 11, p. 4384, 1978.

[31] M. Mézard and G. Parisi, "A replica analysis of the travelling salesman problem," *Journal de Physique*, vol. 47, no. 8, pp. 1285–1296, 1986.

[32] Y. Fu and P. W. Anderson, "Application of statistical mechanics to NP-complete problems in combinatorial optimisation," *Journal of Physics A: Mathematical and General*, vol. 19, no. 9, p. 1605, 1986.

[33] A. Montanari, "Turbo codes: The phase transition," *The European Physical Journal B-Condensed Matter and Complex Systems*, vol. 18, no. 1, pp. 121–136, 2000.

[34] H. Seung, H. Sompolinsky, and N. Tishby, "Statistical mechanics of learning from examples," *Physical Review A*, vol. 45, no. 8, p. 6056, 1992.

[35] Y. Kabashima and D. Saad, "Statistical mechanics of error-correcting codes," *EPL (Europhysics Letters)*, vol. 45, no. 1, p. 97, 1999.

[36] ——, "Statistical mechanics of low-density parity-check codes," *Journal of Physics A: Mathematical and General*, vol. 37, no. 6, p. R1, 2004.

[37] T. Murayama, Y. Kabashima, D. Saad, and R. Vicente, "Statistical physics of regular low-density parity-check error-correcting codes," *Physical Review E*, vol. 62, no. 2, p. 1577, 2000.

[38] A. Montanari and N. Sourlas, "The statistical mechanics of turbo codes," *The European Physical Journal B-Condensed Matter and Complex Systems*, vol. 18, no. 1, pp. 107–119, 2000.

[39] H. Nishimori and K. M. Wong, "Statistical mechanics of image restoration and error-correcting codes," *Physical Review E*, vol. 60, no. 1, p. 132, 1999.

[40] T. Tanaka, "A statistical-mechanics approach to large-system analysis of CDMA multiuser detectors," *IEEE Transactions on Information Theory*, vol. 48, no. 11, pp. 2888–2910, 2002.

[41] ——, "Average-case analysis of multiuser detectors," in *Proceedings of IEEE International Symposium on Information Theory (ISIT)*. IEEE, 2001, p. 287.

[42] D. Guo and S. Verdú, "Multiuser detection and statistical mechanics," in *Proceedings of Communications, Information and Network Security*. Springer, 2003, pp. 229–277.

[43] ——, "Randomly spread CDMA: Asymptotics via statistical physics," *IEEE Transactions on Information Theory*, vol. 51, no. 6, pp. 1983–2010, 2005.

[44] R. R. Müller, "Channel capacity and minimum probability of error in large dual antenna array systems with binary modulation," *IEEE Transactions on Signal Processing*, vol. 51, no. 11, pp. 2821–2828, 2003.

[45] R. Müller, D. Guo, and A. L. Moustakas, "Vector precoding for wireless MIMO systems and its replica analysis," *IEEE Journal on Selected Areas in Communications*, vol. 26, no. 3, pp. 530–540, 2008.

[46] D. Guo, D. Baron, and S. Shamai, "A single-letter characterization of optimal noisy compressed sensing," in *Proceedings of 47th Annual Allerton Conference on Communication, Control, and Computing*. IEEE, 2009, pp. 52–59.

[47] J. Barbier and F. Krzakala, "Replica analysis and approximate message passing decoder for superposition codes," in *Proceedings of IEEE International Symposium on Information Theory (ISIT)*. IEEE, 2014, pp. 1494–1498.

[48] A. Montanari and D. Tse, "Analysis of belief propagation for non-linear problems: The example of CDMA (or: How to prove tanaka's formula)," in *Proceedings of IEEE Information Theory Workshop (ITW)*. IEEE, 2006, pp. 160–164.

[49] W. Huleihel and N. Merhav, "Asymptotic MMSE analysis under sparse representation modeling," *Signal Processing*, vol. 131, pp. 320–332, 2017.

[50] G. Reeves and H. D. Pfister, "The replica-symmetric prediction for compressed sensing with Gaussian matrices is exact," in *Proceedings of IEEE International Symposium on Information Theory (ISIT)*. IEEE, 2016, pp. 665–669.

[51] J. Barbier, M. Dia, N. Macris, and F. Krzakala, "The mutual information in random linear estimation," in *Proceedings of 54th Annual Allerton Conference on Communication, Control, and Computing*. IEEE, 2016, pp. 625–632.

[52] J. Barbier, N. Macris, M. Dia, and F. Krzakala, "Mutual information and optimality of approximate message-passing in random linear estimation," *IEEE Transactions on Information Theory*, vol. 66, no. 7, pp. 4270 – 4303, July 2020.

[53] J. Barbier, M. Dia, and N. Macris, "Threshold saturation of spatially coupled sparse superposition codes for all memoryless channels," in *Proceedings of IEEE Information Theory Workshop (ITW)*. IEEE, 2016, pp. 76–80.

[54] ——, "Universal sparse superposition codes with spatial coupling and gamp decoding," *IEEE Transactions on Information Theory*, vol. 65, no. 9, pp. 5618–5642, 2019.

[55] S. Rangan, A. K. Fletcher, and V. Goyal, "Asymptotic analysis of MAP estimation via the replica method and applications to compressed sensing," *IEEE Transactions on Information Theory*, vol. 58, no. 3, pp. 1902–1923, 2012.

[56] M. L. Mehta, *Random matrices*, 3rd ed. Elsevier Academic Press, USA, 2004, vol. 142 of Pure and Applied Mathematics.

[57] R. R. Müller, G. Alfano, B. M. Zaidel, and R. de Miguel, "Applications of large random matrices in communications engineering," *arXiv preprint arXiv:1310.5479*, 2013.

[58] A. M. Tulino and S. Verdú, "Random matrix theory and wireless communications," *Foundations and Trends in Communications and Information Theory*, vol. 1, no. 1, pp. 1–182, 2004.

[59] A. Guionnet, M. Maı *et al.*, "A Fourier view on the R-transform and related asymptotics of spherical integrals," *Journal of functional analysis*, vol. 222, no. 2, pp. 435–490, 2005.

[60] A. Dembo and O. Zeitouni, *Large deviations techniques and applications*. Springer Science & Business Media, New York, USA, 2009, vol. 38.

[61] M. Mezard and A. Montanari, *Information, physics, and computation*. Oxford University Press, UK, 2009.

[62] V. Dotsenko, *Introduction to the replica theory of disordered statistical systems*. Cambridge University Press, Cambridge, UK, 2005, vol. 4.

[63] G. Parisi, "A sequence of approximated solutions to the SK model for spin glasses," *Journal of Physics A: Mathematical and General*, vol. 13, no. 4, p. L115, 1980.

[64] B. M. Zaidel, R. Müller, A. L. Moustakas, and R. de Miguel, "Vector precoding for Gaussian MIMO broadcast channels: Impact of replica symmetry breaking," *IEEE Transactions on Information Theory*, vol. 58, no. 3, pp. 1413–1440, 2012.

[65] J. de Almeida and D. J. Thouless, "Stability of the Sherrington-Kirkpatrick solution of a spin glass model," *Journal of Physics A: Mathematical and General*, vol. 11, no. 5, p. 983, 1978.

[66] G. Parisi, "Toward a mean field theory for spin glasses," *Physics Letters A*, vol. 73, no. 3, pp. 203–205, 1979.

[67] ——, "The order parameter for spin glasses: a function on the interval 0-1," *Journal of Physics A: Mathematical and General*, vol. 13, no. 3, p. 1101, 1980.

[68] F. Guerra, "Broken replica symmetry bounds in the mean field spin glass model," *Communications in mathematical physics*, vol. 233, no. 1, pp. 1–12, 2003.

[69] M. Talagrand, "The parisi formula," *Annals of mathematics*, pp. 221–263, 2006.

[70] G. Parisi, "Order parameter for spin-glasses," *Physical Review Letters*, vol. 50, no. 24, p. 1946, 1983.

[71] M. Mézard, G. Parisi, and M. Virasoro, *Spin glass theory and beyond: An Introduction to the Replica Method and Its Applications*. World Scientific Publishing Company, Singapore, 1987, vol. 9.

[72] M. Mézard, G. Parisi, N. Sourlas, G. Toulouse, and M. Virasoro, "Replica symmetry breaking and the nature of the spin glass phase," *Journal de Physique*, vol. 45, no. 5, pp. 843–854, 1984.

[73] A. L. Moustakas and S. H. Simon, "On the outage capacity of correlated multiple-path MIMO channels," *IEEE Transactions on Information Theory*, vol. 53, no. 11, pp. 3887–3903, 2007.

[74] G. Reeves and H. D. Pfister, "The replica-symmetric prediction for random linear estimation with Gaussian matrices is exact," *IEEE Transactions on Information Theory*, vol. 65, no. 4, pp. 2252–2283, 2019.

[75] M. Yoshida, T. Uezu, T. Tanaka, and M. Okada, "Statistical mechanical study of code-division multiple-access multiuser detectors—analysis of replica symmetric and one-step replica symmetry breaking solutions—," *Journal of the Physical Society of Japan*, vol. 76, no. 5, pp. 054 003–054 003, 2007.

[76] D. J. Ryan, I. B. Collings, I. V. L. Clarkson, and R. W. Heath Jr, "Performance of vector perturbation multiuser MIMO systems with limited feedback," *IEEE Transactions on Communications*, vol. 57, no. 9, p. 2633, 2009.

[77] Y. Kabashima, T. Wadayama, and T. Tanaka, "A typical reconstruction limit for compressed sensing based on ℓ_p-norm minimization," *Journal of Statistical Mechanics: Theory and Experiment*, vol. 2009, no. 09, p. L09003, 2009.

[78] N. I. Akhiezer, *The classical moment problem: and some related questions in analysis*. Oliver & Boyd, Edinburgh, UK, 1965, vol. 5.

[79] B. Simon, "The classical moment problem as a self-adjoint finite difference operator," *Advances in Mathematics*, vol. 137, no. 1, pp. 82–203, 1998.

[80] J. A. Shohat and J. D. Tamarkin, *The problem of moments*. American Mathematical Society, USA, 1943, no. 1.

[81] W. Feller, *An introduction to probability theory and its applications*. John Wiley & Sons, New Jersey, USA, 2008, vol. 2.

[82] M. Nygaard and E. M. Schmidt, *Transition systems: Algorithms and data structures*. Department of Computer Science, University of Aarhus, Aarhus, Denmark, February 2004, vol. DAIMI-FN-64.

[83] A. Finkel and P. Schnoebelen, "Fundamental structures in well-structured infinite transition systems," in *Proceedings of Latin American Symposium on Theoretical Informatics*. Springer, 1998, pp. 102–118.

[84] D. N. Tse and S. V. Hanly, "Linear multiuser receivers: Effective interference, effective bandwidth and user capacity," *IEEE Transactions on Information Theory*, vol. 45, no. 2, pp. 641–657, 1999.

[85] D. N. Tse and O. Zeitouni, "Linear multiuser receivers in random environments," *IEEE Transactions on Information Theory*, vol. 46, no. 1, pp. 171–188, 2000.

[86] Y. C. Eldar and A. M. Chan, "On the asymptotic performance of the decorrelator," *IEEE Transactions on Information Theory*, vol. 49, no. 9, pp. 2309–2313, 2003.

[87] S. Verdú and S. Shamai, "Spectral efficiency of CDMA with random spreading," *IEEE Transactions on Information Theory*, vol. 45, no. 2, pp. 622–640, 1999.

[88] J. Zhang, E. K. Chong, and D. N. Tse, "Output MAI distributions of linear MMSE multiuser receivers in DS-CDMA systems," *IEEE Transactions on Information Theory*, vol. 47, no. 3, pp. 1128–1144, 2001.

[89] D. Guo, S. Verdú, and L. K. Rasmussen, "Asymptotic normality of linear multiuser receiver outputs," *IEEE Transactions on Information Theory*, vol. 48, no. 12, pp. 3080–3095, 2002.

[90] D. Guo, L. K. Rasmussen, and T. J. Lim, "Linear parallel interference cancellation in long-code CDMA multiuser detection," *IEEE Journal on Selected Areas in Communications*, vol. 17, no. 12, pp. 2074–2081, 1999.

[91] S. Shamai and S. Verdú, "The impact of frequency-flat fading on the spectral efficiency of CDMA," *IEEE Transactions on Information Theory*, vol. 47, no. 4, pp. 1302–1327, 2001.

[92] R. R. Müller and W. H. Gerstacker, "On the capacity loss due to separation of detection and decoding," *IEEE Transactions on Information Theory*, vol. 50, no. 8, pp. 1769–1778, 2004.

[93] R. R. Müller, "On channel capacity, uncoded error probability, ML-detection, and spin glasses," in *Proceedings of Workshop on Concepts in Information Theory*, 2002, pp. 79–81.

[94] A. M. Tulino, G. Caire, S. Verdu, and S. Shamai, "Support recovery with sparsely sampled free random matrices," *IEEE Transactions on Information Theory*, vol. 59, no. 7, pp. 4243–4271, 2013.

[95] C. Chen and J. Huang, "Compressive sensing MRI with wavelet tree sparsity," in *Proceedings Advances in Neural Information Processing Systems*, 2012, pp. 1115–1123.

[96] J. Sun, H. Li, Z. Xu *et al.*, "Deep ADMM-Net for compressive sensing MRI," in *Proceedings Advances in Neural Information Processing Systems*, 2016, pp. 10–18.

[97] N. S. Rao, R. D. Nowak, S. J. Wright, and N. G. Kingsbury, "Convex approaches to model wavelet sparsity patterns," in *Proceedings of 18th IEEE International Conference on Image Processing*. IEEE, 2011, pp. 1917–1920.

[98] M. Lustig, D. L. Donoho, J. M. Santos, and J. M. Pauly, "Compressed sensing MRI," *IEEE Signal Processing Magazine*, vol. 25, no. 2, p. 72, 2008.

[99] M. Lustig, D. Donoho, and J. M. Pauly, "Sparse MRI: The application of compressed sensing for rapid MR imaging," *Magnetic Resonance in Medicine: An Official Journal of the International Society for Magnetic Resonance in Medicine*, vol. 58, no. 6, pp. 1182–1195, 2007.

[100] J. Bobin, J.-L. Starck, J. Fadili, and Y. Moudden, "Sparsity and morphological diversity in blind source separation," *IEEE Transactions on Image Processing*, vol. 16, no. 11, pp. 2662–2674, 2007.

[101] C. F. Caiafa and A. Cichocki, "Computing sparse representations of multidimensional signals using kronecker bases," *Neural computation*, vol. 25, no. 1, pp. 186–220, 2013.

[102] E. J. Candès, J. Romberg, and T. Tao, "Robust uncertainty principles: Exact signal reconstruction from highly incomplete frequency information," *IEEE Transactions on Information Theory*, vol. 52, no. 2, pp. 489–509, 2006.

[103] E. J. Candes and T. Tao, "Near-optimal signal recovery from random projections: Universal encoding strategies?" *IEEE Transactions on Information Theory*, vol. 52, no. 12, pp. 5406–5425, 2006.

[104] R. Tibshirani, "Regression shrinkage and selection via the lasso," *Journal of the Royal Statistical Society. Series B (Methodological)*, pp. 267–288, 1996.

[105] D. L. Donoho, A. Maleki, and A. Montanari, "Message-passing algorithms for compressed sensing," *Proceedings of the National Academy of Sciences*, vol. 106, no. 45, pp. 18 914–18 919, 2009.

[106] ——, "Message passing algorithms for compressed sensing: I. motivation and construction," in *Proceedings of IEEE Information Theory Workshop (ITW)*. IEEE, 2010, pp. 1–5.

[107] D. L. Donoho and J. Tanner, "Precise undersampling theorems," *Proceedings of the IEEE*, vol. 98, no. 6, pp. 913–924, 2010.

[108] R. Couillet and M. Debbah, *Random matrix methods for wireless communications*. Cambridge University Press, Cambridge, UK, 2011.

[109] M. Vehkaperä, Y. Kabashima, and S. Chatterjee, "Analysis of regularized LS reconstruction and random matrix ensembles in compressed sensing," *IEEE Transactions on Information Theory*, vol. 62, no. 4, pp. 2100–2124, 2016.

[110] D. Agrawal and A. Vardy, "The turbo decoding algorithm and its phase trajectories," *IEEE Transactions on Information Theory*, vol. 47, no. 2, pp. 699–722, 2001.

[111] S. Chen, S. A. Billings, and W. Luo, "Orthogonal least squares methods and their application to non-linear system identification," *International Journal of control*, vol. 50, no. 5, pp. 1873–1896, 1989.

[112] S. Qian and D. Chen, "Signal representation using adaptive normalized Gaussian functions," *Signal processing*, vol. 36, no. 1, pp. 1–11, 1994.

[113] L. F. Villemoes, "Best approximation with walsh atoms," *Constructive Approximation*, vol. 13, no. 3, pp. 329–355, 1997.

[114] D. L. Donoho and P. B. Stark, "Uncertainty principles and signal recovery," *SIAM Journal on Applied Mathematics*, vol. 49, no. 3, pp. 906–931, 1989.

[115] L. Breiman, "Better subset regression using the nonnegative garrote," *Technometrics*, vol. 37, no. 4, pp. 373–384, 1995.

[116] L. Breiman and P. Spector, "Submodel selection and evaluation in regression. the X-random case," *International statistical review (revue internationale de Statistique)*, pp. 291–319, 1992.

[117] I. Daubechies, S. Jaffard, and J.-L. Journe, "A simple Wilson orthonormal basis with exponential decay," *SIAM Journal on Mathematical Analysis*, vol. 22, no. 2, pp. 554–573, 1991.

[118] D. L. Donoho, "Orthonormal ridgelets and linear singularities," *SIAM Journal on Mathematical Analysis*, vol. 31, no. 5, pp. 1062–1099, 2000.

[119] S. Mallat, *A wavelet tour of signal processing*, 2nd ed. Elsevier Academic Press, California, USA, 1999.

[120] K. R. Rao and P. Yip, *Discrete cosine transform: algorithms, advantages, applications*, 1st ed. Elsevier Academic Press, California, USA, 2014.

[121] D. L. Donoho and X. Huo, "Uncertainty principles and ideal atomic decomposition," *IEEE Transactions on Information Theory*, vol. 47, no. 7, pp. 2845–2862, 2001.

[122] M. Elad and A. M. Bruckstein, "A generalized uncertainty principle and sparse representation in pairs of bases," *IEEE Transactions on Information Theory*, vol. 48, no. 9, pp. 2558–2567, 2002.

[123] D. L. Donoho and M. Elad, "Optimally sparse representation in general (nonorthogonal) dictionaries via ℓ_1 minimization," *Proceedings of the National Academy of Sciences*, vol. 100, no. 5, pp. 2197–2202, 2003.

[124] G. B. Folland and A. Sitaram, "The uncertainty principle: a mathematical survey," *Journal of Fourier Analysis and Applications*, vol. 3, no. 3, pp. 207–238, 1997.

[125] E. J. Candès and M. B. Wakin, "An introduction to compressive sampling [a sensing/sampling paradigm that goes against the common knowledge in data acquisition]," *IEEE Signal Processing Magazine*, vol. 25, no. 2, pp. 21–30, 2008.

[126] R. G. Baraniuk, "Compressive sensing," *IEEE Signal Processing Magazine*, vol. 24, no. 4, 2007.

[127] S. Chen and D. Donoho, "Basis pursuit," in *Proceedings of the Asilomar Conference on Signals, Systems and Computers*, vol. 1. IEEE, 1994, pp. 41–44.

[128] S. S. Chen, D. L. Donoho, and M. A. Saunders, "Atomic decomposition by basis pursuit," *SIAM review*, vol. 43, no. 1, pp. 129–159, 2001.

[129] D. Needell and J. A. Tropp, "Cosamp: Iterative signal recovery from incomplete and inaccurate samples," *Applied and Computational Harmonic Analysis*, vol. 26, no. 3, pp. 301–321, 2009.

[130] W. Dai and O. Milenkovic, "Subspace pursuit for compressive sensing signal reconstruction," *IEEE Transactions on Information Theory*, vol. 55, no. 5, pp. 2230–2249, 2009.

[131] T. T. Cai and L. Wang, "Orthogonal matching pursuit for sparse signal recovery with noise," *IEEE Transactions on Information Theory*, vol. 57, no. 7, pp. 4680–4688, 2011.

[132] R. G. Baraniuk, V. Cevher, M. F. Duarte, and C. Hegde, "Model-based compressive sensing," *IEEE Transactions on Information Theory*, vol. 56, no. 4, pp. 1982–2001, April 2010.

[133] E. J. Candes, "The restricted isometry property and its implications for compressed sensing," *Comptes rendus mathematique*, vol. 346, no. 9-10, pp. 589–592, 2008.

[134] R. Baraniuk, M. Davenport, R. DeVore, and M. Wakin, "A simple proof of the restricted isometry property for random matrices," *Constructive Approximation*, vol. 28, no. 3, pp. 253–263, 2008.

[135] Y. Kabashima, T. Wadayama, and T. Tanaka, "Statistical mechanical analysis of a typical reconstruction limit of compressed sensing," *Proceedings of IEEE International Symposium on Information Theory (ISIT)*, pp. 1533–1537, 2010.

[136] C.-K. Wen, J. Zhang, K.-K. Wong, J.-C. Chen, and C. Yuen, "On sparse vector recovery performance in structurally orthogonal matrices via lasso," *IEEE Transactions on Signal Processing*, vol. 64, no. 17, pp. 4519–4533, 2016.

[137] L. Zheng, A. Maleki, H. Weng, X. Wang, and T. Long, "Does ℓ_p-minimization outperform ℓ_1-minimization?" *IEEE Transactions on Information Theory*, 2017.

[138] D. L. Donoho, A. Maleki, and A. Montanari, "How to design message passing algorithms for compressed sensing," *preprint*, 2011.

[139] A. Maleki and D. L. Donoho, "Optimally tuned iterative reconstruction algorithms for compressed sensing," *IEEE Journal of Selected Topics in Signal Processing*, vol. 4, no. 2, pp. 330–341, April 2010.

[140] S. Rangan, "Generalized approximate message passing for estimation with random linear mixing," in *Proceedings of IEEE International Symposium on Information Theory (ISIT)*. IEEE, 2011, pp. 2168–2172.

[141] A. Montanari, "Graphical models concepts in compressed sensing," *Compressed Sensing: Theory and Applications*, pp. 394–438, 2012.

[142] M. Bayati and A. Montanari, "The dynamics of message passing on dense graphs, with applications to compressed sensing," *IEEE Transactions on Information Theory*, vol. 57, no. 2, pp. 764–785, 2011.

[143] E. Bolthausen, "Random dynamical generation of thetap equations and the high-temperature solution of the skmodel," in *Presented in Seminar at European Institute for Statistics, Probability, Stochastic Operations Research and its Applications (Eurandom), Eindhoven*, December 2009.

[144] S. Rangan, P. Schniter, and A. K. Fletcher, "Vector approximate message passing," in *Proceedings of IEEE International Symposium on Information Theory (ISIT)*. IEEE, 2017, pp. 1588–1592.

[145] K. Takeuchi, "Rigorous dynamics of expectation-propagation-based signal recovery from unitarily invariant measurements," *arXiv preprint arXiv:1701.05284*, 2017.

[146] Y. Wu and S. Verdú, "Optimal phase transitions in compressed sensing," *IEEE Transactions on Information Theory*, vol. 58, no. 10, pp. 6241–6263, 2012.

[147] ——, "MMSE dimension," *IEEE Transactions on Information Theory*, vol. 57, no. 8, pp. 4857–4879, 2011.

[148] D. L. Donoho, A. Javanmard, and A. Montanari, "Information-theoretically optimal compressed sensing via spatial coupling and approximate message passing," *IEEE Transactions on Information Theory*, vol. 59, no. 11, pp. 7434–7464, 2013.

[149] F. Krzakala, M. Mézard, F. Sausset, Y. Sun, and L. Zdeborová, "Statistical-physics-based reconstruction in compressed sensing," *Physical Review X*, vol. 2, no. 2, p. 021005, 2012.

[150] S. Haykin and M. Moher, *Communication systems*, 5th ed. John Wiley & Sons, New Jersey, USA, 2009.

[151] H. Q. Ngo and E. G. Larsson, "EVD-based channel estimations for multicell multiuser MIMO with very large antenna arrays," in *Proceedings of IEEE International Conference on Acoustics, Speech and Signal Processing (ICASSP)*. IEEE, 2012, pp. 3249–3252.

[152] F. Kaltenberger, H. Jiang, M. Guillaud, and R. Knopp, "Relative channel reciprocity calibration in MIMO/TDD systems," in *Proceedings of Future Network and Mobile Summit*. IEEE, 2010, pp. 1–10.

[153] J. W. Ketchum, M. S. Wallace, J. R. Walton, and S. J. Howard, "Channel estimation and spatial processing for TDD MIMO systems," Jan. 26 2010, US Patent 7,653,142.

[154] E. G. Larsson, O. Edfors, F. Tufvesson, and T. L. Marzetta, "Massive MIMO for next generation wireless systems," *IEEE Communications Magazine*, vol. 52, no. 2, pp. 186–195, 2014.

[155] C. B. Peel, B. M. Hochwald, and A. L. Swindlehurst, "A vector-perturbation technique for near-capacity multiantenna multiuser communication-part I: channel inversion and regularization," *IEEE Transactions on Communications*, vol. 53, no. 1, pp. 195–202, 2005.

[156] S. K. Mohammed and E. G. Larsson, "Per-antenna constant envelope precoding for large multi-user MIMO systems," *IEEE Transactions on Communications*, vol. 61, no. 3, pp. 1059–1071, 2013.

[157] D. Spano, M. Alodeh, S. Chatzinotas, and B. Ottersten, "Symbol-level precoding for the non-linear multiuser MISO downlink channel," *IEEE Transactions on Signal Processing*, 2017.

[158] M. Alodeh, D. Spano, A. Kalantari, C. Tsinos, D. Christopoulos, S. Chatzinotas, and B. Ottersten, "Symbol-level and multicast precoding for multiuser multiantenna downlink: A state-of-the-art, classification and challenges," *IEEE Communications Surveys & Tutorials*, 2018.

[159] J. Hoydis, S. Ten Brink, and M. Debbah, "Massive MIMO in the UL/DL of cellular networks: How many antennas do we need?" *IEEE Journal on selected Areas in Communications*, vol. 31, no. 2, pp. 160–171, 2013.

[160] H. Li, L. Song, and M. Debbah, "Energy efficiency of large-scale multiple antenna systems with transmit antenna selection," *IEEE Transactions on Communications*, vol. 62, no. 2, pp. 638–647, 2014.

[161] J. Xu and L. Qiu, "Energy efficiency optimization for MIMO broadcast channels," *IEEE Transactions on Wireless Communications*, vol. 12, no. 2, pp. 690–701, 2013.

[162] O. Tervo, L.-N. Tran, H. Pennanen, S. Chatzinotas, M. Juntti, and B. Ottersten, "Energy-efficient coordinated multi-cell multi-group multicast beamforming with antenna selection," in *Proceedings of IEEE International Conference on Communications Workshops (ICC Workshops)*, 2017, pp. 1209–1214.

[163] S. Asaad, A. M. Rabiei, and R. R. Müller, "Massive MIMO with antenna selection: Fundamental limits and applications," *IEEE Transactions on Wireless Communications*, vol. 17, no. 12, pp. 8502–8516, 2018.

[164] M. Gharavi-Alkhansari and A. B. Gershman, "Fast antenna subset selection in MIMO systems," *IEEE Transactions on Signal Processing*, vol. 52, no. 2, pp. 339–347, 2004.

[165] A. Gorokhov, D. A. Gore, and A. J. Paulraj, "Receive antenna selection for MIMO spatial multiplexing: Theory and algorithms," *IEEE Transactions on Signal Processing*, vol. 51, no. 11, pp. 2796–2807, 2003.

[166] A. A. Saleh, "Frequency-independent and frequency-dependent nonlinear models of TWT amplifiers," *IEEE Transactions on Communications*, vol. 29, no. 11, pp. 1715–1720, 1981.

[167] S. C. Cripps, *RF Power Amplifiers for Wireless Communications*, 2nd ed. Artech House Microwave Library, USA, 2006.

[168] D. Schreurs, M. O'Droma, A. A. Goacher, and M. Gadringer, *RF power amplifier behavioral modeling.* Cambridge University Press, Cambridge, UK, 2008.

[169] M. O'Droma, S. Meza, and Y. Lei, "New modified Saleh models for memoryless nonlinear power amplifier behavioural modelling," *IEEE Communications Letters*, vol. 13, no. 6, 2009.

[170] M. O'Droma and L. Yiming, "A new Bessel-Fourier memoryless nonlinear power amplifier behavioral model," *IEEE Microwave and Wireless Components Letters*, vol. 23, no. 1, pp. 25–27, 2013.

[171] M. A. Sedaghat, R. R. Müller, and G. Fischer, "A novel single-RF transmitter for massive MIMO," in *Proceedings of International ITG Workshop on Smart Antennas (WSA).* VDE, 2014, pp. 1–8.

[172] M. A. Sedaghat, R. R. Müller, G. Fischer, and A. Ali, "Discrete load-modulated single-RF MIMO transmitters," in *Proceedings of International ITG Workshop on Smart Antennas (WSA).* VDE, 2016, pp. 1–7.

[173] M. A. Sedaghat, V. I. Barousis, R. R. Müller, and C. B. Papadias, "Load modulated arrays: a low-complexity antenna," *IEEE Communications Magazine*, vol. 54, no. 3, pp. 46–52, 2016.

[174] S. Jacobsson, G. Durisi, M. Coldrey, T. Goldstein, and C. Studer, "Quantized precoding for massive MU-MIMO," *IEEE Transactions on Communications*, vol. 65, no. 11, pp. 4670–4684, 2017.

[175] S. Jacobsson, G. Durisi, M. Coldrey, U. Gustavsson, and C. Studer, "Throughput analysis of massive MIMO uplink with low-resolution ADCs," *IEEE Transactions on Wireless Communications*, vol. 16, no. 6, pp. 4038–4051, 2017.

[176] S. Jacobsson, G. Durisi, M. Coldrey, and C. Studer, "Massive MU-MIMO-OFDM downlink with one-bit dacs and linear precoding," in *Proceedings of IEEE Global Communications Conference (GLOBECOM).* IEEE, 2017, pp. 1–6.

[177] A. K. Saxena, I. Fijalkow, and A. L. Swindlehurst, "Analysis of one-bit quantized precoding for the multiuser massive MIMO downlink," *IEEE Transactions on Signal Processing*, vol. 65, no. 17, pp. 4624–4634, 2017.

[178] S. Jacobsson, G. Durisi, M. Coldrey, and C. Studer, "Linear precoding with low-resolution dacs for massive MU-MIMO-OFDM downlink," *IEEE Transactions on Wireless Communications*, 2019.

[179] J. W. Silverstein and Z. Bai, "On the empirical distribution of eigenvalues of a class of large dimensional random matrices," *Journal of Multivariate Analysis*, vol. 54, no. 2, pp. 175–192, 1995.

[180] M. Grant and S. Boyd, "CVX: Matlab software for disciplined convex programming, version 2.1," http://cvxr.com/cvx, Mar. 2014.

[181] ——, "Graph implementations for nonsmooth convex programs," in *Recent Advances in Learning and Control*, ser. Lecture Notes in Control and Information Sciences, V. Blondel, S. Boyd, and H. Kimura, Eds. Springer-Verlag Limited, 2008, pp. 95–110, http://stanford.edu/~boyd/graph_dcp.html.

[182] G. J. Foschini, "Layered space-time architecture for wireless communication in a fading environment when using multi-element antennas," *Bell Labs Technical Journal*, vol. 1, no. 2, pp. 41–59, 1996.

[183] P. W. Wolniansky, G. J. Foschini, G. Golden, R. A. Valenzuela *et al.*, "V-BLAST: An architecture for realizing very high data rates over the rich-scattering wireless channel," in *Proceedings of International Symposium on Signals, Systems, and Electronics (ISSSE)*, vol. 98, 1998, pp. 295–300.

[184] G. J. Foschini and M. J. Gans, "On limits of wireless communications in a fading environment when using multiple antennas," *Wireless Personal Communications*, vol. 6, no. 3, pp. 311–335, 1998.

[185] E. Biglieri, G. Caire, and G. Taricco, "Limiting performance of block-fading channels with multiple antennas," *IEEE Transactions on Information Theory*, vol. 47, no. 4, pp. 1273–1289, 2001.

[186] R. R. Müller, A. Lampe, and J. Huber, "Gaussian multiple-access channels with weighted energy constraint," in *Proceedings of IEEE Information Theory Workshop (ITW)*. IEEE, 1998, pp. 106–107.

[187] R. R. Müller, "An asymptotic analysis of BLAST-like systems," in *Proceedings of IEEE International Conference on Communications (ICC)*, vol. 2. IEEE, 2001, pp. 560–564.

[188] E. Telatar, "Capacity of multi-antenna Gaussian channels," *European Transactions on Telecommunications*, vol. 10, no. 6, pp. 585–595, 1999.

[189] P. Viswanath, D. N. C. Tse, and V. Anantharam, "Asymptotically optimal water-filling in vector multiple-access channels," *IEEE Transactions on Information Theory*, vol. 47, no. 1, pp. 241–267, 2001.

[190] C. Windpassinger, R. F. Fischer, T. Vencel, and J. B. Huber, "Precoding in multiantenna and multiuser communications," *IEEE Transactions on Wireless Communications*, vol. 3, no. 4, pp. 1305–1316, 2004.

[191] D. Tse and P. Viswanath, *Fundamentals of wireless communication*. Cambridge University Press, Cambridge, UK, 2005.

[192] V. Tarokh, N. Seshadri, and A. R. Calderbank, "Space-time codes for high data rate wireless communication: Performance criterion and code construction," *IEEE Transactions on Information Theory*, vol. 44, no. 2, pp. 744–765, 1998.

[193] S. Alamouti, "A simple transmit diversity technique for wireless communications," *IEEE Journal on Selected Areas in Communications*, vol. 16, no. 8, pp. 1451–1458, 1998.

[194] V. Tarokh, H. Jafarkhani, and A. R. Calderbank, "Space-time block codes from orthogonal designs," *IEEE Transactions on Information theory*, vol. 45, no. 5, pp. 1456–1467, 1999.

[195] A. J. Paulraj and T. Kailath, "Increasing capacity in wireless broadcast systems using distributed transmission/directional reception (DTDR)," Sep. 6 1994, US Patent 5,345,599.

[196] D. Gesbert, H. Bölcskei, D. A. Gore, and A. J. Paulraj, "Outdoor MIMO wireless channels: Models and performance prediction," *IEEE Transactions on Communications*, vol. 50, no. 12, pp. 1926–1934, 2002.

[197] R. U. Nabar, H. Bölcskei, V. Erceg, D. Gesbert, and A. J. Paulraj, "Performance of multiantenna signaling techniques in the presence of polarization diversity," *IEEE Transactions on Signal Processing*, vol. 50, no. 10, pp. 2553–2562, 2002.

[198] P. Viswanath and D. Tse, "Sum capacity of the vector Gaussian broadcast channel and uplink-downlink duality," *IEEE Transactions on Information Theory*, vol. 49, no. 8, pp. 1912–1921, 2003.

[199] B. M. Hochwald, T. L. Marzetta, and V. Tarokh, "Multiple-antenna channel hardening and its implications for rate feedback and scheduling," *IEEE Transactions on Information Theory*, vol. 50, no. 9, pp. 1893–1909, 2004.

[200] D. Bai, P. Mitran, S. Ghassemzadeh, R. Miller, and V. Tarokh, "Rate of channel hardening of antenna selection diversity schemes and its implication on scheduling," *IEEE Transactions on Information Theory*, vol. 10, no. 55, pp. 4353–4365, 2009.

[201] R. Müller, "A random matrix model of communication via antenna arrays," *IEEE Transactions on Information Theory*, vol. 48, no. 9, pp. 2495–2506, 2002.

[202] G. Caire, R. Müller, and T. Tanaka, "Iterative multiuser joint decoding: optimal power allocation and low-complexity implementation," *IEEE Transactions on Information Theory*, vol. 50, no. 9, pp. 1950–1973, 2004.

[203] T. S. Rappaport, S. Sun, R. Mayzus, H. Zhao, Y. Azar, K. Wang, G. N. Wong, J. K. Schulz, M. Samimi, and F. Gutierrez, "Millimeter wave mobile communications for 5G cellular: It will work!" *IEEE Access*, vol. 1, pp. 335–349, 2013.

[204] Z. Pi and F. Khan, "An introduction to millimeter-wave mobile broadband systems," *IEEE Communications Magazine*, vol. 49, no. 6, pp. 101–107, 2011.

[205] C. H. Doan, S. Emami, A. M. Niknejad, and R. W. Brodersen, "Millimeter-wave CMOS design," *IEEE Journal of Solid-State Circuits*, vol. 40, no. 1, pp. 144–155, 2005.

[206] S. Rangan, T. S. Rappaport, and E. Erkip, "Millimeter-wave cellular wireless networks: Potentials and challenges," *Proceedings of the IEEE*, vol. 102, no. 3, pp. 366–385, March 2014.

[207] W. Roh, J.-Y. Seol, J. Park, B. Lee, J. Lee, Y. Kim, J. Cho, K. Cheun, and F. Aryanfar, "Millimeter-wave beamforming as an enabling technology for 5G cellular communications: Theoretical feasibility and prototype results," *IEEE Communications Magazine*, vol. 52, no. 2, pp. 106–113, 2014.

[208] T. L. Marzetta, "Noncooperative cellular wireless with unlimited numbers of base station antennas," *IEEE Transactions on Wireless Communications*, vol. 9, no. 11, pp. 3590–3600, 2010.

[209] F. Rusek, D. Persson, B. K. Lau, E. G. Larsson, T. L. Marzetta, O. Edfors, and F. Tufvesson, "Scaling up MIMO: Opportunities and challenges with very large arrays," *IEEE Signal Processing Magazine*, vol. 30, no. 1, pp. 40–60, 2013.

[210] T. L. Marzetta, "Massive MIMO: an introduction," *Bell Labs Technical Journal*, vol. 20, pp. 11–22, 2015.

[211] E. Björnson, E. G. Larsson, and T. L. Marzetta, "Massive MIMO: Ten myths and one critical question," *IEEE Communications Magazine*, vol. 54, no. 2, pp. 114–123, 2016.

[212] T. L. Marzetta, E. G. Larsson, H. Yang, and H. Q. Ngo, *Fundamentals of Massive MIMO*. Cambridge University Press, Cambridge, UK, 2016.

[213] L. Lu, G. Y. Li, A. L. Swindlehurst, A. Ashikhmin, and R. Zhang, "An overview of massive MIMO: Benefits and challenges," *IEEE Journal of Selected Topics in Signal Processing*, vol. 8, no. 5, pp. 742–758, 2014.

[214] B. R. Vojcic and W. M. Jang, "Transmitter precoding in synchronous multiuser communications," *IEEE Transactions on Communications*, vol. 46, no. 10, pp. 1346–1355, 1998.

[215] R. F. H. Fischer, *Precoding and signal shaping for digital transmission.* John Wiley & Sons, New Jersey, USA, 2005.

[216] E. Visotsky and U. Madhow, "Space-time transmit precoding with imperfect feedback," *IEEE Transactions on Information Theory*, vol. 47, no. 6, pp. 2632–2639, 2001.

[217] Z. Tang and S. Cheng, "Interference cancellation for DS-CDMA systems over flat fading channels through pre-decorrelating," in *Proceedings of 5th IEEE International Symposium on Personal, Indoor and Mobile Radio Communications (PIMRC)*, vol. 2. IEEE, 1994, pp. 435–438.

[218] R. F. Fischer, C. Windpassinger, A. Lampe, and J. B. Huber, "Space-time transmission using Tomlinson-Harashima precoding," *Proc. of 4th ITG Conference on Source and Channel Coding*, pp. 139–147, January 2002.

[219] ——, "Tomlinson-Harashima precoding in space-time transmission for low-rate backward channel," in *Proceedings of International Zurich Seminar (IZS) on Broadband Communications Access-Transmission-Networking.* IEEE, 2002, pp. 7–7.

[220] K. Kusume, M. Joham, W. Utschick, and G. Bauch, "Efficient Tomlinson-Harashima precoding for spatial multiplexing on flat MIMO channel," in *Proceedings of IEEE International Conference on Communications (ICC)*, vol. 3. IEEE, 2005, pp. 2021–2025.

[221] B. M. Hochwald, C. B. Peel, and A. L. Swindlehurst, "A vector-perturbation technique for near-capacity multiantenna multiuser communication-Part II: Perturbation," *IEEE Transactions on Communications*, vol. 53, no. 3, pp. 537–544, 2005.

[222] S. Sanayei and A. Nosratinia, "Antenna selection in MIMO systems," *IEEE Communications Magazine*, vol. 42, no. 10, pp. 68–73, 2004.

[223] A. F. Molisch and M. Z. Win, "MIMO systems with antenna selection-an overview," *IEEE Microwave Magazine*, vol. 5, no. 1, pp. 46–56, 2004.

[224] A. F. Molisch, M. Z. Win, and J. H. Winters, "Capacity of MIMO systems with antenna selection," in *Proceedings of IEEE International Conference on Communications (ICC)*, vol. 2. IEEE, 2001, pp. 570–574.

[225] R. W. Heath, S. Sandhu, and A. Paulraj, "Antenna selection for spatial multiplexing systems with linear receivers," *IEEE Communications letters*, vol. 5, no. 4, pp. 142–144, 2001.

[226] R. S. Blum and J. H. Winters, "On optimum MIMO with antenna selection," *IEEE Communications Letters*, vol. 6, no. 8, pp. 322–324, 2002.

[227] A. Gorokhov, "Antenna selection algorithms for mea transmission systems," in *Proceedings of IEEE International Conference on Acoustics, Speech, and Signal Processing (ICASSP)*, vol. 3. IEEE, 2002, pp. III–2857.

[228] M. Di Renzo, H. Haas, A. Ghrayeb, S. Sugiura, and L. Hanzo, "Spatial modulation for generalized MIMO: Challenges, opportunities, and implementation," *Proceedings of the IEEE*, vol. 102, no. 1, pp. 56–103, 2014.

[229] R. Y. Mesleh, H. Haas, S. Sinanovic, C. W. Ahn, and S. Yun, "Spatial modulation," *IEEE Transactions on Vehicular Technology*, vol. 57, no. 4, pp. 2228–2241, 2008.

[230] J. Jeganathan, A. Ghrayeb, and L. Szczecinski, "Spatial modulation: Optimal detection and performance analysis." *IEEE Communications Letters*, vol. 12, no. 8, pp. 545–547, 2008.

[231] M. D. Renzo, H. Haas, A. Ghrayeb, S. Sugiura, and L. Hanzo, "Spatial modulation for generalized MIMO: challenges, opportunities and implementation," *Proceedings of the IEEE*, vol. 102, no. 1, pp. 56–103, 2014.

[232] A. Younis, N. Serafimovski, R. Mesleh, and H. Haas, "Generalised spatial modulation," in *Proceedings of the Asilomar Conference on Signals, Systems and Computers*. IEEE, 2010, pp. 1498–1502.

[233] M. Di Renzo, H. Haas, and P. Grant, "Spatial modulation for multiple-antenna wireless systems: A survey," *IEEE Communications Magazine*, vol. 49, no. 12, pp. 182–191, 2011.

[234] L. Liang, W. Xu, and X. Dong, "Low-complexity hybrid precoding in massive multiuser MIMO systems," *IEEE Wireless Communications Letters*, vol. 3, no. 6, pp. 653–656, 2014.

[235] F. Sohrabi and W. Yu, "Hybrid digital and analog beamforming design for large-scale antenna arrays," *IEEE Journal of Selected Topics in Signal Processing*, vol. 10, no. 3, pp. 501–513, 2016.

[236] S. S. Ioushua and Y. C. Eldar, "A family of hybrid analog-digital beamforming methods for massive MIMO systems," *IEEE Transactions on Signal Processing*, 2019.

[237] A. F. Molisch, V. V. Ratnam, S. Han, Z. Li, S. L. H. Nguyen, L. Li, and K. Haneda, "Hybrid beamforming for massive MIMO: A survey," *IEEE Communications Magazine*, vol. 55, no. 9, pp. 134–141, 2017.

[238] I. Ahmed, H. Khammari, A. Shahid, A. Musa, K. S. Kim, E. de Poorter, and I. Moerman, "A survey on hybrid beamforming techniques in 5G: Architecture and system model perspectives," *IEEE Communications Surveys & Tutorials*, vol. 20, no. 4, pp. 3060–3097, 2018.

[239] A. Alkhateeb, O. El Ayach, G. Leus, and R. W. Heath, "Hybrid precoding for millimeter wave cellular systems with partial channel knowledge," in *Proceedings of Information Theory and Applications Workshop (ITA)*. IEEE, 2013, pp. 1–5.

[240] J. Barbier and N. Macris, "The stochastic interpolation method: A simple scheme to prove replica formulas in Bayesian inference," *Probability theory and related fields*, vol. 174, no. 3-4, pp. 1133–1185, 2019.

[241] S. F. Cotter, B. D. Rao, K. Engan, and K. Kreutz-Delgado, "Sparse solutions to linear inverse problems with multiple measurement vectors," *IEEE Transactions on Signal Processing*, vol. 53, no. 7, pp. 2477–2488, 2005.

[242] E. J. Candès and B. Recht, "Exact matrix completion via convex optimization," *Foundations of Computational mathematics*, vol. 9, no. 6, p. 717, April 2009.

[243] E. J. Candes and Y. Plan, "Matrix completion with noise," *Proceedings of the IEEE*, vol. 98, no. 6, pp. 925–936, April 2010.

[244] A. K. Jain, R. P. W. Duin, and J. Mao, "Statistical pattern recognition: A review," *IEEE Transactions on Pattern Analysis and Machine Intelligence*, vol. 22, no. 1, pp. 4–37, January 2000.

[245] C. M. Bishop, *Pattern recognition and machine learning*. Springer, New York, USA, 2006.

[246] I. H. Witten, E. Frank, M. A. Hall, and C. J. Pal, *Data Mining: Practical machine learning tools and techniques*. Morgan Kaufmann, Massachusetts, USA, October 2016.

[247] Y. C. Eldar and M. Mishali, "Robust recovery of signals from a structured union of subspaces," *IEEE Transactions on Information Theory*, vol. 55, no. 11, pp. 5302–5316, November 2009.

[248] S. Sarvotham, D. Baron, M. Wakin, M. F. Duarte, and R. G. Baraniuk, "Distributed compressed sensing of jointly sparse signals," pp. 1537–1541, June 2005.

[249] D. Baron, M. F. Duarte, M. B. Wakin, S. Sarvotham, and R. G. Baraniuk, "Distributed compressive sensing," *arXiv preprint arXiv:0901.3403*, January 2009.

[250] A. El Gamal and Y.-H. Kim, *Network information theory*. Cambridge University Press, Cambridge, UK, 2011.

[251] H. Chandra, "Differential operators on a semisimple Lie algebra," *American Journal of Mathematics*, pp. 87–120, 1957.

[252] C. Itzykson and J.-B. Zuber, "The planar approximation. II," *Journal of Mathematical Physics*, vol. 21, no. 3, pp. 411–421, 1980.

[253] A. Guionnet and O. Zeitouni, "Large deviations asymptotics for spherical integrals," *Journal of functional analysis*, vol. 188, no. 2, pp. 461–515, 2002.

[254] A. M. Mathai and S. B. Provost, *Quadratic forms in random variables: theory and applications*. Marcel Dekker, New York, USA, 1992.

[255] H. Robbins, "A remark on Stirling's formula," *The American Mathematical Monthly*, vol. 62, no. 1, pp. 26–29, 1955.